MOLECULAR STUDIES OF THE RESPONSE OF PERIODONTAL LIGAMENT CELLS TO MECHANICAL STRAIN *IN VITRO*

AARTHI SAMINATHAN

(MSc, UNIVERSITY OF ABERDEEN)

A THESIS SUBMITTED FOR THE DEGREE OF

DOCTOR OF PHILOSOPHY

FACULTY OF DENTISTRY
NATIONAL UNIVERSITY OF SINGAPORE
2013

DECLARATION

I hereby declare that the thesis is my original work and it has been written by me in its entirety. I have duly acknowledged all the sources of information which have been used in the thesis.

This thesis has also not been submitted for any degree in any university previously.

AARTHI SAMINATHAN

23 August 2013

Acknowledgement

This doctoral thesis could not have been completed without the support of several people. I wish to acknowledge all of them.

Foremost, I owe my sincere and deepest gratitude to my main supervisor of this research, Professor Murray Clyde Meikle for his unfaltering faith in me as well as for maintaining a light-hearted work environment throughout my four years at NUS. His steady support even during phases of hindrances has been a source of motivation and aided me to mould myself to savour the coarse stages of this research. His knowledge, guidance and his constructive criticism were invaluable and enduring and I could not have imagined a better expert and mentor for my Ph.D. It was indeed a wonderful journey all along.

Secondly, I would like to express my thanks to co-supervisor, Associate Professor Cao Tong, who provided his expertise and aid and for granting permission to utilise his equipments and laboratory which contributed greatly towards the smooth progress of my research experiments.

Besides my supervisors, I am grateful to Dr. Vinoth Kumar, who introduced and gave me a good opportunity to work in this research topic. I am much obliged for the strong confidence he had in me and for all the effort he spent in aiding me. A special thanks for his initial teachings on experimental techniques which were the important basis of my research work.

My intellectual debt is to Dr. Sriram Gopu whose persistant help and enormous support for the research, not to mention the brain-storming discussions have been illuminating. His patience and experience have guided me in preparing my research papers and conferences that I have attended. I wish to share the stage with him for each of my successful experimental breakthroughs.

I also want to thank Mr. Chan Swee Heng for the special provisions and maintenance of the necessary hardware and tools in the lab that were highly needed for conducting the experiments, without any obstacles. My sincere thanks to Ms Lee Shu Ying of confocal microscopy unit, DSO staffs, colleagues for their help and support when needed.

Lastly, I owe my deepest thanks to my family who guided me in the right path and were supportive of my choices and especially Thamarai Selvan and Morgan Saminathan, without whose moral support and of course the patient editing of my paper works all through my academic life, my path would not have been easier to walk through. Things would not have been possible if not for you both.

Dedicating to

Prof. Meikle, Saminathan, Sooriyakala, Thamarai Selvan, Morgan & Muruganandham

Table of Contents

Summary

The periodontal ligament (PDL) is a thin fibrous connective tissue, embedded between the cementum covering the roots of the teeth and supporting alveolar bone that evolved in mammals to provide for the eruption and attachment of teeth to the bones of the jaw.

Since the PDL functions in a mechanically-active environment, we initially investigated the effect of a cyclic in-plane tensile deformation of 12% on human PDL cells in 2-dimensional culture over a 6–24 h time-course in a Flexercell FX-4000 Strain Unit. Eighty-four adhesion related genes were screened using real time RT-PCR microarrays, and of these 73 were expressed. Fifteen genes were mechanoresponsive, four of which were upregulated (*ADAMTS1*, *CTGF*, *ICAM1* and *SPP1*) and 11 downregulated, with the range extending from a 1.76-fold induction of *SPP1* at 12 h to a 2.49-fold downregulation of *COL11A1* at 24 h. Mechanically-deformed cells also showed a significant reduction in metabolic and caspase 3/7 activity at 6–12 hours suggesting a positive effect of mechanical stress on apoptosis.

Cells are normally embedded in a complex extracellular network of collagens, proteoglycans and noncollagenous proteins – not attached to tissue culture plastic, or to films composed of collagen or fibronectin. We therefore developed 3-dimensional constructs incorporating PDL cells into thin films (80–100 μm) of a hyaluronan (HA)–gelatin hydrogel matrix (Extracel™) which were subjected to 12% cyclic tensile strain, 6h/day for 1–3 weeks.

Eighteen connective-tissue related genes were analyzed. With the exception of *P4HB, TGFB1* and *RANKL,* each was upregulated in mechanically active cultures at some point in the time scale, as was the synthesis of MMPs and TIMP-1 detected by ELISAs. *SOX9, MYOD, SP7, BMP2, BGLAP or COL2A1* were not detected in either stationary or mechanically active cultures. Mechanical stress had no significant effect on cell proliferation.

Studies of compressive force require thicker constructs (900–1000 μm), and this was achieved by incorporating type I rat tail collagen into the HA-gelatin matrix. A compressive of 33.4 kPa (340.6 gm/cm^2) applied for 6, 12 and 24 h upregulated *COL1A1*, *MMP1*, *MMP3* expression with the matricellular protein *CTGF* being the most mechanoresponsive with a 3.15 fold induction. Compressive strain significantly increased apoptotic cell death by the upregulation of 8 caspase encoding genes. At the protein level, compressive strain significantly increased MMP and TIMP-1 levels while *MYOD*, *SP7*, *BGLAP*, *COL2A1* genes were again not expressed.

In summary, 3-dimensional tissue constructs provide additional complexity to monolayer culture systems, and suggest some of the assumptions regarding cell growth, differentiation and matrix turnover based on 2-dimensional cultures may not apply to cells in 3-dimensional matrices. Primarily developed as a transitional in vitro model for studying cell-cell and cell-matrix interactions in tooth support, the system is also suitable for investigating the pathogenesis of periodontal diseases, and importantly from the clinical point of view, in a mechanically active environment.

List of Tables

List of Figures

1. Review of Literature

1.1 Orthodontic Tooth movement

Orthodontic tooth movement is the result of a biological response to interfere in the physiological equilibrium of the dentofacial complex by an externally applied force (Profitt, 2000). The movement is characterized by remodelling changes in the dental and periodontal tissues, including the dental pulp, periodontal ligament (PDL), alveolar bone and gingival tissues (Krishnan, 2009). In contrast to the slow process of physiological dental drift or tooth eruption, orthodontic tooth movement can occur rapidly or slowly depending on the physical characteristics of the applied force and the size and biological response of PDL (Rygh, 1995). The present study utilizes cells derived from PDL and therefore, it would be appropriate to discuss the anatomy, the biology and the unique characteristics of the PDL in respective to its involvement in the orthodontic tooth movement.

1.1.1. PDL structure and biology

The PDL is a structure that separates the alveolar bone and the tooth in the periodontium derived from the dental follicle and the development of the PDL starts during root formation before tooth eruption. The width of the periodontal ligament ranges 0.15mm to 0.38 mm, which can vary depending upon patient, age, systemic conditions and functional status of the tooth (Shimono *et al*., 2003; Verna and Melsen, 2003).

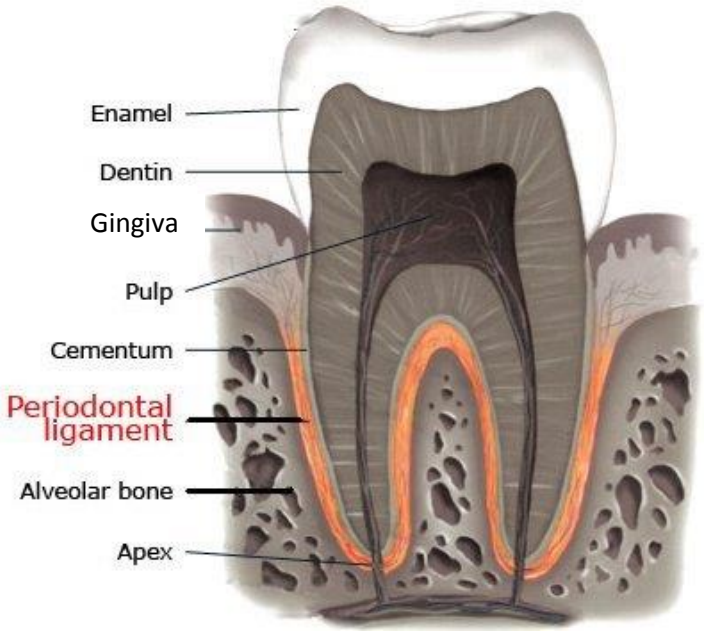

Figure 1.1. A schematic diagram illustrating the periodontal ligament attaching the cementum of the tooth root to the alveolar bone of the socket. Adapted - www.studiodentaire.com/en/glossary/periodontal_ligament.php.

1.1.2. PDL fibres

The PDL is a thin fibrous connective tissue that connects the surface of the tooth root with the bony tooth socket. The fibres are primarily composed of Type I collagen, with lesser amounts of type III, IV, V, XII (Berkovitz *et al*., 1995). In addition, the PDL also consists of a small quantity of elastic fibres, including oxytalan, reticulin and elastin fibres. The collagen fibres are arranged in bundles of connective tissue of approximately 5µm in diameter. Based on their orientations, distributions and functions, the bundles form six distinct groups: i) transeptal fibres; ii) alveolar fibres; iii) horizontal fibres; iv) oblique fibres; v) apical fibres and vi) interradicular fibres (Krishnan and Davidovitch, 2009). The principal fibres which are embedded in the cementum

are known as Sharpey's fibres as first described by the English anatomist William Sharpey in 1846.

In addition to the principal fibres, numerous collagen fibres are arranged with random directions, forming an indifferent fiber plexus. In 1923, Sicher introduced another term, the intermediate plexus, which he described as an intercalation of fibres near the middle of the PDL; these fibres did not pass directly from the tooth to the bone. This concept was later denied by Sloan (1979) as he did not observe any plexus in the SEM findings.

1.1.3. PDL cells

The periodontal ligament is a highly cellular structure with a heterogeneous cell population that includes fibroblasts, osteoblasts, osteoclasts, cementoblasts, cementoclasts, defence cells and epithelial cells (McCulloch and Bordin, 1991; Seo *et al*., 2004) PDL harbours stem cell niches and ECM microenvironments where multipotent stem cells can synthesize and remodel the periodontium when subjected to aging and injury. Many experiments further investigated the phenotypes in a PDL cell population (Seo *et al*., 2004; Nagatomo *et al*., 2006; Kim *et al*., 2012; Wang *et al*., 2012). These experiments have shown that PDL cell population is heterogeneous due to the existence of a small sub-population of mesenchymal stem cells. These studies have also reported that human PDL cells express the mesenchymal stem cell markers STRO-1 and CD146/MUC18 and have the potential to differentiate into cementoblast-like cells and adipocytes. Gay *et al*. (2007) found that this small sub population of human post-natal stem cells can be induced to

differentiate into the number of different cell types including osteoblasts, chondrocytes and adipocytes. Jo *et al*. (2007) isolated postnatal stem cells from human dental tissues which included dental pulp, PDL, periapical follicle and surrounding mandibular marrow. Stem cells were identified in these populations using STRO-1 as a stem cell marker, as well as through expression of the mesenchymal stem cell markers CD29 and CD44. They also demonstrated that post-natal stem cells in dental tissues, including the PDL, can differentiate into adipocytes and osteoblasts depending upon the environment.

1.1.4. PDL fibroblasts

The predominant cells of the periodontal ligament are the fibroblasts. These cells can synthesize extracellular matrix products which plays an important role in the development, structure and function of the tooth support apparatus (Ten Cate, 1994). The cells are arranged in parallel manner to the collagen fibres within the PDL and interaction is noted with the oxytalan fibres of the PDL (Beertsen *et al*., 1974). The fibroblasts are polarized, with Golgi complex and the centriolar region situated between the leading edge of the cell and the posteriorly located nucleus. The leading edge is the nuclear pole anterior to which are the elements such as rough endoplasmic reticulum, mitochondria, microfilaments (predominantly composed of cellular protein called actin) and microtubules (made of the protein tubulin), which are considered to be the indicators of polarity (Berkovitz *et al*., 1995). Polarization of the intracellular organelles influences the directed migration of the fibroblasts, synthesis and breakdown of matrix components (Beersten *et al*., 1979; Garant and Cho,

1979). Microfilaments are important for the contraction and movement of the cells.

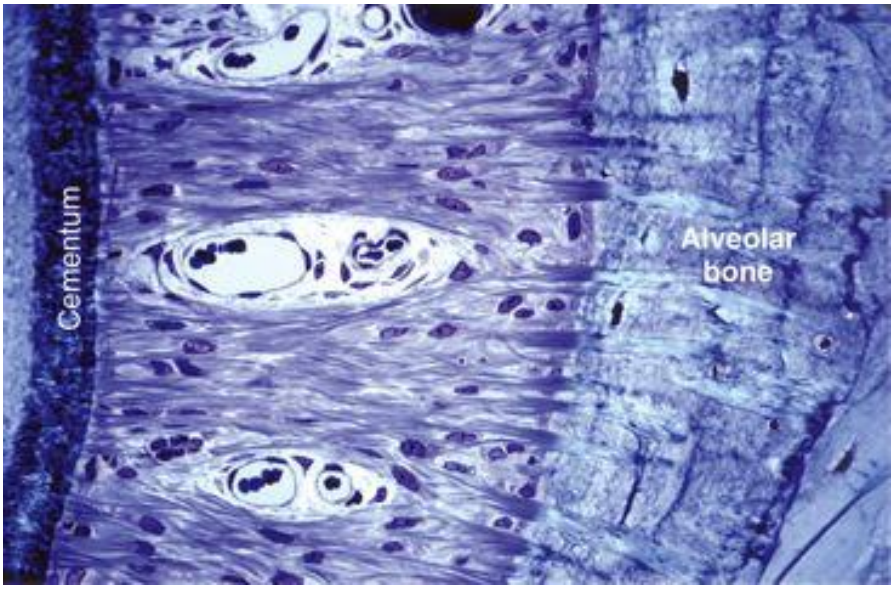

Figure 1.2. Low-power light micrograph showing arrangement and insertion of periodontal ligament fiber bundles into the root cementum on the left and alveolar bone on the right in a monkey. Adapted - Rose, (2004).

The PDL fibroblasts present with characteristics which make them unique from other cells in the connective tissues and one of properties includes the higher alkaline phosphatise (ALP) activity (Murakami *et al*., 2003; Jacobs *et al*., 2013; Kook *et al*., 2013). The periodontal ligament is found to have higher ALP activity at the region lining the alveolar wall compared to the tooth related regions and the supracrestal extensions. This enzyme is a characteristic marker for osteoblasts-like cells, and closely associated with mineralization. High ALP levels have been reported in PDL fibroblasts and osteoblasts (Piche *et al*., 1989; Nojima *et al*., 1990). Murakami and co-workers (2003) made use of an immunomagnetic method to isolate ALP-positive subsets from the PDL cells. Somerman *et al*. (1988) compared the PDL and the gingival fibroblasts

in vitro and reported that the PDL fibroblasts have higher ALP activity and greater protein and collagen production, than gingival fibroblasts. Similar findings were also reported by Kuru *et al*. (1998) who studied the difference between PDL and gingival fibroblasts, using flow cytometry. Basdra and Komposch (1997) measured increasing basal ALP activity in PDL cell cultures and significantly higher ALP when the cells are subjected to 1α, 25-dihydroxyvitamin D3.

PDL fibroblasts also demonstrate immunofluorescence against osteocalcin, an osteoblast marker (Basdra and Komposch, 1997; Murakami *et al*., 2003). Cho *et al*. (1992) noted the formation of mineralized nodules by rat PDL cells, and Basdra and Komposch (1997) also showed formation of mineral nodules by human PDL cells with the use of Von Kossa staining. These results indicate that human PDL fibroblasts exhibit some of the *in vitro* phenotypic characteristics of osteoblast-like cells, suggesting these cells can potentially differentiate into osteoblasts and or cementoblasts (Basdra and Komposch, 1997). The involvement of PDL cells in bone remodelling was also reported by Yang *et al*. (2006) who carried out intermittent mechanical loading on the PDL cells *in vitro* and found that osteoblast markers are expressed (increased ALP and osteocalcin and decreased osteoprotegerin). The presence of osteoblastic markers illustrates the potential of PDL fibroblasts to differentiate into osteoprogenitor cells, which could contribute to bone remodelling during orthodontic movement.

1.1.5. Viscoelastic nature of PDL

The response of the tooth subjected to intrusive load showed that the PDL acts as a viscoelastic gel that helps cushion against mechanical loading (Bien and Ayers, 1965). *In vivo* experiments have been conducted on tooth displacement (Wills *et al*., 1972) and demonstrated the nonlinearity and the time dependence of the relationship between load and tooth displacement. A study by Natali *et al*. (2004), attempted to implement the viscoelastic model in a general purpose finite element code. In this study, experimental tests were carried out *in vitro* on PDL specimens of adult pigs to obtain stress-relaxation and cyclic stress-strain curves. When the experimental and numerical results were compared, good correspondence was noted and confirmed the capability of the formulation to properly interpret the viscoelastic behaviour of the PDL.

1.2. Phases of orthodontic tooth movement

When the rate of orthodontic tooth movement was plotted against time, three phases of response can be recognized and termed by Burstone as: the initial phase, the lag phase and the post-lag phase (Burstone, 1962). Likewise, Graber and Vanarsdall (1994) have also divided tooth movement into three elements of tooth displacement as initial strain, lag phase and progressive tooth displacement based on report of Schwartz (1932).

The initial phase is represented by rapid tooth movement as a result of displacement of the tooth within the PDL space, which occurs immediately after force application. The definition of initial strain extends to bone strain and extrusion that can span for one to three days, up to a week, followed by a

lag period in which there are low rates of displacement or no displacement of the tooth. The lag phase mainly involves in the hyalinization or undermining resorption of the PDL in areas of compression. The duration of the lag period varies between two to ten weeks, depending on the patient's age, density of the bone and the extent of the PDL necrotic tissue (Graber and Vanarsdall, 1994). Once the necrotic tissues are completely removed by the macrophages, the rate of tooth displacement increases and tooth movement enters the post-lag or the progressive tooth displacement phase. Progressive tooth movement takes place at a relatively fast rate depending upon two key factors: frontal resorption of the PDL and remodelling of the alveolar bone (Graber and Vanarsdall, 1994).

Two studies were conducted to measure the rate of tooth displacement with varying force magnitudes and patterns subsequent to which a new time/displacement model for tooth displacement was proposed (Pilon *et al*., 1996; van Leeuwen *et al*., 1999). Instead of three phases, four phases of tooth displacement were identified from beagle dog experiments: (1) Initial tooth movement, (2) Arrest of tooth movement, (3) Acceleration of tooth movement, (4) linear tooth movement. Initial tooth movement within the bony socket lasts for a few days but not greater than a week. During this phase the tooth movement is limited by the hydrodynamic damping and viscoelasticity of the PDL. Within twenty-four hours there were signs of cellular and tissue reactions (Von Bohl *et al*., 2004) while PDL fibres were compressed and stretched at the pressure and tension sides respectively. Osteoblastic and osteoclastic numbers were also increasing.

Next phase of arresting tooth movement occurs due to the presence of hyalinization. This takes place for about four to twenty days. This period involved the recruitment of phagocytes into the necrotic areas and proliferation of osteoblastic progenitors and fibroblasts in the tension areas to prepare for acceleration of tooth movement in the third phase. After 40 days of initial force application (von Bohl *et al*., 2004), remodelling of the PDL and alveolar bone took place at a maximal capacity to allow for continuous tooth movement with an increasing rate (Pilon *et al*., 1996). This was the third phase. Once the limit for rate of tooth movement is reached, constant tooth displacement takes place and usually occurs 80 days after force application. Hyalinized areas and irregular bone surfaces were still detectable due to direct bone resorption during the last two phases. The collagen fibres were not properly orientated at the sites of pressure while the tension site had bone deposition on which the bone surfaces were covered with ALP-positive osteoblastic cells (von Bohl *et al*., 2004).

1.3. Optimal forces of orthodontic tooth movement

In 1932, (Schwartz) proposed the classic definition of optimal force as 'the force leading to a change in tissue pressure that approximated the capillary vessels' blood pressure, thus preventing their occlusion in the compressed periodontal ligament'. According to Schwarz, forces below the optimal level caused no reaction in the PDL, whereas forces exceeding the optimal level would lead to vascular occlusion and tissue necrosis, preventing frontal bone resorption. He concluded that the forces delivered as part of orthodontic treatment should not exceed the capillary blood pressure (20–25g/cm^2 of root

surface). Oppenheim (1942) advocated the use of very light force to move teeth and this concept was supported by Reitan (1957) when he noted cell-free compressed areas within the pressure sites even in cases where light forces are applied. The concept of optimal force has changed considerably over the past 70 years.

Storey and Smith in 1952 determined the optimal force for orthodontic tooth movement by using heavy and light retraction springs to move canine teeth in nine patients. They found that forces below 150 g did not cause the canine to move significantly. However, when the forces ranged from 150-250 g, the canine moved rapidly into the premolar extraction site. They also found that heavy springs applying a force of 400-600 g did not cause the canine to move, but rather resulted in the anchor unit moving significantly. These findings say that the optimal force required for maximum rate of tooth movement varies with individual patients in which the magnitude of the applied force is the main variable that affects the rate of tooth movement giving rise to the concept of differential force.

1.3.1. Continuous, interrupted and intermittent forces

The current concept of optimal force, views it as a force of certain magnitude and certain characteristics (continuous versus intermittent, constant versus declining, etc) capable of producing a maximum rate of tooth movement without tissue damage. Although light continuous forces are used in fixed orthodontic appliances, a long duration can cause the force to subside and get interrupted. However, interrupted movements occur for a short period of time

making it difficult to get distinguished from the continuous force (Thilander *et al*., 2000). When the force gets interrupted with a low initial magnitude, formation of hyalinized zones in the compressed sites of PDL occurs eliminating the necrotic tissue and tooth moves. During this passive period, new osteoid layer forms, the tissues get reorganized and favouring cell proliferation for any further changes when the appliance gets reactivated (Gianelly, 1969). A histochemistry study involving staining with tartarate-resistance acid phosphatase (TRAP) on rat molars subjected to continuous force evaluated the compressed areas of PDL found resorption of alveolar bone parallel to the new bony tissue formation on the tension sites PDL (Bonafe-Oliveira *et al*., 2003).

Intermittent forces are periodically delivered by removable appliances like springs resting on tooth surfaces which generate a force as an impulse or with many interruptions for a short period (Thilander *et al*., 2000). These forces produce small compression zones in the PDL, short hyalinization periods and when the appliances are removed intermittently it results in longer resting periods. This treatment helps the PDL fibres to retain a functional arrangement thus promoting the increase in the number of PDL cells (Gianelly, 1969). The condition where in the compressed PDL with only some of them undergoing necrosis was termed as ‘’semihyalinization’’ (Reitan, 1960). This leads to the formation of osteoclasts along bone surface and bone resorption is less disturbed by hyalinization effecting a uniform movement of teeth.

1.3.2. Forces and the rate of tooth movement

Quinn and Yoshikawa (1985) noted that the true mechanical parameter in tooth movement is not the magnitude of force applied by the appliance, but rather refers to the magnitude of stress generated by the appliance in the surrounding periodontium. Four hypotheses have been proposed regarding the relationship between stress magnitude and tooth movement (Quinn and Yoshikawa, 1985): (1) a constant relationship between rate of movement and stress, in which rate of movement does not increase as the stress level is increased; (2) a linear increase in the rate of tooth movement as stress increases; (3) increasing stress causes the rate of tooth movement to increase to a maximum. However, once the optimal level is reached, additional stress can cause the rate of tooth movement to decline, and (4) a linear relationship exists between stress magnitude and rate of tooth movement up to a point, after which, an increase in stress causes no appreciable increase in tooth magnitude.

The magnitude of force determines the duration of hyalinization but its duration depends on the rate at which it is removed by macrophages and giant cells. With light force, the duration of the hyalinization period is shorter, while excessively strong forces can result in a longer hyalinization period with formation of secondary hyalinized zones (Viecilli *et al*., 2013).

There are four main problems encountered throughout the literature that look at the force magnitude and tooth movement (Quinn and Yoshikawa, 1985; Ren *et al*., 2003). When a tipping movement is performed, the stress distribution

within the PDL is uneven and it I difficult to determine the centre of resistance. In addition, clinical tooth movement is accompanied by dynamic changes in stress/strain in the PDL, which ranges from compression to tension (Isaacson *et al*., 1993). Secondly, it is technically difficult to calculate a precise distribution of stress and strains at the level of the PDL, which are more critical when evaluating the optimal force magnitude for inducing biological reactions in tooth movement. The third problem encountered is that the evaluation of tooth movement is conducted only over a short period, leading to data pertaining to the first two phases of the process and not to the third or fourth phase in which true orthodontic tooth movement is considered to take place. Lastly, there are large inter-individual variations and measurement errors encountered in both human and animal studies. The rates of tooth movement can vary substantially and standardized controlled force between patients and between quadrants in an individual; on the other hand, rates of tooth movement may be almost the same among or within individuals when the applied forces are substantially different (Quinn and Yoshikawa, 1985; Ren *et al*., 2003; Melsen B, 2007). As a result it is impossible to determine the optimal force required for orthodontic tooth movement in individual patients.

1.4. Orthodontic tooth movement theory

The concept of force induced tooth movement being related to bone resorption and bone deposition within a tooth socket dates back to the time of Chapin Harris in the 19th century (Meikle, 2006). Many theories were developed by

different researchers of which two main theories have primarily dominated the literature to date: the pressure-tension theory and bone bending.

1.4.1. The pressure-tension theory

The pressure-tension theory was hypothesized to explain that orthodontic tooth movement generates a pressure and tension side in the PDL. A sequence of biological events occurs on both sides to result in the tooth movement. On the pressure side, reduced blood flow, cell death, resorption of hyalinized tissue by macrophages. In contrast, on the tension side, blood flow is increased where the PDL is stretched promoting the osteoblastic activity resulting in bone deposition.

Histological research by Sandstedt using dogs as his experimental model resulted to frame the foundation of pressure-tension theory. He induced tooth movement on six maxillary incisors over 3 weeks and found that both light and heavy forces resulted in bone deposition on the alveolar bone on the tension side of the tooth. With light forces on the pressure side, osteoclasts were found to induce bone resorption directly at the bone-PDL interface, whereas with heavy forces, cell death and capillary thrombosis took place, creating localized cell-free areas which Sandstedt termed as ‘hyalinization’ (Bister and Meikle, 2013). Once the necrotic tissues and the underside bone immediately adjacent to the necrotic PDL area, were removed by the macrophages, multinucleate giant cells from the adjacent undamaged tissues, tooth movement resumed. This process is known as ‘undermining resorption’. In contrast, Oppenheim (1911, 1912) a few years later carried out a

histological study on the primary teeth of monkeys and noted a transformation of the entire architecture of bone by the simultaneous occurring of bone resorption and deposition of new bone tissue. Schwarz in his 1932 review paper explained the difference between the theories postulated by Sandstedt and Oppenheim. Sandstedt was proven correct in his interpretations. Oppenheim had sacrificed the animals several days after the orthodontic tooth movement had ceased.

A half century later, Reitan carried out histological works extensively on human material to study the tissue reaction of the periodontium following orthodontic force applications further supported the pressure-tension theory. He found that even minimal forces can create areas of hyalinization and it happened at a greater degree for teeth with shorter roots. He also observed that intermittent forces produced shorter periods of hyalinization than continuous forces.

Though firmly embedded in the orthodontic literature, this theory was not supported by some experiments. Two conceptual flaws have been raised regarding the pressure-tension theory. The first being the question of the production of tension by stretched PDL fibres. It is believed that the tension created in the PDL by the stretched collagen fibres provides the stimulus responsible for the deposition of bone. To test this theory, Heller and Nanda (1979) disrupted the normal metabolism and function of the collagen in rat molars by the administration of the lathyrogen beta-aminopropionitrile (BAPN) and found that there was no interference to bone formation or

orthodontic tooth movement. The agent increases collagen solubility by inhibiting lysine 6-oxidase activity, an enzyme that cross-links the polypeptide chains of collagen and elastin molecules (Levene and Carrington, 1985). The collagen in the periodontal ligament was devoid of its normal architecture, which suggests that one remodelling during orthodontic tooth movement occurred despite the presence of a physically altered periodontium. It was concluded that the tension created in the PDL and thought to be transferred to the alveolus through Sharpey's fibres may not be necessary to stimulate bon formation.

In Baumrind's experiment on young male rats to determine the dimensional and metabolic changes of the PDL by applying an orthodontic force, increased cell replication and metabolic activity were observed on both pressure and tension sides of the tooth while collagen synthesis was decreased. This raised the question whether there was any qualitative difference between the two sides of the tooth. In regards to this second conceptual flaw Baumrind proposed that PDL is a closed hydrostatic system and applied Pascal's law to dispute the pressure-tension theory. Pascal's law stated that for all points at the same absolute height in a connected body of an incompressible fluid at rest, the fluid pressure is the same, even if additional pressure is applied on the fluid at some place. But can PDL be considered as a closed system and be classified as a fluid? Gingival cervical fluid is expressed through gap junctions in the epithelium following the application of continuous force to a tooth in addition to the walls of the alveolus are highly perforated by the vascular system suggesting it could not be a closed system and PDL consists of cells,

collagen proteoglycans, blood vessels as well as tissue fluids and henceforth not a fluid (Meikle, 2006). Baumrind hypothesized that orthodontic forces creates differential pressure-tension areas in the solid periodontium which contains the bone, tooth and the solid fractures of the PDL. Thus an alternative hypothesis of bone ending theory was suggested.

1.4.2. Bone bending theory

The concept of bone bending was first proposed by Farrar (1888) who suggested that alveolar bone bending plays a pivotal role in orthodontic tooth movement. Farrer wrote in 1888:

> "Teeth move by one of two kinds of tissue changes in the alveolus by the reduction of the alveolus through what is called absorption on one side of the tooth, followed by the growth of new supporting tissue on the other; and by bending of the alveolar tissue"

The theory was further confirmed by the experiments of Baumrind (1969) and Grimm (1972). Baumrind suggested this as an alternative hypothesis consequent to his previous experiments. According to him, the bone was found to be more elastic and deforms more readily than the periodontal ligament. He also made reference to Hook's law that states the amount by which a material body is deformed (the strain) is linearly related to the force causing the deformation (the stress). Grimm (1972) measured bone deflection in two 12-year-old patients and bending of alveolar bone was detected at forces less than 50g and up to 35μm with a load of 1.5 kg. A transient effect was observed as an initial deflection of the socket wall was in the opposite direction from the tooth movement and resolved after 1 minute. Despite the

small sample size, this study provides additional evidence that bone bending occurs during tooth movement.

The idea of bone bending due to orthodontic forces result in resorption and deposition of bone to allow tooth movement is reasonable, but does not agree with orthopaedic theory which states that bone under compression results in bone deposition and bone in tension results in bone resorption (Melsen, 1999). Epker and Frost (1965) described areas of compression and tension by suggesting that during orthodontic tooth movement, the socket wall in the direction of the applied force is in tension and the socket wall on the opposite side is in compression. Being opposite to the pressure tension theory, it was explained that a load causes a tooth to apply a compression force perpendicular to the surface of the socket wall in the direction of the applied load. Recent finite element analysis would suggest otherwise. FEA is a computer based numerical technique for calculating the strength and behaviour of engineering structures. By breaking structures down into elements, FEA can be used to calculate strain, stress and vibration behaviour of a structure. FEA of teeth undergoing orthodontic tooth movement has previously been used to support the pressure-tension theory around the periodontium. Periodontal ligament was not correctly defined in the computer model of these studies (Edmundson, 1984; Middleton *et al*., 1990; Williams and Wilson *et al*., 1994). These computer models generally incorporated homogenous, isotropic, linear elastic and continuous periodontal ligament properties. The periodontal ligament has been found to possess non-linear mechanical properties and provides non-uniform geometric data (Toms *et al*.,

2002). Recent FEA show very complex pattern of compression and tension in the alveolar bone. Cattaneo *et al*. (2005) attempted to use FEA to determine the impact of the modelling process on the outcome. Their findings were seen to be consistent with the hypothesis of Melsen (2001), that direct bone resorption in front of the roots along the movement direction starts as a consequence of a hypo physiological loading characterized by strain values below the minimum effective strain as defined by Frost' mechanostat theory (Frost, 1992). However Cattaneo *et al*'s study was based on the anatomy of a single donor.

The contribution of bone bending theory to orthodontic tooth movement has been explained by the production of piezoelectric signals (Bassett and Becker, 1962), which may be associated with a biological response created at the bone surface during the mechanical deformation of the supporting alveolar bone (Epker and Frost, 1965). Grimm (1972) also noted that '..strain-induced electric or chemical phenomenon may be the mediating factor between the mechanotherapy and cellular bone response' with the bending of the alveolus during orthodontic treatment.

1.4.3. Piezoelectric signals

Piezoelectricity is the phenomenon of some materials to generate electric potential in response to the deformation of the material. Materials that exhibit this property are crystals and ceramics. Bone is capable of producing piezoelectric signal due to the presence of apatite crystals.

Piezoelectric signals have two characteristics: (1) a quick decay rate, where the piezoelectric signal created in response to the force application, rapidly dies off even when the force is maintained. (2) Production of an equivalent signal in the opposite direction when the force is released (WR, 2000). The ion interacts in the fluid on the bone, and when the bone bends, electric signals are generated with the electric signals generated resulting in the formation of streaming potential.

Basset and Becker (1962) suggested that the piezoelectric properties of bone play an important role in the development and growth remodelling of the skeleton. The authors demonstrated the release of an electrical potential upon bone bending and the amplitude of electrical potentials released in stressed bone was dependent upon the rate and magnitude of bone deformation. The polarity was determined by the direction of bending. Epker and Frost (1965) analysed the relationship between the physical loads on bones and the change of osteogenic activity at the bone surface. When an external force is applied to the bone, opposite effects are produced on the tension and compression sides. While bending, the tension surface of the bone elongates, becomes less concave and results in bone resorption; compression side shortens and becomes more concave resulting in bone formation electronegative potentials was associated with the concave area of the bent bone where bone formation takes place while the convex surface is electropositive with bone resorption. As hypothesized by Epker and Frost (1965), the production of an electrical potential on deformed or bent bone surfaces can be associated with a

biological signal created and this signal may be responsible for the observed osteogenic response.

The nature of the electromechanical relationship of the dentoalveolar complex using simulated orthodontic forces was analysed by Zengo *et al*. (1973). They related the polarity of the stress-induced potentials with histologic responses which occurs during orthodontic tooth movement and function. This result supported the findings of Bassett and Becker (1962) and Epker and Frost (1965). The areas which were electronegative corresponded to the areas of expected osteoblastic activity during an application of a similar orthodontic force. Conversely, positivity was observed in regions characterized by osteoclasia. Since piezoelectric currents in mechanically stressed bone were implicated in the activation of bone cells, Davidovitch (1980) aimed to determine the usefulness of exogenous electric currents in accelerating orthodontic tooth movement and found that teeth treated by force and electricity moved significantly faster with increased cyclic adenosine monophosphate (cAMP) and PGE, than those treated by force alone. Enhanced bone resorption was observed near the anode (PDL compression site), while bone formation was pronounced near the cathode (PDL tension site). In addition to the piezoelectric signals, bone also possesses an electric double layer, which exists at the fluid-bone matrix interface. Pollack *et al*., (1984) noted that this region could affect the amplitude and polarity of the stress-generated potentials, which in turn can influence bone growth and remodelling.

However, piezoelectric signals are also present in dead bones. Shamos and Lavine (1967) demonstrated that dried bone exhibits piezoelectric properties, by direct observation of electric potentials generated when a dried specimen of bone is stressed, Since piezoelectricity can exist in dead bone and as more information is derived about the cellular basis of orthodontic tooth movement and the involvement of cytokines and growth factors. Meikle (2006) has argued that the stress-generated electric potentials are more likely to be a by-product of deformation rather than an explanation of bone remodelling.

1.5. Biology of orthodontic tooth movement

Remodelling changes involve a complex interplay of cell-cell and cell-matrix interactions. Applied mechanical forces are transduced from the strained ECM to the cytoskeleton through cell surface proteins. Adhesion of the ECM to these receptors can induce reorganization of the cytoskeleton, secretion of stored cytokines, neurotransmitters, leukotrienes, growth factors, colony-stimulating factors, arachidonic acid derivatives and gene transcription (Sandy, 1998; Kerrigan *et al*., 2000).

1.5.1. Prostaglandins

The name prostaglandin was derived from the prostate gland and was first isolated from seminal fluid in 1935 by the Swedish physiologist Ulf von Euler. Prostaglandins are found in almost all tissues and organs. They serve as autocrine or paracrine mediators of cellular activity. Arachidonic acid which is the main component of cell membrane is released due to the action of phospholipase enzymes. The intermediate product can pass into both the

cyclooxygenase pathway to form PGs and thromobaxanes and the lipoxygenase pathway to form leukotrienes.

Hong *et al*., (1976) showed the first evidence of PGs playing a role in mechanical force transduction by observing an increase in PG synthesis when the cells were mechanically detached from the culture dishes. The study suggests that the force had changed the conformation of the cell membrane which exposes phospholipids to the action of phospholipases thereby releasing arachidonic acid. Harell *et al*., (1977) conducted an *in vitro* experiment to investigate the cellular production of PGs in response to mechanical stimuli. The authors suggested that the activation of the phospholipase A2 with subsequent release of arachidonic acid resulted in increased PGE_2 production, which in turn increased cAMP production. At the same time, there was also an elevation in intracellular calcium ion and stimulation of DNA synthesis.

The production of PGs in response to orthodontic tooth movement has been widely demonstrated. Yamasaki *et al*. (1980) found that the administration of indomethacin, a specific inhibitor of PGs synthetase, suppressed the appearance of osteoclasts and alveolar bone resorption induced by experimental tooth movement. When the gingival tissues near upper molar of the rat were injected with PGE1 or PGE2, appearance of osteoclasts and alveolar bone resorption were seen. These findings suggest that mechanical stress on PDL induces the PGs synthesis which stimulates osteoclastic activity. Sandy and Harris (1984) also noted a reduction of osteoclast numbers in the bone adjacent to compression sites following the injection of a non-

steroidal anti-inflammatory agent, flubiprofen and hypothesized that inhibition of PG synthesis and bone resorption had occurred. Saito and co-workers (1991) found an increased PGE production in periodontal cells when subjected to mechanical stress *in vivo* and *in vitro* and recently, Liu *et al*. (2006) reported that clodronate inhibits PGE_2 production in compressed PDL cells through its inhibitory effects on the expression of cyclooxygenase-2 (COX-2) and receptor activator of nuclear factor-kappa B ligand (RANKL).

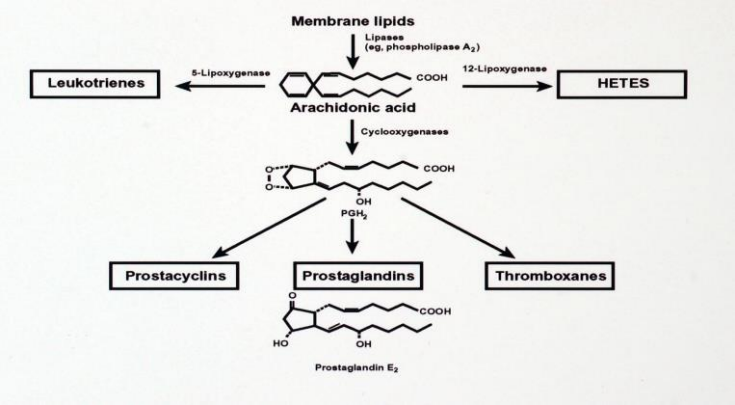

Figure 1.3. Arachidonic acid metabolites. PGs are metabolites of arachidonic (eicosatetraenoic) acid, discovered by von Euler (1934) in the prostate gland – hence the name. PGs are now known to be ubiquitous. Arachidonic acid is present in precursor form in membrane lipids from which it is released through the action of phospholipases. Arachidonic acid can be (1) converted to PGs, prostacyclins and thromboxanes via the cyclooxygenase pathway, or (2) can be acted upon to form leukotrienes and HETEs via the lipoxygenase pathway. Adapted - Berridge (1985).

Mechanical stress transducing into biochemical signals have been proposed by the following mechanisms: Activation of phospholipase A2 activity on phospholipids produce PGE_2 upon an application of mechanical stress (Binderman *et al*., 1988). Sandy *et al*., (1989) noted that inositol triphosphate pathway is involved when osteoblasts are exposed to PGE, and mechanical

deformation. It was suggested that inositol triphosphate induced calcium intake and phospholipid breakdown resulting in increased phospholipase A2 activity and PGE production (Yamaguchi *et al*., 1994). The same group of authors had also proposed that tensile force has stimulated phospholipase C in the PDL cells leading to increased inositol triphosphate and diacylglycerol. The breakdown of diacylglycerol may also result in increased arachidonic acid metabolites such as PGE2.

Several experiments have been carried out on animals and at clinical level to identify the role of prostaglandins in the bone resorptive activity. When exogenous PGEs were administered in monkeys' and rats' teeth, tooth movement was enhanced (Yamasaki *et al*., 1982; Leiker *et al*., 1995). PGE was found to enhance the replication and differentiation of osteoclast and osteoblast precursors partly mediated by cAMP (Kawaguchi *et al*., 1995). Yamasaki *et al*., (1982) confirmed the involvement of cAMP and prostaglandins in bone resorption when the appearance of osteoclasts was inhibited by the administration of imidazole (an activator of adenosine 3′ 5′ - phosphodiesterase and an inhibitor of thromboxane synthetase) and verapamil (calcium blocker) and enhanced with theophylline (an inhibitor of adenosine 3′5′ - phosphodiesterase) and ouabain (calcium transfer). Okuda *et al*., (2003) reported PGs stimulate osteoclastic activity by the induction of RANKL expression by osteoblasts and enhancement of the action of RANKL on osteoclast precursors by inhibiting granulocyte macrophage-colony stimulating factor (GM-CSF).

PGE_2 production and regulation to effect bone remodelling and tooth movement was shown to be regulated by several other agents like growth factors, interleukins, systemic hormones and other cytokines (Tashjian *et al*., 1982; Saito *et al*., 1990; Kale *et al*., 2004). Richards and Rutherford (1988) incubated human PDL fibroblasts with parathyroid hormone and cytokines (IL-α, IL-β, TNF) and noted an increased production of PGE_2. Similar result was noted when PDL cells were combined with cytokines and hormones.

1.5.2. Second messenger systems

Sutherland and Rall first identified the presence of free glucose in the bathing media of liver slices exposed to adrenaline and established the second messenger basis in 1958. They postulated that the adrenaline acts as the first messenger that binds to the cell membrane receptor and triggers the production of an intracellular second messenger (Sandy *et al*., 1993; Krishnan and Davidovitch, 2006) which interacts with cellular enzymes inducing protein synthesis or glycogen breakdown. Numerous second messenger systems have shown to be activated by mechanical deformation, but two most closely studied are cyclic nucleotide pathway and phosphatidyl inositol pathway.

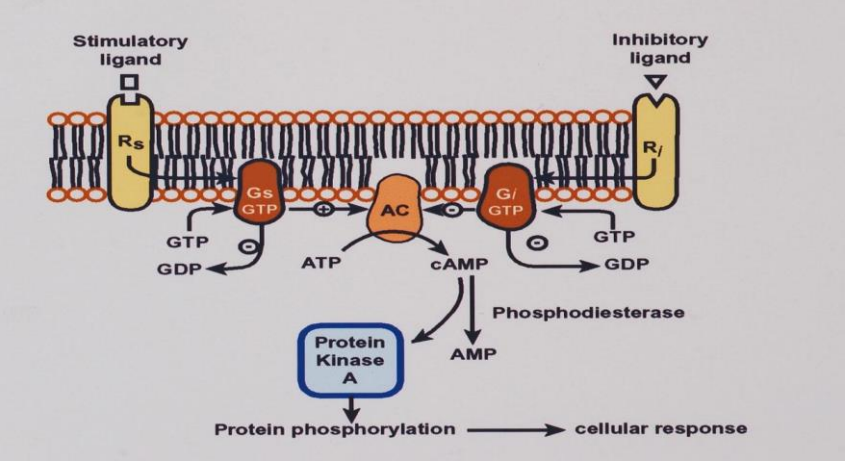

Figure 1.4. The cyclic AMP pathway. External messengers are regulated by stimulatory (Rs) and inhibitory (Ri) receptors. These interact with G proteins to stimulate or inhibit adenylate cyclase (AC) which converts ATP to cAMP. cAMP binds to the regulatory component of its protein kinase to liberate the catalytic component which is then free to phosphorylate specific proteins that regulate the cellular response. Inactivation of cAMP is effected by the enzyme phosphodiesterase. Adapted - Berridge (1985).

Cyclic AMP and cyclic cGMP are two second messengers associated with bone remodelling. Traditionally, the second messenger which is associated with mechanical force transduction is cAMP. Rodan *et al*., (1975a) and Davidovitch and Sanfield (1975) were the first to report on the involvement of the cAMP pathway in mechanical signal transduction. During orthodontic force application, the cells of immune and nervous system produce signal molecules that bind to the receptors on cell membrane, leads to enzymatic conversion of cytoplasmic ATP and GTP into cyclic AMP and cyclic GMP respectively. Davidovitch and Sanfield tested a cat subjected to orthodontic force for its alveolar bone from the compression and tension sites an initial decrease of cAMP levels in the compression site due to necrosis of PDL cells. The levels increased two weeks later due to the bone remodelling activity. A later study by Davidovitch *et al*., (1976) on cellular localization of cAMP

observed the areas of PDL where bone resorption or deposition occurred has higher levels of cAMP-positive cells. The actions of cAMP are mediated through phosphorylation of specific substrates. cGMP, in contrast to the role of cAMP is an intracellular regulator of endocrine and non-endocrine mechanisms (Davidovitch, 1995). The action of cGMP is mediated by cGMP –dependent protein kinases and plays a role in nucleic acid and protein synthesis and secretion of cellular products (Davidovitch, 1995).

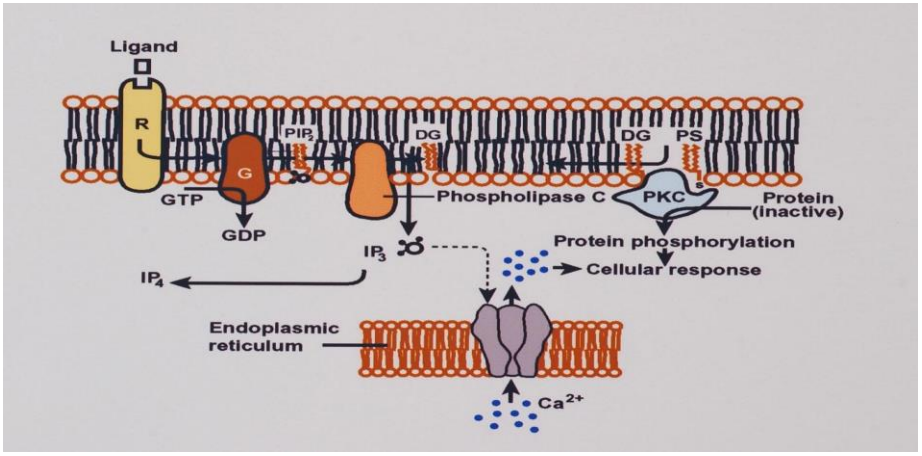

Figure 1.5. The phosphoinositide pathway. External ligands transmit information through a stimulatory G protein (G) to activate phospholipase C which cleaves PIP_2 into diacylglycerol (DG) and inositol triphosphate (IP_3). IP_3 is water soluble and diffuses into the cytoplasm where it mobilizes Ca^{2+} from the ER. DG remains within the cell membrane and activates PKC which then phosphorylates a protein. The continued action of these two second messenger pathways accounts for early and sustained cellular responses. Adapted - Berridge (1985).

The phosphotidyl inositol (PI) signalling pathway was first investigated, by Hokin and Hokin in 1953. However, this mechanism was only better appreciated in the 1980s when Streb *et al*. (1983) demonstrated that the

products of inositol lipid breakdown could cause release of intracellular calcium (Sandy *et al*., 1993). The PI pathway is responsible for the changes seen in mechanically deformed tissues, including the elevation of intracellular calcium and increased DNA synthesis (Meikle, 2006) and the stimulation of PGE production described earlier. PGE_2 and parathyroid hormone (PTH) are physiologic agonists, which stimulate bone resorption and the release of inositol phosphates. The production of cAMP was triggered in murine calvarial osteoblasts when subjected to PGE_2 and parathyroid hormone (Farndale *et al*., 1988). In addition to the release of PGE_2 when subjected to mechanical stress, Sandy *et al*., (1989) reported a dual elevation Camp and inositol phosphates when osteoblasts are mechanically deformed and Yamguchi *et al*. (1994) confirmed this observation in human PDL cells when subjected to tensile strain in a force magnitude-dependent manner.

1.5.3. Cell-matrix interactions

The ECM is a collection of fibrous proteins embedded in a hydrated polysaccharide gel (Kerrigan *et al*., 2000). The tissue mainly contains macromolecules such as collagen and glycosaminoglycans (GAGs), secreted by fibroblasts, osteoblasts and chondroblasts. The extracellular matrix (ECM) provides a physical framework that plays an integral part in signalling cells to proliferate, migrate and differentiate (Holmbeck and Szabova, 2006). Extensive studies have been done on this mechanotransducers transforming mechanical forces into biochemical signals in which role of cell adhesion molecules in has received close attention (Kerrigan *et al*., 2000; Sandy *et al*., 1989; Sandy, 1998).

The ECM molecules involved in this process include collagen, proteoglycans, laminin, and fibronectin. Immunohistochemistry studies on the periodontium have identified proteoglycans components such as versican, decorin, biglycan, syndecan and CD44 (Hakkinen *et al*., 1993). The cell interactions of these adhesive proteins are mediated by the presence of peptide sequence Arg-Gly-Asp (RGD). The mechanical force gets transduced by ECM proteins binding the cell surface receptors (integrins) which in turn induces the reorganization of the cytoskeleton, local synthesis of cytokines, growth factors, leukotrienes, neurotransmitters, colony-stimulating factors and arachidonic acid derivatives.

1.5.4. Integrins

Integrins are a family of heterodimeric transmembrane receptors which mediates the attachment between the ECM and the actin filaments of the cytoskeleton (Sandy, 1998). Cells in culture are 'tack welded' at specialized sites of cell attachment called focal adhesions. Extracellularly, integrins recognize and bind to ECM proteins forming the focal complexes during cell adhesion and migration. Integrins are heterodimeric receptors, composed of structurally different α and β subunits. The integrin properties are classified by their β subunit (Table 1.1). αvβ3 is the major integrin focal complex, which recognizes various ECM proteins via their RGD peptide motifs. After a mechanically stable contact has been made, the activated integrins connect to the actin cytoskeleton mediated by the clustering of adaptor proteins such as talin, vinculin, α-actinin and paxilin. Integrin-mediated cell adhesion regulates intercellular signalling and promotes cell migration, proliferation, apoptosis,

cell polarity and differentiation (Brakebusch and Fassler, 2005; Clark and Brugge, 1995).

Table 1.1. The integrin receptor family. Adapted - Meikle (2002).

Subunits		Ligands	Minimal sequence of binding site
β_1	α_1	Collagens, laminin	
	α_2	Collagens, laminin	DGEA
	α_3	Fibronectin, laminin, collagens	RGD
	α_4	Fibronectin (V25), VCAM-1	EILDV
	α_5	Fibronectin (RGD)	RGD
	α_v	Vitronectin, fibronectin	RGD
β_2	α_X	Fibrinogen	GPRP
β_3	α_v	Fibrinogen, fibronectin, vitronectin, thrombospondin	RGD, KQAGDV
	α_v	Vitronectin, fibrinogen, thrombospondin, fibronectin, osteopontin, collagen	RGD
β_4	α_6	Laminin	
β_5	α_v	Vitronectin	RGD
β_6	α_v	Fibronectin	RGD
β_7	α_4	Fibronectin	EILDV

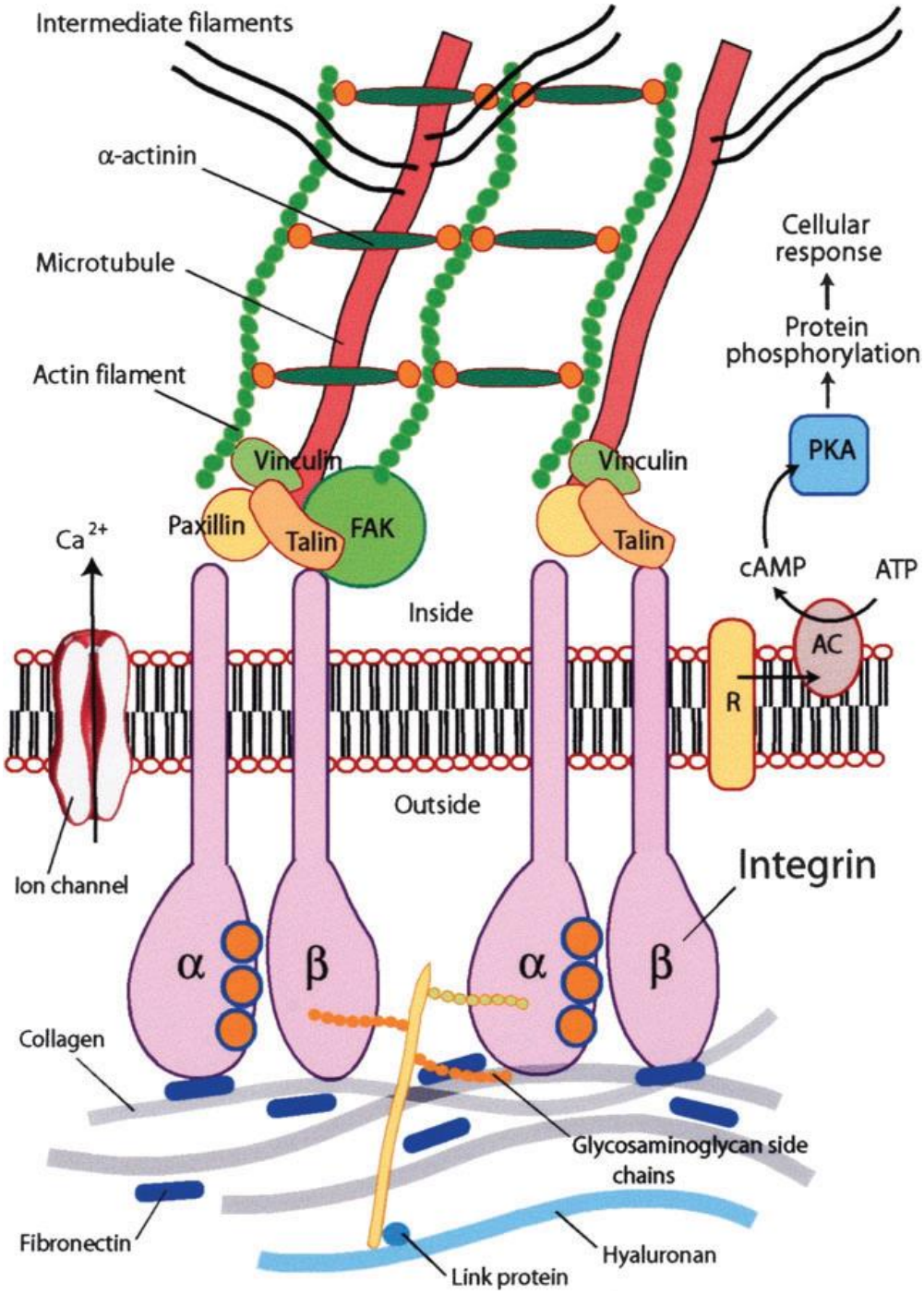

Figure 1.6. Diagram of integrin receptor. Integrins are composed of α and β subunits that combine to produce heterodimeric receptors which can bind proteins in the ECM and regulate intracellular signal transduction pathways. Adapted - Meikle, (2006).

In response to the mechanical stimuli, a multitude of intracellular signalling pathways can be induced. Integrins mediate signals that are involved in regulating the activities of the cytoplasmic tyrosine kinases (MAP kinases), serine/threonine kinases, ion channels and the control of the organization of the intracellular actin cytoskeleton. Activation of calcium-dependent signalling and increases in intracellular calcium through mechanosensitive ion channels, stimulation of nuclear factor kappa-B, changes in Rab Rho family have also been reported previously for mechanoreceptive studies. Meyer *et al*. (2000) conducted a study to establish whether cells sense mechanical signals through generalized membrane distortion or through specific transmembrane receptors, such as integrins. It was found that the mechanical stress applied to the cell surface altered the cyclic AMP signalling cascade and downstream gene transcription by activated integrins receptors in a G-protein dependent manner. Integrins, in association with the cytoskeleton intracellularly is seen to partly regulate gene expression (Hynes, 1992; Ingber, 1991).

RT-PCR quantification done on PDL cells exposed to tensile strain showed an induction in the expression of the mRNAs encoding α6 and β1. These receptors can transduce signals from the matrix to the intracellular environment or effectors in the cytoplasm can affect the affinity of the integrins for the ECM ligands.

1.5.5. Cytokines

Cytokines are extracellular, low molecular weight (mw < 25 kDa) signalling proteins that are produced in low concentrations acting on target cells in a

paracrine (acting on adjacent cells) or autocrine (acting on the cell of origin) manner. Cytokines evokes synthesis and secretion of substances such as prostaglandins, growth factors and cytokines by their target cells, in the presence of other systemic and local signal molecules. This induces cellular proliferation and differentiation facilitating the distortion of extracellular matrix of the periodontium to remodel the paradental tissues. The definition thus includes the interleukins (IL), tumor necrosis factors (TNFs), interferons (IFN), growth factors (GF) and colony stimulating factors (CSF).The complexity in understanding the cytokine biology is their sheer numbers and redundancy and pleiotropy of the signalling molecules (Meikle, 2006). The action of cytokines can be divided into osteogenic and osteolytic in nature.

1.5.5.1. Regulation by Cytokines in bone resorption and bone formation

1.5.5.1.1. Interleukins

The first cytokine shown to stimulate bone resorption was IL-1 (Gowen *et al*., 1983). Interleukins encompass biological activities such as leukocyte endogenous mediator, lymphocyte activating factor, stimulation of fibroblasts, endothelial cells, osteoclasts and osteoblasts. Experiments have reported that IL-1 is the most potent in bone resorption by stimulating osteoclast formation (Lee *et al*., 2006; Kim *et al*., 2009). This was dependent on the presence of osteoblasts as target cells for IL-1, signalling the osteoclasts.

This polypeptide has two isoforms, IL-1α and IL-1β.Many in-vitro and in-vivo studies, demonstrated increased expression of IL-1β during orthodontic tooth movement. This action was reported to have stimulatory effect on PGE

production. Increased levels of IL-1β and PGE2 were found in the gingival cervical fluid during the early phases of tooth movement (Grieve *et al*., 1994; Uematsu *et al*., 1996; Dudic *et al*., 2006). Inducing orthodontic tooth movement in rats have also noted increased levels of IL-1β. Interestingly, the velocity of tooth movement has been seen to be associated with the role of IL-1β gene (Iwasaki *et al*., 2006). A 50 % reduction in tooth velocity was reported after an intra-peritoneal injection of soluble receptors to IL-1 (sIL-R11) and TNF-α (sTNF-αR1). TRAP-positive cells reduced considerably on the surface of bone and roots. Saito *et al*. (1991) provided the first experimental evidence of the role of IL-1β in the periodontal tissues of the cat canine after an application of 80 g tipping force and also noted increased levels of cAMP and PGE2. A down regulation of IL-1 gene was also seen. This was supported in a recent tensile strain study by Pinkerton *et al*. (2008). In another study, PDL cells were subjected to tensile strain which induced the synthesis of IL-1β, IL-6 and inhibited IL-8 (Long *et al*., 2001). de Araujo *et al*. (2007) and Lee *et al*. (2007) measured increased levels of IL-8, PGE2 and IL-6, respectively after compressing human PDL cells. Both the studies support the phenomenon of bone deposition in areas of tension and bone resorption in the areas of compression. IL-2, IL-3 are the other interleukins that stimulate bone resorption, while IL-4, IL-10, 1L-12 and IL-13 inhibits bone resorption. IL-10 inhibits the production of IL-1, IL-6, IL-8, TNF-α and G-CSF (Pretolani, 1999)

Table 1.2. Cytokines involved in tooth movement. Adapted - Krishnan, (2009)

Cytokines (isoforms)	**Functional effect on tooth movement**
Interleukin-1α (IL-1a)	Proliferation and differentiation of cells, ECM remodeling and bone resoprtion
Interleukin-1β (IL-1b)	Promotes bone resorption by stimulating osteoclasts
Interleukin-4 (IL-4)	Inhibits bone resorption and increases OPG
Interleukin-6 (IL-6)	Inhibits bone formation, stimulates osteoclasts and ECM remodelling
Interleukin-8 (IL-8)	Expressed in PDL tension site, stimulates osteoclasts, bone formation
Interleukins 10,12 (IL-10,12)	Inhibits bone resorption
Interleukin-13 (IL-13)	Increases OPG and inhibits bone resorption
Tumour necrosis factor-alpha (TNF-α)	Stimulates bone resorption and osteoclasts, ECM remodelling
Osteoprotegerin (OPG)	Inhibits bone resorption by inhibiting osteoclast differentiation
Osteoprotegerin ligand (OPGL)	Osteoclasts formation. Identical to Receptor activator of nuclear factor kappa B ligand (RANKL)

1.5.5.1.2. Tumor necrosis factor (TNF) and the RANK/RANKL/OPG system

Tumor necrosis factor-alpha (TNF-α) is another pro-inflammatory cytokine shown to stimulate bone resorption. Increased expression levels of TNF-α was always noted along with the IL-1 in the studies done with gingival cervical fluid as mentioned before (Grieve *et al*., 1994; Uematsu *et al*., 1996; Alhashimi *et al*., 2001). In the presence of M-CSF, TNF can stimulate the differentiation of osteoclast progenitors to osteoclasts (Pérez-Sayáns *et al*., 2010).

Osteoprotegerin (OPG), also called osteoclastogenesis inhibitory factor was first identified (OCIF) as the member of tumor necrosis factor receptor superfamily during a fetal rat intestine cDNA-sequencing project (Simonet *et al*., 1997). It helps in inhibiting osteoclast differentiation during its terminal stages and suppresses activation of matrix osteoclasts thereby protecting the bone. OPG is not a bone specific protein as it is seen to be expressed in many tissues apart from osteoblasts, including heart, kidney, liver, spleen and bone marrow.

Bone remodelling is a balanced interplay of the receptor activator of nuclear factor kappa (RANK), OPG and its decoy receptor -the receptor activator of nuclear factor kappa B ligand (RANKL) (Khosla, 2001; Yamaguchi, 2009; Ogasawara *et al*., 2004; Pérez-Sayáns *et al*., 2010;). RANK was first discovered by Anderson *et al*. (1997) while sequencing cDNAs from a dendritic cell library. Two research teams isolated and cloned RANKL simultaneously (Lacey *et al*., 1998; Yasuda *et al*., 1998) and termed it as Osteoprotegerin Ligand. To reduce the confusion and redundancy by the proliferation of synonyms for the three new TNF ligand/receptor systems in the literature, the Nomenclature Committee of the ASBMR (American Society for Bone and Mineral Research) recommended the usage of RANK for the receptor and RANKL for the ligand.

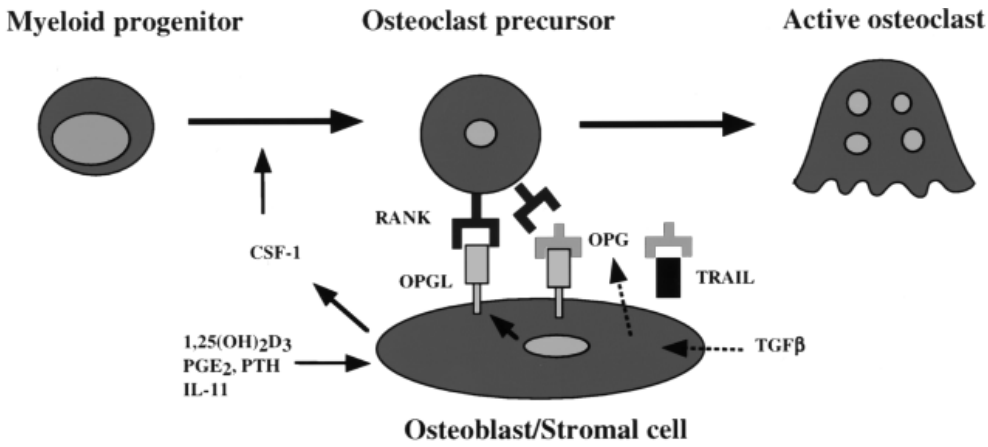

Figure 1.7. Proposed roles for RANK, OPGL and OPG system in osteoclastogenesis. Adapted - Meikle, (2002).

RANKL is expressed on the osteoblast cell lineage which binds to RANK, expressed on the osteoclast lineage cells leading to differentiation of haematopoietic osteoclast precursors to mature osteoblasts. The level of RANKL expressions in PDL cells after mechanical loading were investigated by a number of studies. Increase of RANKL and decrease in OPG secretion were reported after human PDL cells were exposed to compressive force *in vitro* (Kanzaki *et al*., 2002) in a time and force-magnitude dependent manner (Nishijima *et al*., 2006). Nakao *et al*. (2007) has reported an increase in expression of RANKL levels when the cells were compressed for 8 or 24 h/day for 2-4 days. Addition of IL-1 receptor to the culture medium had inhibited the increase in RANKL levels. (Yamaguchi *et al*., 2006) found an increase in RANKL and decrease in OPG in the human PDL cells removed from the teeth that experienced root resorption during an orthodontic tooth movement. The maxillary molars were moved laterally for 1-7 days in 55-day old rats and immunohistochemistry done after one day treatment on these compressed PDL cells showed a positive staining for RANKL, suggesting its

role in bone resorption. Another interesting finding is the gene transfer experiment by Kanzaki and co-workers (2004) where an OPG plasmid in an envelope of an inactivated virus, was injected into the periodontium of rat molars, which resulted in the inhibition of osteoclastogenesis, reducing the tooth movement. In contrast, the RANKL gene transfer in rats, stimulated osteoclastogenesis and accelerated tooth movement (Kanzaki *et al*., 2006).

1.5.6. Growth factors

The transforming growth factor- beta (TGF-β) family is the group of abundant growth factors seen to be associated with the cell growth, differentiation, apoptosis, bone formation and remodelling. The family consist of three isoforms: TGF-β1, TGF-β2, TGF-β3 and Bone Morphogenetic proteins (BMPs) (Katagiri and Takahashi, 2002). Cat PDL cells and alveolar bone were stained for the presence of TGF-β after orthodontic tooth movement, showing an increase in TGF-β while the control PDL cells showed no staining for TGF-β (Davidovitch, 1995). TGF-β encourages bone formation through the attraction of osteoblasts by chemotaxis, enhancement of osteoblasts proliferation and differentiation, as well as the production of type II collagen and proteoglycans by chondrocytes (Janssens *et al*., 2005). In addition, TGF-β inhibits bone resorption by suppressing osteoclast formation and activation (Bonewald and Mundy, 1990). It reduces the differentiation of B- and T-cell lineages *in vitro*, and negates the effects of pro-inflammatory cytokines such as IL-1 and the expression of IL-1 receptors (Wahl, 1992) and it has been suggested that TGF-β acts as a 'bone-coupling factor linking bone resorption to bone formation' (Bonewald and Mundy, 1990).

Fibroblast growth factors (FGF) are aother group of important growth factors in bone formation. The two main forms of FGFs have been identified as acidic FGF and basic FGF, both of which can be found in bone matrix (Hauschka *et al*., 1986) and the latter form is commonly involved in bone remodelling activities. Basic FGF (FGF-2) was noted for its involvement in bone resorption, by the stimulation of osteoclasts formation when the murine bone marrow cultures were exposed to FGF-2 (Hurley *et al*., 1998). Nakajima *et al*. (2008) evaluated the effect of compression force on the production of FGF-2 and RANKL and found that the compression significantly increased the secretion of FGF-2 in a time- and magnitude-dependent manner.

Insulin-like growth factors (IGF-I and-II) involves in cellular differentiation, proliferation, morphogenesis. These actions of these growth factors are regulated by factors like PTH, vitamin D3, TGF-β, IL-1 and PDGF. To investigate their roles in tooth movement, the first molar of rat maxillae was moved by means of an orthodontic appliance. In the immunostaining pattern of the periodontal ligament, increased immunostaining was seen for all components on the pressure sides and resorption lacunae, suggesting its involvement in resorption processes (Gotz *et al*., 2006).

Vascular endothelial growth factors (VEGFs), originally isolated from bovine pituitary folliculo-stellate cells (Leung *et al*., 1989) are recognized to involve in bone resorption during orthodontic tooth movement by its effect on osteoclasts differentiation. Injection of recombinant human VEGF during experimental tooth movement stimulated osteoclasts differentiation (Kaku *et*

al., 2001). Yao *et al*. (2006) reported an increase in RANK gene expression but not osteoclastogenesis. When coupled with colony-stimulating factor-1 (M-CSF), the proliferation of osteoclasts can be enhanced (Niida *et al*., 1999).

1.5.7. Extracellular Matrix degradation

Remodelling of the ECM plays a vital role in orthodontic tooth movement with forces exerted on tooth and transmitted to surrounding tissues of the periodontium. To achieve this, breakdown of collagen fibres and removal of other macromolecules take place. Several proteolytic enzymes are involved in this breakdown of extracellular matrix. They are grouped into four major classes as metalloproteinases, serine proteinases, cysteine proteinases and aspartate proteinases (Waddington and Embery, 2001). Although enzymes from each of these classes are involved in resorptive cascade, cysteine proteinases and particularly matrix metalloproteinases (MMPs) or matrixins are recognized to play important role in remodelling the extracellular matrix during cell migration (Schnaper *et al*., 1993; Fisher *et al*., 1994;).

Table 1.3. Classes and properties of major groups of matrix metalloproteinases. Adapted - Meikle, (2002).

	MMP number	**MW (latent; kDa)**	**MW (active; kDa)**	**Matrix substrates of group**
Collagenases	MMP-1	55	45	Collagen types I, II, III, VII, VIII, X, aggrecan, tenasin
	MMP-8	75	58	Collagen types I,II, III, VII, X, aggrecan
	MMP-13	65		Proteoglycan core protein, type II collagens
Gelatinases	MMP-2	72	66	Specific locus in type IV collagen, gelatin, vironectin, fibronectin, elastin, laminin, aggrecan
	MMP-9	92	86	Types V, VII, X, XI collagens, Elastin
Stromelysins	MMP-3	57	45	Proteoglycan core protein, non-helical regions of type IV collagen
	MMP-10	57	44	Types I, IV, X, XI collagen, laminin
	MMP-11	51		Elastin, fibronectin, gelatins, procollagens I, II, III

1.5.7.1 Matrix metalloproteinases and their inhibitors

MMPs are endopeptidases that are excreted by connective tissues and pro-inflammatory cells such as fibroblasts, osteoblasts, endothelial cells, macrophages, neutrophils and lymphocytes (Verma and Hansch, 2007). MMPs are mostly expressed as inactive zymogens and are activated by proteinase cleavage (DeCarlo *et al*., 1997; Syggelos *et al*., 2013). During normal physiological conditions, the proteolytic activity of MMPs are

controlled by transcription, activating the zymogens and inhibiting the active forms by tissue inhibitors of MMPs (TIMPs).In contrast, this equilibrium shifts to the MMPs activity during pathological conditions. MMPs can digest any molecule in the extracellular matrix. Based on their ability to degrade the matrix proteins, 22 different homologues have been characterized and grouped into collagenases, gelatinases, stromelysins, matrilysins, metalloelastase and membrane type MMPs.

Collagenases MMP-1 (Fibroblast collagenase), MMP-8 (Neutrophil collagenase), MMP-13 (collagenase-3) cleave interstitial collagens I, II and III at a specific site 3 /4 from the N terminus. Collagenases can also digest other ECM and non ECM molecules. Gelatinases MMP-2 (Gelatinase A), MMP-9 (Gelatinase B) readily digest denatured collagens and gelatins with the help of their type II fibronectin domain that binds to gelatin, collagens and laminin.MMP-2, but not MMP-9 digests collagens I, II, III similar to the collagenases. Stromelysins are similar to collagenases in domain arrangement but functions in digesting ECM molecules and activating the proMMPs. MMP-3 (Stromelysin I), MMP-10 (Stromelysin II) and MMP-11 (Stromelysin III) belong to this group.MT-MMPs are displayed on the surface of cells and are capable of activating proMMP-2. MT-MMPs can efficiently degrade a number of matrix macromolecules including denatured collagen and aggrecan, the principle proteoglycans in cartilage (Meikle, 2002).

MMPs are counteracted by the tissue inhibitors of matrixmetalloproteinases, thereby restricts the ECM breakdown. All the four homologs of TIMPs

(TIMP-1,-2,-3,-4) can bind to the activated form of MMPs and inhibit its proteolytic activity. On the other hand, TIMPs can also bind to the latent forms of MMPs and inhibit their activations. The expression of MMPs and TIMPs by cells is regulated by many cytokines, particularly IL-1 and growth factors. Expression levels of MMP-8, MMP-13 mRNA transiently increased during the orthodontic tooth movement study *in vivo* by Takahashi *et al*. (2003). The same author did an *in vivo* study of orthodontic tooth movement in rats and reported a transient increase in the mRNA expression levels of MMP-2, MMP-9 and TIMPs-1, -2, -3 PDL cells on the compression side including cementoblasts, fibroblasts, osteoblasts and osteoclasts on tension side the increases were mainly limited to osteoblasts and cementoblasts. This altered gene expression pattern is associated with determination of the rate and extent of remodelling the collagenous ECM in periodontal tissues during orthodontic tooth movement (Takahashi *et al*., 2003, 2006). The MMP-8 is associated with the pathophysiological PDL remodelling during tooth eruption and MMP-13 was seen to be associated with osteoblasts and osteocytes in alveolar bone (Tsubota *et al*., 2002). Thereby, the delicate interplay of MMPs and TIMPs is important in during tooth movement and the integrity of healthy tissues is maintained by the balance between MMPs and TIMPs.

1.6. Methods of mechanical cell stimulation

Systematic *in vitro* cell culture models have been developed for better understanding of the cellular response to mechanical stimuli of the complex *in vivo* environment. These are laboratory based systems with a controlled

delivery of strain regimens to cell cultures at differing levels of accuracy and homogeneity.

The early mechanostimulus systems provided strain of non-quantitative nature. Glücksmann (1939) initially studied compressive force on endosteal cells cultures grown unexplanted intercostals muscle to which pairs of neighbouring ribs were attached applied tensile loads on hanging drop cultures by utilizing the force of surface tension. With advances in technology, several models were designed so the strain applied could be quantified (Rodan *et al*., 1975a; Rodan *et al*., 1975b).

1.6.1. Tensile loading systems

The early static loading systems were first developed by Harell *et al*.,Harell *et al*. (1977) and Meikle *et al*. (1979) to study the effect of continuous mechanical strain on fibrous joints. Cranial sutures from new born rabbits were attached to split circular mounts and a force of 20-30 g applied using a stainless steel open spring. Somjen *et al*. (1980) stimulated a tensile load on rat embryo calvarial cells cultured on a plastic dish was a orthodontic expansion screw was bonded to the base.

Longitudinal stretch systems provide controlled uniaxial force to deformable substrates (Fig 1.8a). These systems have been refined to provide control over the magnitude and timing of the tensile mechanical stimulus applied to cell culture. The substrates used varied from rectangular elastin (Leung *et al*., 1977), rectangular strips of polyetherurethane urea (Ives *et al*., 1986), silastic

membranes (Vandenburgh and Karlisch, 1989), Silicone membranes (Neidlinger-Wilke *et al*., 1994; Carano and Siciliani, 1996), to which motor driven force was stimulated. Later Xu *et al*. (1996) imposed 5% cyclic uniaxial strain on cultured rat fetal lung cells within Gelfoam® rectangular sponges and Mitton *et al*. (1997) performed a 10% static strain on rectangular silicon substrates. Four point bending system was introduced as an alternative (Fig 1.8b), to deliver low strain levels in range encountered by bone *in vivo.* However, due to poisson effect, it involves compressive strain perpendicular to the direction of tension; both the systems do not stimulate a homogenous strain pattern across the cells. Despite this inability, longitudinal stretch systems are still widely used in tensile experiments (Wang *et al*., 2011).

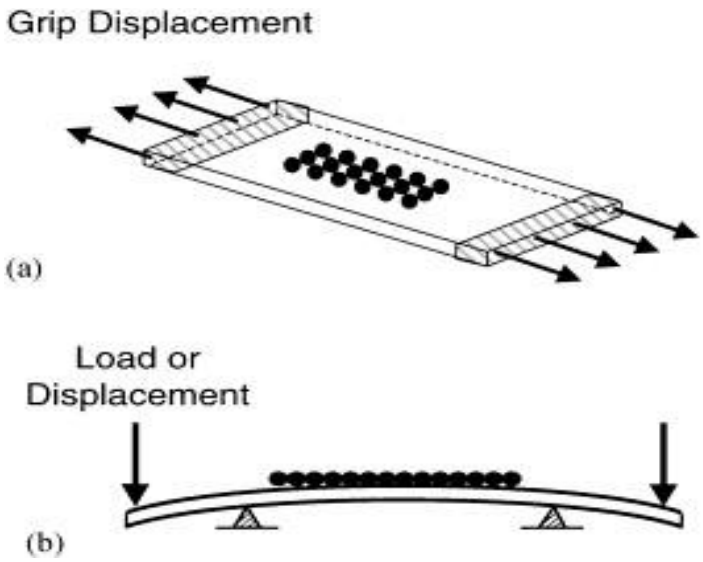

Figure 1.8. Techniques to achieve longitudinal substrate stretch. (a) Uniaxial tension. (b) Flexure by so-called four-point bending. Adapted - Brown, (2000).

The next broad class of mechanostimulatory systems is called the out-of plane substrate distension. The device was first reported by Hasegawa *et al*. (1985). Rat calvarial bone cell cultures were cultured on a flexible membrane in a culture dish and a static weight was placed to press the membrane on a convex surface. It was reported that the cells on the periphery of curved surfaces were less strained than the ones in the middle. Several other platen-driven systems were later developed by many researchers. In 1985, Banes *et al*., designed the flexible-bottomed circular cell culture plates, interfaced with vacuum manifold system. The set up was controlled by a computer to alter and maintain the vacuum magnitude, frequency and duty cycle. The vacuum from the bottom stretched the substrate downward providing the tensile strain to the culture layer. The whole unit was commercialized under the name Flexercell®. The system was characterized for stimulus studies and strain measurement on substrates (Pedersen *et al*., 1993; Gilbert *et al*., 1994). A homogenous radial tensile strain was found across a thin circular membrane, but not for a thick circular membrane.

Flexercell® system followed the in-plane substrate distension to overcome the above difficulty. This was done by retrofitting with an immobile flat circular platen (Fig.1.9a). Vacuum was applied around this platen giving a tensile strain across the substrate membrane. Biaxial strain can be applied using the circular shaped loading post or uniaxial strain for oblong-shaped loading post (Arctangle™ Loading Station™) designed for a homogenous strain field. Finite Element Analysis was performed on this unit by several researchers. Four different vacuum pressures (20kPa, 40kPa, 60kPa and 80kPa) were analysed

on the strain field within the Flexercell™ membranes by Vande Geest *et al*. (2004). The strain field was quantified for both uniaxial and biaxial loading posts. The validation experiment showed that the magnitude of loading strain was constant at the centre and reduced at the edges of the loading post. Matheson *et al*. (2006) also characterized the Flexcell™ Uniflex system by applying 10% longitudinal sinusoidal strain (0.25Hz) for 48 hours to U937 macrophage-like cells. It was observed that 10% strain was highly reproducible and relatively uniform (10.6%±0.2%) in the central rectangular membrane after an image analysis.

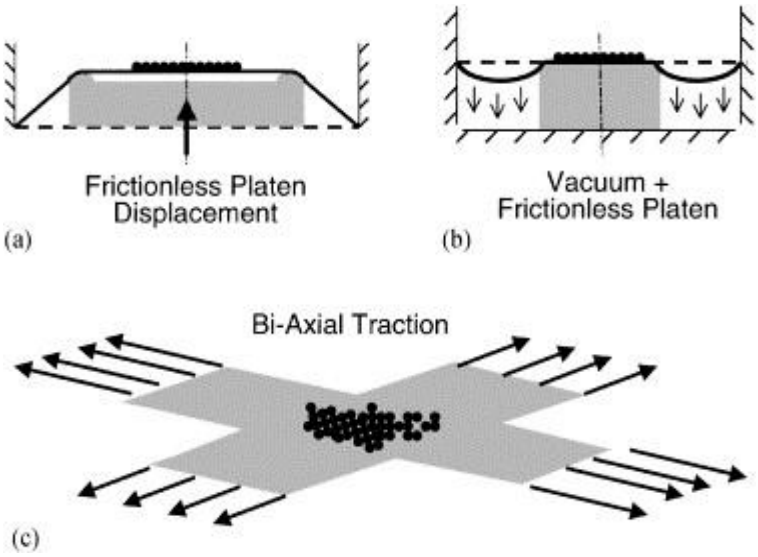

Figure 1.9. Methods to achieve in-plane substrate distension. (a) Concurrent radial and circumferential strain input by motion of a frictionless platen. (b) Retro-fit of the Flexercell system, achieving radial and circumferential substrate strains by means of a fixed central stage. (c) Bi-directional substrate traction. Adapted - Brown, (2000).

Further validation upon the magnitude of the strain experienced by the substrate compared to the cells exposed was done by Wall *et al*. (2007). They

found that, on average, cellular strain was 63±11% of the applied uniaxial strain and largest strain values for the cells oriented parallel to the direction of applied uniaxial strain. Also, strain magnitudes within each cell were heterogeneous.

The variance in strain magnitude within or between cells may be due to the cell adhesion connection between the cell and substrate. Normally, strain is imparted to the cell via focal adhesion between the substrate and cytoskeleton via integrins. Loss of this connection from the deformable substrate can result in the alteration of the imparted strain to the cells. Cyclic uniaxial strains align the cells perpendicular to the axis of the strain after which the cells perceive different mechanical inputs compared to their initial orientation (Syedain *et al*., 2008). In cases of equibiaxial strain, major strain axis is lacked and hence cell alignment does not occur. Although, a proper morphological verification on cells exposed to the strains has become an essential study for these types of experiments.

1.6.2. Compressive loading systems

Two types of compressive loading systems are utilized in the mechanical stimulation of cell and tissue culture *in vitro*, namely hydrostatic pressurization and direct platen abutment. Hydrostatic pressurization (Fig.1.10a) is mostly used for cell, tissue compression studies due to its simplicity of the equipment, spatial homogeneity of the stimulus, ease of configuring multiple loading replicates, and ease of delivering and transducing either static or transient loading inputs (Brown, 2000). Negative and positive

pressure loading can also be performed (Yousefian *et al*., 1995). Unlike direct platen abutment loading, there is no issue concerning pre-loading the specimen and interference of metabolite transport processes between the cell culture and the nutrient medium. In addition, the adhesion of the cell culture and the substrate does not affect the hydrostatic compression loading. However, there are limitations of the hydrostatic pressurization system. The use of high hydrostatic pressure will increase the level of high pO2 and pCO2 in the nutrient medium which require compensatory treatment steps (Ozawa *et al*., 1990) and it is difficult to duplicate the *in vivo* stress conditions with *in vitro* hydrostatic loading even though a dilatational component can be identified for an loading regimen (Brown, 2000).

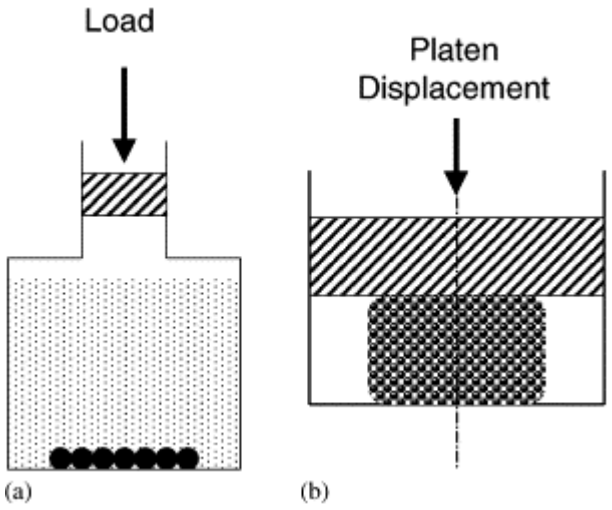

Figure 1.10. Common methods for compressive loading. (a) Hydrostatic pressure. Embodiments have included systems both with (as shown here) and without an incubator gas phase pressurized atop the liquid nutrient medium. (b) Platen abutment. Adapted - Brown, (2000).

Direct platen abutment (Fig.1.10b) is a commonly used method for studying solid specimens, such as cartilage, bone or biomimetic scaffolds. The use of

abutment requires either a tissue explant or cells embedded in matrix. Early compression studies mainly involved cartilage explants which involved flat ended porous platen and manual application of dead weights (Burton-Wurster *et al*., 1993; Torzilli *et al*., 1997). Guilak *et al*. (1994) performed multi-hour experiments with three orders of magnitude (0.001-1.0Pa) controlled by a motorized micrometer and high-sensitivity load cell. In 1994, Freeman *et al*., performed a study on chondrocyte metabolism. Chondrocytes isolated and embedded in 2% agarose gel and exposed to 5, 10 and 15% of strain. The team devised a microscope stage-mounted compression system for the study.

Kanai *et al.* (1992) developed compression loading system where a cell disk was placed over nearly confluent cell layers and compression force was controlled by inserting lead granules in the cylinder. The force was controlled by adjusting the number of lead granules. This method was used in many other studies to look at the response of PDL cells to compressive loading. Kanzaki *et al*., (2002) compressed PDL cells with 0.5, 1.0, 2.0 or 3.0 g/cm^2 for 0.5, 1.5, 6, 24 or 48 h to study the induction of osteoclastogenesis by RANKL in PDL cells. At 4 g/cm^2, PDL cells were partially damaged. Yamaguchi *et al*. (2004) subjected the PDL cells to 0.5, 1.0, 2.0 or 3.0 g/cm^2 of compressive force for 24 hours to investigate the role of Cathepsins B and L. Lee *et al.* (2007) and Araujo *et al.* (2007) modified the technique and incorporated the cells in a type I collagen gel matrix to study the effect of mechanical stress on PDL cells. A new high-thorough put technique capable of simultaneously applying compressive forces to cells encapsulated in an array of micropatterned biomaterials has been developed by Moraes *et al*. (2010). The

first study was on mouse mesenchymal stem cells encapsulated within poly(ethylene glycol) hydrogels were subjected to 6% to 26% of compressive force simultaneously.

The latest Flexercell™ compression system applies intermittent compressive force to cells encapsulated in a hydrogel matrix (Fig.1.11). For this set up, a positive air pressure is generated, which compresses the gel against the surface of the platen.

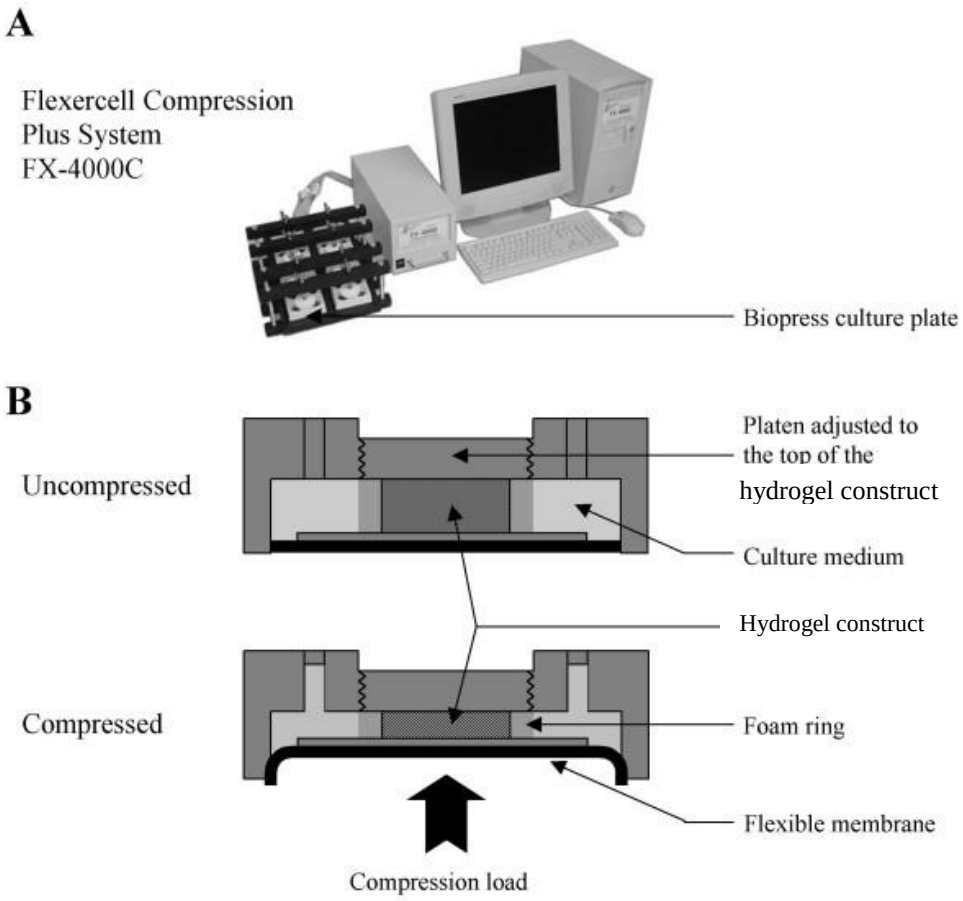

Figure 1.11. Compression system**.** A) FX-4000C™ Flexercell® Compression Plus™ System (Flexcell International). A positive pressure compresses samples between a piston and stationary platen on the BioPress™ culture. B) Schematic diagram of the BioPress™ culture plate compression chamber in uncompressed or compressed position. Adapted -Bougault, (2008).

1.7. Cell Culture systems

The development and remodelling of bone in part depends upon the mechanical signals in its growth environment. In the last several decades, importance has been given to understand the scope of mechanobiological effects on cells in integrin-mediated signalling pathways, mechanics of the cell and cytoskeletal components. This has been done by studying the cell adhesive interaction with their microenvironment which is required for the cell differentiation, proliferation and migration.

Traditional 2-dimensional (2D) experiments continue to provide valuable insights of the dynamic relationship between cell function and interactions with the cellular microenvironment, cytoskeletal mechanics. 2D surfaces such as tissue culture flasks, Petri dishes, micro-well plates have been used for such cell culture studies due to its ease, convenience and high cell viability of 2D culture. The differentiation of human mesenchymal stem cells was reported to be dependent on the stiffness of the 2D substrate (Engler *et al*., 2006, 2007).

Natural ECM is a complex meshwork of collagen and elastic fibres surrounded in an environment of glycosaminoglycans, proteoglycans and glycoproteins (Lee *et al*., 2008; Wiltz *et al*., 2013). In addition to the biophysical and biochemical functions, the cellular microenvironment contributes to complex signalling domain that directs cell phenotype. Cell interactions with ECM showed its phenotype can overtake the genotype. Hence, a solitary entity of a genome is evaluated in the context of ECM, soluble growth factors and other molecules (Tibbitt and Anseth, 2009). Cell

migration, differentiation and morphologies of 2D culture cells behaves unnaturally in contrast to the more complex forms observed *in vivo*, as the cells are forced to adjust on an artificial flat, rigid surface, which lacks the unique ECM environment of each cell type. This may be due to the homogenous concentration of nutrients, growth factors and cytokines present in bulk media contacts only a section of the membrane. Migration of cells in 2D environment is another restricted to a plane phenomenon compared to a normal migration in a surrounding ECM (Pedersen and Swartz, 2005). Hence, a proper 3D model microenvironment is vital for a better understanding the studies on cell mechanobiology.

Three dimensional cell culture matrices were introduced as a mimic of the ECM and also to overcome the limitations of 2D culture systems (Pedersen and Swartz, 2005; Lee *et al*., 2008; Tibbitt and Anseth, 2009; Kang *et al*., 2013). To date, cells have been encapsulated within microporous (Levenberg *et al*., 2003; Cai *et al*., 2012; Mazzitelli *et al*., 2013), nanofibrous (Silva *et al*., 2004; Zhong *et al*., 2013) and hydrogel scaffolds (Musah *et al*., 2012; Grevesse *et al*., 2013) for mechanotransduction studies. Microporous scaffolds effectively serves as 2D scaffolds due to their large porous nature (approximately 100 μm). Nanofibrous scaffolds, closely mimics the architecture formed by fibrillar ECM proteins (Tibbitt and Anseth, 2009). However, they are too weak to handle the stress needed for proper mechanotransduction. Hydrogels do not have these limitations, making them widely used in mechanobiological studies. Hydrogels are reticulated structures of crosslinked polymer chains that can be formed from an array of natural and

synthetic materials (Prestwich, 2011). These are highly attractive material to develop synthetic ECM analogs due to its varied mechanical and chemical properties, facile transport of oxygen, nutrients and waste. They can be formed under mild, cytocompatible conditions, can be easily modified to possess cell adhesion ligands, viscoelasticity and degradability.

Natural gels-scaffolds from natural sources for cell culture are complex to use due to risk of contaminations, batch-batch variability that can confound cell proliferation, differentiation and migration. The naturally derived polymers include agarose, alginate, chitosan, collagen, gibrin and hyaluronic acid (Drury and Mooney, 2003). Hydrogels formed from non-natural molecules have been used and reported in many studies. The molecules such as Poly (ethylene glycol) (Sawhney *et al*., 1993), poly (vinyl alcohol) (Martens and Anseth, 2000), poly(2-hydroxy ethyly methacrylate) (Chirila *et al*., 1993), These hydrogels have been shown to maintain cell viability and allows the deposition of ECM as they degrade. Hence these synthetic gels can function as 3D cell culture systems. Although, they are inert gels, without integrins-binding ligands and therefore lack the endogenous factors required for cell behaviour (Cushing and Anseth, 2007). The cross linking of the polymeric chains can be initiated using physical stimuli such as changes in temperature, pH, ionic environment and shear stress, or by chemical means via that of cross-linking agent, enzymatic reaction or exposure to light (photopolymerization) (Fedorovich *et al*., 2007). Other than providing a three dimensional structure for the organization and differentiation of cells in tissue engineering, hydrogels are also used as space filling agents which provide

bulking and act as biological adhesives or anti-adhesives. They can also act as delivery vehicles for bioactive molecules such as VEGFs or be used to encapsulate secretory cells which release biological mediators (Drury and Mooney, 2003).

Hyaluronan is a non-sulphated GAG which forms the major constituent of the ECM. It is biocompatible and biodegradable and functions in organizing the ECM, regulates cell adhesion, proliferation and differentiation. The present study utilizes HA-derived hydrogel (Prestwich, 2011) which is semi-synthetic in nature, composed of thiol-modified hyaluronic acid (Glycosil™) and gelatin (Gelin-S™) that are co-crosslinked with polyethylene glycol diacrylate (Extralink™).Hydrogel serves to encapsulate the cells in a three-dimensional structure to facilitate the application of mechanical strain with Flexercell® machine.

2. The effect of mechanical strain on PDL cells in two-dimensional culture system

2.1 Introduction

The periodontal ligament functions in a mechanically active and undergoes tension and compression when subjected to excessive occlusal loading, not only during mastication, deglutition and speech, but also due to occlusal trauma and man-made orthodontic appliances. PDL cells have been widely investigated using various techniques to study the effects of both tensile and compressive strain (see literature review) *in vitro* and most have focussed on the expression of cytokine and osteogenic genes (Yamaguchi *et al*., 1994; Tsuji *et al*., 2004; Yang *et al*., 2006 Wescott *et al*., 2007; Yamashiro *et al*., 2007; Pinkerton *et al*., 2008; Tang *et al*., 2012; Xie *et al*., 2012). Remodelling changes involve a complex interplay of cell-cell and cell-matrix interactions and applied mechanical forces are transduced from the strained ECM to the cytoskeleton through cell surface proteins. Adhesion of the ECM to cell surface receptors can induce reorganization of the cytoskeleton, secretion of stored cytokines, ribosomal activation, and gene transcription (Sandy, 1998; Kerrigan *et al.,* 2000), and the role of cell adhesion molecules in the transformation of mechanical forces into biochemical signals has been widely studied (Sandy *et al*., 1989; Sandy, 1998; Kerrigan *et al.*, 2000).

All cells have a finite life span, and apoptosis, a form of programmed cell death in which cells are induced to activate their own death or suicide, plays an important role in many pathophysiologcal processes, including tissue

remodelling and homeostasis (Wyllie *et al.*, 1980; Elmore, 2007). However, cultured bone and PDL cells deprived of the normal functional loading to which they are exposed *in vivo* are in a physiological default state, raising the question of what effect mechanical stimuli might have on apoptosis-mediated cell death. The *in vitro* evidence to date is equivocal. Although complicated by the use of different model systems and strain regimens, unlike cultured bone cells, where mechanical stimuli have typically been shown to inhibit apoptosis (Bakker *et al*., 2004; Aguirre *et al*., 2006), cyclic mechanical strain has been reported to trigger a transient increase in apoptosis in cultured human PDL cells (Zhong *et al*., 2008; Hao *et al*., 2009). This is important because any reductions in metabolic activity may compromise quantification of alterations in gene expression.

In the present investigation, human PDL cells in two-dimensional culture were screened for adhesion-related genes using targeted real-time RT-PCR microarrays, and we report, for the first time, the effect that a predominantly tensile cyclic mechanical strain has on their expression. We further show that the immediate response of the cells to a change in their biophysical environment was a short-term reduction in overall cellular activity, including the expression of two apoptosis executioner caspases (Saminathan *et al.*, 2012).

The RNA extraction was carried out by our collaborators from the Department of Oral Sciences, Faculty of Dentistry, University of Otago, Dunedin and the real-time RT-PCR microarrays by SAB Biosciences. Kindly refer the published work of this study attached in the appendix section (Appendix 1).

2.2 Materials and methods

2.2.1 Isolation and culture of periodontal ligament cells

Approval for the use of human PDL cells was granted by the National University of Singapore Institutional Review Board (Reference: OSHE/RA/03/04/FOMo-28). All the teeth used in the study were healthy, pathology-free premolars extracted for orthodontic purposes. They were obtained following informed consent with permission from the donor/ guardian. Human PDL cells were prepared from extracted premolars using the method described by Somerman *et al*. (1988).

Subgingival scaling and chlorhexidine were first carried out to remove visible plaque and calculus to reduce the source of contamination during culture. A sulcular incision and gingival curettage were made under local anaesthesia to minimize gingival attachment before extraction by simple forceps delivery. The teeth were placed in 50 mL Falcon tubes containing 20 mL of pre-incubated culture medium and transported to the laboratory. Teeth were washed with culture medium to remove excess blood and adherent PDL tissue removed from the middle third of the root with a scalpel. All procedures were carried out in laminar flow hood under aseptic conditions. Tissue explants were plated onto 35mm Petri-dishes covered with drops of culture media and then placed in a carbon dioxide incubator in a humidified atmosphere of 5% CO_2 and 95% air at 37^{o}C. The explants were checked for attachment at 48 hours before additional culture media was added to cover the surface of the Petri dish completely. The culture media consisted of Dulbecco's modification of Eagle's medium (DMEM; GIBCO, Invitrogen), 10% fetal calf serum

(GIBCO), antibiotic-antimycotic reagent (10,000 units, penicillin, 10,000 µg streptomycin and 25 µg/mL amphotericin B), 200 mM L-glutamine (Invitrogen) and Gentamicin reagent solution. Media changes were performed at three to four day intervals, with regular examination of the specimens under light microscopy (Leica, DMI 3000) to assess for outgrowth of cells from the tissue explants. Once the primary explanted cells (P0 cell line) reached confluence, the cells were trypsinized and cultured in a 100mm Petri dish. This first passage of cell was labelled P1. Subsequent passages of cells (P2, P3 and so on) were cultured in 75 cm^2 and 150cm^2 tissue flasks. Until the cells reached confluence, media was changed for every two days. From a 75 cm^2 flask, each passage of cells were expanded by washing with PBS and trypsinizing with 2.5mL of Trypsin/EDTA (Gibco, Invitrogen, Singapore) for 5 minutes in the 37^oC incubator. Once the cells had lifted, they were homogenized with 2.5 mL of media; for a 150 cm^2 flask, the volumes of the reagents added were doubled. The suspension was centrifuged at 1200 rpm (290 x g) for 3 minutes and the pellet re-suspended with 1mL media and transferred to a 150cm^2 flask containing 20 mL of media or three 75 cm^2 flasks each containing 10 mL of media. Flasks were again incubated at 37^oC incubator for subsequent expansion; P3 and P4 cells were used in all experiments and the excess cells were frozen at -80^oC liquid nitrogen for future use.

2.2.2 Storage of periodontal ligament cells

After each passage of cells has reached confluence, the cells were first trypsinized with Trypsin/EDTA and homogenized and centrifuged as described above. From the cell pellet suspension, 10 µL was taken to count the number of cells by using a haemocytometer. Cell number was calculated as below:

Average number of cells counted x Volume of original mixture x 10^4

The dispersed cells were again centrifuged at 1200 rpm for 3 minutes and the pellet suspended in freezing media (1 part of dimethyl sulfoxide: 9 parts FBS) to obtain a concentration of 1 x 10^6 cells/mL. The diluted cells were aliquoted into 1 mL cryogenic vials and stored in -20^{o}C overnight and transferred to -80^{o}C for storage until used for experiments.

2.2.3 Application of tensile strain

The PDL cells were trypsinized and counted to subculture 3 x 10^5 cells per well into the six-well, 35 mm flexible-bottomed UniFlex® culture plates (Figure 2.1, Flexcell International Corporation, Hillsborough, NC, USA) containing a centrally located rectangular strip (15.25 x 24.18 mm) coated with type I collagen.

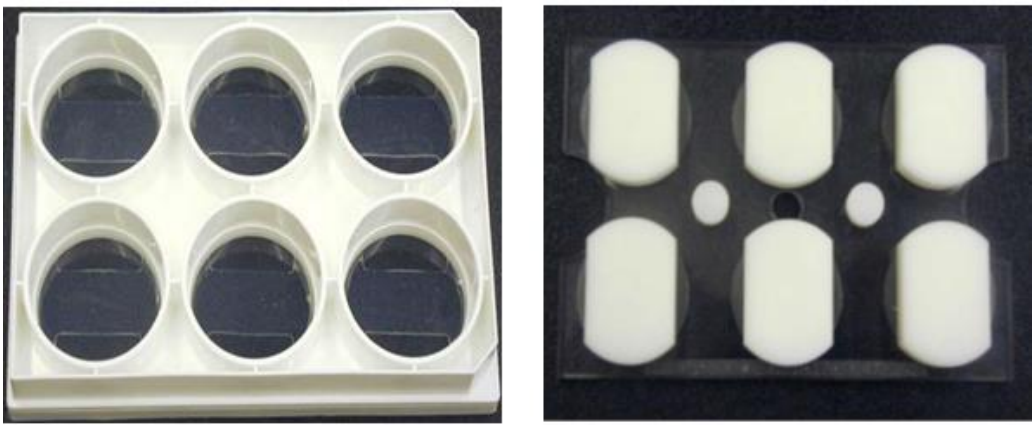

Figure 2.1. Left: 35 mm six well UniFlex® flexible bottomed cell culture plate; Right: Arctangle® Loading stations™ 3.3" x 5" Lexan® plate and six removable Delrin® planar faced semi-rectangular posts. Adapted - Flexcell International technical report.

Uniflex® culture plates are designed to apply an in-plane uniaxial strain to monolayer cell cultures. The strain was applied (Figure 2.2) to the central rectangular strip (0.952 in^2) in the orientation along the 24.18 mm axis providing uniaxial strain to an area of 3.68 cm^2 (0.57 in^2). Specially designed Arctangle® Loading Stations® (Figure 2.1) were used to expose the selectively controlled portion to regulated vacuum. The loading stations comprised a 3.3" x 5" Lexan® plate and six removable Delrin® planar faced semi-rectangular posts positioned to be perpendicular to the central rectangular strip beneath the flexible membrane of each well of the UniFlex® plate.

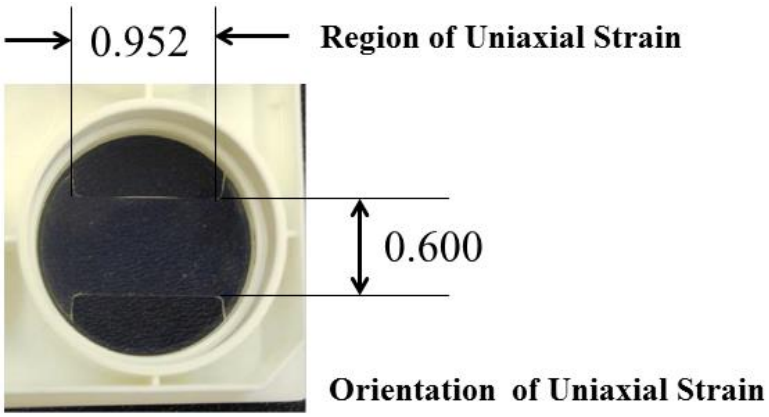

Figure 2.2. A single UniFlex® well showing region and orientation of uniaxial strain. Total strain area = 0.57 in^2. Adapted - Flexcell International technical report.

When the cells had reached confluence (commonly 3–4 d), the plate and loading stations were placed in the BioFlex® baseplate and the gaskets which hold the plate and prevent leak of the vacuum sealed tight. The whole set up was placed in a 37°C, 5% CO_2 incubator and the silicon rubber membranes were subjected to an in-plane deformation of 12% for 5 s (0.2 Hz) every 90 s using a square waveform in a Flexercell FX-4000 strain unit (Figure 2.3) (Flexcell Corp., Hillsborough, NC, USA).

Figure 2.3. Flexcell® FX-4000™ Tension system. UniFlex® plate with confluent human PDL cells were assembled in the standard BioFlex® baseplate with Arctangle® Loading station. The set up was connected to the FX-4000™ Tension system and subjected to a programmed regimen of 12% for 5 s (0.2 Hz) every 90 s.

The strain value of 12% was based on data derived from a finite element model, which suggested that maximal PDL strains for horizontal displacements of a human maxillary central incisor under physiological loading lies in the vicinity of 8–25%, depending upon the apico-crestal position – a deformation of 12% correlates well with strain conditions predicted at the mid-root (Natali *et al*., 2004). Experimental and control plates were allocated to each of the three time points (6, 12 and 24 h) and separate experiments performed for light microscopy, cell activation, caspase activity and RNA extraction. As discussed in detail later, the deformation of the silicon membrane is not uniform, but generates a tension gradient; any changes in expression will therefore represent the global average of cells exposed to different amounts of strain.

2.2.4 Changes in cell morphology

At the end of the experimental period, plates were removed from the baseplate and loading stations were detached. To determine changes in the orientation of the cells and evidence of cellular detachment or collagen delamination, some cultures were fixed with acetic methanol (1 part glacial acetic acid:3 parts methanol) for 5 mins at 25^{o}C, and after aspirating the fixative, 1% Giemsa stain (G9641; Sigma-Aldrich, Singapore) in acetic methanol added for 2–5 mins at 25^{o}C. After washing with 60% methanol in water for 1–2 mins, rectangular segments were cut from the silicon membranes and after mounting on glass slides, viewed by light microscopy.

2.2.5 MTT assay

Cell activation was measured by the MTT assay (Sigma-Aldrich), a colorimetric assay for estimating mammalian cell survival, proliferation and activation based on the ability of viable cells to reduce yellow 3-(4, 5-dim-ethythiazol-2-yl)-2, 5-diphenyl tetrazolium bromide (MTT) by mitochondrial succinate dehydrogenase (Twentyman and Luscombe., 1987; Mosmann, 1989). At the end of each time point, the cells were harvested by trypsinization and re-suspended in fresh media; 50 µL of this cell suspension was added to 96-well plates and spun at 4000 rpm (1900 x g) for 5 min. The supernatant was removed and 50µL of the MTT solution (4 mg/mL in DMEM) added to each well. The cells were incubated at 37^{o}C for 2 h in the dark. Following incubation, the plate was centrifuged and the supernatant discarded; the resulting formazan crystals were dissolved by the addition of 200µL of

dimethylsulfoxide (Sigma-Aldrich), and absorbance was measured at 570 nm in a microplate reader (Tecan SpectrophorPlus, Singapore).

2.2.6 Caspase 3/7 assay

Caspases, a family of cysteine proteinases that specifically cleave proteins after aspartate residues play key roles in mammalian cell apoptosis. Two 'executioner' caspases (3 and 7) were measured by the Caspase-Glo 3/7 Assay (Promega Corporation, Madison, WI) which provides a luminescent Caspase-3/7 substrate containing the tetrapeptide sequence (Asp-Glu-Val-Asp) in a reagent optimized for caspase activity, luciferase activity and cell lysis. At the end of each time point, the collagen coated rectangular area was cut and treated with the Caspase-Glo® 3/7 reagent for 1 hour in dark at room temperature. Each sample was aliquoted into triplicates. Luminescence was measured with a Sirius Single tube luminometer (Berthold Detection Systems).

2.2.7 Gene expression analysis

RNA extraction and real-time PCR array analysis was performed by SAB Biosciences.

2.3 Results

Under light microscopy, a difference in cellular orientation was observed as early as 6 h after the application of cyclic strain, with no evidence of cell detachment or plate delamination. While control cells remained randomly orientated, mechanically deformed cells had become reorientated away from the direction of the applied force, as previously reported (Buckley *et al.*, 1988; Neidlinger-Wilke *et al.*, 2002). However, realignment of the cells was not uniform across the whole surface of the centrally located collagen strip, tending to be more pronounced towards the edges (Figure 2.4).

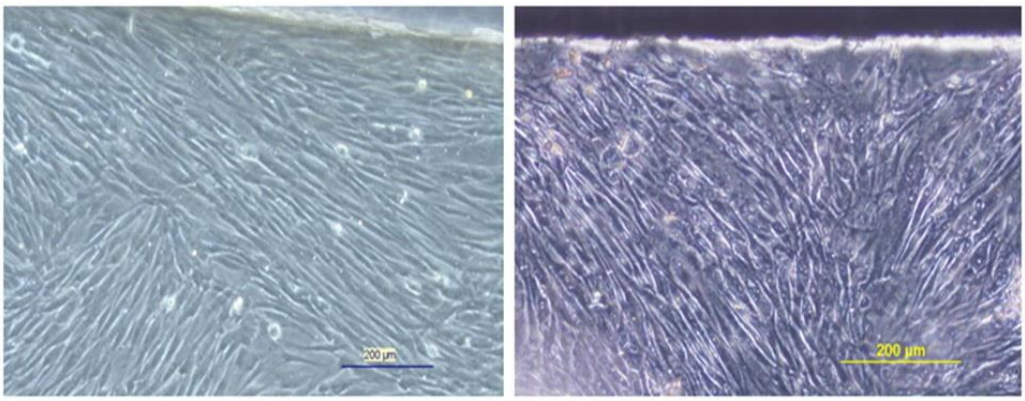

Figure 2.4. Reorientation of cells observed by light microscopy after 12% deformation. Both images were taken at the edge of the centrally located type I collagen strip. Left: Control culture in which cells tend to be randomly orientated. Right: 12h stressed culture stained by the Giemsa method. Cells become aligned at varying angles to the long axis of the applied strain (Saminathan *et al.*, 2012).

The MTT assay showed that intermittent substrate deformation resulted in a small, but statistically significant, reduction in overall metabolic activity at 6 h (Figure 2.5). There was also a reduction in caspase-3 and -7 activity by

mechanically strained cells at 6 and 12 h, suggesting that the strain regimen had delivered a transient anti-apoptotic signal to the cells (Figure 2.6).

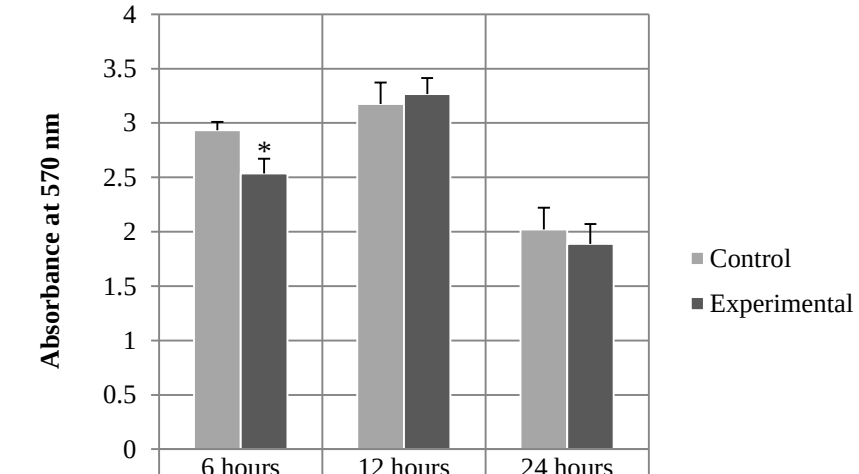

	6 hours	12 hours	24 hours
Control	2.932	3.176	2.021
Experimental	2.535*	3.266	1.888

Figure 2.5. The effect of uniaxial, cyclic strain on the viability of cells; MTT assay. Data represented as means of absorbance values from three separate experiments measured at 570 nm. *$p < 0.05$. (Saminathan *et al*., 2012).

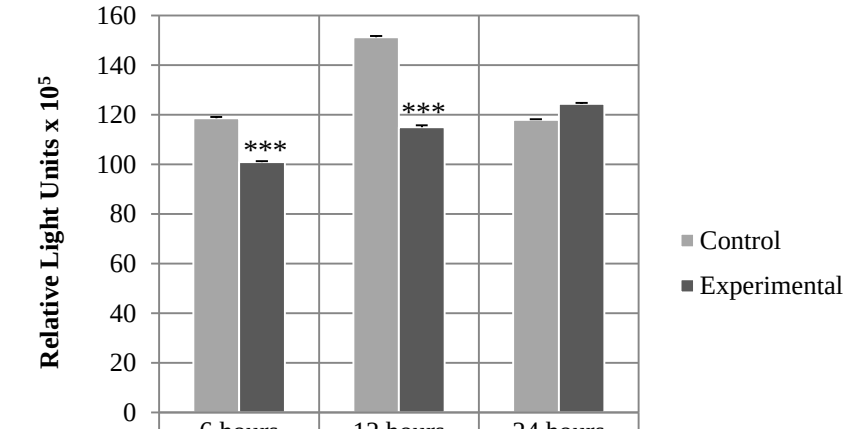

	6 hours	12 hours	24 hours
Control	118.50	151.20	117.83
Experimental	100.87	114.86	124.32

Figure 2.6. The effect of cyclic mechanical strain on the activity of two 'executioner' caspases, -3 and -7, detected by Caspase 3/7 assay. Data is expressed in relative light units (RLU) as mean for 6-wells from three separate experiments. ***$P < 0.001$. (Saminathan *et al*., 2012).

2.4 Discussion

The study showed that intermittent tensile strain on human PDL cells in 2-dimensional culture had a significant effect on the regulation of adhesion-related molecules and the metabolic activity of the cells (Appendix 1). In response to biomechanical cues, PDL cells undergo alterations in cell proliferation and differentiation of the various cell populations in the ligament (Mabuchi *et al*., 2002). PDL fibroblasts being the most predominant cells in the human PDL (see literature review), (Lekic and McCulloch, 1996) serve to regenerate the PDL and maintain its structural integrity during bone remodelling. Thus for PDL homeostasis, the proliferative capacity of PDL is essential.

In the present study, the MTT assay suggested that the application of mechanical strain to quiescent cells resulted in transient reduction in cellular activity. At first sight this supports the findings of Wang *et al*. (2011), which reported that a cyclic tensile strain as low as 0.5% applied to human PDL cells for 2 h in an out-of-plane, four-point bending system had an inhibitory effect on cell proliferation and viability. However, the signal generated in the MTT assay is dependent upon the number as well as activity of living cells (Twentyman and Luscombe, 1987; Sieuwerts *et al*., 1995). Our findings suggest that mechanical stress is not cytotoxic, but the reductions in the MMT formazon product at 6h result, from a temporary reduction in metabolic activity associated with the alteration in their functional environment (Saminathan *et al.,* 2012). Moreover, Wang *et al.* also performed a microarray analysis using a whole genome oligonucleotide chip and were able to identify

110 genes that were differentially expressed, 97 of which were upregulated. A recent study on PDL fibroblasts stretched by less than 10% strain showed a reduction in proliferation without any cytotoxic effect, and that proliferation was mediated by a MAPK dependent pathway (Kook and Lee, 2012). A cyclic stretch of 9% strain with 6 cycles/min inhibited PDL cells proliferation (Matsuda *et al*., 1998) and in an *in vivo* study the rate of proliferation was observed to be lower on the tension side than the resorption side (Zentner *et al.*, 2000). In contrast, PDL cells subjected to 2.5% elongation showed significant increase in DNA synthesis (Kletsas *et al.*, 1998), while an *in vivo* study on orthodontic tooth movement using male Sprague-Dawley rats found that the tension sides of PDL was found to show higher proliferation than the compression side (Mabuchi *et al.,* 2002). These latter data and the findings of the present study suggest that mechanically deformed cells remain metabolically active, and suggest that any changes in the MTT assay represent a short-term adjustment to alterations in their biophysical environment.

Apoptosis, a conserved form of programmed cell death following a specialized cellular process plays a critical role in cell proliferation and differentiation and also protects the cell from any extracellular stress induced by removal of growth factors (Jacobson *et al.*, 1997; Jilka *et al.*, 1998; Fuchs and Steller, 2011). The process involves activation of a cascade of proteolytic enzymes called caspases responsible for cleaving cellular substrates in many apoptotic pathways (Saminathan *et al*., 2012). They are induced by initiator caspases 8 and 9 which triggers the executioner caspases -3. -6 and -7, with caspase-3 being the most effective to respond to the direct activation (Hao *et al*., 2009).

Our caspase-3 and -7 data suggest that the application of an in-plane cyclic strain to PDL cells has a positive, albeit transient, effect on apoptosis, an observation supported by comparable data for gingival fibroblasts (Danciu *et al.*, 2004). However, the results are contradictory to previous reports on out-of-plane cyclic mechanical strain which showed a transient increase of apoptosis in PDL cells (Zhong *et al*., 2008; Hao *et al*., 2009). This seems likely to have been due to the more vigorous strain regimens used (1, 10 and 20% deformation at 0.25 Hz for 10 and 6 cycles/min, respectively), suggesting that the cells might have been overstressed. Experiments conducted on human lung fibroblasts, for example, have shown that 20% cyclic deformation activated apoptotic signalling pathways (Boccafoschi *et al.*, 2010), while 25% strain induced cell death (Boccafoschi *et al.*, 2007).

PDL cells in order to maintain homeostasis, may undergo cell death after the completion of functions such as synthesis, resorption and remodelling of the periodontal tissues (Mabuchi *et al*., 2002), and apoptotic cell death has been reported in the both the pressure and tension sides of the tooth during orthodontic tooth movement (Hatai *et al.*, 2001; Mabuchi *et al*., 2002; Yamamoto *et al*., 2006). In summary, induction of apoptosis in mechanically deformed cells *in vitro* appears to be related to the magnitude and frequency of the applied strain. This is likely to be reflected in real life, where the PDL will be more heavily stressed by occlusal loading during mastication than in swallowing. Moreover, the slowdown in proliferation can be viewed as an adaptation and protection mechanism to enable cells respond to external stimuli (Wang *et al*., 2011). The relationship between the biophysical

environment of a cell and the mechanisms of programmed cell death and its balance with cell proliferation appears to be a complicated one and would benefit from further investigation.

The effects of strain magnitude and frequency have been widely investigated but the relationship between signalling and strain direction remains unknown. Fibroblasts were seen to align perpendicular to the direction of the force in the *in vitro* studies done by Zhong *et al*. (2008) and Culbertson *et al.* (2011). The authors explain that when a mechanical stimulus was applied to the teeth, there will be an increase in PDL cell proliferation, strengthening the physical properties of PDL fibers and hence increases PDL space. Therefore, the perpendicular alignment to the direction of force applied may be an essential characteristic role played to maintain the structure PDL. Cyclic uniaxial strain applied to cardiac fibroblasts *in vitro* induced the expression of genes encoding TGFβ1, collagen III and fibronectin, while equibiaxial strain induced extracellular matrix molecules at mRNA levels (Lee *et al*., 1999). A further study relating the deposition of ECM molecules that could possibly influence the cell alignment is necessary for a better understanding of the physiological response of cells to mechanical stimuli.

In the Flexercell system, a silicone membrane is stretched across a loading post by the application of vacuum pressure and, depending on the shape of the loading post, either a biaxial or a uniaxial strain (as in the present study) may be applied to the cells. Although the most widely used commercially available apparatus for delivering controlled mechanical strain to cells *in vitro*, the

Flexercell system does have limitations, particularly when it comes to determining the physical characteristics of the strain. First, the mechanical in-plane deformation applied to UniFlex® plates does not produce a purely tensional strain because tension in one plane is always accompanied by compressive and shear strains due to the Poisson effect (Vande Geest *et al*., 2004; Matheson *et al.*, 2006) Second, cells cultured on a UniFlex® plate will experience about half the applied substrate strain programmed into the computer (Wall *et al.*, 2007). And third, the amount of cellular deformation will vary with the distance from the middle of the membrane; cells near the perimeter of the field will experience greater deformation (Matheson *et al.*, 2006). Nevertheless, despite the shortcomings of all existing model systems in precisely defining the strain profile, *in vitro* methodology still remains the most effective way to screen cells for the expression of mechanoresponsive genes. Another consideration is that the traditional 2-dimensional culture systems in widespread use for investigating the response of cells to mechanical strain *in vitro* have a number of limitations, not least the fact that periodontal ligament cells are normally surrounded by a complex network of collagens, proteoglycans and non-collagenous proteins, which are not grown on tissue culture plastic or films of matrix proteins, such collagen or fibronectin. In other words, the cells cultured in this system are in a double default state. Some attempt has been made to address this shortcoming for compressive force application by seeding periodontal ligament cells into type I collagen gels (de Araujo *et al*., 2007; Lee *et al.*, 2007), but collagen is only one of the major structural macromolecules found in extracellular matrices. For the field to progress, therefore, it is clear that future *in vitro* analyses of

mechanoresponsive gene and protein expression require well characterized three-dimensional models incorporating periodontal ligament cells into hydrogel matrices designed to produce a tissue construct resembling more closely the periodontal ligament *in vivo*.

3. Preliminary study

3.1 Introduction

Traditional two-dimensional culture systems have a number of limitations since they are in a double default state. To bridge the gap between 2-dimensional cultures and animal models we created 3-dimensional tissue constructs to more closely resemble the structure of the PDL *in vivo* by seeding cells into hydrogel matrices. Hydrogels are class of polymer material that have properties which resemble naturally occurring extracellular matrices. They have been widely used to create 3-dimensional tissue constructs for use in cell biology, bioengineering and regenerative medicine (Serban *et al*., 2008). In the present investigation, PDL cells were encapsulated in two hydrogel matrices : (1) agarose, a linear polysaccharide composed of galactose subunits obtained from agar which has been widely used in orthopaedic research due to its ability to support the chondrocyte phenotype (Buschmann *et al*., 1995; Chowdhury *et al*., 2003; Toyoda *et al*., 2003; Kelly *et al*., 2006; Bougault *et al*., 2008, 2012), and (2) Extracel™, a commercially-available hydrogel composed of hyaluronan (HA) and gelatin, cross-linked with polyethylene glycol diacetate (PEGDA) forming a semi-synthetic extracellular matrix (Serban *et al*., 2008).

3.2 Materials and methods

3.2.1 Culture of periodontal ligament cells

Primary human PDL cells were purchased from a commercial source (ScienCell Research Laboratories, Carlsbad, CA, USA; Lot number: 5145). The cells were isolated from several donors and cryopreserved at passage 0. The cells were delivered frozen on dry ice which was transferred immediately to liquid nitrogen. Each 1mL vial containing 5 x 10^6 cells was cultured by first thawing in a 37^{o}C water bath and diluting with 1 mL of Dulbecco's modification of Eagle's medium (DMEM; GIBCO, Invitrogen, Singapore) with all essential supplements as described before, under sterilized conditions in a biosafety cabinet. The mixture was centrifuged at 1200 rpm (290 x g) for 3 minutes and the supernatant was discarded. The pellet was re-suspended with 1 mL of media and transferred to a 75cm^2 tissue culture flask (Corning® cell culture flasks) containing 10 mL of DMEM. The flask was incubated in a humidified atmosphere of 5% carbon dioxide and 95% air at 37^{o}C. Media was changed after 24 hours to remove any residual freezing media.

3.2.2 Cells encapsulation in hydrogels

Preliminary experiments were done to optimize the cell number and growth conditions in the hydrogels. Four hydrogel construct cultures were set up and maintained to be examined for one, two, three and four weeks.

3.2.2.1 Extracel™ constructs

Human PDL cells were incorporated into Extracel™ hydrogel as per manufacturer's instructions. Passages 3 and 4 of the PDL cells were used for all our studies. Extracel™ kits (Figure 3.1) purchased from Glycosan Biosystems were stored in -20^{o}C on arrival; each consists of three individual vials of Glycosil, Gelin-S, Extralink and degassed deionized water (DG water). Glycosil, Gelin-S and Extralink come as lyophilized solids blanketed by argon and under a slight vacuum.

Prior to use in experiments, the kit components were brought to room temperature and reconstituted according to the manufacturer's instructions. Under aseptic conditions, DG water was added to dissolve Glycosil and Gelin-S using a syringe. Syringes were always used to add water and remove product from the vials since Glycosil and Gelin-S tends to cross link in the presence of oxygen. Glycosil and Gelin-S were reconstituted to produce a 1% (w/v) solution. To dissolve the solids, both the vials were placed in a 37^{o}C shaker for approximately 30 minutes until the solutions were clear and viscous. Extralink was reconstituted to produce a 2 % (w/v) solution.

Figure 3.1. Extracel™ hydrogel kit containing DG water, Glycosil, Gelin-S and Extralink in its lyophilized form.

Human PDL cells were trypsinized and pelleted. Equal volumes of Gelin-S and Glycosil were mixed and added to the cell pellet and mixed well for complete dispersion of cells by pipetting back and forth. One part of Extralink was added to the mixture at a ratio of 1: 4 to produce a final concentration of the cells to be 2.5 x 10^6/mL.

Glass rings of about 13 mm diameter and 1.5 mm thickness were sterilized and placed in a 60 mm Petri dish (Figure 3.2). 300 µL of the hydrogel mixture was added to each glass ring to form a construct of about 800–1000 µm thickness. The constructs gelled at 37^o C for 30 minutes; 10mL of culture media added to each dish and the constructs were cultured at 37^o C incubator at 5% CO_2/95% air. Culture media were changed every 2 days.

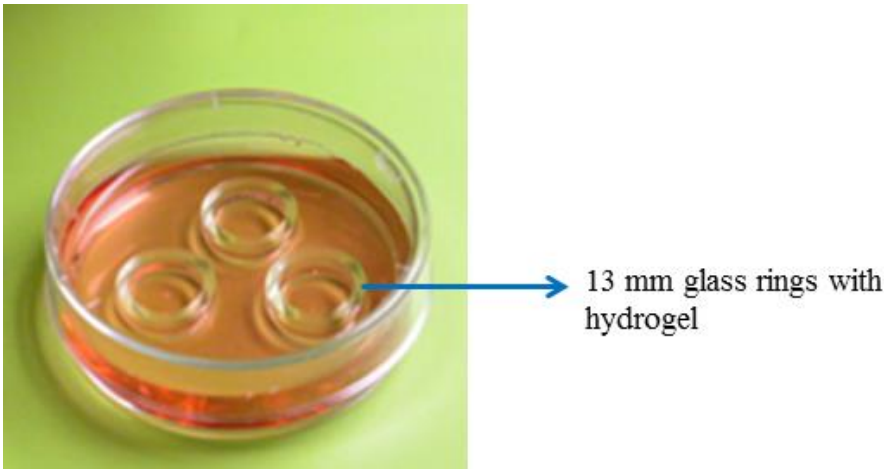

Figure 3.2. Image taken when hydrogel encapsulated with human PDL cells were cast into glass rings of 13 mm diameter x 1.5 mm thickness placed in 60 mm Petridish.

3.2.2.2 Agarose constructs

Low melting agarose was used for the constructs. To prepare 2 % gel construct, 0.1mg of low melting agarose was dissolved in 5 mL of PBS and the solution was heated for approximately 1-2 minutes until the agarose was dissolved completely and cooled to bearable temperature in a 37^{o} C water bath before adding the PDL cells which were trypsinized and pelleted to 2.5 x 10^{6}. After the pellet was re-suspended slowly using a pipette for a uniform suspension and avoid air bubbles, 300 µL of the gel was transferred to the glass rings as described above for Extracel™. The constructs were left to gel for 10 min in a 37^{o} C incubator before 10 mL culture media was added and maintained along with the Extracel™ culture constructs. Culture media was changed every 2 days.

3.2.2.3 Growth factors

In order to accelerate the growth of PDL cells and direct the cells towards the fibroblast phenotype, connective tissue growth factor (CTGF) and fibroblast growth factor (FGF-2) were incorporated into the constructs; 100 ng/mL of CTGF (BioVendor Laboratories, Guangzhou, China) and 10 ng/mL of FGF-2 (10 ng/mL; Gibco) were added to both the hydrogel matrix and the culture media. Cultures without growth factors were maintained as controls.

3.2.3 Confocal microscopy

Cell viability was determined by staining with Fluorescent dyes, fluorescein diacetate (FDA) and propidium iodide (PI) (Jones and Senft, 1985). The FDA is a lipid-soluble, non-fluorescent probe that passes through the cell membrane and is hydrolyzed by cytoplasmic esterase to yield a fluorescent product, fluorescein. It is a polar compound that passes slowly through a living cell membrane, accumulates inside the cell and exhibits green fluorescence when excited by blue light (Johnson *et al*., 2001; Jones and Senft, 1985). PI, on the other hand, passes through damaged cell membranes and intercalates with DNA and RNA to form a bright red fluorescent complex seen in the nuclei of dead cells. Since the dye is excluded by intact cell membranes, PI is an effective stain to identify nonviable cells.

A stock solution of fluorescein diacetate (Sigma Aldrich, Singapore) was prepared by dissolving it in acetone to produce a concentration of 5 mg/mL. The working solution of FDA was freshly prepared each time, by adding 0.04 mL of stock solution to 10 mL of phosphate buffered saline (PBS). The stock

solution of PI was prepared by dissolving 1 mg in 50 mL of PBS. The prepared stock solutions were stable for up to 6 months when stored in dark at $4^{o}C$.

At the end of each time point, culture medium was aspirated from the Petri dishes and gels stained by adding 0.1 mL (2µg) of FDA working solution and 0.03 mL (0.6µg) of PI. The procedure was carried out in the dark and the gels were left to stain for 3 minutes at room temperature. The Petri dishes were covered with aluminium foil and transported in ice to the Confocal Microscopy Unit (National University Medical Institutes) and viewed with a Olympus Fluoview FV 1000 (Olympus, Japan) confocal imaging system at 10x magnification. Viable cells appear as fluorescent bright green at 470 nm and non-viable cells are bright red at 559 nm. Three fields (120µm x 120µm) with one center and two periphery were chosen and scanned for analysis from each disc and the numbers of viable and non-viable cells were counted using the Imaris version 6.1.5 software.

3.3 Results and discussion

Over 4 week time course, PDL cells retained high viability in Extracel™ compared to agarose. Observing after 24 h, there was almost 50% of cell death in agarose compared to just 3-4% in Extracel™, although, there was an improvement in the cell growth from the second week onwards (Table 3.1). Addition of CTGF and FGF-2 has significantly increased the viability of cells in both the hydrogels compared to the corresponding controls (Table 3.1 below).

Hydrogels without CTGF/FGF-2

Days in culture	Extracel™		Agarose	
	Viable cells (FDA)	Dead cells (PI)	Viable cells (FDA)	Dead cells (PI)
1 day	341.22	16.11	171	121.89
7 days	921.67	46.67	150.33	473.11
14 days	1191.11	155.44	396.56	275.67
21 days	2021.44	124	1401.22	131.11
28 days	2257.78	123.78	1278.33	98.78

Hydrogels with CTGF/FGF-2

Days in culture	Extracel™ + GFs		Agarose + GFs	
	Viable cells (FDA)	Dead cells (PI)	Live cells (FDA)	Dead cells (PI)
1 day	1696	65.56	719.67	641.89
7 days	1904.11	55.56	593.67	547.89
14 days	2302.78	105.11	869.11	73.22
21 days	3479.11	60.22	1294.22	144.89
28 days	4082.44	146.56	1611.56	134.44

Table 3.1. Comparative tabulation of cell viability in the hydrogels without (above) and with (below) addition of CTGF/FGF-2, calculated by FDA/PI staining-laser confocal microscopy method. Three fields were chosen from each glass ring in the Petri-dish and the number of viable/non-viable cells were counted using Imaris version 6.1.5 software. Data represented is means of 9 readings/Petri-dish.

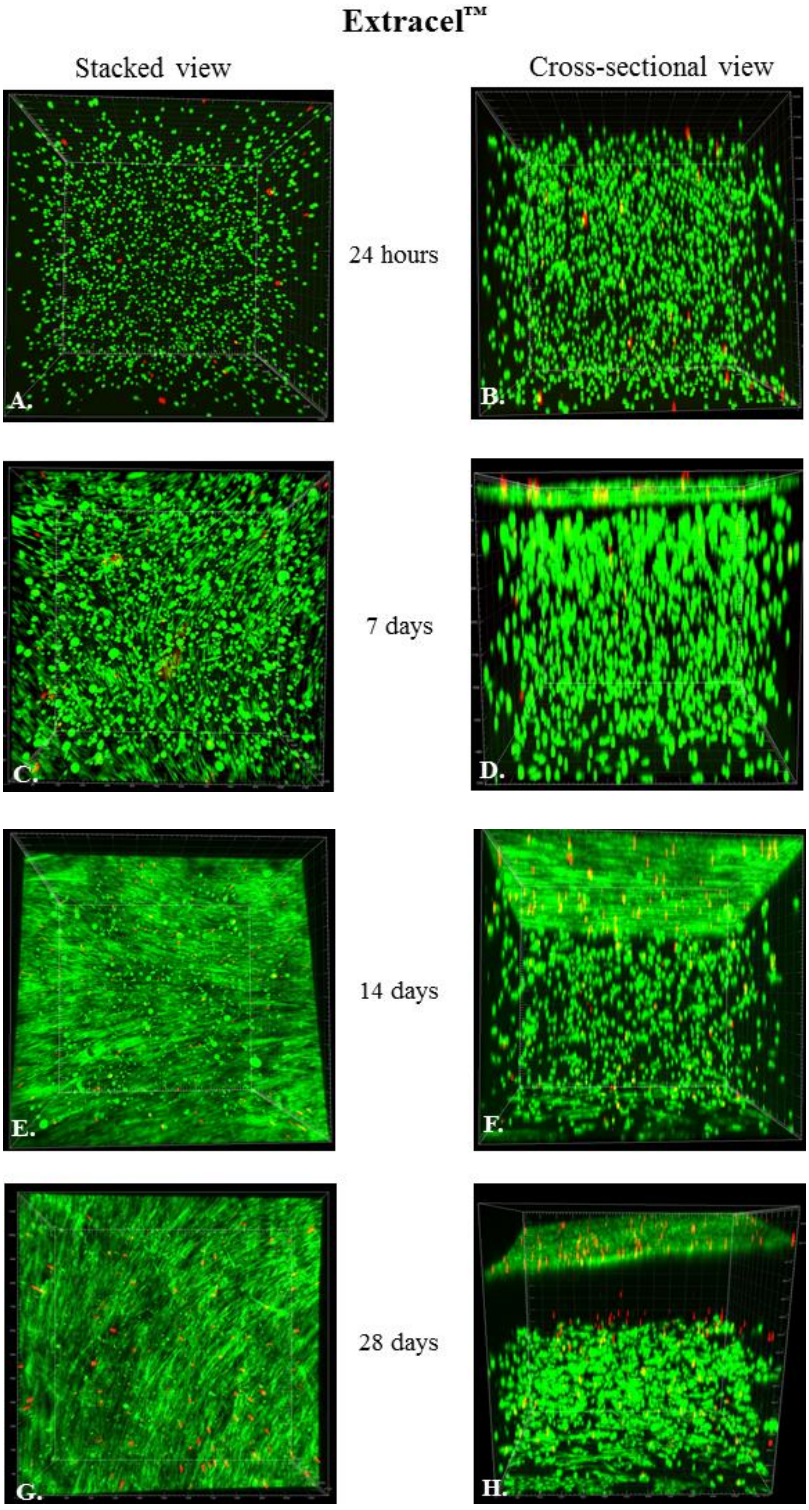

Figure 3.3. Images were taken at 10 x magnification after each experimental time point by Olympus Fluoview FV 1000 (Olympus, Japan) confocal imaging system and processed by Imaris software version 6.1.5. The left aligned images (A, C, E, G) are the stacked view from the top of the Extracel™ hydrogels in an area of 1200 x 1200 µm of each sample ; Right aligned images (B, D, F, H) are the cross-sectional view (900-1000 µm thickness). Viable cells appear green and non-viable cells appear red after staining with Fluorescein diacetate and propidium iodide.

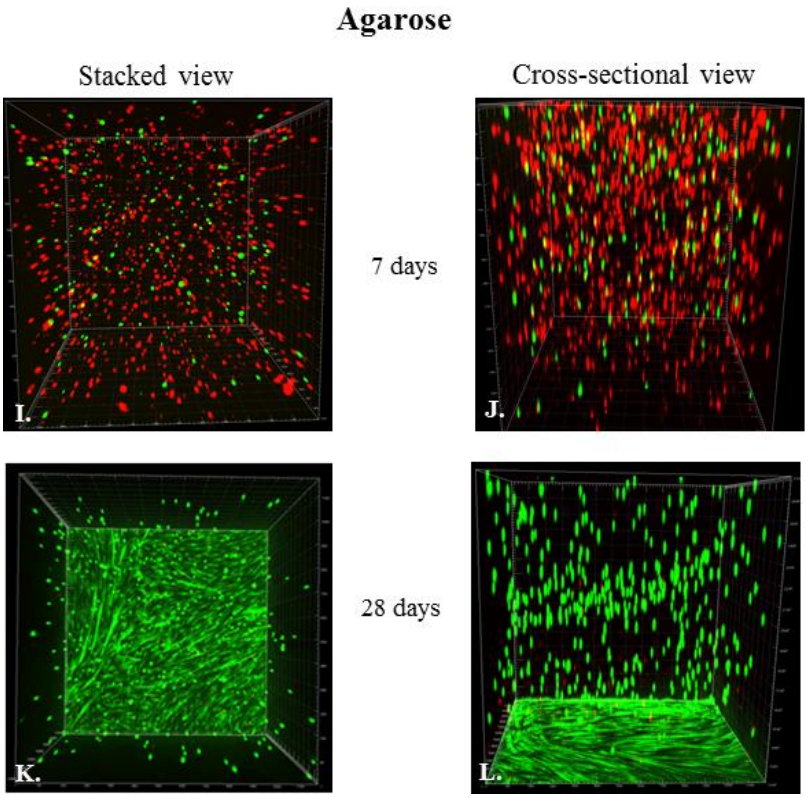

Figure 3.4. Confocal images (10 X) of PDL cells in Agarose showing a higher number of dead cells by 7 days of culture (I, J) and its migration towards the gel-substrate interface by the end of 28 days.

The morphology of the cells at the end of 4 weeks' time course varied with the planes of the gel. A characteristic fibroblast phenotype was assumed by the cells on the gel-substrate interface (Figure 3.3H), but the cells remained rounded within the body of the gel. One of the ways cells adapt to their environment is through adhesive interactions with their substrate, typically extracellular matrix proteins such as collagen or fibronectin via focal adhesions. Retention of a rounded morphology suggests the biophysical characteristic of the hyaluronan-gelatin substrate, unlike the gel-plastic interface, does not provide a sufficiently stiff scaffold to enable the cells to attach and spread. Since PDL cells constitute a heterogeneous population including mesenchymal stem cells (MSCs) and it is possible that some of the

rounded cells within the gel matrix were chondrocytes. Another peculiar behavior of cells organization was seen within the gel from the second week onwards (Figure 3.3F). Cells with a fibroblast phenotype formed a densely packed network in the top layer with some cells migrating towards the bottom of the gel leaving an empty space in the gel (Figure 3.3H); this was observed in both the hydrogels. In other words, the cell number was higher towards exterior region of the gel than the interior. This may be due to the fact that, as the cells grow to fill in the pores, diffusion of nutrients might have become limited to reach (Carrier *et al*., 2002; Dunn *et al*., 2006) and the cells might have to migrate towards these directions for adhesion and growth. Cell growth in agarose exhibited similar characteristics except that the cells were migrating to organize as a dense layer towards the gel-plastic interface alone **(**Figure 3.4**)**. Though previous studies (Bougault *et al*., 2008, 2012) have used agarose for molecular studies on mechanical deformation, while our preliminary data shows an increased cell death rate compared to the Extracel™, we chose Extracel™ for our further studies.

4. Engineering and characterizing three-dimensional tissue constructs in a tensile environment

4.1 Introduction

The forces that orthodontic appliances apply to the teeth are transmitted through the PDL to the supporting alveolar bone leading to the deposition or resorption of bone depending upon whether the tissues are exposed to a tensile or compressive mechanical strain. These strains initiate changes in the metabolic and proliferative activity of the PDL leading to tissue remodelling and formation or resorption of bone depending upon whether the cells at bone-PDL interface are exposed to an osteogenic or osteoclastic signalling cascade.

The extracellular matrix (ECM) provides a physical framework that plays an integral part in signalling cells to proliferate, migrate and differentiate (Holmbeck and Szabova, 2006). Remodelling of the ECM plays a vital role in orthodontic tooth movement with forces exerted on the teeth and transmitted to the surrounding tissues of the periodontium. The ECM molecules involved in this process include collagen, proteoglycans, laminin, and fibronectin. As most *in vitro* studies done on investigating these aspects using two-dimensional culture systems do not provide a complete understanding of the complex interplay occurring *in vivo*, a three-dimensional model is required. To overcome the limitation of cells being organized as double layer resulting in a construct with a non-uniform distribution of cells, we designed a thin film construct that measures about 80-100 µm thickness. Here we describe

preliminary experiments to characterize the thin film constructs before we implemented for mechanical deformation.

4.2 Aims

1) To engineer a three dimensional model that closely resembles the structure of PDL.
2) To characterize the behaviour of tissue construct in a tensile environment using Flexcell FX-4000T Tension Plus Strain Unit.

4.3 Materials and Methods

4.3.1 Stationary culture – Preliminary characterization

Human PDL cells were incorporated in Extracel™ at a concentration of 2.5 x 10^6/mL as described in chapter 3, section 3.2.2.1 and 300µL of the gel was transferred to each well of 35 mm diameter in Type-1 collagen coated 6 well plates (Sigma-Aldrich, Singapore). The solution was spread in the well which after 20 minutes of gelling in a 37^{o}C incubator, formed an 80-100 microns thick gel construct. We term these constructs as thin film constructs throughout the study. The cells were cultured for up to 6 weeks with and without CTGF (100 ng/mL) and FGF-2 (10 ng/mL) in the hydrogels and culture media. Media was changed every two days.

4.3.2 Microscopy

4.3.2.1 Analysis of cell viability

At the end of each time point, culture media was aspirated and the gels were directly stained with FDA and PI as per the same procedure elaborated in chapter 3, section 3.2.3. One center and two periphery fields were scanned and analyzed from each well (n = 9).

4.3.2.2 Immunostaining

The gels were washed with phosphate-buffered saline (PBS) and fixed in 4% formaldehyde at room temperature for 15 minutes. For detection of actin filaments, the thin film constructs were permeabilized with 0.1% Triton X-100 in PBS, and blocked with 5% normal goat serum or fetal bovine serum (FBS) for 1 hour at room temperature. The primary antibody Anti-Vinculin (1mg/mL: Millipore, Singapore) was diluted with blocking solution and in the ratio of 1:150 and incubated with the prepared cells at 4°C overnight. After 2 hours wash with PBST (0.1% Tween-20 in PBS), Goat anti-Mouse IgG Antibody, (H+L) FITC Conjugated (2mg/mL) was added at 1:300 dilution. For the actin staining, tetramethyl rhodamine isothiocyanate (TRITC)-conjugated phalloidin (60µg/mL) (Millipore, Singapore) added at a dilution of 1:250. After 60 minutes incubation, the cells were washed three times with PBST and incubated with 4', 6-Diamidino-2-phenylindol (Millipore, Singapore). The whole procedure was carried out in the dark. The samples were covered with aluminium foil and transported on ice to the confocal microscopy unit. Immunostained cells were viewed with an Olympus

Fluoview FV 1000 (Olympus, Japan) confocal imaging system at 60X magnification and processed using Imaris version 6.1.5 software.

4.3.2.3 Scanning electron microscopy

Culture media was aspirated from the 35 mm culture dishes and the constructs fixed in 2.5 % Glutaraldehyde at 4^0C overnight, washed in PBS twice and then post-fixed for 2h at room temperature in 2% osmium tetroxide. They were then dehydrated in a graded series of ethanol and dried by transferring the specimens in a 100% ethanol to a critical point drying apparatus (Leica EM CPD030, Singapore) and ethanol exchanged for liquid CO_2 under pressure. After six cycles of this exchange, the temperature of the chamber was raised to 40^0C, a point at which the liquid changes into a gas and drying occurs. After this stage, the specimens shrunk to small pieces and required careful handling. The dried specimens were mounted onto aluminium specimen stubs with a conductive tape and sputter coated with gold-palladium alloy for 120s, placed in a vacuum and viewed in a scanning electron microscope (Philips/FEI XL30 FEG SEM).

4.3.3 Application of mechanical strain to gel constructs

Human PDL cells were incorporated at a concentration of 2.5 x 10^6 cells/ mL of Extracel™ as described earlier and 300 µL of the hydrogel was cast on to each of the type I collagen-coated 35 mm flexible-bottomed silicone membranes in six-well Tissue Train® culture plates (Figure 4.1, Flexcell International Corporation, Hillsborough, NC, USA). The membranes are fitted with matrix-bonded foam circular for improved cell attachment. Another set of

cultures was also prepared with and without addition of CTGF (100 µg/mL) and FGF-2 (10 µg/mL) in the hydrogel and culture media.

Figure 4.1. Left: Tissue train circular foam culture plate. Right : six removable Delrin® planar Bioflex® loading posts .

An in-plane equibiaxial cyclic strain was applied to the cells by the combined usage of Tissue Train® plates and Bioflex® Loading Stations™ (Figure 4.1 right). The Loading stations are comprised of a 3.3" x 5" Lexan® plate and six removable Delrin® planar faced posts positioned in such a way that each is centred beneath the flexible membrane of each well of the 35 mm Tissue Train® culture plate.

This provides the cell culture in a uniform biaxial environment with all cells stretched over loading posts receiving uniform radial and circumferential strain (Figure 4.2). The gel constructs were strained using the Flexercell FX-4000™ strain unit (Flexercell Corporation, Hillsborough, North Carolina). The biaxial strain was regulated by the hardware platform FX-4000™ Tension Plus™ System and FlexSoft™ software. This was carried out by placing the culture plates According to the manufacturer's design, cells attached to the

areas of membrane over the post when membrane is in its fully stretched position are the ones that receive uniform strain.

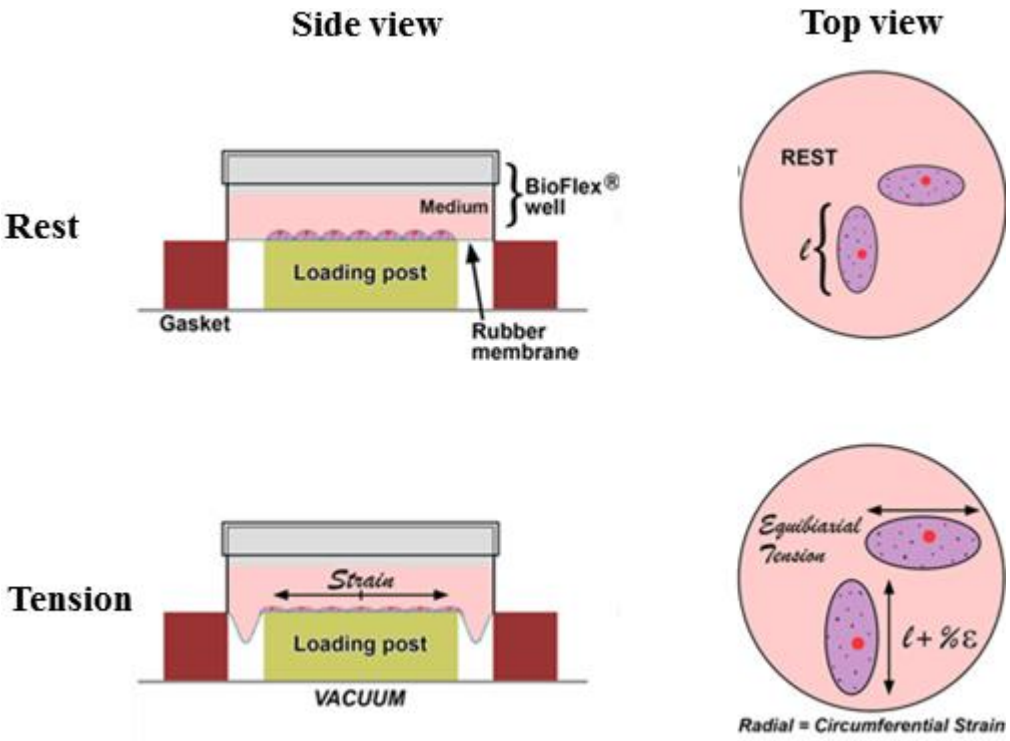

Figure 4.2. Schematic of the type I collagen coated Tissue Train® membrane in rest and when deformed by equibiaxial strain across the Bioflex® loading posts. Picture adapted from Flexcell International corporation user's manual.

4.3.4 Cell recovery from Extracel™

Cells embedded in the hydrogel were recovered by a two stage process (Glycosan Biosystem® Company) involving trypsinization and break down of the collagen and hyaluronic acid cross-link using the enzymes collagenase/hyaluronidase.

At the end of each experiment time period, the media was aspirated and stored in cryogenic vials at -80^{o}C for protein quantification. The hydrogel was

washed with PBS and 1.5 mL of Trypsin/EDTA (Invitrogen, Singapore) was added to each 300 µL gel construct and incubated for 3 hours in 37^{o}C incubator. After incubating for 3 hours at 37^{o}C, 1.5 ml of 10X collagenase/hyaluronidase (StemCell Technologies) enzyme was added to each well. The plate was left at 37^{o}C for overnight gel digestion. This was based upon the protocol suggested by Glycosan Biosystems®, the manufacturer of Extracel™. 3 ml of DMEM supplemented with 10% fetal bovine serum was added to the dissolved gel solution. The solution from all the 6 wells were then transferred to one 50 mL falcon tube and centrifuged at 1200 rpm for 5 minutes. The pellet was re-suspended with 1.5 ml of fresh media and again centrifuged at 10,000 rpm (6708 x g) for 2 minutes to obtain the pellet for RNA extraction.

4.3.5 RNA extraction

RNA extraction was carried out using RNeasyplus Mini kit (Qiagen).The pellet was loosened by flicking the tube to which 350µl of buffer RLT plus containing guanidine thiocyanate was added to disrupt the cells. The mixture was pipetted well to mix and the lysate was homogenized by passing 5 times through a 20-guage needle (0.9 mm) attached to an RNAase-free syringe. The homogenized lysate was transferred to a gDNA Eliminator spin column placed in a 2ml collection tube and centrifuged at 10,000 rpm for 30 seconds. The flow through was mixed well with 1 volume of 70% ethanol. The sample was then transferred to a RNeasy spin column placed in a 2ml collection tube and centrifuged at 10,000rpm for 15 seconds. The flow through was discarded. To the RNAeasy spin column 700µl of RW1 buffer was added and centrifuged

for 15 seconds for 10,000 rpm. The flow through was discarded. To the same spin column 500µl of buffer RPE was added but centrifuged at 10,000 rpm for 2 minutes. The spin column was placed in a new 2ml collection tube and centrifuged for 15 seconds at 10,000 rpm to remove any ethanol left. The spin column was transferred to a new RNase-free 1.5 ml collection tube and 30µl RNase-free water was added directly to the spin column membrane. RNA was eluted by centrifuging for 1 minute at 10,000 rpm. The eluted RNA samples were aliquoted and stored in -80^{o}C freezer.

4.3.6 RNA quality check

The RNA extracted was quantified and checked for quality and integrity before proceeding to downstream application, in this case was Real Time RT-PCR. Impurities such as contaminating proteins, genomic DNA, organic solvents such as phenol and ethanol, any enzymatic inhibitors in RNA samples can affect the accuracy of gene expression. It is important to check the quality and quantity of the RNA after thawing each time as impure RNA samples can degrade due to multiple freeze and thaw cycles.

The quality and quantity of the extracted RNA was assessed using a Nanodrop® ND-1000 UV-Vis Spectrophotometer. The RNA samples were removed from the -80^{o}C freezer and thawed by placing on ice to prevent any nuclease activity. The spectrophotometer was calibrated with 5µL RNase free water. One µL of the RNA sample was loaded onto the receiving optic fibre cable and measured. The instrument is connected and controlled by special software installed in the PC which displays the wavelength vs. absorbance

graph and the absorbance ratios (Figure 4.3). The absorbance is measured at three different wavelengths, 230 nm, 260 nm and 280 nm. The optical density values are represented as ratios: A260/280, specific for the level of protein contamination and A260/230, specific for the level of any presence of guanidine salts or phenol left from the RNA extraction process. The A260/280 value of a pure RNA sample should be approximately 2.0 and values between 1.8 and 2.0 are however acceptable.

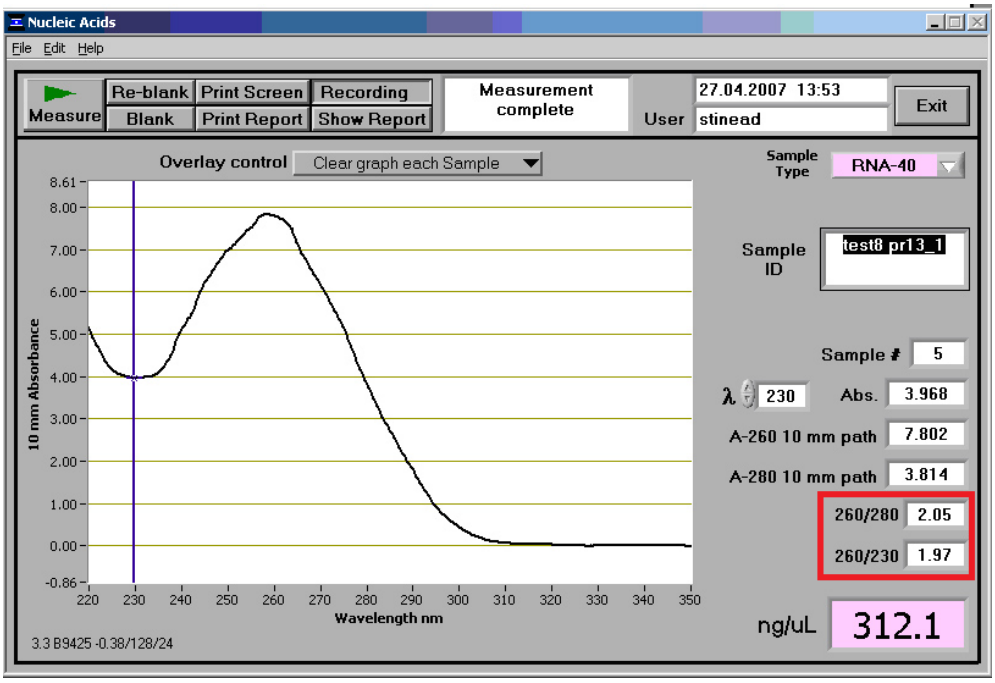

Figure 4.3. A Screenshot of the Nanodrop® ND-1000 software display indicating the A230/280 values and the quantity of RNA present in the tested sample.

4.3.7 RNA integrity check

Extracted RNA has a possibility to get degraded and shorter fragments of RNA can occur in the sample which compromises the results of downstream applications. We chose to evaluate the degree of its degradation by using the

Agilent 2100 Bioanalyzer, an automated device introduced in 1991 for the analysis of RNA samples which provides a RNA integrity number (RNA). The RIN number is a software algorithm value assigning the RNA based on a number system from 1 to 10, with 1 being the most degraded and 10 being more intact. This technology is more advanced and accurate than the traditional 28S to 18S rRNA ratio technique which is subjective to a user's interpretation. RNA samples were analyzed for its integrity using the RNA 6000 Nano LabChip kit as per the Agilent 2100 bioanalyzer protocol. The following steps were followed.

4.3.7.1 Reagents and sample set up

1. The RNA Nano 6000 reagents were brought to room temperature in the dark.
2. Aliquot 1µL of the RNA 6000 ladder and 2 µL of RNA sample into separate tubes.
3. Using the electrode cleaner chips provided in the kit and RNAase ZAP and RNA free DI water, the electrodes on Bioanalyzer was decontaminated.
4. The Dye concentrate was mixed thoroughly and spun down for 10 sec. One µL of it was mixed with 65 µL of the filtered gel matrix. This gel-dye mix was vortexed well, centrifuged at 13000 g for 10 min.

4.3.7.2 Sample loading

1. A new Lab Nano chip (Figure 4.4.1) was placed on the chip priming station. Nine µL of the gel-dye mix was pipetted into one of the appropriate wells.

2. The timing was set to 1 min and the plunger on the priming station was pulled up to 1 mL mark. The chip priming station was closed the plunger of the syringe was pressed until it was held by the clip. After 30 sec wait, the plunger was released. In less than one second, the plunger quickly moved back to 0.3 mL mark which is an indication of a proper pressurizing of the chip (Figure 4.4.2).
3. Nine µL of the gel-dye mix was dispensed to each of the remaining wells marked with G.
4. Five µL of the Nano marker was dispensed to each of the 12 sample wells and the ladder well.
5. Before loading, the RNA samples and the ladder were denatured at 70^{o}C for 2 min. A quick-spin was done to collect the evaporation.
6. One µL of the ladder and RNA samples were loaded on to corresponding wells. Empty wells were filled with 1 µL DI water to maintain the volume and avoid any errors when the chip was read.
7. The components were mixed by vortex for 1 min at 240 rpm, and any liquid spills were wiped off before placing the chip into the Bioanalyzer.
8. Within 5 min (to prevent evaporation of the sample from wells), the chip was inserted into the Bioanalyzer (Figure 4.4.3) and let to read by the software program installed in the connecting PC.

4.3.7.3 Analysis

The results will be displayed (Appendix 2) with the calculation of RNA concentration and RIN numbers of the RNA samples by plotting a graph for plotting the peaks of 18S and 28S strands (Figure 4.4).

Figure 4.4. Images of summarized steps involved in RNA integrity check process. (1) RNA 6000 Nano LabChip®; (2) Sample set up in chip priming station; (3) Chip with samples placed in Bioanalyzer; (4) Bioanalyzer read by a software program installed in the connecting PC.

4.3.8 Reverse transcription of mRNA to cDNA

The purpose of converting mRNA to a single strand of complementary DNA (cDNA) to analyze the mRNA template is because DNA strands are more stable than RNA. We used the iScript cDNA Synthesis Kit (Bio-Rad Laboratories, Hercules, CA, USA) and followed its instructions. The cDNA was synthesized from a known amount of total RNA (500 ng) using iScript Reverse Transcriptase (RT) (the protein reverse transcriptase) and the reaction

requires primers, which can be either oligodT (annealing to polyA tails of mRNA) or random hexamers; nucleotides for DNA synthesis (dNTPs); MgC_2 and buffers required by the enzyme which was all present in the 5x iScript Reaction Mix. The reaction was set up as below:

Reaction components	**Volume**
5x iScript Reaction Mix	4 µL
iScript Reverse Transcriptase	1 µL
Total RNA (500 ng)	x µL
Nuclease free water	x µL
Total	**20 µL**

The reaction was set up in nuclease free PCR tubes and carried out using a MyCycler™ thermal cycler (Bio-Rad). The reaction process was programmed for incubation in series as specified below:

Temperature	**Time**
25ºC	5 minutes
42ºC	30 minutes
85ºC	5 minutes
4ºC	Hold

To avoid any contaminations RNA handling and reaction set ups were always carried out on clean bench top, pipettes, racks and gloves which were sprayed with RNaseZap, left for few minutes and carefully wiped off using Kim® wipes.

4.3.9 Real Time RT-PCR

The novel fluorescent DNA labelling technique using fast SYBR green was used for the quantification of gene expression. SYBR green is an asymmetric canine dye (Bengtsson *et al*., 2003) that fluoresces upon binding with double stranded DNA. The intensity of fluorescent signals is proportional to the accumulation of PCR products (Zipper *et al*., 2004). This technique does not involve designing of probes like the Taqman or Molecular Beacon probes, it is easier and economical to use for repeated experiments. SYBR green can perform in terms of dynamic range and sensitivity comparable to the TaqMan probe (Wilhelm *et al*., 2003; Wong and Bai, 2006). The Fast SYBR Green Master Mix (Applied Biosystems, Singapore) we used in this study contains SYBR Green® dye I; AmpliTaq® Fast DNA Polymerase, UP (Ultra Pure) which amplifies the target sequence creating the PCR product; Uracil-DNA Glycosylase (UDG) to prevent any re-amplification of carryover PCR products; ROX™ dye Passive Reference provides an internal fluorescence reference to which the report-dye signal can be normalized during data analysis.

4.3.9.1 Reaction set up

The primers of the genes of interest (Page 103) were purchased (First Base, Singapore) and stored at -20^{o}C upon its arrival. From the stock solution (100 X), 20 µL was diluted in 80 µL of Nuclease free water to prepare a working solution. This working solution was always stored in -20^{o}C and was thawed on ice during each PCR set up. The primers mix and cDNA mix were prepared

separately before the reaction was set up in nuclease free tubes as tabulated below:

Reaction component	**Volume**
Forward primer	0.2 µL
Reverse primer	0.2 µL
Nuclease free water	4.6 µL
Total	**5 µL**

The primers used at the above specified volume gave a concentration of 200 nm for an optimal performance. Next, the cDNA was thawed on ice and the reaction mix was set up as tabulated below:

Reaction component	**Volume**
Fast SYBR Green Master Mix	10 µL
cDNA	0.5 µL
Nuclease free water	4.5 µL
Total	**15 µL**

The PCR reaction was setup by adding the 15 µL of cDNA mix and 5 µL of primer mix into each well of the 96-well MicroAmp™ Fast Optical 96-Well Reaction Plate to get a total reaction volume of 20 µL per well . The plate was sealed properly with optical adhesive cover (Applied Biosystems®, Singapore) and centrifuged for 2 min at 900 x g to eliminate any air bubbles.

HGNC Agreed Gene Symbol	Description	Primer Sequences	Annealing Temperature
ACTB	Actin, Beta	F: CCAAGGCCAACCGCGAGAAGATGAC R:AGGGTACATGGTGGTGCCGCCAGAC	58
GAPDH	Glyceraldehyde-3-phosphate dehydrogenase	F:ACCACAGTCCATGCCATCAC R:TCCACCACCCTGTTGCTGTA	60
P4HB	Prolyl- 4-hydroxylase, Beta subunit	F: GTCTTTGTGGAGTTCTATGCCC R: GTCATCGTCTTCCTCCATGTCT	62
RUNX2	Runt-related transcription factor 2	F: TGAGAGCCGCTTCTCCAACC R: GCGGAAGCATTCTGGAAGGA	58
SOX9	SRY (sex determining region Y)-Box 9	F: GAACGCACATCAAGACGGAG R: TCTCGTTGATTTCGCTGCTC	58
PPAR-γ	Peroxisome proliferator-activated receptor-gamma	F: ATTGACCCAGAAAGCGATTC R: CAAAGGAGTGGGAGTGGTCT	62
MYOD	Myogenic differentiation antigen1	F: CGGCGGAACTGCTACGAAG R: GCGACTCAGAAGGCACGTC	60
COL1A1	Collagen Type I, Alpha-1	F:GAACGCGTGTCATCCCTTGT R: GAACGAGGTAGTCTTTCAGCAACA	60
COL2A1	Collagen Type II, Alpha-1	F: TTCAGCTATGGAGATGACAATC R: AGAGTCCTAGAGTGACTGAG	58
COL3A1	Collagen Type III, Alpha-1	F: AACACGCAAGGCTGTGAGACT R: GCCAACGTCCACACCAAATT	60
MMP1	Matrix metalloproteinase1; Collagenase-1	F:GGGAGATCATCGGGACAACTC R: GGGCCTGGTTGAAAAGCAT	60
MMP2	Matrix metalloproteinase2; Gelatinase A (72 kDa)	F:TGATCTTGACCAGAATACCATCGA R: GGCTTGCGAGGGAAGAAGTT	60
MMP3	Matrix metalloproteinase3; Stromelysin-1	F:TGGCATTCAGTCCCTCTATGG R: AGGACAAAGCAGGATCACAGTT	60
TIMP1	Tissue inhibitor of metalloproteinases-1	F: CTGTTGTTGCTGTGGCTGATA R: CCGTCCACAAGCAATGAGT	60
TGFB1	Transforming growth factor, Beta-1	F:GCAACAATTCCTGGCGATACCTC R: AGTTCTTCTCCGTGGAGCTGAAG	60
BGLAP	Gamma carboxyglutamic acid protein; Osteocalcin	F: ATGAGAGCCCTCACACTCCTC R: GCCGTAGAAGCGCCGATAGGC	60
SP7	Transcription factor Sp7; Osterix (OSX)	F: TGGCGTCCTCTCTGCTTGA R: TCAGTGAGGGAAGGGTGGGT	60
BMP2	Bone morphogenetic protein 2	F: CAGAGACCCACCCCCAGCA R: CTGTTTGTGTTTGGCTTGAC	58
TNFSF11	Tumour necrosis factor ligand superfamily, member 11; RANKL	F: TCCCATCTGGTTCCCATAAA R: GGTGCTTCCTCCTTTCATCA	60
TNFRSF11B	TNF receptor superfamily member 11B; Ostoprotegerin (OPG)	F: CGTCAAGCAGGAGTGCAATC R: CCAGCTTGCACCACTCCAA	60

The plate was checked for any air bubbles before it was loaded on the StepOnePlus™ Real-Time PCR System (Applied Biosystems®, Singapore). The reaction conditions and reaction of wells were labelled using the software. The amplification was carried out as follows:

Step	Temperature	Duration	Cycles
AmpliTaq® Fast DNA Polymerase, UP Activation	95°C	10 min	HOLD
Denature	95°C	15 sec	40
Anneal/Extend	Specific to primer	10 sec	40

The SYBR green dye I when added to the sample, immediately binds to all the double stranded DNA. The AmpliTaq® Fast DNA Polymerase amplifies the target which creates the PCR product. The next step of denaturing double-stranded DNA to single-stranded molecules releases the SYBR Green I dye. The primers anneal the single-stranded DNA molecules which get amplified by AmpliTaq Gold creating double-stranded DNA which will be the PCR product. The SYBR Green I dye now binds to these newly formed double amplicons and as the products increase, intensity of the fluorescent signal increases reflecting the quantity of the amplicons.

For stationary cultures, the samples without growth factors were considered as the reference sample while the cultures which were not subjected to any mechanical deformation were reference samples in the mechanical deformation study. *ACTB* (β-actin) and *GAPDH* (glyceraldehyde-3-phosphate dehydrogenase) were the two housekeeping genes used as endogenous

controls. The reaction for each sample was set up as duplicates in the 96-well reaction plate.

4.3.9.2 Data analysis – Comparative C_T method:

The changes in gene expression of the test sample relative to the reference sample were represented as relative quantification (RQ) values which were determined using the comparative C_T ($\Delta\Delta C_T$) method. The StepOne Plus™ Version 2.1 software (Applied Biosystems®, Singapore) measured the target amplification of the endogenous control in the samples and the reference sample. Measurements were normalized using the endogenous control. The cycle threshold (C_T) values, the relative measure of the concentration of the target were measured and averaged for the duplicates to get the mean C_T value. The relative quantity of a gene in a sample was calculated and displayed by the software using the $2^{-\Delta\Delta CT}$ formula and by comparing its normalized value to the normalized target quantity in the reference sample. The gene expression was quantified and averaged for four individual (biological replicates) runs with duplicates.

4.3.10 Agarose gel electrophoresis

The PCR products were checked by electrophoresis with 1.5% agarose gel stained with 1 X SYBR™ safe gel stain (Invitrogen, Singapore). 2µl of 6X loading Dye (10Mm Tris-Hcl0.03% bromophenol blue, 0.03% xylene cyanol FF, 60% glycerol and 60Mm EDTA) (Fermentas, Singapore) was mixed with 8µl of the PCR products and loaded against 8 µl of 100 bp DNA ladder (Fermentas, Singapore). The gels were run for 55 min at 75v in 1xTBE. The

gels were observed by a UV transillumination in a BioRad imaging system using Quantity One® v 4.6 software.

4.3.11 MTS assay for cell proliferation

For the mechanical deformation experiments, the measurement of cell proliferation using confocal microscopy was not possible as the laser beam could not penetrate the silicone membrane used to support cell cultures in Flexcell Bioflex plates. Hence, cell proliferation was measured by the CellTiter 96® AQueous One Solution Cell Proliferation Assay (Promega, Singapore), a colorimetric assay for estimating cell viability in proliferation based on the ability of viable cells to reduce novel tetrazolium compound [3-(4,5-dimethylthiazol-2-yl)-5-(3-carboxymethoxyphenyl)-2-(4-sulfophenyl)-2H-tetrazolium, inner salt; MTS(a)] and an electron coupling reagent (phenazine ethosulfate; PES) by mitochondrial NADPH or NADH dehydrogenase enzymes (1,2) into a colored formazan product soluble in tissue culture medium. At the end of each time point, the supernatant was removed and 1.2ml of MTS solution (200µl of CellTiter 96® AQueous One Solution reagent/ml of DMEM) was added to each well of the tissue train plates. The plates were incubated at 37^{o}C, 5% CO_2 atmosphere for 30 minutes in the dark from which 100µL was transferred to a 96-well flat bottomed plate. The absorbance measured at 490nm by an uQuant microplate spectrophotometer (Biotek, Singapore) for the quantity of formazan product is directly proportional to the number of viable cells in the culture. The incubation time was chosen to be 30 minutes as the solution reached a

saturation level which was above the detectable reading limit of the spectrophotometer.

4.3.12 Enzyme-linked immunosorbent assays

The enzymes and growth factors secreted in the media which was collected at the end of each experiment were estimated by using Enzyme-linked immunosorbent assays (ELISAs). The media stored in cryogenic vials at -80^{o}C were brought to room temperature by leaving it to thaw on bench top. A selection of four proteolytic enzymes used by fibroblasts to remodel the extracellular matrices were assayed: Matrix metalloproteinase MMP-1 (collagenase-1); MMP-2 (gelatinase-A; 72 kDa); MMP-3 (stromelysin-1); and TIMP-1 (tissue inhibitor of metalloproteinase-1) (Quantikine® colorimetric sandwich ELISAs, R&D Systems China, Shanghai, China) and two growth factors: CTGF (connective tissue growth factor) and FGF-2 (fibroblast growth factor) (Aviscera Bioscience, Santa Clara, CA, USA). The protocol was followed as per the manufacturer's instructions. Each kit was tested for the working concentration of samples prior to the experimental use. Though the volumes of reagents and samples were used based on each kit's protocol, the basic procedure involved the steps below:

1. Reagents, samples and standards were brought to room temperature and prepared to the concentrations as instructed.
2. The specified volume of assay diluent was added to each well of the 96-well plate, pre-coated with monoclonal antibody specific for each protein.
3. The standards and samples were pipetted into each well and incubated for 2 hours at room temperature on a horizontal orbital shaker set at 200 ± 50

rpm. During this time, the desired protein present in the sample is bound by the immobilized antibody.

4. Each well was aspirated and washed four times with the wash buffer for any unbound substances. After the last wash, the plate was inverted on clean paper towels and made sure of removing any remaining wash buffer.
5. An enzyme-linked polyclonal antibody specific for the protein was added to each well.
6. The plate was again washed as in step.4, to remove any unbound antibody-enzyme reagent.
7. Equal volumes of stabilized hydrogen peroxide and chromogen (tetramethylbenzidine) were mixed together to form the substrate solution which was added to each well and incubated for 30 minutes and protected from light. The colour developed during this time is proportion to the amount of the protein bound in the initial step.
8. 50 µL of stop solution containing 2N sulphuric acid was added to each well in the same order as the substrate solution to stop the activity of substrate solution. The colour changes from blue to yellow upon addition after a thorough mixing of both the solutions.
9. Intensity was measured at 450 nm using a microplate spectrophotometer (Biotek, Singapore).

4.3.13 Statistical analysis

Differences between groups were determined by Student's t-test (two-tailed) using GraphPad Prism (GraphPad Software Inc., San Diego, CA, USA) with the level of significance set at $P < 0.05$.

4.4 Results

The preliminary experiments were done on the 35 mm 6-well Type 1 collagen coated plates as tissue cultures since the wells were the same diameter as the Type 1 collagen coated wells of Tissue Train plates with the added advantage of allowing the confocal microscopy's laser beam pass through the wells' surface. During the initial few days of culture, the cells remained rounded and randomly distributed in the construct (Figure 4.5 A, B). By the first week, some cells were starting to resume fibroblast morphology with the central two-thirds of the wells being densely populated and the one-third towards the periphery (Figure 4.5 C, D). After two weeks onwards, the cells became organized at gel-substrate interface and the surface as two layers (Figure 4.5 E-H).

The effect on addition of CTGF/FGF-2 showed a significant increase in the number of viable cells when compared to the controls (Table 4.1). However, the number of viable cells progressively increased every week and plateaued (Figure 4.6) from two weeks onwards in both the experimental and control cultures with the number of non-viable cells constantly remaining around 5%. The cells formed a dense fibrillar closely clustered layer of growth. This could be a possible reason for the plateaued effect on the number of live cells as the cells were constrained to proliferate in a limited growth space. Though the addition of growth factors had an effect on cells' viability, there were no marked morphological changes seen between the two cultures. In order to optimize the growth-time and conditions of the cells in these hydrogel constructs, the culture was observed until 6 weeks. The number of viable cells

started to decrease after five weeks while the number of non-viable cells increased to 14 % in cultures with growth factors and 12% in those without growth factors.

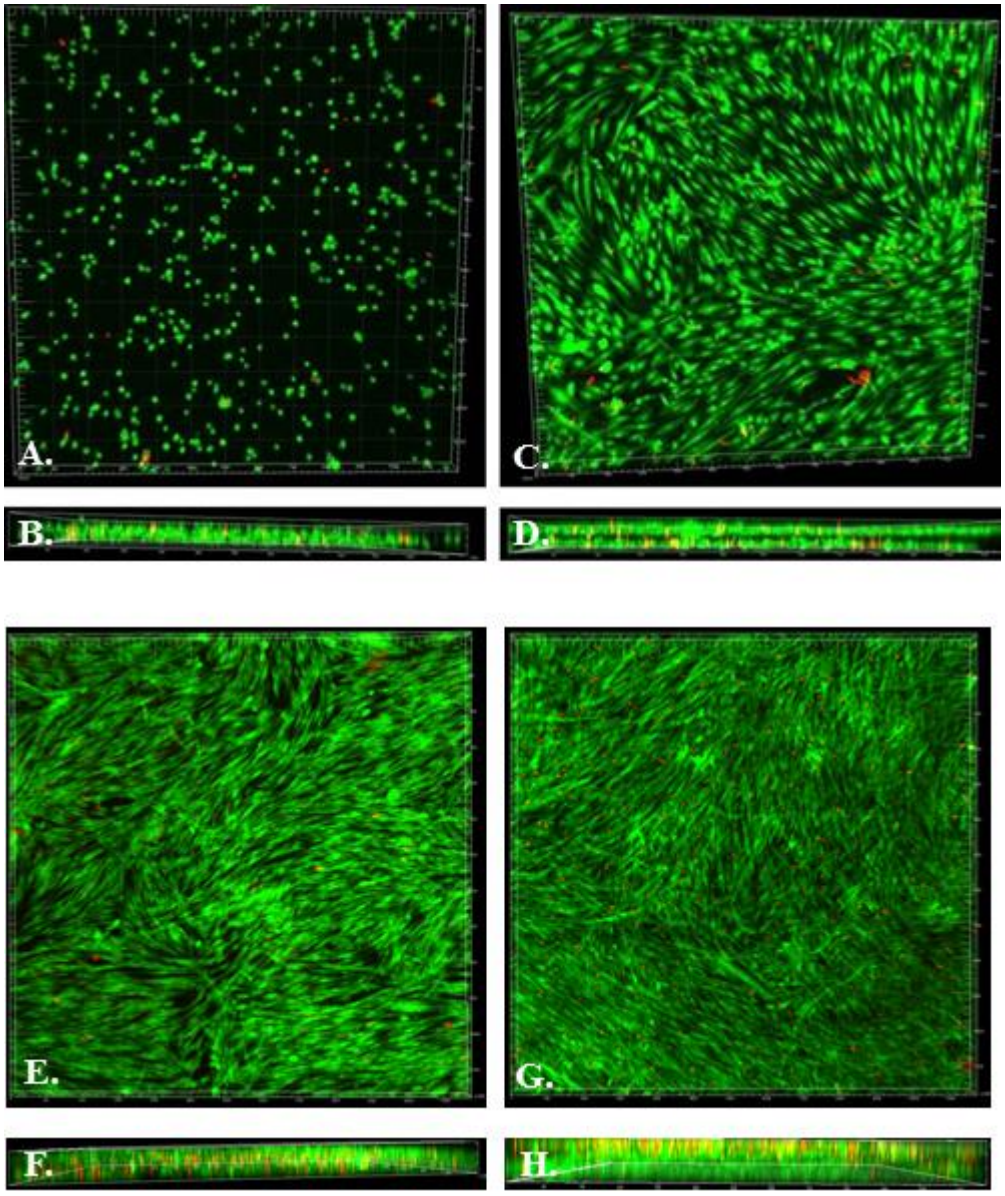

Figure 4.5. Human periodontal ligament cells in Extracel™ thin films constructs cultured in 35 mm diameter type I collagen coated six-well plates and images taken after each time point at 10 x magnification during confocal microscopy as described in previous chapters. The images A, C, E, G are taken as view from above (stacked view) and the images B, D, F, H are their cross-sectional view. (A &B) 24 hours, cells remain rounded and randomly distributed; (C & D) 7 days when proliferated cells organize themselves as double layer ; (E & F) 14 days, cell viability number reached its plateau; (G & H) 21 days (Saminathan *et al*., 2013).

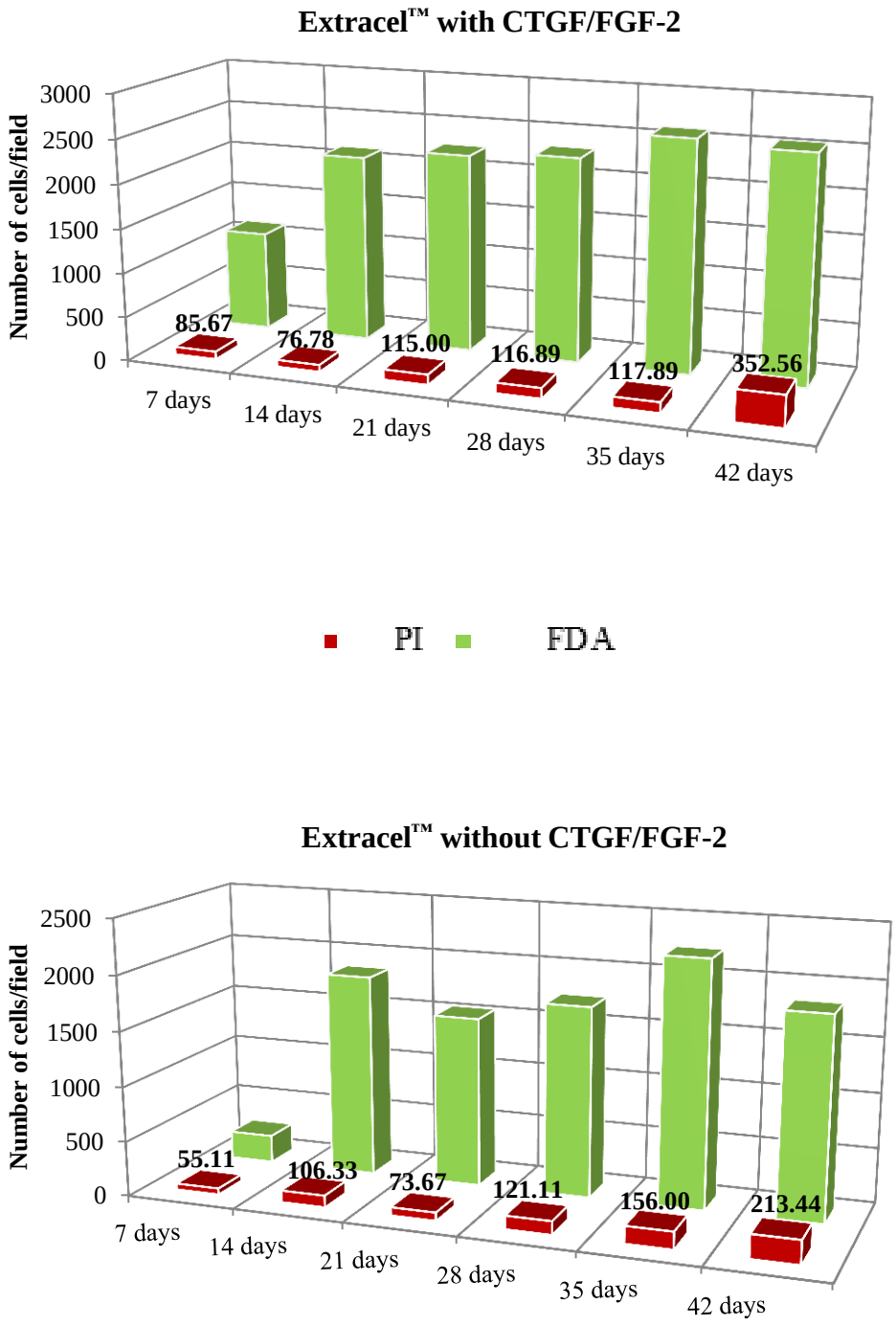

Figure 4.6. Viability of human periodontal ligament cells incorporated into Extracel™ thin film constructs. Data represents the average number of cells counted from three chosen fields (1200 µm x 1200 µm) of the samples to give 9 readings (n = 9) and counted using Imaris software (version 6.1.5) after confocal microscopy.

Time	Control	Experimental
7 Days	288.44 ± 47.04	1127.44 ± 59.22 ***
14 Days	1619.67 ± 234.50	2185.89 ± 156.14 ***
21 Days	1543.00 ± 76.36	2239.78 ± 44.52 ***
28 Days	1731.67 ± 117.89	2304.89 ± 52.43 ***

Table 4.1. A comparative tabulation of the average number of viable cells in cultures of Extracel™ with (Experimental) and without (Control) CTGF/FGF-2. Addition of CTGF/FGF-2 has significantly increased cell viability. ***$p < 0.001$.

Triple staining for actin, vinculin and DNA and observing under confocal imaging gave a detailed imaging concept of the cells behavior in the hydrogel matrix. Figure 4.7 shows the orientation of actin filaments within the cell (stained red) linked to the matrix through the focal adhesion points (stained green) and the cell's nuclei stained with the blue fluorescence. The images showed a morphological difference between the growth of cells on the gel-substrate interface and the surface. The cells appeared as elongated fusiform fibroblasts on the surface (Figure 4.7A) which resembled a two-dimensional culture while the cells assumed an amoeboid-like morphology (Figure 4.7C) at the gel-substrate interface.

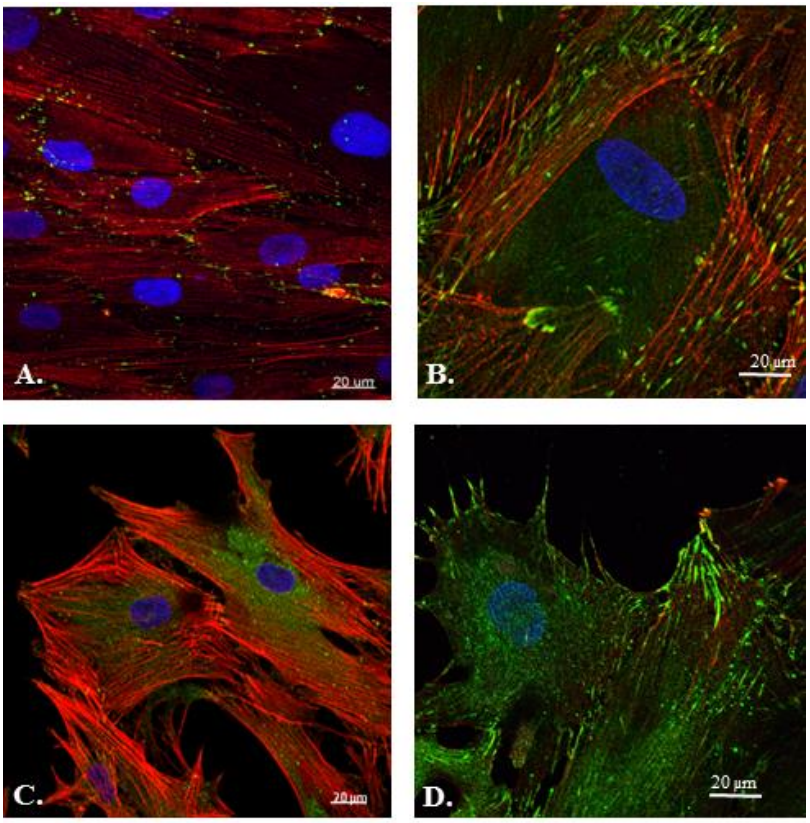

Figure 4.7. Confocal immunofluorescent images of human PDL cells in Extracel™ thin films stained with vinculin antibody for focal adhesions (green), TRITC conjugated-phalloidin for actin filaments, DAPI for DNA. (A,B) Fusiform fibroblasts formed on the surface of hydrogel; (C,D) Fibroblasts with amoeboid-morphology at the gel-surface interface. Scale bar measures 20 µm (Saminathan *et al*., 2013).

Scanning electron microscopy provided a closer view to understand the surface structure of the cells and the hydrogel yielding high resolution three-dimensional images of the cells, the dense network of hyaluronan and gelatin fibrils (Figure 4.8). However, the lack of stiffness of the gel was a disadvantage when attempting to examine the tissue constructs by SEM, the specimens collapsing during the critical point drying stage of preparation. Hence, the images showing the density of the fibrillary matrix (Figure 4.8F) are likely to be exaggerated by shrinkage during dehydration.

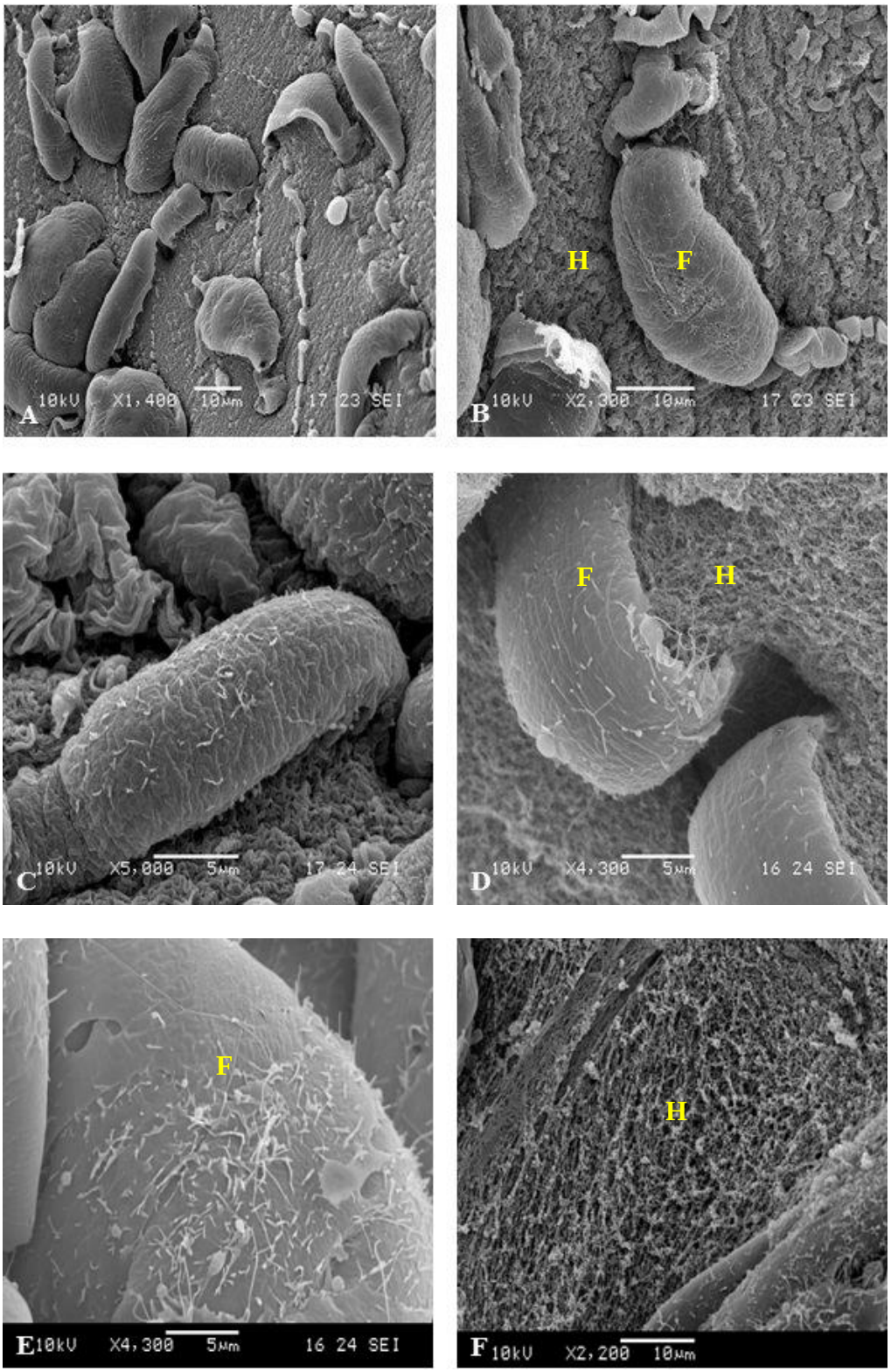

Figure 4.8. Scanning electron micrograph of (A) & (B) Human PDL fibroblasts embedded on the surface of Extracel™; (C) & (D) Cells' interaction with the hydrogel at a higher magnification; (E) Surface of a single fibroblast; (F) Dense network of cross-linked hyaluronan and gelatin fibrils of the hydrogel matrix; this is likely exaggerated to some extent by dehydration during specimen preparation. Yellow labels: F - Fibroblast; H- Hydrogel.

The effect on gene expression by the addition of CTGF and FGF-2 was analyzed on a panel of 18 genes. The detectable threshold cycle number in the RT-PCR was chosen to be < 35. Any gene that crossed this fractional cycle number was considered non-detectable. The C_t values obtained from the analysis of both the stationary and mechanically stressed cultures suggested that 12 genes were detected with C_t values < 35 (Table 4.2, 4.3). In stationary cultures, the RQ values suggested that addition of growth factors had modest effects on gene expression. There was at least one fold induction at some experimental time point for all the genes except *TIMP1*. *COL1A1, TGFB1* and the osteoblast-specific transcription factor *RUNX2* were upregulated with more than two-fold inductions (RQ > 2) after two weeks of culture while the collagenase gene *MMP1* was upregulated during all the three time points. The six genes which failed to express with C_t values > 35 are *SOX9, MYOD, SP7, BMP2, BGLAP* or *COL2A1*. Melt curve analysis was done for these failed genes and it showed multiple peaks. To eliminate the possibility for the presence of any DNA contaminants or formation of primer dimers in addition to a low yield of PCR product by these genes, agarose gel electrophoresis results confirmed that there was no PCR product for these non-detectable genes. Clear, single bands were obtained from the amplicons of 12 expressed genes matching with their corresponding molecular weights calculated while designing the primers. The intensity of the bands from the experimental cultures was slightly higher than its controls. However, the intensity did not totally represent the RQ values obtained from RT-PCR. Hence, agarose gel analysis was only used to check the quality of the PCR products (Figure 4.9). In mechanically active environment, the RQ values show that the tensile force

had induced gene expression at least to one fold increase at some experimental time point for all the genes.

Table 4.2. Effect of growth factors on gene expression by human periodontal ligament cells.

	7 days	14 days	21 days
P4HB	1.41 ± 0.73	0.72 ± 0.25	0.44 ± 0.19
RUNX2	0.94 ± 0.27	2.01 ± 0.77	2.21 ± 0.82
PPARG	1.48 ± 0.84	0.95 ± 0.30	0.53 ± 0.25
COL1A1	0.81 ± 0.35	3.35 ± 0.49	1.27 ± 0.82
COL3A1	0.89 ± 0.37	1.35 ± 0.25	0.61 ± 0.27
MMP1	4.02 ± 1.18	4.62 ± 1.42	3.16 ± 0.86
MMP2	1.21 ± 0.82	0.47 ± 0.26	1.45 ± 1.03
MMP3	0.42 ± 0.18	0.31 ± 0.09	1.15 ± 0.46
TIMP1	0.78 ± 0.26	0.3 ± 0.19	0.66 ± 0.57
TGFB1	0.97 ± 0.35	0.82 ± 0.38	3.07 ± 0.71
RANKL	1.06 ± 0.16	1.14 ± 0.28	0.61 ± 0.22
OPG	0.67 ± 0.37	1.29 ± 1.08	0.83 ± 0.23

Gene expression was quantified by real-time RT-PCR. The data is cross-sectional, expressed as RQ (relative quantity), and represents the mean of four separate determinations. RQ values >1.00 signify an increase in gene expression by growth factor-treated cultures over controls; those exceeding 2.00 are highlighted (Saminathan *et al*., 2013).

COL3A1, *MMP1*, *TIMP1*, and *OPG* were seen to be upregulated with RQ > 2.00 in the mechanically stressed cultures with and without CTGF/FGF-2. In the absence of the growth factors, *RUNX2* and *PPARG* were seen to be upregulated in addition to *MMP3* across all the three time points. *MMP3* showed a RQ value of 13 after 21 days of stress in both the cultures (Table 4.3 A). *COL1A1* and *MMP2* were upregulated (Table 4.3 B) by mechanical stress in the presence of CTG/FGF-2 with just one fold higher than being expressed in the absence of the growth factors. To summarize, except for *PPARG*, there was no significant synergistic effects between the effects of mechanical stress alone and CTGF/FGF-2. The PCR products checked on agarose gel gave clear, single bands matched to their molecular weights as calculated. The six

genes which were not expressed showed multiple peaks in the melt curve. No bands were obtained on the agarose from their PCR products confirming the absence of any non-specific products or primer dimers (Figure 4.5 and Appendix 3).

Table 4.3.A. No growth factors ± mechanical stress

	7 days	14 days	21 days
P4HB	0.78 ± 0.21	0.84 ± 0.15	1.08 ± 0.10
RUNX2	0.86 ± 0.29	1.13 ± 0.12	2.62 ± 0.48
PPARG	0.49 ± 0.15	1.00 ± 0.39	3.00 ± 0.41
COL1A1	0.87 ± 0.21	1.53 ± 0.45	1.40 ± 0.09
COL3A1	2.02 ± 0.92	0.98 ± 0.19	3.14 ± 1.15
MMP1	0.44 ± 0.18	1.48 ± 0.67	4.31 ± 1.46
MMP2	1.00 ± 0.25	1.44 ± 0.58	1.83 ± 0.17
MMP3	2.66 ± 0.47	2.56 ± 0.26	13.47 ± 2.27
TIMP1	0.88 ± 0.23	2.10 ± 0.17	2.71 ± 0.62
TGFB1	0.78 ± 0.27	1.13 ± 0.48	1.03 ± 0.14
RANKL	0.12 ± 0.01	0.56 ± 0.38	1.12 ± 0.40
OPG	1.26 ± 0.11	2.31 ± 0.84	5.02 ± 1.37

Table 4.3.B. Growth factors ± mechanical stress

	7 days	14 days	21 days
P4HB	0.85 ± 0.10	0.91 ± 0.42	1.02 ± 0.22
RUNX2	1.20 ± 0.41	1.66 ± 0.17	1.38 ± 0.37
PPARG	1.47 ± 0.36	1.78 ± 0.18	1.00 ± 0.26
COL1A1	0.85 ± 0.08	2.01 ± 0.73	0.84 ± 0.15
COL3A1	1.49 ± 0.24	1.35 ± 0.52	3.46 ± 0.45
MMP1	1.06 ± 0.26	2.05 ± 1.13	5.41 ± 1.70
MMP2	0.88 ± 0.27	2.34 ± 0.65	2.11 ± 0.33
MMP3	0.77 ± 0.10	1.53 ± 0.62	13.00 ± 4.49
TIMP1	1.17 ± 0.22	3.45 ± 0.62	5.54 ± 1.70
TGFB1	0.63 ± 0.11	1.39 ± 0.22	1.05 ± 0.46
RANKL	0.12 ± 0.05	0.05 ± 0.02	0.63 ± 0.59
OPG	0.37 ± 0.13	2.58 ± 1.06	2.28 ± 0.31

Table 4.3.A&B. Effect of mechanical stress on gene expression by human periodontal ligament cells ± CTGF (100 ng/mL) and FGF-2 (10 ng/mL), ± cyclic mechanical strain for 6 h/day and gene expression quantified by real-time RT-PCR. The data is cross-sectional, expressed as RQ (relative quantity), and represents the mean of four separate determinations. RQ values >1.00 signify an increase in gene expression by mechanically-active cultures over the corresponding controls; those exceeding 2.00 are highlighted.

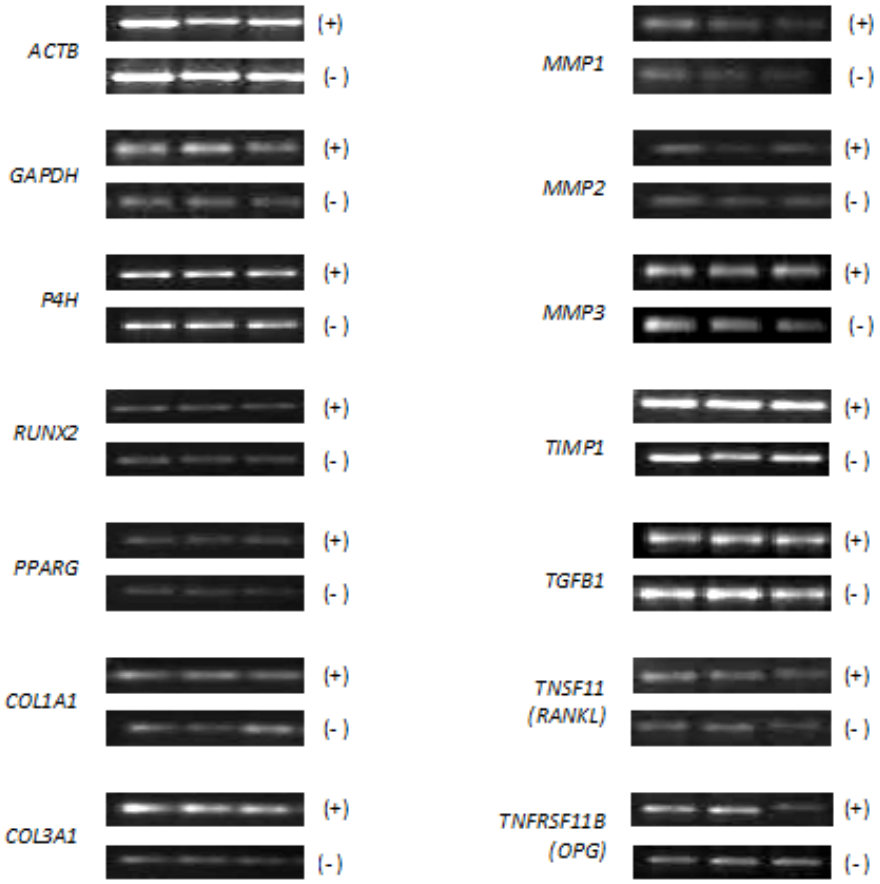

Figure 4.9. Agarose gel electrophoresis of amplified real-time PCR products following reverse transcription of RNA extracted from PDL/Extracel constructs cultured with (+) and without (–) CTGF (100 ng/mL) and FGF-2 (10 ng/mL) for 7, 14 and 21 days in 35 mm 6-well plates. The images are representative examples of the results of four independent experiments (Saminathan *et al*., 2013).

At protein level, mechanical stress had induced the synthesis of MMP-3 and TIMP-1 at a significant level during all the time points in the absence of CTGF/FGF-2 (Figure 4.10). MMP-1 and 2 were at significantly higher levels after 7 days and 21 days of mechanical stimulation. In cultures supplemented with CTGF/FGF-2, mechanical stress for 3 weeks had significantly increased the synthesis of MMP-1-2-3 and TIMP-1 (Figure 4.11). After 7 days, significantly higher levels of MMP-2 and TIMP-1 were synthesized while

their levels decreased after 21 days in both the control and experimental cultures. At the same time point, decrease in synthesis at a significant level was also seen in the MMP-1 and MMP-3 of the control cultures.

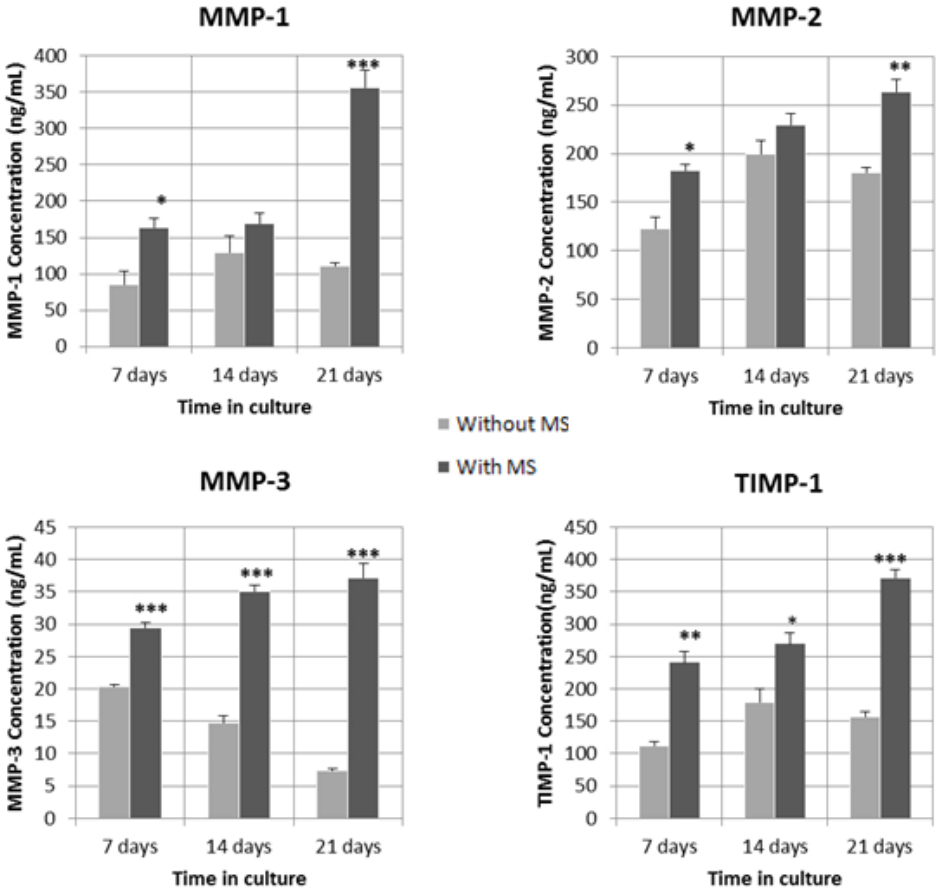

Figure 4.10. MMP-1–3 and TIMP-1 synthesis by human PDL cells in Extracel films subjected to mechanical stress. At each end-point the culture media from 6 wells was pooled in pairs and assayed in triplicate. The data is cross-sectional and expressed as means ± SEM. *$p < 0.05$, ** $p < 0.01$, ***$p < 0.001$ (Saminathan *et al*., 2013).

Cell culture with CTGF/FGF-2

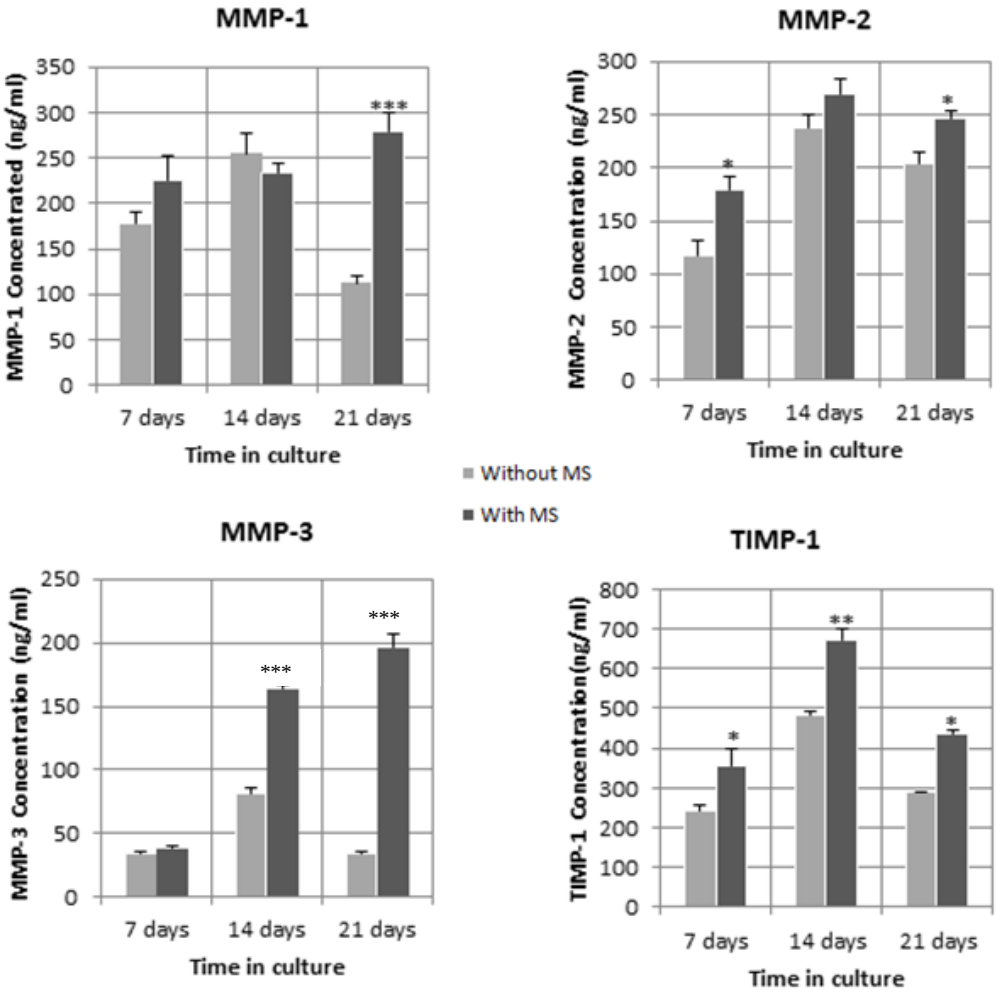

Figure 4.11. MMP-1–3 and TIMP-1 synthesis by human PDL cells supplemented with CTGF/FGF-2 in Extracel films subjected to mechanical stress. At each end-point the culture media from 6 wells was pooled in pairs and assayed in triplicate. The data is cross-sectional and expressed as means ± SEM. *$p < 0.05$, ** $p < 0.01$, ***$p < 0.001$.

MTS (tetrazolium) assay was performed to exclude the possibility that the increase in gene and protein expression in mechanically-stressed cultures were due to an increase in cell population. The results (Table 4.4**)** showed that mechanical stress did not have a significant effect on the cell proliferation across all the three time points. Supernatants from these cultures were also

assayed to check if CTGF was constitutively synthesized by the cells. Picograms level of CTGF was synthesized (Figure 4.12) by the cells but mechanical strain did not have any significant effect on the synthesis.

Table 4.4. Effect of mechanical strain on periodontal ligament cell proliferation measured by the colorimetric MTS (tetrazolium) assay to detect living cells; data represented are mean ± SEM absorbance values measured at 490 nm for six wells from three separate experiments. Mechanical strain did not have a significant effect on cell number.

	7 days	**14 days**	**21 days**
Control	0.281 ± 0.017	0.864 ± 0.136	1.104 ± 0.105
Experimental	0.225 ± 0.015	0.838 ± 0.116	0.996 ± 0.100

Figure 4.12. Effect of mechanical strain on synthesis of CTGF by human PDL cells. The data are cross-sectional and expressed as means ± SEM. There was no statistically significant difference between control and mechanically stressed cultures (Saminathan *et al*., 2013).

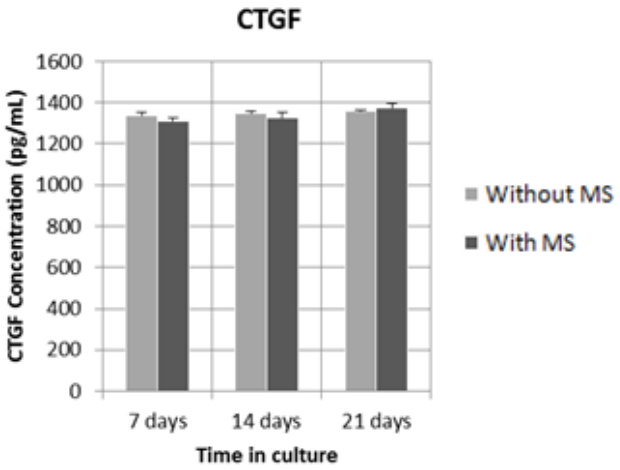

4.5 Discussion

This study has demonstrated an attempt to analyze the complex *in vivo* environment by engineering a three dimensional construct which overcomes the limitations of the existing two dimensional systems. Numerous previous studies have employed various natural and synthetic biomaterials like polyesters (poly(lactic acid) and poly(glycolic acid)) and type I collagen as hydrogels or scaffolds for such investigations (literature review). While synthetic materials lack biochemical signals occurring *in vivo*, type I collagen, though a naturally occurring major structural protein in connective tissues, it tends to contract when seeded with fibroblasts and cultured for longer period of time (Haas *et al*., 2001; Huang *et al*., 2006) unless in the presence MMP inhibitors (Myers and Wolowacz, 1998; Bildt *et al*., 2009). Various studies on the characterization of ECM molecules suggest at least two important molecules as the primary structural component of the matrix which varies from collagen, heparin, fibrin, hyaluronan. These molecules contributes to the structural integrity while the matrix proteins regulate the cell-matrix interactions for the cells to function in a three dimensional environment.

In this study, the commercially available Extracel™ provided a combined matrix form of two major structural molecules hyaluronan and collagen (Saminathan *et al*., 2013). Preliminary experiments on designing thin-film constructs supported a growth pattern that enabled the cells to assume the fibroblast phenotype though it formed a double layer one at the gel-substrate interface and gel-surface.

In order to accelerate the growth of PDL cells, connective tissue growth factor (CTGF) and fibroblast growth factor-2(FGF-2) were incorporated into the gel matrix and culture media (Dangaria *et al*., 2009; Tong *et al*., 2011). Connective tissue growth factor (CTGF/CCN2) is a cysteine-rich, extracellular matrix (ECM) protein that acts as an anabolic growth factor for fibroblasts and other connective tissue cells (Igarashi *et al*., 1993). CTGF has been implicated as a key regulatory factor in complex biological and pathological processes including wound healing, angiogenesis and fibrotic disorders (Igarashi *et al*., 1993; Grotendorst, 1997; Alfaro *et al*., 2013). CTGF is mitogenic and chemostatic for fibroblasts and is selectively induced by TGF-β (Kothapalli *et al*., 1997). Recently, CTGF has been shown to direct fibroblast differentiation from PDL progenitor cells (Dangaria *et al*., 2009) and mesenchymal stem cells, which strongly suggests that CTGF functions in the PDL to maintain the fibroblast phenotype. FGFs exert their physiological roles through binding FGFR and regulate developmental pathways, controlling events such as mesoderm patterning in the early embryo through development of multiple organ systems, mitogenesis, cellular migration, differentiation, angiogenesis, and wound healing (Shimabukuro *et al*., 2005; Yun *et al*., 2010). In this study, though addition of CTGF/FGF-2 to stationary cultures had significantly increased cell viability, effect at mRNA level was limited. The concentrations of CTGF/FGF-2 used in this study were referred from Dangaria *et al*., 2009. The authors found that addition of CTGF/FGF-2 showed a significant up regulation of *COL1A1* and *COL3A1* by the PDL cells seeded in the collagen gel constructs. The present data partially supports this finding since there was at least one fold induction of these genes but not at significant level. But

COL1A1 and *COL3A1* were found to be mechanoresponsive genes even in the absence of growth factors.

Previous studies including ours on two dimensional culture systems, have shown that CTGF is a mechanoresponsive gene. However, our present data does not confirm this finding and the addition of CTGF/FGF-2 to either stationary or mechanically stressed constructs was of limited benefit. In retrospect this is not surprising, given that, real-time RT-PCR microarrays (Wescott *et al*., 2007; Pinkerton *et al*., 2008) have shown that *in vitro* PDL cells express numerous cytokines and growth factors that exhibit overlapping biological activities (redundancy), as well as multiple biological effects (pleiotropy); suggesting that endogenous production of growth factors by the cells was sufficient to promote growth (Saminathan *et al*., 2013).

PDL cells contain a heterogenous group of cells and also show multipotential capability to differentiate into osteoblasts, chondroblasts, myoblasts and adipocytes (Seo *et al*., 2004; Gay *et al*., 2007). CTGF/FGF-2 and mechanical stress had upregulated the osteoblast-specific transcription factor *RUNX2* However, we could not detect the downstream mediators of osteogenesis such as SP7 (Osterix), BMP2 or BGLAP (Osteocalcin) suggesting that *RUNX2*-expressing osteoprogenitor cells were part of the mesenchymal stem cell pool. Whereas, Tang *et al*.,(2012) found an up-regulation of the *RUNX2*, and *SP7* when PDL cells were subjected to a cyclic tensile force. Although it was not surprising that *MYOD*, a key regulator of skeletal muscle lineage and *SOX9*, a chondrocyte specific collagen II regulator were not detected, adipocyte related

transcription factor PPARG and its responsiveness to mechanical strain was intriguing. PPAR-c ligands induce bone marrow stem cell adipogenesis but also inhibit osteogenesis (Zhao *et al*., 2008a), and the secretion of adipocyte hormones such as leptin, which affect bone development, goes some way to explaining the poorly understood pathophysiological association between fat and bone.

The genes for RANKL and OPG, were expressed in both the stationary and mechanically induced cultures where OPG being highly responsive to mechanical stress while RANKL was downregulated. Regardless of the initiating signal, the RANK/RANKL/OPG triad is a ligand-receptor system regulates the final stages of bone resorptive cascade (Khosla, 2001; Kanzaki *et al*., 2002). The finding that PDL cells also express RANKL and OPG has drawn wide interests on *in vitro* studies of bone remodelling and has found that both genes are upregulated by compressive and tensile mechanical strain (Kanzaki *et al*., 2002; Tsuji *et al*., 2004; Kanzaki *et al*., 2006; Kim *et al*., 2013). The reasons for this are not clear, but may be related to limiting ossification of the ligament; the clinical observation that most ankylosed teeth are lower deciduous molars out of occlusion (Biederman, 1962) is perhaps relevant. Estimating the OPG protein synthesis after mechanical stress would be more interesting to investigate the role of osteoclastogenesis.

MMPs playing key role in cell-cell and cell-matrix interactions, function at neutral pH and are released as latent proforms, activation of which involves the loss of a propeptide of about 80 residues (Reynolds and Meikle, 1997).

TIMP-1 is the major form, closely regulates MMP activity as an inhibitor by forming high affinity, essentially irreversible complexes with the activated enzyme to prevent uncontrolled resorption. Mechanical stress had stimulated the three major secreted MMPs, MMP-1 (collagenase- 1), MMP-2 (gelatinase-A) and MMP-3 (stromelysin-1), as well as their inhibitor TIMP-1 at a significant level and the genes encoding these proteins were also upregulated. Although the level of TIMP-1 synthesis was higher than the MMPs, it is difficult to conclude whether the latter is involved in the degradation of pericellular matrix. A study using a 3D finite element model by Zhao *et al*., (2008b) found a significant increase of TIMP-1 and type I collagen being increased in the tensile zones while MMP-1 was increased in both the zones. The MMP-1 ELISA we have used, only recognizes proMMP-1. Hence, it will be appropriate to do additional research using activity assays and gelatin and casein zymography to establish whether the enzymes are in the active, latent or complex forms. Our two dimensional culture study, we found that human PDL cells constitutively expressed 16 members of the MMP family (Saminathan *et al*., 2012) which included seven MMPs, three MT-MMPs (membrane type-MMPs) and three ADAMTSs (a disintegrin and metalloproteinase with thrombospondin motifs), a family of proteinases anchored to the extracellular matrix whose actions include cleavage of the matrix proteoglycans aggrecan and versican (Porter *et al*., 2005), plus three TIMPs. This establishes that there are plenty of alternative enzymes for matrix degradation depending on the substrate. It will be more interesting to quantify type I collagen to draw the regulation sequence after determining the existing forms of the degrading enzymes. But it should also be noted that enzymes like

for example, MMP-1 which cleaves native collage can act as gelatinase (Saminathan *et al*., 2013).

This study was a novel technique in an aspect of engineering a 3-dimensional construct using a hydrogel with two primary molecules of ECM as the matrix component (Saminathan *et al*., 2013). Understanding of cell alignment is of concern in tissue engineering because cells tend to orientate relating to the loading direction (Lee *et al*., 2007; Xie *et al*., 2012). From our previous study, we found that under tensile stress, cells align to the direction of the stress (Saminathan *et al*., 2012) and many studies done both on 2D and 3D cultures have reported cells aligning along or perpendicular to the direction of stretch (Neidlinger-Wilke *et al*., 2002; Wang *et al*., 2004; Park *et al*., 2006). Cell alignment being a passive process (Pedersen and Swartz, 2005), it still remains unclear of how much it is an active cellular response to the force. Studies on subjecting cells in collagen gels, to mechanical strain reported and interpreted for its cells alignment as to deposit more collagen along its direction to shield themselves from the strain (Birk and Trelstad, 1984; Eastwood *et al*., 1998; Roeder *et al*., 2002).This reinforcement by producing more ECM has been reported from a study on cyclic strain on 2D synthesizing collagen, hyaluronate (Leung *et al*., 1976) and while in a 3D environment, collagen XII was increased both at mRNA and protein expression level. These reports of cellular alignment and increase in matrix synthesis together suggest that cells are involved in reinforcing their environment in the principle direction of strain (Pedersen and Swartz, 2005). Failure of penetration of laser beam through the silicone membrane during confocal microscopy was a drawback

and limitation to observe these changes after mechanical stretch. It would have been interesting to co-relate these sequential events in our model.

Effect of cyclic stretch have been reported to increase (Butcher *et al*., 2006; Webb *et al*., 2006) or decrease (Hannafin *et al*., 2006) or have no difference (Balestrini and Billiar, 2006) on cell proliferation. Our study showed no significant difference in cell proliferation due to mechanical stress while our previous study showed a contrasting result. With all these data, it seems that effect of tensile strain on cell proliferation still remains controversial and unclear.

In summary, we have demonstrated that the addition of a third dimension provides another level of complexity to the existing two-dimensional culture systems designed to investigate the mechanobiology of the PDL. While thin films are suitable for studies of tensile strain, thicker constructs will be needed for investigating the effects of compression. This will require increasing the complexity of the scaffold by incorporating additional structural molecules such as type I collagen and fibronectin into the matrix to provide extra RGD (Arg-Gly-Asp) binding sites; these will aid cell attachment, proliferation and function, enabling cells to populate the entire gel, while the triple helices of intact collagen will stiffen the matrix. Although primarily developed as a transitional in vitro model for studying cell–cell and cell–matrix interactions in tooth support, the system is also suitable for investigating the pathogenesis of periodontal diseases, and importantly from the clinical point of view, in a mechanically active environment.

5. Engineering and characterizing three-dimensional tissue constructs under compressive force

5.1. Introduction

Mechanical stress applied to the crowns of teeth during orthodontic treatment and/or mastication stimulates the tissues of the PDL, setting in motion the series of cellular and molecular events that lead to bone remodelling and tooth movement. At this point, the general agreed theory is that tissue tension generated in the PDL is associated with bone formation, and compression with bone resorption. As discussed in previously *in vitro* attempts to understand the biochemical responses of the PDL to mechanical stimuli involved the simulation of such mechanical/functional environment, by subjecting bones or osteoblasts to a variety of mechanical forces, including fluid shear, uni-axial or bi-axial stretching, hydrostatic compression, or a combination of two or more of these forces. Most of the *in-vitro* investigations that have been conducted to date have looked at the expression of chemical mediators such as prostaglandins (PGs), interleukins (IL-1, IL-6, IL-8, IL-10) and alkaline phosphatase (ALP) activity by human PDL cells subjected to tensile strain (Saito *et al*., 1991; Yamaguchi *et al*., 1994; Chiba and Mitani, 2004; Tang *et al*., 2012) and microarrays which allow the activity of numerous genes to be monitored simultaneously have also been reported (de Araujo *et al*., 2007; Wescott *et al*., 2007; Yamashiro *et al*., 2007; Pinkerton *et al*., 2008; Saminathan *et al*., 2012). Very few studies have investigated the effect of compressive strain on the genetic expression of PDL cells *in vitro*; most have

applied compression to PDL cells by the method developed by Kanai *et al.* (1992), where a cylindrical disk was placed over nearly confluent PDL cell layers and compression applied by inserting lead granules in the cylinder. The technique was later taken to a 3-dimenisonal level by incorporating PDL cells into a type I collagen gel matrix (de Araujo *et al*., 2007; Lee *et al*., 2007; Li *et al*., 2013). All these model systems employed only a static force to simulate the *in vivo* orthodontic tooth movement.

In this study, human PDL cells cultured in Extracel™ were subjected to a programmed cyclic compressive force using the FX-4000C™ Flexercell® Compression Plus™ System (Flexercell Corporation, Hillsborough, North Carolina). To date, compressive loading has not been carried out on human PDL cells using this 3 dimensional model and machine. The 80-100μm thick thin film constructs designed for tensile studies were not suitable for investigating the effects of compression, which required thicker constructs. To increase the gel's complexity and provide extra RGD (Arg-Gly-Asp) binding sites, type I collagen was added to the HA-GLN matrix before subjecting it to cyclic pressure.

5.2. Aims

1) To engineer a tissue construct model of a human PDL at a 3-dimenional level that can be subjected to a compressive force using the Flexercell® machine.
2) To study the effects of cyclic compressive strain on gene expression and apoptosis of human PDL cells.

5.3. Materials and methods

5.3.1. Stationary culture –Preliminary characterization

Equal volumes of Gelin-S and Glycosil from the Extracel™ kit were mixed well as described in Chapter 3, section 3.2.2.1. Rat tail type I collagen (Cat# C3867-1VL; Sigma Aldrich, Singapore) solution was added to the mix at an optimized concentration of 1.3 mg/mL to give a ratio of 1:1:1. Human PDL cells were mixed in this Gelin-Glycosil-Col1 solution at a concentration of 5 X 10^6 cells/mL, to which 1 part of Extralink was added to produce a ratio of 1: 3. Three hundred µL of the hydrogel mix was transferred to each of the 13 mm rings placed in a 60 mm Petri dish. These constructs measure about 1000 µm in thickness which mimics the samples that will be subjected to compression as described in the next section. After one hour incubation for gelation at 37^{o}C incubator, 10 mL of culture media was added and the growth was observed for three weeks.

5.3.2. Application of compressive strain

5.3.2.1. Sample preparation

Human PDL cells were incorporated in the hydrogel as described above. Compression strain was carried out using the BioPress™ culture plates (Figure 5.1) and baseplate clamping assembly (Flexcell International Corporation, Hillsborough, NC). The BioPress™ culture plate contains a foam ring and sample holder. As the thickness of the compressed foam is 350 µm, to ensure compressibility, the optimum thickness of the sample should be 1000 µm. The sample holders were removed from the foam rings using a pair of sterile

forceps and 300 µL was transferred to each of the 13 mm (internal diameter) foam rings in the six well BioPress™ plate. Gelation occurred for one hour in the 37^{o} C incubator ; 5 mL of culture media was added to each well and cultured at 37^{o}C in a humidified atmosphere of 5% CO_2/95% air for two weeks prior to mechanical loading using the FX-4000C™ Flexercell® Compression Plus™ System (Figure 5.1, Flexercell Corporation, 61, Hillsborough, North Carolina).

5.3.2.2. Sample loading

Stationary platens were placed over the gel samples in both the experimental and control plates (Figure 5.1). The platens were adjusted by rotating the center screws until it touches the gel. Care was taken to not screw the center down too far to avoid preloading of the sample which might give inaccurate force readings. The experimental group of BioPress™ compression plates was placed on top of the gaskets in the baseplate.

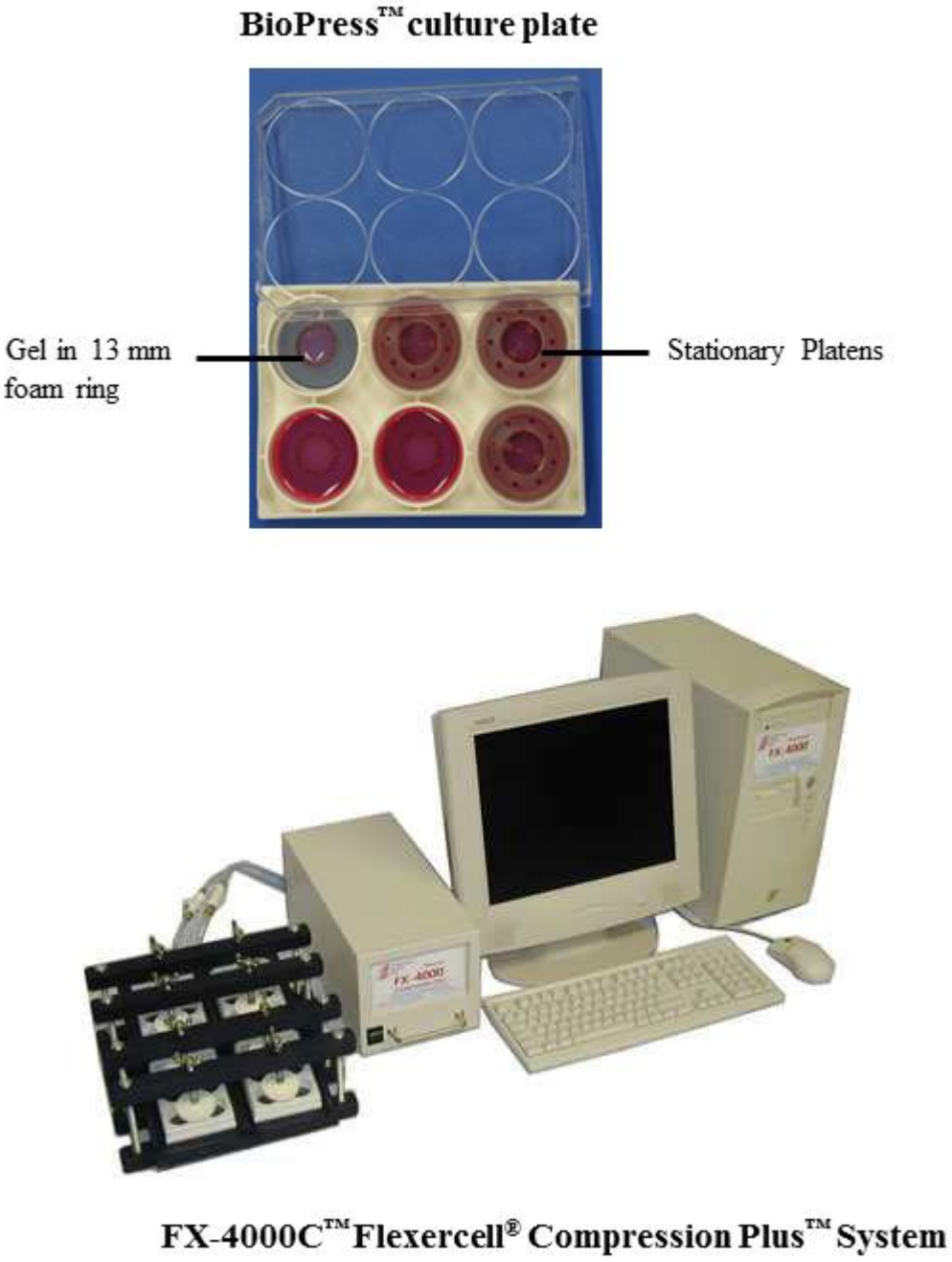

Figure 5.1. BioPress™ plate (above) with human PDL cells embedded in Extracel™ cast in the central 13 mm foam ring to form thicker constructs (900-1000µm). Below: A picture adapted from the Flexcell user's manual showing the Stationary platens placed in the wells and assembled with Plexiglas® window in the clamping system and connected to a PC controlled by installed software.

In the clamping system, the eight clamping pads were adjusted to their maximum height and turned so that the bottom of each pad was parallel with the surface of each baseplate. The Plexiglas® window was placed into the clamping system, evenly along the bottom of the four clamping bars. The baseplate assembly was carefully slid into the clamping system so that the BioPress™ plates were centered under the clamping pads. The wing nuts on the clamping pads were turned until they were finger tight. This was to compress the plates downward onto the gaskets, creating a seal. The entire assembly was placed into the incubator and the *FLEX IN* and *FLEX OUT* fittings were attached on the compression baseplate. A positive pressure is created underneath the BioPress™ compression plates by the compressor and this pressure provides the force required to push the BioPress™ culture plates against the stationary platen. This results in compression of the gel samples. The control group with the platens was also placed in the incubator and was termed as the positive control group.

5.3.2.3. Compression Regimen

The pressure applied to the sample in the well of the BioPress™ plate is dependent on the surface area of the sample to which the force is being applied (Flexercell® Compression Plus™ V4.0 user's manual). The pressure was programmed by using the formula provided by the company which converts the desired force to pressure.

$$P_{MPa} = (5.65* Force_{lbs})/(D_{mm}{}^{2})$$

Where P_{MPa} is the pressure applied to the sample in megapascals (MPa), $Force_{lbs}$ is the force entered into the regimen or displayed on the software screen in pounds and D_{mm} is the diameter of a single sample in mm.

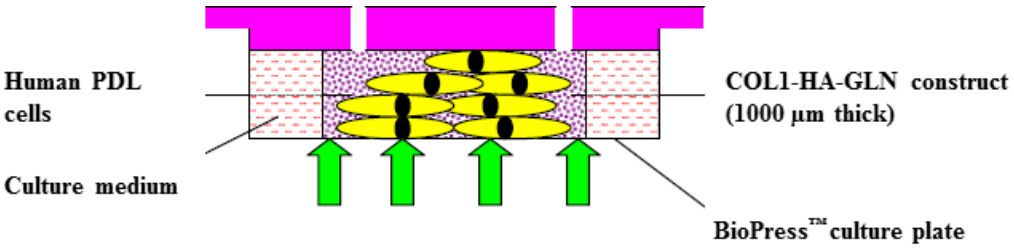

Figure 5.2. Compression loading on human PDL cells using the Flexcell® machine. The cells were embedded in 13 mm COL1-HA-GLN constructs in the culture plate. Pressure was applied underneath the membrane and the hydrogel is compressed against the surface of the platen.

The compression regimen was programmed to expose the gel the samples to a cyclic compression of 1.0 lbs (0.453 kg) for 1.0 sec (1 Hertz) every 60 sec, for 6, 12 and 24 hours. As per the formula, 1.0 lbs force translates into a compressive strain of 33.4 kPa (340.6 gm/cm^2). The minimum force recommended by the Flexcell Corporation for operating the Flexercell FX-4000C unit is 0.5 lbs; in view of the likelihood that about half the applied strain will be transmitted to the cells, a force of 1.0 lb was programmed into the computer.

5.3.3. Cell viability and apoptosis

The effect of compression on cell viability and apoptosis was determined by the FDA/PI staining method and Caspase 3/7 assay respectively.

5.3.3.1. Confocal microscopy

After each experimental time period, the BioPress™ plates were carefully removed from the clamping system. The platens were removed from both the experimental and control groups. Media was aspirated from the wells. As the laser beam of the confocal microscope does not pass through the membranes of the BioPress™ plates, samples had to be transferred to a surface which allows viewing of the cells. Hence, the membranes were cut off using a scalpel and using a sterile pair of forceps, the foam ring around the sample was carefully removed without disturbing the sample. Using a sterile flat bottomed spatula, the gel was lifted up and transferred to a 24-well flat bottomed (Corning® Costar® cell culture plates, Sigma Aldrich, Singapore) plate. The same technique was followed for the apoptosis assay and overnight cell recovery process for RNA extraction. FDA/PI staining and confocal microscopy was carried out as described in Chapter 3, section 3.2.3.

5.3.3.2. Caspase 3/7 assay

At the end of each time point the constructs were removed and transferred as described in section 1.3.3.1. Two constructs were placed in each well to which 500 µL of the Caspase Glo® 3/7 reagent was added and incubated for 1 h in the dark at room temperature according to the manufacturer's instructions. Each sample was aliquoted into triplicate tubes and luminescence, expressed

as relative light units (RLU), measured with a Sirius Single Tube Luminometer (Berthold Detection Systems GmbH, Pforzheim, Germany).

5.3.4. RNA extraction and RT-PCR

The gel constructs were transferred as described in section 5.3.3.1 and the cells were recovered and RNA extracted as described in Chapter 4, section 4.3.4**.** The quality of RNA was checked before proceeding with the cDNA synthesis.

The effect of compression on gene expression was investigated on apoptotic genes (Table 5.1) in addition to the 18 extracellular genes of (Page 103), using real time RT-PCR as described in Chapter 4, section 4.3.1. Genes with threshold values from 33-35 were considered non-detectable.

5.3.5. Protein quantification

Media was aspirated before the gel constructs were treated for cell recovery process and stored in -80^{o}C for protein quantification using ELISAs. Commercially available kits were purchased to estimate the following:

1) A selection of proteolytic enzymes; MMP-1 (matrix metalloproteinase-1; collagenase-1); MMP-2 (gelatinase-A); MMP-3 (stromelysin-1) and TIMP-1 (tissue inhibitor of metalloproteinases-1) obtained from (R&D Systems China, Shanghai, China)
2) The cell-cell signaling molecules RANKL (receptor activator of nuclear kappa factor B) and OPG (osteoprotegerin) from (Cusabio Biotech, Wuhan, China).

3) The growth factors CTGF (connective tissue growth factor) from (Aviscera Bioscience, Santa Clara, CA, USA) and FGF-2 from (R&D Systems China).

The stored media was thawed to room temperature and were assayed in triplicates for protein according to the manufacturer's instructions.

5.3.6. Statistical analysis

Differences between groups were determined by Student's t-test (two-tailed) using GraphPad Prism (GraphPad Software Inc., San Diego, CA, USA) with the level of significance set at $P < 0.05$.

Table 5.1. Apoptosis-related genes and primer sequences used for real-time RT-PCR.

HGNC agreed gene symbol	Description	Primer sequence	Annealing temperature
TNFA	Tumor necrosis factor, alpha	F: GAGCACTGAAAGCATGATCC R: CGAGAAGATGATCTGACTGCC	60
TNFRSF1A	Tumor necrosis factor receptor superfamily, member 1A	F: TGCCTACCCCAGATTGAGAA R: ATTTCCCACAAACAATGGAGTAG	60
TNFRSF1B	Tumor necrosis factor receptor superfamily, member 1B	F: GCGAGTTACAGCTAAAGCAT R: TTATGCAACATGACCTTGGA	60
TNFSF10	Tumor necrosis factor receptor (ligand) superfamily, member 10	F: GAGCTGAAGCAGATGCAGGAC R: TGACGGAGTTGCCACTTGACT	60
IL1A	Interleukin 1-Alpha	F: CCCAACACCTGGACCTCGGC R: CGTAGGCACGGCTCCTCAGC	60
IL1B	Interleukin 1-Beta	F: AAGCTGAGGAAGATGCTG R: ATCTACACTCTCCAGCTG	60
IL6	Interleukin 6 (interferon, beta 2)	F: TGCGTCCGTAGTTTCCTTCT R: GCCTCAGACATCTCCAGTCC	60
CASP1	Caspase 1, apoptosis-related cysteine peptidase	F:AATACTGTCAAATTCTTCATTGCAGATAAT R: AAGTCGGCAGAGATTTATCCAATAA	60
CASP2	Caspase 2, protein phosphatase 1, regulatory subunit 57	F: GCACTGAGGGAGACCAAGCA R: CACAGCTCAACGGTGGGAGTA	60
CASP3	Caspase 3, apoptosis-related cysteine protease	F: AGAACTGGACTGTGGCATTGAG R: GCTTGTCGGCATACTGTTTCAG	60
CASP6	Caspase 6, apoptosis-related cysteine peptidase	F: GGCAGTTCCCTGGAGTTCAC R: GACCTTCCTGTTCACCAGCG	60
CASP7	Caspase 7, apoptosis-related cysteine peptidase	F: AGTGACAGGTATGGGCGTTCG R: GCATCTATCCCCCCTAAAGTGG	60
CASP8	Caspase 8, apoptosis-related cysteine peptidase	F: CTCCCCAAACTTGCTTTATG R: AAGACCCCAGAGCATTGTTA	60
CASP9	Caspase 9, protein phosphatase 1, regulatory subunit 56	F: CGAACTAACAGGCAAGCAGC R: ACCTCACCAAATCCTCCAGAAC	60
CASP10	Caspase 10, apoptosis-related cysteine peptidase	F: AATCTGACATGCCTGGAG R: ACTCGGCTTCCTTGTCTAC	60

5.4. Results

Our first attempts at engineering PDL constructs for compression studies involved incorporating PDL cells into Extracel in a circular format (13 mm x 1.0 mm), designed to fit BioPress™ culture plates. FDA-PI staining and confocal microscopy showed that on encapsulation the cells adopted a rounded morphology and retained high viability over a 4-week time-course (Chapter 3). Nevertheless, it was clear from side views that the body of matrix was relatively sparsely populated. Only at the hydrogel surface and the gel-substrate interface did the cells appear to achieve confluence and assume a fibroblastic phenotype suggesting the HA-GLN scaffold was insufficiently stiff to facilitate cell attachment (Chapter 3). We therefore added type I rat tail collagen to provide additional RGD (Arg-Gly-Asp) binding sites on the triple-helices of intact collagen, and this enabled the cells to populate the full thickness of the gel (Figure 5.3 B&D). However, by the 3rd and 4th weeks of culture, in common with all collagen containing hydrogels, the constructs showed a tendency to contract. Two-week COLI-HA-GLN constructs were therefore used in all loading experiments which minimized this complication, although we did find that owing to their low modulus of elasticity, the compression regimen reduced the thickness of the constructs to around 300–400 μm.

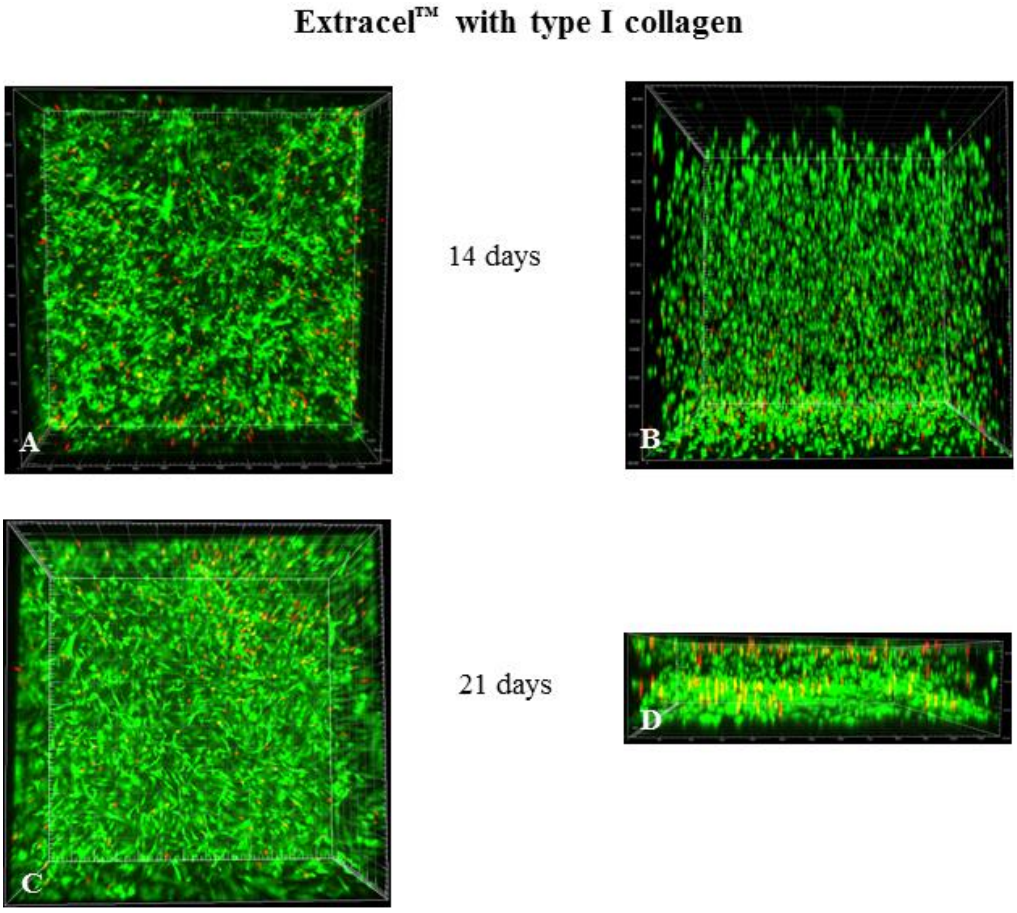

Figure 5.3. Human PDL cells (5 x 10^6 cells/mL) in Extracel™ incorporated with rat tail type I collagen (1.3 mg/mL) and cultured on 13 mm rings placed in 60 mm Petri-dishes. Images were taken by confocal microscopy from an area of 1200 x 1200 µm of each sample at 10 x magnification. (A) View from above after 14 days; (B) Cross-sectional view after 14 days measured 1000µm thick; (C) View from the top after 21 days; (D) Cross-sectional view after 21 days when the hydrogel contracted to 300 µm thickness.

Cyclic compressive strain resulted in a significant increase in the number of nonviable cells after 12 h and 24 h loading (Figure 5.5); however, it was only possible to count the dead cells – the dense fibrillary growth of the viable cells made their quantification impossible (Figure 5.4). The increase in the number of cells undergoing programmed cell death was confirmed by the Caspase 3/7 assay, which was significantly upregulated across all three time-points (Figure 5.5), and to investigate this further, we measured the expression of a number

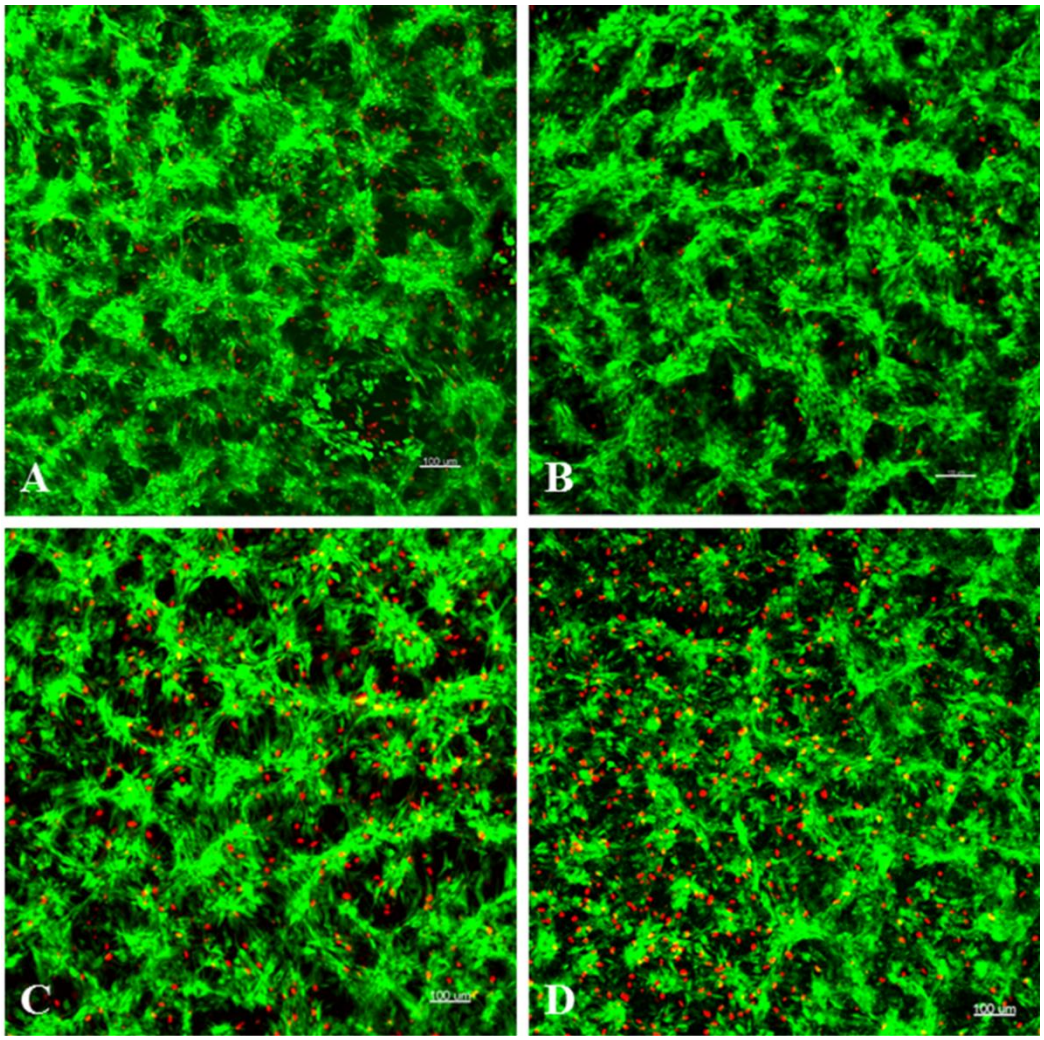

Figure 5.4. Confocal microscopy images (10 x) of the samples after each cyclic compression time point. Non-viable cells (red) were chosen to count due to the dense and clustered appearance of the viable cells (green). (A) Control culture; (B) 6 hours of compression did not make much difference compared to the control culture. A significantly higher number of non-viable cells were seen after 12 hours (C) and 24 hours (D) of 33.4 kPa compressive force.

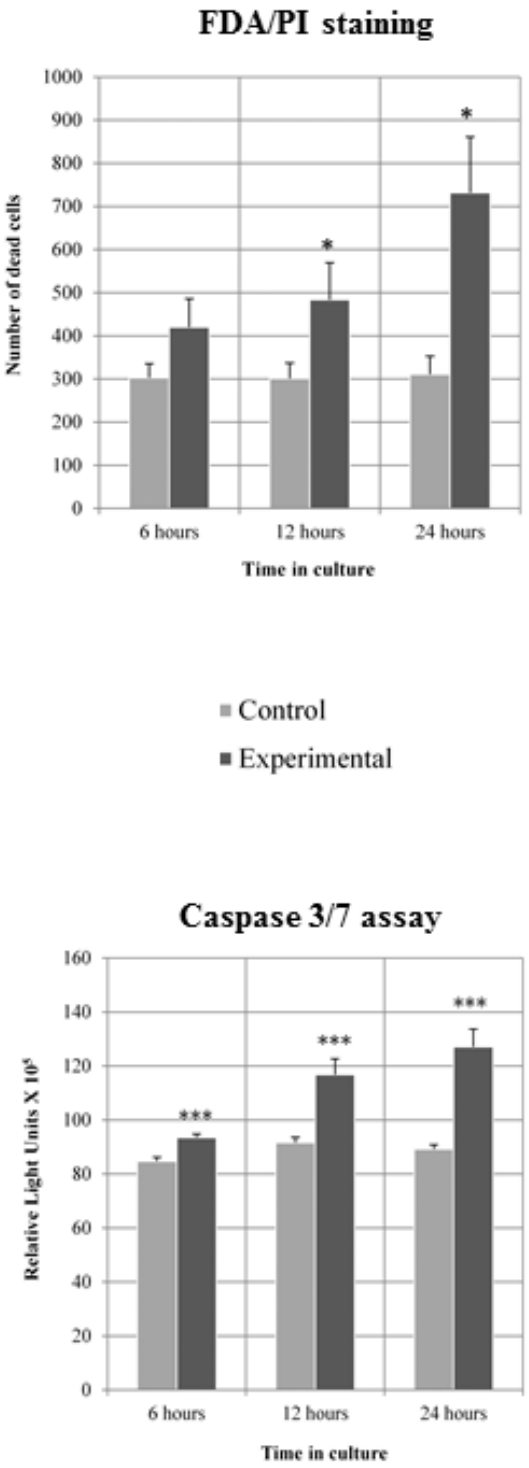

Figure 5.5. A compressive strain of 33.4 kPa has a significantly increased induced cell death of human PDL cells in COL1-HA-GLN constructs. Confocal microscopy cell count showed a significant effect after 12 and 24 hours (histogram above); Caspase 3/7 assay showed results of a very high significance on the induction of apoptotic-cell death after all the three time points. *$p < 0.05$; ***$p < 0.001$.

Table 5.2. Effect of cyclic compressive strain on the gene expression of apoptosis-related genes.

	6 h	12 h	24 h
TNFA	0.28	1.56	0.24
TNFRSF1A	0.26	0.38	1.24
TNFRF1B	ND	ND	ND
TNFSF10	0.80	0.70	2.45
IL1A	0.64	0.52	2.00
IL1B	0.39	1.17	0.74
IL6	1.17	0.60	0.71
CASP1	0.53	1.40	1.76
CASP2	0.68	0.96	1.48
CASP3	0.35	0.73	0.89
CASP6	0.23	1.08	1.17
CASP7	0.40	0.49	1.03
CASP8	0.67	0.55	1.59
CASP9	0.49	0.20	1.11
CASP10	0.24	0.68	2.18

The significant increase in apoptotic cell death assayed (previous page) was confirmed by the up-regulation of apoptosis-related genes quantified by real-time RT-PCR. The data are cross-sectional, expressed as relative quantity (RQ) and the mean of two separate determinants. All the genes were up-regulated by at least one fold induction (RQ > 1.00) at some time point. Relative quantity values > 2.00 are highlighted. ND: Not detected.

of genes playing key roles in apoptosis (Table 5.2). *TNFRSF1A*, *TNFSF10* (*TRAIL*) and *IL1A* were all significantly upregulated after 24 h, the latter two by RQ values > 2.00. TNFA, IL1B, and the caspase inhibitor gene *IL6* in contrast, were downregulated at the same time-point. Each of the eight caspases (cysteine-dependent aspartate-directed proteinases) involved in the apoptosis signalling cascade showed a progressive increase in expression (Table 5.2). These included the interleukin-1-converting enzyme *CASP1*, and the initiator caspases *CASP2, CASP8, CASP9* and *CASP10*, which cleave the inactive proforms of the executioner caspases *CASP3*, *CASP6* and *CASP7*;

these in turn cleave other intracellular protein substrates to trigger the apoptotic process.

While the osteoblast-specific transcriptions factor *RUNX2* and its chondrogenic counterpart *SOX9* were initially expressed, they were not detectable in 24h cultures; and adipocyte and myoblast-specific transcription factors *PPARG* and *MYOD* were not detected at any time point. However, *P4HB* a gene that is abundantly expressed by cells synthesizing collagen and a useful marker for the fibroblast phenotype was expressed at 6h and 12h, although it had declined by 24h (Table 5.3). Of the fifteen extracellular matrix genes screened, twelve were detected at Ct values < 35; BGLAP, the gene encoding the bone matrix protein osteocalcin, SP7 (Osterix) the osteoblast transcription factor acting downstream of RUNX2, and the cartilage-specific collagen gene COL2A1, all failed to be identified. At 6h cyclic compressive strain significantly increased the expression of COL1A1, MMP1 and MMP3 by RQ values > 2.00, and in the case of CTGF > 3.00 at both 6h and 12h. Although most genes were upregulated at some point with RQ values > 1.00 after 6h and/or 12h deformation, all were down-regulated in the 24h cultures except for the three MMPs and CTGF (Table 5.3).

Table 5.3. Effect of cyclic compressive strain on gene expression by PDL cells

	6 h	12 h	24 h
P4HB	1.05 ± 0.14	0.96 ± 0.11	0.54 ± 0.05
RUNX2	0.43±0.07	0.96 ± 0.09	ND
SOX9	0.76 ± 0.19	1.60 ± 0.18	ND
PPARG	ND	ND	ND
MYOD	ND	ND	ND
COL1A1	2.89 ± 0.54	1.08 ± 0.15	0.93 ± 0.29
COL2A1	ND	ND	ND
COL3A1	1.61 ± 0.23	1.2 ± 0.09	0.31 ± 0.04
MMP1	2.2 ± 0.28	0.45 ± 0.12	1.12 ± 0.23
MMP2	1.51 ± 0.20	0.81 ± 0.16	1.23 ± 0.21
MMP3	2.41 ± 0.98	1.08 ± 0.19	1.30 ± 0.42
TIMP1	0.71 ± 0.16	0.78 ± 0.13	0.59 ± 0.06
TGFB1	0.5 ± 0.14	1.41 ± 0.66	0.47 ± 0.06
BGLAP	ND	ND	ND
SP7	ND	ND	ND
BMP2	1.41 ± 0.08	1.17 ± 0.07	0.34 ± 0.08
RANKL	1.39 ± 0.39	0.82 ± 0.23	ND
OPG	0.42 ± 0.16	1.13 ± 0.51	0.38 ± 0.11
CTGF	3.15 ± 0.56	3.09 ± 0.97	1.92 ± 0.56
FGF2	1.56 ± 0.23	1.77 ± 0.63	0.63 ± 0.21

Gene expression was quantified by real-time RT-PCR on a panel of 20 extracellular matrix genes. Of the 15 genes expressed, 12 were up-regulated with RQ >1.00 at some time point of the compression. The data are cross-sectional, expressed as relative quantity and represents the mean ± SEM of four separate determinants. RQ values > 2.00 are highlighted. ND: Not detected.

Proteins levels of all three MMPs plus TIMP-1 were identified by ELISAs in culture supernatants from both experimental and control cultures, although the concentrations of MMP-2 and MMP-3 were low in comparison with MMP-1 and TIMP-1. Both of these proteins were significantly upregulated by cyclic compressive strain (Figure 5.6), although after 24h, the concentration of free TIMP-1 (760 ng/mL) in compressed cultures was more than twice that of the pro-form of MMP-1 (360 ng/mL). Mechanical stress did not seem to have a significant effect on RANKL, OPG and FGF-2. But the concentration of OPG

secretion was higher (82-106 ng/mL) compared to the RANKL detected at 61-73 pg/mL. While FGF-2 was detected at low levels of 13-16 pg/mL, CTGF was lower than the detectable levels of the assay (Table 5.4).

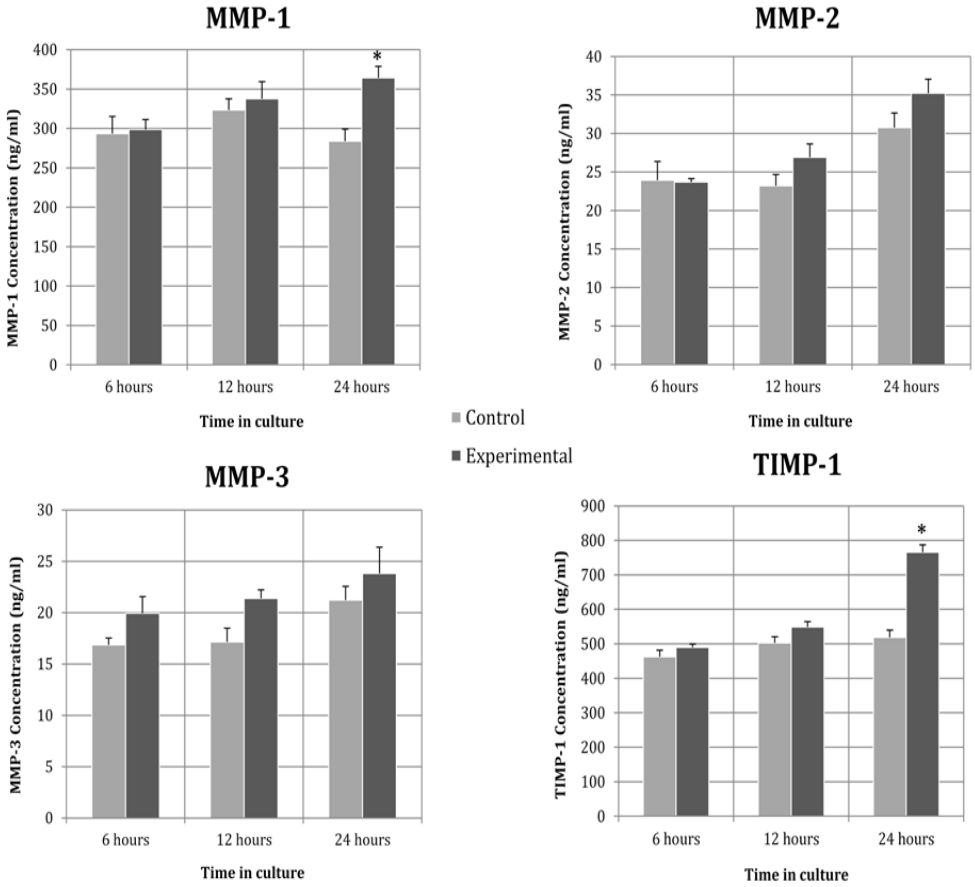

Figure 5.6. A significant up-regulation of MMP-1 and TIMP-1 synthesis by human PDL cells ,was seen after subjecting to 24h of compressive force. At each end-point the culture media from 6 wells was pooled in pairs and assayed in triplicate. The data is cross-sectional and expressed as means ± SEM. *$p <$ 0.05.

Table 5.4. No significant up-regulation was seen on the synthesis of RANKL/OPG, FGF-2. CTGF was synthesized below the detection limit of the assay.

Enzyme		**6 hours**	**12 hours**	**24 hours**
RANKL (pg/mL)	Control	73.69 ± 1.2	61.6±2.4	62.9±2.89
	Experimental	62.5±4.18	59.88±2.2	64.6±4.3
OPG (ng/mL)	Control	82.28±5.3	82.98±4.4	82.42±7.9
	Experimental	91.94±8.3	94.38±1.2	106.21±6.2
FGF-2 (pg/mL)	Control	14.40±0.73	14.01±0.71	13.29±0.20
	Experimental	14.92±0.83	15.28±0.08	16.07±1.01
CTGF (pg/mL)	Con/Exp	ND	ND	ND

5.5. Discussion

This study provided progressive insight into the effects of compressive strain on PDL cells through the development of a novel 3D hydrogel construct. The BioPress™ Compression Plus™ system has been used in several studies (http://www.flexcellint.com/documents/FlexcellPublications.pdf) to investigate the effects of compression on chondrocytes, and tissues like cartilage, and meniscus cultured or embedded in gel scaffolds to simulate functional compressive loading.

Unlike collagen fibres, fibroblasts and smooth muscle cells cultured in 3D collagen gels which become aligned perpendicular to the direction of the applied force (Girton *et al*., 2002), PDL cells in COLI-HA-GLN constructs viewed by confocal microscopy showed no particular alignment. However, the amount of deformation in the Girton *et al*. study was much greater at about

50%. A study by (Kwok *et al*., 2013) of human mesenchymal stem cells in collagen gel constructs subjected to cyclic compressive loading for 1 h per day for 1, 3, 5, or 7 consecutive days at a frequency of 1 Hz found that cell alignment did not occur until the 5th day – by day 7, an obvious pattern of alignment was observed along the compression loading axis. Interestingly, the authors found that compression-induced cell alignment was dependent on the concentration of the collagen in the construct.

In the present study a force of 0.5 lbs (230g) was chosen to simulate the orthodontic force. This translates to a pressure of 16.7 kPa (170.3g/cm^2) which is much higher than previous studies; these used forces in the range of 0.5g/cm^2 to 25.0g/cm^2 but were applied continuously not intermittently (de Araujo *et al*., 2007; Lee *et al*., 2007; Kang *et al*. 2013; Li *et al*., 2013). The difficulty in an *in vitro* study such as this, given the wide variety of occlusal loading to which teeth are subjected during mastication, swallowing and speech, is to decide how much force to apply to the cells. In a clinical study of the ideal force levels to be applied to the clinical crowns of teeth during orthodontic tooth movement, Storey and Smith (1952) found the optimal force required to distalize a canine in an orthodontic patient was 200–300 g. However, no clinical studies have yet been reported quantifying force levels in the PDL when a certain level of force is applied to the clinical crown. Technically, it is difficult to determine the stress/strain within the PDL and finite element studies have shown that the stress/strain field is a very complex (Jones *et al*., 2001). In any event, the force magnitude chosen to simulate occlusal force was much lower than that reported by Gibbs et al. (1981) for the

forces produced during swallowing (about 66.5 lbs) and chewing (about 58.7 lbs).

PDL cells, as discussed in the previous chapter are a heterogeneous group of cells which includes mesenchymal stem cells that can differentiate into osteoblast, chondrocytes, adipocytes and myoblasts. The osteoblast-specific transcription factor *RUNX2* and the chondrogenic regulator *SOX9* were expressed initially by 6 and 12 hours, but were not detectable at 24 h. The adipocyte and myoblast-specific transcription factors *PPARG* and *MYOD* were not detected at any time point. However, *P4HB* a gene that is abundantly expressed by cells synthesizing collagen and a useful marker for the fibroblast phenotype was expressed at 6h and 12h, although it had declined by 24h (Table 5.3). Of the fifteen extracellular matrix genes screened, twelve were detected at Ct values < 35; *BGLAP*, the gene encoding the bone matrix protein osteocalcin, *SP7* (Osterix) the osteoblast transcription factor acting downstream of *RUNX2*, and the cartilage-specific collagen gene *COL2A1*, all failed to be identified. At 6h compressive strain significantly increased the expression of *COL1A1*, *MMP1* and *MMP3* by RQ values > 2.00, and in the case of *CTGF* > 3.00 at both 6h and 12h. Although most genes were upregulated at some point with RQ values > 1.00 after 6h and/or 12h deformation, all were down-regulated in the 24h cultures except for the three *MMPs* and *CTGF* (Table 5.3). CTGF serves to regulate cell-matrix interactions and cell functions and directs cells to fibroblast phenotype. These findings together suggest that the stem cell pool was directed towards fibrosis.

Orthodontic tooth movement is characterized by bone resorption at sites of compressive strain (Sandstedt, 1904, 1905; Bister and Meikle, 2013), and because of their role in osteoclast formation and function, RANKL and OPG are considered to be important mediators of resorption at the bone-PDL interface (Khosla, 2001; Yamaguchi, 2009). However, in the present study, although *RANKL* was upregulated at 6 hours, it was downregulated by 12 hours and not expressed at 24 hours; *OPG* was upregulated at 12 hours only, and at the protein level, mechanical stress did not alter the synthesis of either RANKL or OPG. This is in contrast to previous studies with 2-dimensional (Kanzaki *et al*., 2002; Yamamoto *et al*., 2006; Nakajima *et al*., 2008) and 3-dimensional culture systems (Li *et al*., 2013), which have consistently reported increases in *RANKL* or *OPG* expression in PDL cells.

PDL cells and gingival fibroblasts play important roles in bone remodelling and protect abnormal bone resorption respectively (Kook *et al*., 2009). Kook *et al*., (2009) found that mechanical force induced OPG production, inhibiting the osteoclastogenesis through ERK-mediated signalling pathway. The same authors in their investigation on osteoclastogenesis in response to compression force, found that PDL fibroblasts predominantly produced OPG than RANKL . In the present investigation, although there were no significant differences in the synthesis of either OPG or RANKL by PDL cells in response to compression, the levels of OPG detected in the culture supernatants were an order of magnitude (80–100 ng/mL) greater than those for RANKL (60–73 pg/mL).

In a recent analysis of the effect of compressive stress on gene expression of PDL cells, Kang *et al*. (2013) reported an upregulation of RANKL after and 2 and 48 hours of compression in both 2- and 3- dimensional culture systems. Surprisingly, they did not report on OPG activity.

Apoptosis, a form of programmed cell death in which cells are induced to activate their own death or suicide, plays an important role in many pathophysiological processes including embryonic development, tissue remodelling and homeostasis (Wyllie *et al*., 1980; Elmore, 2007). The significant increase in the number of dead cells and the increased expression of a number of apoptosis-related genes, including four initiator caspases (*CASP2*, *CASP8*, *CASP9* and *CASP10*) and three executioner (*CASP3*, *CASP6* and CASP7) caspases (Fan *et al*., 2005; Chowdhury *et al*., 2008), established that apoptotic signaling pathways had been upregulated by the compressive strain. Prolonged exposure to compressive strain inhibits cell proliferation (Li *et al*., 2013). This contrasts with the effect of cyclic tensile strain on cultured PDL cells in 2-dimensional culture systems, which we have previously shown to have a positive, albeit transient effect on apoptosis (Saminathan *et al*., 2012), unless more vigorous strain regimens are applied (Zhong *et al*., 2008; Hao *et al*., 2009; Xu *et al*., 2011) experiments on human lung fibroblasts, for example, have shown that regimens producing 20% cyclic deformation activated apoptotic signaling pathways and cell death (Boccafoschi *et al*., 2007; Boccafoschi *et al*., 2010). In other words, the induction of apoptosis in mechanically-deformed cells appears to be related as one might expect, to the magnitude and frequency of the applied strain, whether it is predominantly

compressive or tensile, and in the case of the PDL, will vary throughout the ligament depending on its anatomical relationship with the roots of the various teeth.

However, the osteoclasts differentiation from M-CSF derived macrophages was assumed to be induced by TNF-α, in a RANKL-independent manner (Azuma *et al*., 2000). TNF-α also promotes RANKL expression by stromal cells and osteoblasts and also induces osteoclast differentiation and bone resorption in the presence of M-CSF, facilitated by RANKL, during orthodontic tooth movement (Takayanagi, 2005; Cho *et al*., 2010; Kook *et al*., 2011). The present finding showed an upregulation of TNF-α at mRNA level only by 12 hours and was down regulated during the remaining two time points.

Furthermore, interleukin genes *IL1A*, *IL1B* and *IL6* that are involved in osteoclast differentiation in addition to TNF and RANKL were upregulated by 24 h, 12 h and 6h of compression respectively while the cytokine *TGF-β* , that has inhibitory effects on osteoclastogenesis (Pérez-Sayáns *et al*., 2010) was upregulated by 12 hours like its counterpart *OPG*. Interestingly, the apoptosis inducing TNF-related ligand *TRAIL* (*TNFSF10*) was expressed, but upregulated after 24 hours of compression. OPG binds and neutralizes TRAIL to block the TRAIL-induced apoptosis (Emery *et al*., 1998). A recent study (Li *et al*., 2013) using static compression force for 6h, 24 h and 72 h on PDL cells encapsulated in PLGA scaffolds has found an increase of osteoclastogenesis inducers initially and longer exposure (72 h) had increased its inhibitors. But

CTGF was reported to be down-regulated due to compression. From our data, we noted a random up and down-regulations of these cytokines and interleukins across the time points at mRNA level, a further understanding of the osteoclastogenesis regulation can be done by the enzyme estimations of *TNFSF10* and *IL1A*.

MMPs are a family of proteolytic enzymes synthesized as either secreted forms or bound to the plasma membrane that function at neutral pH, and play key roles in connective tissue resorption during growth, morphogenesis and pathophysiological remodelling (Murphy and Nagase, 2008; Zitka *et al*., 2010). All are synthesized in latent pro-forms with activation involving the loss of a pro-peptide of around 80 residues. To prevent uncontrolled resorption, the actions of MMPs are closely regulated by TIMPs through the formation of high affinity, essentially irreversible complexes with the activated forms of the enzymes (Reynolds and Meikle, 1997); TIMP-1 is the major form, but four have been described to date. In addition to increased expression of *MMP1*, *MMP2* and *MMP3* following compression, MMP-1, MMP-2, MMP-3 and TIMP-1 protein were all released into the culture media, and interestingly MMP-1 and TIMP-1 levels were significantly higher in 24h cultures despite *TIMP1* expression being downregulated, suggesting increased matrix turnover. However, because these ELISAs only recognize latent proMMP-1 and free TIMP-1, we are not in a position to say whether the enzymes are in the active, latent or complex forms without performing activity assays and zymography. In any event, human PDL cells constitutively express

sixteen members of the MMP family (Saminathan *et al*., 2012), so there are plenty of other alternatives for degrading the matrix.

One problem encountered with incorporating type I collagen into Extracel was a failure of the components to gel with some batches of collagen. Hence, repetitions of the experiments with the new batch of type I collagen was limited. The hydrogel construct with type I collagen incorporation was optimized for two weeks growth when the cells assumed the fibroblast phenotype, as a higher concentration (>1.3 mg/mL) and longer periods of culture caused the hydrogel to contract quickly. Moreover, the commercially purchased rat tail type I collagen (Sigma Aldrich, Singapore) was available by reconstituting in 20mM acetic acid by the manufacturers. PDL cells, initially experienced a survival shock which might be due to the shift in pH to acidic range. A significantly ($p < 0.001$) lower viability rate compared to the Extracel™ without the addition of type I collagen was noted after first week of culture during the preliminary experiments. By the end of second week, the viability number continued to be less, but not at significant level ($p = 0.21$).

Overcoming such limitation, this culture system can be used as a novel construct and investigated for variations in time periods and stress magnitudes so that the effects of compressive loading can be studied in a time- and magnitude-dependent manner that mimics a particular loading concept occurring *in vivo.*

.

6. Overall discussion and future work

To date, attempts to build tissue-engineering strategies are still at the early stage of development to make a significant impact either at the clinical or commercial level (Taba *et al*., 2005; Chen and Jin, 2010; Izumi *et al*., 2011). Nevertheless, our objective in developing 3-dimensional *in vitro* models of the PDL for advancing our understanding of the mechanisms of tooth support and tooth movement derived from 2-dimensional models and *in vivo* animal studies was achieved by this study.

6.1. Mechanical view

The challenge in engineering 3-dimensional constructs using biodegradable biomaterials for *in vitro* studies is to replicate not only tissue complexity, but also the mechanical and viscoelastic characteristics (resistance to elastic deformation or stiffness) of the native tissue, and it is clear that further improvements in the composition of the present constructs are required. For the compression study, although we used close to the minimum level recommended for use with the Flexercell Compression Plus system, a force of 32.4 kPa was at the limit appropriate for deforming the constructs in their present format, highlighting one of the disadvantages of hydrogels – their poor mechanical properties, resulting in tissue constructs with significantly poorer mechanical strength than the real tissue. Analysis of the rheological properties of cross-linked HA-gelatin hydrogels for use in soft tissue engineering has shown that the elastic moduli range from 11 Pa to 3.5 kPa depending on the concentration of the HA; increasing the ratio of gelatin reduced gel stiffness

by diluting the concentration of the HA component. Extracel has a shear elastic modulus of around 70 Pa (Vanderhooft *et al*., 2009), and although it has not been measured, the elastic modulus of the present constructs is likely to be similar to the 90 Pa reported recently for a 3-dimensional collagen gel populated with PDL cells (Kim *et al*., 2011). Type I collagen, a commonly used scaffold material has specific mechanical properties that has been widely investigated (Pedersen and Swartz, 2005; Billiar, 2011) would have altered the existing mechanical property of the Extracel™. The basic changes to be considered are the pH and concentration – pH has been found to be co-related to the stiffness of the gel by altering fibril diameters (Christiansen *et al*., 2000). For example, a gelation pH from 5 to 8 alters the stiffness from 5 to 25 kPa (Yamamura *et al*., 2007).

While this construct may be suitable for imaging cell–cell and cell–matrix interactions in studies of tooth support and periodontitis by immunological methods and confocal microscopy, for tissue engineering applications a much higher stiffness is required. One problem in trying to reconstruct the biophysical properties of the human PDL, a complex fibre-reinforced tissue that responds to mechanical loading in a viscoelastic and nonlinear manner (Jónsdóttir *et al*., 2006), is that for all practical purposes the elastic modulus is unknown. The difficulty of examining a thin tissue (0.1–0.4 mm) sandwiched between bone and cementum has resulted in a lack of consistency regarding its elastic properties, highlighted by a recent systematic review of 23 studies that had used finite element analysis, which found that Young's modulus ranged from 10 kPa to 1750 MPa, a difference approaching six orders of magnitude

(Fill *et al*., 2011). In comparison, the elastic moduli of soft mammalian tissues range from near 100 Pa for soft organs such as the brain, to tens of thousands in muscle and around 300 MPa for Achilles tendon (Levental *et al*., 2006).

Culturing cells in three dimensions complicates the perennial question of the strain profile experienced by the cells. As discussed previously (Chapter 2), this is difficult enough to determine with the methods commonly used to deform cells in two dimensions. When a substrate is deformed, irrespective of whether in-plane or out-of-plane, uniaxial or biaxial, the cells will be exposed to a combination of tensile, compressive and shear strains; the amount of deformation will also vary with the position of the cells within the field, and in the Flexercell system deformation of the substrate will only be about half that programmed into the computer (Vande Geest *et al*., 2004; Wall *et al*., 2007). In the present study, the strain experienced by the cells at the gel–substrate interface, will clearly be different from that experienced by the cells of the surface layer or within the body of the gel. The stress profile is therefore likely to be similar to the complexity revealed by the finite element analysis of the von Mises and principal stresses generated are mechanically loaded *in vivo* (Milne *et al*., 2009).

One thing is certain, understanding the strain distribution within the hydrogel matrix and its effect on the biomechanical behavior of the cells will require sophisticated three dimensional finite element modeling (Pfeiler *et al*., 2008). This suggests that recapitulating the biophysical properties of the next generation of artificial PDL constructs, requires a much more robust

extracellular matrix. Since type I collagen is the major structural protein of the PDL, rather than add collagen to the hydrogel matrix, a more rational approach would be to permeabilize preformed type I collagen scaffolds with a mixture of PDL cells and Extracel followed by gelation.

6.2. Biological view

The molecular data established from both the tensile and compression studies have given a basic knowledge of mechanoresponsive genes to a certain level although not exactly as it occurs *in vivo* which still remains unknown. Introducing a new form of hydrogel and regimen used, although seems novel, the data obtained was not comparable with similar studies. This could be clearly observed from the interpretation of results done in all the chapters. The frequency and magnitude of strain can be similar or referred from previous studies using fibroblasts. But, it should be considered that the mechanical forces which can variedly be shear, compression or tension and the biochemical signals vary with microenvironment of the fibroblasts which can be from lungs, dermal or tendon fibroblasts. The work done by Kook et al., (2012) found that the proliferation rate was stimulated in gingival fibroblasts, while it was inhibited in periodontal ligament fibroblasts by tensile force. In another example, fibroblast cultured in collagen gels exhibit a "compaction" process (Billiar, 2011) and exogenous addition of TGF-β (Halliday and Tomasek, 1995) activates the fibrotic pathway (wound healing) by differentiating fibroblasts into myofibroblasts (Tomasek *et al*., 2002; Li and Wang, 2011). Myofibroblasts have been identified on the tension side of the PDL *in vivo* and in 2D *in vitro* cultures (Meng *et al*., 2010) and the present

tissue constructs could be used to investigate this aspect of oral wound healing.

The results of RANKL and OPG expression did not exactly agree with the previous established studies of PDL cells in 2-D cultures (elaborated in discussion section). The complex up- and down-regulation of transcription factors, apoptotic genes and interleukins still requires a deeper understanding of other possible factors such as other growth factors, effect of cell density, alterations of mechanical properties like stiffness due to collagen incorporation that could have induced different entropy. Another example is the interesting point about the synergistic effect of compression and hypoxia (Li *et al*., 2013). When PDL is subjected to orthodontic force, the compression side is under hypoxic condition due to the shut blood vessels and nutrient deprivation to the interior.

The study could be taken to a next level by choosing specific pathways and gene profiling using microarray analysis which measures the expression of multiple genes. de Araujo *et al.* (2007) conducted a microarray analysis of the response of the PDL cells subjected to static compressive force and demonstrated the complex interactions of genes involved in the biology of tooth movement. It was shown that 108 of 30,000 genes tested were differentially expressed, out of which 85 genes were up-regulated and 23 were down regulated. However, these data were based in treated/control ratios of ±2 and contained no statistics. Targeted microarrays have shown that this will result in numerous false-positives and false negatives (Wescott *et al.*, 2007;

Pinkerton *et al.*, 2008). A recent study (Li *et al*., 2013) on time course analysis of compression force using microarray analysis showed five significant pathways being expressed which included cytokine–cytokine receptor interaction, MAPK, and cell cycle signalling pathways, and Cell–cell signalling. An interesting bioinformatics analysis comparing 2D and 3D culture systems exposed to compressive force have showed MAPK and focal adhesion kinase pathways to be relevant to the compression-induced cellular response (Kang *et al*., 2013), one of the few microarrays on PDL cells exposed to compressive force. Coupled with greater knowledge on the physiological function of the individual gene, the vast information obtained from microarray analysis may help facilitate the understanding of the complex interactions of biological genes during tooth movement.

.

Technical handling of the hydrogel involved a lot more care and attention. The reconstituted Gelin-S and Gelatin of the Extracel™ becomes oxidized if exposed to repeated freeze-thaw cycles. Incubation with trypsin for longer time (Chapter 4, section 4.3.4) during cell recovery process can also reduce cell viability to yield less RNA. Batch to batch variation of type I collagen purchased limited any further repetitions of experiments. These were the technical obstacles and limitations faced while handling the hydrogel.

7. Bibliography

Aguirre JI, Plotkin LI, Stewart SA, Weinstein RS, Parfitt AM, Manolagas SC *et al.* (2006). Osteocyte apoptosis is induced by weightlessness in mice and precedes osteoclast recruitment and bone loss. *Journal of Bone and Mineral Research* **21(4)***:*605-615.

Alfaro MP, Deskins DL, Wallus M, DasGupta J, Davidson JM, Nanney LB (2013). A physiological role for connective tissue growth factor in early wound healing. *Laboratory investigation; a Journal of Technical Methods and Pathology* **93(1)***:*81-95.

Alhashimi N, Frithiof L, Brudvik P, Bakhiet M (2001). Orthodontic tooth movement and de novo synthesis of proinflammatory cytokines. *American journal of orthodontics and dentofacial orthopedics* **119(3)***:*307-312.

Anderson DM, Maraskovsky E, Billingsley WL, Dougall WC, Tometsko ME, Roux ER *et al.* (1997). A homologue of the TNF receptor and its ligand enhance T-cell growth and dendritic-cell function. *Nature* **390(6656)***:*175-179.

Azuma Y, Kaji K, Katogi R, Takeshita S, Kudo A (2000). Tumor necrosis factor-α induces differentiation of and bone resorption by osteoclasts. *Journal of Biological Chemistry* **275(7)***:*4858-4864.

Bakker A, Klein-Nulend J, Burger E (2004). Shear stress inhibits while disuse promotes osteocyte apoptosis. *Biochemical and Biophysical Research Communications* **320(4)***:*1163-1168.

Balestrini JL, Billiar KL (2006). Equibiaxial cyclic stretch stimulates fibroblasts to rapidly remodel fibrin. *Journal of Biomechanics* **39(16)***:*2983-2990.

Banes AJ, Gilbert J, Taylor D, Monbureau O (1985). A new vacuum-operated stress-providing instrument that applies static or variable duration cyclic tension or compression to cells *in vitro*. *Journal of cell science* **75***:*35-42.

Basdra EK, Komposch G (1997). Osteoblast-like properties of human periodontal ligament cells: an *in vitro* analysis. *European Journal of Orthodontics* **19(6)***:*615-621.

Bassett CA, Becker RO (1962). Generation of electric potentials by bone in response to mechanical stress. *Science (New York, NY)* **137(3535)***:*1063-1064.

Baumrind S (1969). A reconsideration of the propriety of the "pressure-tension" hypothesis. *American journal of Orthodontics* **55(1)***:*12-22.

Beertsen W, Everts V, van den Hooff A (1974). Fine structure of fibroblasts in the periodontal ligament of the rat incisor and their possible role in tooth eruption. *Archives of Oral Biology* **19(12)***:*1087-1098.

Bengtsson M, Karlsson HJ, Westman G, Kubista M (2003). A new minor groove binding asymmetric cyanine reporter dye for real-time PCR. *Nucleic Acids Research* **31(8)***:*e45.

Berkovitz BKB, Moxham BJ, Newman HN (1995). Cells of the periodontal ligament In:The periodontal ligament in health and disease. 2nd edition. Mosby-Wolfe.

Berridge MJ (1985). The molecular basis of communication within the cell. *Scientific American* **253(4)***:*142-152.

Biederman W (1962). Etiology and treatment of tooth ankylosis. *American Journal of Orthodontics* **48(9)***:*670-684.

Bien SM, Ayers HD (1965). Responses of rat maxillary incisors to loads. *Journal of Dental Research* **44***:*517-520.

Bildt MM, Bloemen M, Kuijpers-Jagtman AM, Von den Hoff JW (2009). Matrix metalloproteinase inhibitors reduce collagen gel contraction and alpha-smooth muscle actin expression by periodontal ligament cells. *Journal of Periodontal Research* **44(2)***:*266-274.

Billiar K (2011). The Mechanical Environment of Cells in Collagen Gel Models. In: Cellular and Biomolecular Mechanics and Mechanobiology. A Gefen editor: Springer Berlin Heidelberg, pp. 201-245.

Binderman I, Zor U, Kaye AM, Shimshoni Z, Harell A, Somjen D (1988). The transduction of mechanical force into biochemical events in bone cells may involve activation of phospholipase A2. *Calcified Tissue International* **42(4)***:*261-266.

Birk DE, Trelstad RL (1984). Extracellular compartments in matrix morphogenesis: collagen fibril, bundle, and lamellar formation by corneal fibroblasts. *The Journal of Cell Biology* **99(6)***:*2024-2033.

Bister D, Meikle MC (2013). Re-examination of 'Einige Beitrage zur Theorie der Zahnregulierung' (Some contributions to the theory of the regulation of teeth) published in 1904-1905 by Carl Sandstedt. *European Journal of Orthodontics* **35(2)***:*160-168.

Boccafoschi F, Bosetti M, Gatti S, Cannas M (2007). Dynamic fibroblast cultures: response to mechanical stretching. *Cell Adhesion & Migration* **1(3)***:*124-128.

Boccafoschi F, Sabbatini M, Bosetti M, Cannas M (2010). Overstressed mechanical stretching activates survival and apoptotic signals in fibroblasts. *Cells, Tissues, Organs* **192(3)***:*167-176.

Bonafe-Oliveira L, Faltin RM, Arana-Chavez VE (2003). Ultrastructural and histochemical examination of alveolar bone at the pressure areas of rat molars

submitted to continuous orthodontic force. *European Journal of Oral Sciences* **111(5)***:*410-416.

Bonewald LF, Mundy GR (1990). Role of transforming growth factor-beta in bone remodeling. *Clinical Orthopaedics and Related Research* **250***:*261-276.

Bougault C, Aubert-Foucher E, Paumier A, Perrier-Groult E, Huot L, Hot D *et al.* (2012). Dynamic compression of chondrocyte-agarose constructs reveals new candidate mechanosensitive genes. *PloS one* **7(5)***:*e36964.

Bougault C, Paumier A, Aubert-Foucher E, Mallein-Gerin F (2008). Molecular analysis of chondrocytes cultured in agarose in response to dynamic compression. *BMC Biotechnology* **8(71)**.

Brakebusch C, Fassler R (2005). beta 1 integrin function in vivo: adhesion, migration and more. *Cancer Metastasis reviews* **24(3)***:*403-411.

Brown TD (2000). Techniques for mechanical stimulation of cells *in vitro*: a review. *Journal of Biomechanics* **33(1)***:*3-14.

Buckley MJ, Banes AJ, Levin LG, Sumpio BE, Sato M, Jordan R (1988). Osteoblasts increase their rate of division and align in response to cyclic, mechanical tension *in vitro*. *Bone and Mineral* **4(3)***:*225-236.

Burstone CJ (1962). The biomechanics of tooth movement. In: Kraus BS, Riedal RA, editors. Vistas in Orthodontics. Philadelphia: Lea & Febiger.

Burton-Wurster N, Vernier-Singer M, Farquhar T, Lust G (1993). Effect of compressive loading and unloading on the synthesis of total protein, proteoglycan, and fibronectin by canine cartilage explants. *Journal of Orthopaedic Research* **11(5)***:*717-729.

Buschmann MD, Gluzband YA, Grodzinsky AJ, Hunziker EB (1995). Mechanical compression modulates matrix biosynthesis in chondrocyte/agarose culture. *Journal of Cell Science* **108 (Pt 4)**1497-1508.

Butcher JT, Barrett BC, Nerem RM (2006). Equibiaxial strain stimulates fibroblastic phenotype shift in smooth muscle cells in an engineered tissue model of the aortic wall. *Biomaterials* **27(30)***:*5252-5258.

Cai YZ, Zhang GR, Wang LL, Jiang YZ, Ouyang HW, Zou XH (2012). Novel biodegradable three-dimensional macroporous scaffold using aligned electrospun nanofibrous yarns for bone tissue engineering. *Journal of Biomedical Materials Research Part A* **100(5)***:*1187-1194.

Carano A, Siciliani G (1996). Effects of continuous and intermittent forces on human fibroblasts *in vitro*. *European Journal of Orthodontics* **18(1)***:*19-26.

Carrier RL, Rupnick M, Langer R, Schoen FJ, Freed LE, Vunjak-Novakovic G (2002). Effects of oxygen on engineered cardiac muscle. *Biotechnology and Bioengineering* **78(6)***:*617-625.

Cattaneo PM, Kofod T, Dalstra M, Melsen B (2005). Using the finite element method to model the biomechanics of the asymmetric mandible before, during and after skeletal correction by distraction osteogenesis. *Computer Methods in Biomechanics and Biomedical engineering* **8(3)***:*157-165.

Chen FM, Jin Y (2010). Periodontal tissue engineering and regeneration: current approaches and expanding opportunities. *Tissue Engineering Part B, Reviews* **16(2)***:*219-255.

Chiba M, Mitani H (2004). Cytoskeletal changes and the system of regulation of alkaline phosphatase activity in human periodontal ligament cells induced by mechanical stress. *Cell Biochemistry and Function* **22(4)***:*249-256.

Chirila TV, Constable IJ, Crawford GJ, Vijayasekaran S, Thompson DE, Chen Y-C *et al.* (1993). Poly(2-hydroxyethyl methacrylate) sponges as implant materials: in vivo and *in vitro* evaluation of cellular invasion. *Biomaterials* **14(1)***:*26-38.

Cho E-S, Lee K-S, Son Y-O, Jang Y-S, Lee S-Y, Kwak S-Y (2010). Compressive mechanical force augments osteoclastogenesis by bone marrow macrophages through activation of c-Fms-mediated signaling. *Journal of Cellular Biochemistry* **111(5)***:*1260-1269.

Cho MI, Matsuda N, Lin WL, Moshier A, Ramakrishnan PR (1992). *In vitro* formation of mineralized nodules by periodontal ligament cells from the rat. *Calcified Tissue International* **50(5)***:*459-467.

Chowdhury I, Tharakan B, Bhat GK (2008). Caspases - an update. *Comparative Biochemistry and Physiology Part B, Biochemistry & Molecular Biology* **151(1)***:*10-27.

Chowdhury TT, Bader DL, Shelton JC, Lee DA (2003). Temporal regulation of chondrocyte metabolism in agarose constructs subjected to dynamic compression. *Archives of Biochemistry and Biophysics* **417(1)***:*105-111.

Christiansen DL, Huang EK, Silver FH (2000). Assembly of type I collagen: fusion of fibril subunits and the influence of fibril diameter on mechanical properties. *Matrix Biology : Journal of the International Society for Matrix Biology* **19(5)***:*409-420.

Clark EA, Brugge JS (1995). Integrins and signal transduction pathways: the road taken. *Science (New York, NY)* **268(5208)***:*233-239.

Culbertson EJ, Xing L, Wen Y, Franz MG (2011). Loss of mechanical strain impairs abdominal wall fibroblast proliferation, orientation, and collagen contraction function. *Surgery* **150(3)***:*410-417.

Cushing MC, Anseth KS (2007). Materials science. Hydrogel cell cultures. *Science (New York, NY)* **316(5828)***:*1133-1134.

Danciu TE, Gagari E, Adam RM, Damoulis PD, Freeman MR (2004). Mechanical strain delivers anti-apoptotic and proliferative signals to gingival fibroblasts. *Journal of Dental Research* **83(8)***:*596-601.

Dangaria SJ, Ito Y, Walker C, Druzinsky R, Luan X, Diekwisch TG (2009). Extracellular matrix-mediated differentiation of periodontal progenitor cells. *Differentiation; Research in Biological Diversity* **78(2-3)***:*79-90.

Davidovitch Z (1995). The periodontal ligament in health and disease. 2nd ed. Philadelphia: Mosby-Wolfe.

Davidovitch Z, Finkelson MD, Steigman S, Shanfeld JL, Montgomery PC, Korostoff E (1980). Electric currents, bone remodeling, and orthodontic tooth movement. I. The effect of electric currents on periodontal cyclic nucleotides. *American journal of Orthodontics* **77(1)***:*14-32.

Davidovitch Z, Montgomery PC, Gustafson GT, Eckerdal O (1976). Cellular localization of cyclic AMP in periodontal tissues during experimental tooth movement in cats. *Calcified Tissue Research* **19(4)***:*317-329.

Davidovitch Z, Shanfeld JL (1975). Cyclic AMP levels in alveolar bone of orthodontically-treated cats. *Archives of Oral biology* **20(9)***:*567-574.

de Araujo RM, Oba Y, Moriyama K (2007). Identification of genes related to mechanical stress in human periodontal ligament cells using microarray analysis. *Journal of Periodontal Research* **42(1)***:*15-22.

DeCarlo AA, Jr., Windsor LJ, Bodden MK, Harber GJ, Birkedal-Hansen B, Birkedal-Hansen H (1997). Activation and novel processing of matrix metalloproteinases by a thiol-proteinase from the oral anaerobe Porphyromonas gingivalis. *Journal of Dental Research* **76(6)***:*1260-1270.

Dena W, Arevalos CA, Liezl RB, Alicia AB, Matthew CS, Xing Z *et al.* (2013). Extracellular Matrix Organization, Structure, and Function.

Drury JL, Mooney DJ (2003). Hydrogels for tissue engineering: scaffold design variables and applications. *Biomaterials* **24(24)***:*4337-4351.

Dudic A, Kiliaridis S, Mombelli A, Giannopoulou C (2006). Composition changes in gingival crevicular fluid during orthodontic tooth movement: comparisons between tension and compression sides. *European Journal of Oral Sciences* **114(5)***:*416-422.

Dunn JC, Chan WY, Cristini V, Kim JS, Lowengrub J, Singh S *et al.* (2006). Analysis of cell growth in three-dimensional scaffolds. *Tissue Engineering* **12(4)***:*705-716.

Earnshaw WC, Martins LM, Kaufmann SH (1999). MAMMALIAN CASPASES: Structure, Activation, Substrates, and Functions During Apoptosis. *Annual Review of Biochemistry* **68(1)***:*383-424.

Eastwood M, Mudera VC, McGrouther DA, Brown RA (1998). Effect of precise mechanical loading on fibroblast populated collagen lattices: morphological changes. *Cell Motility and the Cytoskeleton* **40(1)***:*13-21.

Elmore S (2007). Apoptosis: a review of programmed cell death. *Toxicologic Pathology* **35(4)***:*495-516.

Emery JG, McDonnell P, Burke MB, Deen KC, Lyn S, Silverman C (1998). Osteoprotegerin is a receptor for the cytotoxic ligand TRAIL. *The Journal of Biological Chemistry* **273(23)***:*14363-14367.

Engler AJ, Rehfeldt F, Sen S, Discher DE (2007). Microtissue elasticity: measurements by atomic force microscopy and its influence on cell differentiation. *Methods in Cell Biology* **83***:*521-545.

Engler AJ, Sen S, Sweeney HL, Discher DE (2006). Matrix elasticity directs stem cell lineage specification. *Cell* **126(4)***:*677-689.

Epker BN, Frost HM (1965). Correlation of bone resorption and formation with the physical behaviour of loaded bone. *Journal of Dental Research* 44*:*33-41.

Fan TJ, Han LH, Cong RS, Liang J (2005). Caspase family proteases and apoptosis. *Acta Biochimica et Biophysica Sinica* **37(11)***:*719-727.

Farndale RW, Sandy JR, Atkinson SJ, Pennington SR, Meghji S, Meikle MC (1988). Parathyroid hormone and prostaglandin E2 stimulate both inositol phosphates and cyclic AMP accumulation in mouse osteoblast cultures. *The Biochemical Journal* **252(1)***:*263-268.

Farrar JN (1888). A treatise on the irregularities of the teeth and their correction; including, with the author's practice, other current methods New York: [The De Vinne press].

Fedorovich NE, Alblas J, de Wijn JR, Hennink WE, Verbout AJ, Dhert WJ (2007). Hydrogels as extracellular matrices for skeletal tissue engineering: state-of-the-art and novel application in organ printing. *Tissue Engineering* **13(8)***:*1905-1925.

Fill T, Carey JP, Toogood RW, Major PW (2011). Experimentally determined mechanical properties of, and models for, the periodontal ligament: critical review of current literature. *Journal of Dental Biomechanics* **2011**: 312980.

Fisher C, Gilbertson-Beadling S, Powers EA, Petzold G, Poorman R, Mitchell MA (1994). Interstitial collagenase is required for angiogenesis *in vitro*. *Developmental Biology* **162(2)***:*499-510.

Freeman PM, Natarajan RN, Kimura JH, Andriacchi TP (1994). Chondrocyte cells respond mechanically to compressive loads. *Journal of Orthopaedic Research* **12(3)***:*311-320.

Frost HM (1963). Bone emodelling dynamics. Charles C Thomas, Springfield.

Frost HM (1992). The role of changes in mechanical usage set points in the pathogenesis of osteoporosis. *Journal of Bone and Mineral Research* **7(3)***:*253-261.

Fuchs Y, Steller H (2011). Programmed Cell Death in Animal Development and Disease. *Cell* **147(4)***:*742-758.

Garant PR, Cho MI (1979). Histopathogenesis of spontaneous periodontal disease in conventional rats. I. Histometric and histologic study. *Journal of Periodontal Research* **14(4)***:*297-309.

Gay IC, Chen S, MacDougall M (2007). Isolation and characterization of multipotent human periodontal ligament stem cells. *Orthodontics & Craniofacial Research* **10(3)***:*149-160.

Gianelly AA (1969). Force-induced changes in the vascularity of the periodontal ligament. *American Journal of Orthodontics* **55(1)***:*5-11.

Gibbs CH, Mahan PE, Lundeen HC, Brehnan K, Walsh EK, Holbrook WB (1981). Occlusal forces during chewing and swallowing as measured by sound transmission. *The Journal of Prosthetic Dentistry* **46(4)***:*443-449.

Gilbert JA, Weinhold PS, Banes AJ, Link GW, Jones GL (1994). Strain profiles for circular cell culture plates containing flexible surfaces employed to mechanically deform cells *in vitro*. *Journal of Biomechanics* **27(9)***:*1169-1177.

Girton TS, Barocas VH, Tranquillo RT (2002). Confined compression of a tissue-equivalent: collagen fibril and cell alignment in response to anisotropic strain. *Journal of Biomechanical Engineering* **124(5)***:*568-575.

Glücksmann A (1939). Studies on bone mechanics *in vitro*. II. The role of tension and pressure in chondrogenesis. *The Anatomical Record* **73(1)***:*39-55.

Gotz W, Kunert D, Zhang D, Kawarizadeh A, Lossdorfer S, Jager A (2006). Insulin-like growth factor system components in the periodontium during tooth root resorption and early repair processes in the rat. *European Journal of Oral Sciences* **114(4)***:*318-327.

Gowen M, Wood DD, Ihrie EJ, McGuire MK, Russell RG (1983). An interleukin 1 like factor stimulates bone resorption *in vitro*. *Nature* **306(5941)***:*378-380.

Grevesse T, Versaevel M, Circelli G, Desprez S, Gabriele S (2013). A simple route to functionalize polyacrylamide hydrogels for the independent tuning of mechanotransduction cues. *Lab on a chip* **13(5)***:*777-780.

Grieve WG, 3rd, Johnson GK, Moore RN, Reinhardt RA, DuBois LM (1994). Prostaglandin E (PGE) and interleukin-1 beta (IL-1 beta) levels in gingival crevicular fluid during human orthodontic tooth movement. *American Journal of Orthodontics and Dentofacial Orthopedics* **105(4)***:*369-374.

Grimm FM (1972). Bone bending, a feature of orthodontic tooth movement. *American Journal of Orthodontics* **62(4)***:*384-393.

Grotendorst GR (1997). Connective tissue growth factor: a mediator of TGF-beta action on fibroblasts. *Cytokine & Growth Factor reviews* **8(3)***:*171-179.

Guilak F, Meyer BC, Ratcliffe A, Mow VC (1994). The effects of matrix compression on proteoglycan metabolism in articular cartilage explants. *Osteoarthritis and Cartilage* **2(2)***:*91-101.

Haas VR, Santos AR, Jr., Wada ML (2001). Behaviour of fibroblastic cells cultured in collagen I using the sandwich technique. *Cytobios* **106 (Suppl 2)** *:*255-267.

Hakkinen L, Oksala O, Salo T, Rahemtulla F, Larjava H (1993). Immunohistochemical localization of proteoglycans in human periodontium. *The Journal of Histochemistry and Cytochemistry* **41(11)***:*1689-1699.

Halliday NL, Tomasek JJ (1995). Mechanical properties of the extracellular matrix influence fibronectin fibril assembly *in vitro*. *Experimental Cell Research* **217(1)***:*109-117.

Hannafin JA, Attia EA, Henshaw R, Warren RF, Bhargava MM (2006). Effect of cyclic strain and plating matrix on cell proliferation and integrin expression by ligament fibroblasts. *Journal of Orthopaedic Research* **24(2)***:*149-158.

Hao Y, Xu C, Sun SY, Zhang FQ (2009). Cyclic stretching force induces apoptosis in human periodontal ligament cells via caspase-9. *Archives of Oral Biology* **54(9)***:*864-870.

Harell A, Dekel S, Binderman I (1977). Biochemical effect of mechanical stress on cultured bone cells. *Calcified Tissue Research* **22 (Suppl)***:*202-207.

Hasegawa S, Sato S, Saito S, Suzuki Y, Brunette DM (1985). Mechanical stretching increases the number of cultured bone cells synthesizing DNA and alters their pattern of protein synthesis. *Calcified Tissue International* **37(4)***:*431-436.

Hatai T, Yokozeki M, Funato N, Baba Y, Moriyama K, Ichijo H (2001). Apoptosis of periodontal ligament cells induced by mechanical stress during tooth movement. *Oral Diseases* **7(5)***:*287-290.

Hauschka PV, Mavrakos AE, Iafrati MD, Doleman SE, Klagsbrun M (1986). Growth factors in bone matrix. Isolation of multiple types by affinity chromatography on heparin-Sepharose. *The Journal of Biological Chemistry* **261(27)***:*12665-12674.

Heller IJ, Nanda R (1979). Effect of metabolic alteration of periodontal fibers on orthodontic tooth movement. An experimental study. *American Journal of Orthodontics* **75(3)***:*239-258.

Hokin MR, Hokin LE (1953). Enzyme secretion and the incorporation of P32 into phospholipides of pancreas slices. *The Journal of Biological Chemistry* **203(2)***:*967-977.

Holmbeck K, Szabova L (2006). Aspects of extracellular matrix remodeling in development and disease. *Birth Defects Research Part C, Embryo today : reviews* **78(1)***:*11-23.

Hong SL, Polsky-Cynkin R, Levine L (1976). Stimulation of prostaglandin biosynthesis by vasoactive substances in methylcholanthrene-transformed mouse BALB/3T3. *The Journal of Biological Chemistry* **251(3)***:*776-780.

Huang GT, Sonoyama W, Chen J, Park SH (2006). *In vitro* characterization of human dental pulp cells: various isolation methods and culturing environments. *Cell and Tissue Research* **324(2)***:*225-236.

Hurley MM, Lee SK, Raisz LG, Bernecker P, Lorenzo J (1998). Basic fibroblast growth factor induces osteoclast formation in murine bone marrow cultures. *Bone* **22(4)***:*309-316.

Hynes RO (1992). Integrins: versatility, modulation, and signaling in cell adhesion. *Cell* **69(1)***:*11-25.

Igarashi A, Okochi H, Bradham DM, Grotendorst GR (1993). Regulation of connective tissue growth factor gene expression in human skin fibroblasts and during wound repair. *Molecular Biology of the Cell* **4(6)***:*637-645.

Ingber D (1991). Integrins as mechanochemical transducers. *Current Opinion in Cell Biology* **3(5)***:*841-848.

Isaacson RJ, Lindauer SJ, Davidovitch M (1993). On tooth movement. *The Angle orthodontist* **63(4)***:*305-309.

Ives CL, Eskin SG, McIntire LV (1986). Mechanical effects on endothelial cell morphology: *in vitro* assessment. *In vitro Cellular & Developmental Biology* **22(9)***:*500-507.

Iwasaki LR, Gibson CS, Crouch LD, Marx DB, Pandey JP, Nickel JC (2006). Speed of tooth movement is related to stress and IL-1 gene polymorphisms. *American Journal of Orthodontics and Dentofacial* **130(6)***:*698 e691-699.

Izumi Y, Aoki A, Yamada Y, Kobayashi H, Iwata T, Akizuki T (2011). Current and future periodontal tissue engineering. *Periodontology 2000* **56(1)**: 166-187.

Jacobs C, Grimm S, Ziebart T, Walter C, Wehrbein H (2013). Osteogenic differentiation of periodontal fibroblasts is dependent on the strength of mechanical strain. *Archives of Oral Biology* **58(7)***:*896-904.

Jacobson MD, Weil M, Raff MC (1997). Programmed Cell Death in Animal Development. *Cell* **88(3)***:*347-354.

Janssens K, ten Dijke P, Janssens S, Van Hul W (2005). Transforming growth factor-beta1 to the bone. *Endocrine reviews* **26(6)***:*743-774.

Jeon Y-M, Kook S-H, Son Y-O, Kim E, Park S-S, Kim J-G (2009). Role of MAPK in mechanical force-induced up-regulation of type I collagen and osteopontin in human gingival fibroblasts. *Molecular and Cellularl Biochemistry* **320(1-2)***:*45-52.

Jilka RL, Weinstein RS, Bellido T, Parfitt AM, Manolagas SC (1998). Osteoblast Programmed Cell Death (Apoptosis): Modulation by Growth Factors and Cytokines. *Journal of Bone and Mineral Research* **13(5)***:*793-802.

Jo YY, Lee HJ, Kook SY, Choung HW, Park JY, Chung JH *et al.* (2007). Isolation and characterization of postnatal stem cells from human dental tissues. *Tissue Engineering* **13(4)***:*767-773.

Johnson S, Nguyen V, Coder D (2001). Assessment of Cell Viability. In: Current Protocols in Cytometry: John Wiley & Sons, Inc.

Jones KH, Senft JA (1985). An improved method to determine cell viability by simultaneous staining with fluorescein diacetate-propidium iodide. *The Journal of Histochemistry and Cytochemistry* **33(1)***:*77-79.

Jones ML, Hickman J, Middleton J, Knox J, Volp C (2001). A validated finite element method study of orthodontic tooth movement in the human subject. *Journal of Orthodontics* **28(1)***:*29-38.

Jónsdóttir SH, Giesen EB, Maltha JC (2006). Biomechanical behaviour of the periodontal ligament of the beagle dog during the first 5 hours of orthodontic force application. *European Journal of Orthodontics* **28**: 547–552

Kaku M, Kohno S, Kawata T, Fujita I, Tokimasa C, Tsutsui K *et al.* (2001). Effects of vascular endothelial growth factor on osteoclast induction during tooth movement in mice. *Journal of dental research* **80(10)***:*1880-1883.

Kale S, Kocadereli I, Atilla P, Asan E (2004). Comparison of the effects of 1,25 dihydroxycholecalciferol and prostaglandin E2 on orthodontic tooth movement. *American journal of orthodontics and dentofacial orthopedics* **125(5)***:*607-614.

Kanai K, Nohara H, Handa K (1992) Initial effects of continuously applied compressive stress to human periodontal ligament fibroblasts. *Journal of Japanese Orthodontic Society* **57***:*153-163.

Kang KL, Lee SW, Ahn YS, Kim SH, Kang YG (2013). Bioinformatic analysis of responsive genes in two-dimension and three-dimension cultured human periodontal ligament cells subjected to compressive stress. *Journal of Periodontal Research* **48(1)***:*87-97.

Kanzaki H, Chiba M, Sato A, Miyagawa A, Arai K, Nukatsuka S (2006). Cyclical tensile force on periodontal ligament cells inhibits osteoclastogenesis through OPG induction. *Journal of Dental Research* **85(5)***:*457-462.

Kanzaki H, Chiba M, Shimizu Y, Mitani H (2002). Periodontal ligament cells under mechanical stress induce osteoclastogenesis by receptor activator of nuclear factor kappaB ligand up-regulation via prostaglandin E2 synthesis. *Journal of Bone and Mineral Research* **17(2)***:*210-220.

Kanzaki H, Chiba M, Takahashi I, Haruyama N, Nishimura M, Mitani H (2004). Local OPG gene transfer to periodontal tissue inhibits orthodontic tooth movement. *Journal of Dental Research* **83(12)***:*920-925.

Katagiri T, Takahashi N (2002). Regulatory mechanisms of osteoblast and osteoclast differentiation. *Oral Diseases* **8(3)***:*147-159.

Kawaguchi H, Pilbeam CC, Harrison JR, Raisz LG (1995). The role of prostaglandins in the regulation of bone metabolism. *Clinical Orthopaedics and Related Research* **313***:*36-46.

Kelly TA, Ng KW, Wang CC, Ateshian GA, Hung CT (2006). Spatial and temporal development of chondrocyte-seeded agarose constructs in free-swelling and dynamically loaded cultures. *Journal of Biomechanics* **39(8)***:*1489-1497.

Kerrigan JJ, Mansell JP, Sandy JR (2000). Matrix turnover. *Journal of Orthodontics* **27(3)***:*227-233.

Khosla S (2001). Minireview: The OPG/RANKL/RANK System. *Endocrinology* **142(12)***:*5050-5055.

Kim JH, Jin HM, Kim K, Song I, Youn BU, Matsuo K *et al.* (2009). The mechanism of osteoclast differentiation induced by IL-1. *Journal of Immunology (Baltimore, Md : 1950)* **183(3)***:*1862-1870.

Kim SG, Kim S-G, Viechnicki B, Kim S, Nah H-D (2011). Engineering of a periodontal ligament construct: cell and fibre alignment induced by shear stress. *Journal of Clinical Periodontology* **38**: 1130–1136.

Kim SJ, Park KH, Park YG, Lee SW, Kang YG (2013). Compressive stress induced the up-regulation of M-CSF, RANKL, TNF-alpha expression and the down-regulation of OPG expression in PDL cells via the integrin-FAK pathway. *Archives of Oral Biology* **58(6)***:*707-716.

Kim SS, Kwon DW, Im I, Kim YD, Hwang DS, Holliday LS *et al.* (2012). Differentiation and characteristics of undifferentiated mesenchymal stem cells originating from adult premolar periodontal ligaments. *Korean Journal of Orthodontics* **42(6)***:*307-317.

Kletsas D, Basdra EK, Papavassiliou AG (1998). Mechanical stress induces DNA synthesis in PDL fibroblasts by a mechanism unrelated to autocrine growth factor action. *FEBS Letters* **430(3)***:*358-362.

Kook S-H, Jang Y-S, Lee J-C (2011). Human periodontal ligament fibroblasts stimulate osteoclastogenesis in response to compression force through TNF-α-mediated activation of CD4+ T cells. *Journal of Cellular Biochemistry* **112(10)***:*2891-2901.

Kook SH, Jeon YM, Park SS, Lee JC (2013). Periodontal Fibroblasts Modulate Proliferation and Osteogenic Differentiation of Embryonic Stem Cells Through Production of Fibroblast Growth Factors. *Journal of Periodontology*. 2013 Jun 27. [Epub ahead of print]

Kook S-H, Lee J-C (2012). Tensile force inhibits the proliferation of human periodontal ligament fibroblasts through Ras-p38 MAPK up-regulation. *Journal of Cellular Physiology* **227(3)***:*1098-1106.

Kook S-H, Son Y-O, Hwang J-M, Kim E-M, Lee C-B, Jeon Y-M *et al.* (2009). Mechanical force inhibits osteoclastogenic potential of human periodontal ligament fibroblasts through OPG production and ERK-mediated signaling. *Journal of Cellular Biochemistry* **106(6)***:*1010-1019.

Kothapalli D, Frazier KS, Welply A, Segarini PR, Grotendorst GR (1997). Transforming growth factor beta induces anchorage-independent growth of NRK fibroblasts via a connective tissue growth factor-dependent signaling pathway. *Cell Growth & Differentiation* **8(1)***:*61-68.

Krishnan V, Davidovitch Z (2006). Cellular, molecular, and tissue-level reactions to orthodontic force. *American Journal of Orthodontics and Dentofacial Orthopedics* **129(4)***:*469 e461-432.

Krishnan V, Davidovitch Z (2009). On a path to unfolding the biological mechanisms of orthodontic tooth movement. *Journal of Dental Research* 88(7)*:*597-608.

Krishnan V, Davidovitch Z (2009). Biological mechanisms of tooth movement Chichester, Wiley-Blackwell.

Kuru L, Parkar MH, Griffiths GS, Newman HN, Olsen I (1998). Flow cytometry analysis of gingival and periodontal ligament cells. *Journal of Dental Research* **77(4)***:*555-564.

Kwok CB, Ho FC, Li CW, Ngan AH, Chan D, Chan BP (2013). Compression-induced alignment and elongation of human mesenchymal stem cell (hMSC) in 3D collagen constructs is collagen concentration dependent. *Journal of Biomedical Materials Research Part A* **101(6)***:*1716-1725.

Lacey DL, Timms E, Tan HL, Kelley MJ, Dunstan CR, Burgess T *et al.* (1998). Osteoprotegerin ligand is a cytokine that regulates osteoclast differentiation and activation. *Cell* **93(2)***:*165-176.

Lee AA, Delhaas T, McCulloch AD, Villarreal FJ (1999). Differential responses of adult cardiac fibroblasts to *in vitro* biaxial strain patterns. *Journal of Molecular and Cellular Cardiology* **31(10)***:*1833-1843.

Lee J, Cuddihy MJ, Kotov NA (2008). Three-dimensional cell culture matrices: state of the art. *Tissue Engineering Part B, Reviews* **14(1)***:*61-86.

Lee SK, Gardner AE, Kalinowski JF, Jastrzebski SL, Lorenzo JA (2006). RANKL-stimulated osteoclast-like cell formation *in vitro* is partially dependent on endogenous interleukin-1 production. *Bone* **38(5)***:*678-685.

Lee W-C, Maul T, Vorp D, Rubin JP, Marra K (2007). Effects of uniaxial cyclic strain on adipose-derived stem cell morphology, proliferation, and differentiation. *Biomechanics and Modeling in Mechanobiology* **6(4)***:*265-273.

Lee YH, Nahm DS, Jung YK, Choi JY, Kim SG, Cho M *et al.* (2007). Differential gene expression of periodontal ligament cells after loading of static compressive force. *Journal of Periodontology* **78(3)***:*446-452.

Leiker BJ, Nanda RS, Currier GF, Howes RI, Sinha PK (1995). The effects of exogenous prostaglandins on orthodontic tooth movement in rats. *American Journal of Orthodontics and Dentofacial Orthopedics* **108(4)***:*380-388.

Lekic P, McCulloch CAG (1996). Periodontal ligament cell populations: The central role of fibroblasts in creating a unique tissue. *The Anatomical Record* **245(2)***:*327-341.

Leung DW, Cachianes G, Kuang WJ, Goeddel DV, Ferrara N (1989). Vascular endothelial growth factor is a secreted angiogenic mitogen. *Science (New York, NY)* **246(4935)***:*1306-1309.

Leung DY, Glagov S, Mathews MB (1976). Cyclic stretching stimulates synthesis of matrix components by arterial smooth muscle cells *in vitro*. *Science (New York, NY)* **191(4226)***:*475-477.

Leung DY, Glagov S, Mathews MB (1977). A new *in vitro* system for studying cell response to mechanical stimulation. Different effects of cyclic stretching and agitation on smooth muscle cell biosynthesis. *Experimental Cell Research* **109(2)***:*285-298.

Levenberg S, Huang NF, Lavik E, Rogers AB, Itskovitz-Eldor J, Langer R (2003). Differentiation of human embryonic stem cells on three-dimensional polymer scaffolds. *Proceedings of the National Academy of Sciences of the United States of America* **100(22)***:*12741-12746.

Levene CI, Carrington MJ (1985). The inhibition of protein-lysine 6-oxidase by various lathyrogens. Evidence for two different mechanisms. *The Biochemical journal* **232(1)***:*293-296.

Levental I, Georges PC, Janmey PA (2006). Soft biological materials and their impact on cell function. *Soft Matter* **2**: 1–9.

Li B, Wang JH (2011). Fibroblasts and myofibroblasts in wound healing: force generation and measurement. *Journal of Tissue Viability* **20(4)***:*108-120.

Li Y, Li M, Tan L, Huang S, Zhao L, Tang T (2013). Analysis of time-course gene expression profiles of a periodontal ligament tissue model under compression. *Archives of Oral Biology* **58(5)***:*511-522.

Liu L, Igarashi K, Kanzaki H, Chiba M, Shinoda H, Mitani H (2006). Clodronate inhibits PGE(2) production in compressed periodontal ligament cells. *Journal of Dental Research* **85(8)***:*757-760.

Long P, Hu J, Piesco N, Buckley M, Agarwal S (2001). Low magnitude of tensile strain inhibits IL-1beta-dependent induction of pro-inflammatory cytokines and induces synthesis of IL-10 in human periodontal ligament cells *in vitro*. *Journal of Dental Research* **80(5)***:*1416-1420.

Mabuchi R, Matsuzaka K, Shimono M (2002). Cell proliferation and cell death in periodontal ligaments during orthodontic tooth movement. *Journal of Periodontal Research* **37(2)***:*118-124.

Martens P, Anseth KS (2000). Characterization of hydrogels formed from acrylate modified poly(vinyl alcohol) macromers. *Polymer* **41(21)***:*7715-7722.

Matheson LA, Fairbank NJ, Maksym GN, Paul Santerre J, Labow RS (2006). Characterization of the Flexcell Uniflex cyclic strain culture system with U937 macrophage-like cells. *Biomaterials* **27(2)***:*226-233.

Matsuda N, Morita N, Matsuda K, Watanabe M (1998). Proliferation and Differentiation of Human Osteoblastic Cells Associated with Differential Activation of MAP Kinases in Response to Epidermal Growth Factor, Hypoxia, and Mechanical Stress*in vitro*. *Biochemical and Biophysical Research Communications* **249(2)***:*350-354.

Mazzitelli S, Capretto L, Quinci F, Piva R, Nastruzzi C (2013). Preparation of cell-encapsulation devices in confined microenvironment. *Advanced Drug Delivery Reviews*. 2013 Aug 8 [Epub ahead of print].

McCulloch CA, Bordin S (1991). Role of fibroblast subpopulations in periodontal physiology and pathology. *Journal of Periodontal Research* **26(3 Pt 1)***:*144-154.

Meikle MC (2006). The tissue, cellular, and molecular regulation of orthodontic tooth movement: 100 years after Carl Sandstedt. *European Journal of Orthodontics* **28(3)***:*221-240.

Meikle MC, Reynolds JJ, Sellers A, Dingle JT (1979). Rabbit cranial sutures *in vitro*: a new experimental model for studying the response of fibrous joints to mechanical stress. *Calcified Tissue International* **28(2)***:*137-144.

Melsen B (2001). Tissue reaction to orthodontic tooth movement--a new paradigm. *European Journal of Orthodontics* **23(6)***:*671-681.

Melsen B CP, Dalstra M, Kraft DC (2007). The importance of force levels in relation to tooth movement. *Seminars in Orthodontics* **13(4)***:*220-233.

Meng Y, Han X, Huang L, Bai D, Yu H, He Y (2010). Orthodontic mechanical tension effects on the myofibroblast expression of alpha-smooth muscle actin. *The Angle Orthodontist* **80(5)***:*912-918.

Meyer CJ, Alenghat FJ, Rim P, Fong JH, Fabry B, Ingber DE (2000). Mechanical control of cyclic AMP signalling and gene transcription through integrins. *Nature cell biology* **2(9)***:*666-668.

Middleton J, Jones ML, Wilson AN (1990). Three-dimensional analysis of orthodontic tooth movement. *Journal of Biomedical Engineering* **12(4)***:*319-327.

Milne TJ, Ichim I, Patel B, McNaughton A, Meikle MC (2009). Induction of osteopenia during experimental tooth movement in the rat: alveolar bone remodelling and the mechanostat theory. *European Journal of Orthodontics* **31(3)***:*221-231.

Mitton KP, Tumminia SJ, Arora J, Zelenka P, Epstein DL, Russell P (1997). Transient loss of alphaB-crystallin: an early cellular response to mechanical stretch. *Biochemical and Biophysical Research Communications* **235(1)***:*69-73.

Moraes C, Wang G, Sun Y, Simmons CA (2010). A microfabricated platform for high-throughput unconfined compression of micropatterned biomaterial arrays. *Biomaterials* **31(3)***:*577-584.

Murakami Y, Kojima T, Nagasawa T, Kobayashi H, Ishikawa I (2003). Novel isolation of alkaline phosphatase-positive subpopulation from periodontal ligament fibroblasts. *Journal of Periodontology* **74(6)***:*780-786.

Murphy G, Nagase H (2008). Progress in matrix metalloproteinase research. *Molecular Aspects of Medicine* **29(5)***:*290-308.

Musah S, Morin SA, Wrighton PJ, Zwick DB, Jin S, Kiessling LL (2012). Glycosaminoglycan-binding hydrogels enable mechanical control of human pluripotent stem cell self-renewal. *ACS nano* **6(11)***:*10168-10177.

Myers SA, Wolowacz RG (1998). Tetracycline-based MMP inhibitors can prevent fibroblast-mediated collagen gel contraction *in vitro*. *Advances in Dental Research* **12(2)***:*86-93.

Nagatomo K, Komaki M, Sekiya I, Sakaguchi Y, Noguchi K, Oda S *et al.* (2006). Stem cell properties of human periodontal ligament cells. *Journal of Periodontal Research* **41(4)***:*303-310.

Nakajima R, Yamaguchi M, Kojima T, Takano M, Kasai K (2008). Effects of compression force on fibroblast growth factor-2 and receptor activator of nuclear factor kappa B ligand production by periodontal ligament cells *in vitro*. *Journal of Periodontal Research* **43(2)***:*168-173.

Nakao K, Goto T, Gunjigake KK, Konoo T, Kobayashi S, Yamaguchi K (2007). Intermittent force induces high RANKL expression in human periodontal ligament cells. *Journal of Dental Research* **86(7)***:*623-628.

Natali AN, Pavan PG, Scarpa C (2004). Numerical analysis of tooth mobility: formulation of a non-linear constitutive law for the periodontal ligament. *Dental Materials* **20(7)***:*623-629.

Neidlinger-Wilke C, Grood E, Claes L, Brand R (2002). Fibroblast orientation to stretch begins within three hours. *Journal of Orthopaedic Research* **20(5)***:*953-956.

Neidlinger-Wilke C, Wilke HJ, Claes L (1994). Cyclic stretching of human osteoblasts affects proliferation and metabolism: a new experimental method and its application. *Journal of Orthopaedic Research* **12(1)***:*70-78.

Niida S, Kaku M, Amano H, Yoshida H, Kataoka H, Nishikawa S *et al.* (1999). Vascular endothelial growth factor can substitute for macrophage colony-stimulating factor in the support of osteoclastic bone resorption. *The Journal of Experimental Medicine* **190(2)***:*293-298.

Nishijima Y, Yamaguchi M, Kojima T, Aihara N, Nakajima R, Kasai K (2006). Levels of RANKL and OPG in gingival crevicular fluid during orthodontic tooth movement and effect of compression force on releases from periodontal ligament cells *in vitro*. *Orthodontics & Craniofacial Research* **9(2)***:*63-70.

Nojima N, Kobayashi M, Shionome M, Takahashi N, Suda T, Hasegawa K (1990). Fibroblastic cells derived from bovine periodontal ligaments have the phenotypes of osteoblasts. *Journal of Periodontal Research* **25(3)***:*179-185.

Ogasawara T, Yoshimine Y, Kiyoshima T, Kobayashi I, Matsuo K, Akamine A *et al.* (2004). In situ expression of RANKL, RANK, osteoprotegerin and cytokines in osteoclasts of rat periodontal tissue. *Journal of Periodontal Research* **39(1)***:*42-49.

Oppenheim A (1911/12). Tissue changes, particularly of the bone, incident to tooth movement. *American Journal of Orthodontics* **3**:113-32.

Oppenheim A (1942). Human tissue response to orthodontic intervention of short and long duration. *American Journal of Orthodontics and Oral Surgery* **28**:263-301.

Ozawa H, Imamura K, Abe E, Takahashi N, Hiraide T, Shibasaki Y *et al.* (1990). Effect of a continuously applied compressive pressure on mouse osteoblast-like cells (MC3T3-E1) *in vitro*. *Journal of Cellular Physiology* **142(1)***:*177-185.

Park SA, Kim IA, Lee YJ, Shin JW, Kim C-R, Kim JK (2006). Biological responses of ligament fibroblasts and gene expression profiling on micropatterned silicone substrates subjected to mechanical stimuli. *Journal of Bioscience and Bioengineering* **102(5)***:*402-412.

Pederson DR, Bottlang M, Brown TD, Banes AJ (1993). Hyperelastic constitutive properties for polydimethyl siloxane cell culture membranes. Presented at the ASME Advances in Bioengineering 603-609.

Pedersen JA, Swartz MA (2005). Mechanobiology in the third dimension. *Annals of Biomedical Engineering* **33(11)***:*1469-1490.

Pérez-Sayáns M, Somoza-Martín JM, Barros-Angueira F, Rey JMG, García-García A (2010). RANK/RANKL/OPG role in distraction osteogenesis. *Oral Surgery, Oral Medicine, Oral Pathology, Oral Radiology, and Endodontology* **109(5)***:*679-686.

Pfeiler TW, Sumanasinghe RD, Loboa EG (2008). Finite element modeling of 3D human mesenchymal stem cell-seeded collagen matrices exposed to tensile strain. *Journal of Biomechanics* **41(10)***:*2289-2296.

Piche JE, Carnes DL, Jr., Graves DT (1989). Initial characterization of cells derived from human periodontia. *Journal of Dental Research* **68(5)***:*761-767.

Pilon JJ, Kuijpers-Jagtman AM, Maltha JC (1996). Magnitude of orthodontic forces and rate of bodily tooth movement. An experimental study. *American Journal of Orthodontics and Dentofacial Orthopedics* **110(1)***:*16-23.

Pinkerton MN, Wescott DC, Gaffey BJ, Beggs KT, Milne TJ, Meikle MC (2008). Cultured human periodontal ligament cells constitutively express multiple osteotropic cytokines and growth factors, several of which are responsive to mechanical deformation. *Journal of Periodontal Research* **43(3)***:*343-351.

Pollack SR, Salzstein R, Pienkowski D (1984). The electric double layer in bone and its influence on stress-generated potentials. *Calcified Tissue International* **36 (Suppl 1)***:*77-81.

Porter S, Clark IM, Kevorkian L, Edwards DR (2005). The ADAMTS metalloproteinases. *The Biochemical Journal* **386(Pt 1)***:*15-27.

Prestwich GD (2011). Hyaluronic acid-based clinical biomaterials derived for cell and molecule delivery in regenerative medicine. *Journal of Controlled Release* **155(2)***:*193-199.

Pretolani M (1999). Interleukin-10: an anti-inflammatory cytokine with therapeutic potential. *Clinical and Experimental Allergy* **29(9)***:*1164-1171.

Quinn RS, Yoshikawa DK (1985). A reassessment of force magnitude in orthodontics. *American Journal of Orthodontics* **88(3)***:*252-260.

Ren Y, Maltha JC, Kuijpers-Jagtman AM (2003). Optimum force magnitude for orthodontic tooth movement: a systematic literature review. *The Angle Orthodontist* **73(1)***:*86-92.

Reitan K (1957). Some factors determining the evaluation of forces in orthodontics. *American Journal of Orthodontics* **44***:* 32-45.

Reitan K (1960). Tissue behaviour during orthodontic tooth movement. *American Journal of Orthodontics* **46***:*881-90.

Reitan K, Rygh P (1994). Biomechanical principles and reactions: In Orthodontics-Current Principles and Techniques. Eds Graber TM, Vanarsdall RL. Mosby, St. Louis, pp. 96-192.

Reyna J, Moon HB, Maung V, Panahpour M, *et al*. (2006). Gene expression induced by orthodontic tooth movement and/or root resorption. In Biological Mechanisms of Tooth Eruption, Resorption and Movement. Eds Davidovitch Z, Mah J, Suthanarak S. Harvard Society for the Advancement of Orthodontics, pp 45-75.

Reynolds JJ, Meikle MC (1997). Mechanisms of connective tissue matrix destruction in periodontitis. *Periodontology 2000* **14***:*144-157.

Richards D, Rutherford RB (1988). The effects of interleukin 1 on collagenolytic activity and prostaglandin-E secretion by human periodontal-ligament and gingival fibroblast. *Archives of Oral Biology* **33(4)***:*237-243.

Rodan GA, Bourret LA, Harvey A, Mensi T (1975a). Cyclic AMP and cyclic GMP: mediators of the mechanical effects on bone remodeling. *Science (New York, NY)* **189(4201)***:*467-469.

Rodan GA, Mensi T, Harvey A (1975b). A quantitative method for the application of compressive forces to bone in tissue culture. *Calcified Tissue Research* **18(2)***:*125-131.

Roeder BA, Kokini K, Sturgis JE, Robinson JP, Voytik-Harbin SL (2002). Tensile mechanical properties of three-dimensional type I collagen extracellular matrices with varied microstructure. *Journal of Biomechanical Engineering* **124(2)***:*214-222.

Rygh P (1995). The histological responses of the periodontal ligament to horizontal orthodontic loads, pp. 243-258.

Saito M, Saito S, Ngan PW, Shanfeld J, Davidovitch Z (1991). Interleukin 1 beta and prostaglandin E are involved in the response of periodontal cells to mechanical stress in vivo and *in vitro*. *American Journal of Orthodontics and Dentofacial Orthopedics* **99(3)***:*226-240.

Saito S, Saito M, Ngan P, Lanese R, Shanfeld J, Davidovitch Z (1990). Effects of parathyroid hormone and cytokines on prostaglandin E synthesis and bone resorption by human periodontal ligament fibroblasts. *Archives of Oral Biology* **35(10)***:*845-855.

Saminathan A, Vinoth KJ, Wescott DC, Pinkerton MN, Milne TJ, Cao T (2012). The effect of cyclic mechanical strain on the expression of adhesion-related genes by periodontal ligament cells in two-dimensional culture. *Journal of Periodontal Research* **47(2)***:*212-221.

Saminathan A, Vinoth KJ, Low HH, Cao T, Meikle MC (2013). Engineering three-dimensional constructs of the periodontal ligament in hyaluronan–

gelatin hydrogel films and a mechanically active environment. *Journal of Periodontal Research* [Epub ahead of print].

Sandstedt C (1904). Einige Beiträge zur Theorie der Zahnregulierung. *Nordisk Tandläkare Tidskrift* **5**: 236–256.

Sandstedt C (1905). Einige Beiträge zur Theorie der Zahnregulierung. *Nordisk Tandläkare Tidskrift* **6**: 1–25; 141–168.

Sandy JR (1998). Signal transduction. *British Journal of Orthodontics* **25(4)***:*269-274.

Sandy JR, Farndale RW, Meikle MC (1993). Recent advances in understanding mechanically induced bone remodeling and their relevance to orthodontic theory and practice. *American Journal of Orthodontics and Dentofacial Orthopedics* **103(3)***:*212-222.

Sandy JR, Harris M (1984). Prostaglandins and tooth movement. *European Journal of Orthodontics* **6(3)***:*175-182.

Sandy JR, Meghji S, Scutt AM, Harvey W, Harris M, Meikle MC (1989). Murine osteoblasts release bone-resorbing factors of high and low molecular weights: stimulation by mechanical deformation. *Bone and mineral* **5(2)***:*155-168.

Sawhney AS, Pathak CP, Hubbell JA (1993). Interfacial photopolymerization of poly(ethylene glycol)-based hydrogels upon alginate-poly(l-lysine) microcapsules for enhanced biocompatibility. *Biomaterials* **14(13)***:*1008-1016.

Schnaper HW, Grant DS, Stetler-Stevenson WG, Fridman R, D'Orazi G, Murphy AN *et al.* (1993). Type IV collagenase(s) and TIMPs modulate endothelial cell morphogenesis *in vitro*. *Journal of Cellular Physiology* **156(2)***:*235-246.

Schwartz AM (1932). Tissue changes incidental to orthodontic tooth movement. *International Journal of Orthodontia, Oral Surgery and Radiography* **18***:*331-352.

Seo BM, Miura M, Gronthos S, Bartold PM, Batouli S, Brahim J (2004). Investigation of multipotent postnatal stem cells from human periodontal ligament. *Lancet* **364(9429)***:*149-155.

Serban MA, Scott A, Prestwich GD (2008). Use of hyaluronan-derived hydrogels for three-dimensional cell culture and tumor xenografts. *Current protocols in cell biology* / editorial board, Juan S Bonifacino *et al.*, Chapter 10(Unit 10 14).

Shamos MH, Lavine LS (1967). Piezoelectricity as a fundamental property of biological tissues. *Nature* **213(5073)***:*267-269.

Shimabukuro Y, Ichikawa T, Takayama S, Yamada S, Takedachi M, Terakura M (2005). Fibroblast growth factor-2 regulates the synthesis of hyaluronan by human periodontal ligament cells. *Journal of Cellular Physiology* **203(3)***:*557-563.

Shimono M, Ishikawa T, Ishikawa H, Matsuzaki H, Hashimoto S, Muramatsu T *et al.* (2003). Regulatory mechanisms of periodontal regeneration. *Microscopy Research and Technique* **60(5)***:*491-502.

Sicher H (1923) Zeitschriftfiir Stomatologie **21**, 580-594.

Sieuwerts AM, Klijn JG, Peters HA, Foekens JA (1995). The MTT tetrazolium salt assay scrutinized: how to use this assay reliably to measure metabolic activity of cell cultures *in vitro* for the assessment of growth characteristics, IC50-values and cell survival. *European Journal of Clinical Chemistry and Clinical Biochemistry* **33(11)***:*813-823.

Silva GA, Czeisler C, Niece KL, Beniash E, Harrington DA, Kessler JA *et al.* (2004). Selective differentiation of neural progenitor cells by high-epitope density nanofibers. *Science (New York, NY)* **303(5662)***:*1352-1355.

Simonet WS, Lacey DL, Dunstan CR, Kelley M, Chang MS, Luthy R *et al.* (1997). Osteoprotegerin: a novel secreted protein involved in the regulation of bone density. *Cell* **89(2)***:*309-319.

Somerman MJ, Archer SY, Imm GR, Foster RA (1988). A comparative study of human periodontal ligament cells and gingival fibroblasts *in vitro*. *Journal of Dental Research* **67(1)***:*66-70.

Somjen D, Binderman I, Berger E, Harell A (1980). Bone remodelling induced by physical stress is prostaglandin E2 mediated. *Biochimica et Biophysica Acta* **627(1)***:*91-100.

Storey E SR (1952). Force in orthodontics and its relation to tooth movement. *Australian Dental Journal* **56***:*11-18.

Streb H, Irvine RF, Berridge MJ, Schulz I (1983). Release of Ca2+ from a nonmitochondrial intracellular store in pancreatic acinar cells by inositol-1,4,5-trisphosphate. *Nature* **306(5938)***:*67-69.

Sutherland EW, Rall TW (1958). Fractionation and characterization of a cyclic adenine ribonucleotide formed by tissue particles. *The Journal of Biological Chemistry* **232(2)***:*1077-1091.

Syedain ZH, Weinberg JS, Tranquillo RT (2008). Cyclic distension of fibrin-based tissue constructs: evidence of adaptation during growth of engineered connective tissue. *Proceedings of the National Academy of Sciences of the United States of America* **105(18)***:*6537-6542.

Syggelos SA, Aletras AJ, Smirlaki I, Skandalis SS (2013). Extracellular matrix degradation and tissue remodeling in periprosthetic loosening and

osteolysis: focus on matrix metalloproteinases, their endogenous tissue inhibitors, and the proteasome. *BioMed Research International* [Epub ahead of print].

Taba M, Jr., Jin Q, Sugai JV, Giannobile WV (2005). Current concepts in periodontal bioengineering. *Orthodontics & Craniofacial Research* **8(4)***:*292-302.

Takahashi I, Nishimura M, Onodera K, Bae JW, Mitani H, Okazaki M *et al.* (2003). Expression of MMP-8 and MMP-13 genes in the periodontal ligament during tooth movement in rats. *Journal of Dental Research* **82(8)***:*646-651.

Takahashi I, Onodera K, Nishimura M, Mitnai H, Sasano Y, Mitani H (2006). Expression of genes for gelatinases and tissue inhibitors of metalloproteinases in periodontal tissues during orthodontic tooth movement. *Journal of Molecular Histology* 37(8-9)*:*333-342.

Takayanagi H (2005). Inflammatory bone destruction and osteoimmunology. *Journal of Periodontal Research* **40(4)***:*287-293.

Tang N, Zhao Z, Zhang L, Yu Q, Li J, Xu Z (2012). Up-regulated osteogenic transcription factors during early response of human periodontal ligament stem cells to cyclic tensile strain. *Archives of Medical Science* **8(3)***:*422-430.

Tashjian AH, Jr., Hohmann EL, Antoniades HN, Levine L (1982). Platelet-derived growth factor stimulates bone resorption via a prostaglandin-mediated mechanism. *Endocrinology* **111(1)***:*118-124.

Thilander B (2000). Biological basis for orthodontic relapse. *Seminars in Orthodontics* **6(3)***:*195-205.

Tibbitt MW, Anseth KS (2009). Hydrogels as extracellular matrix mimics for 3D cell culture. *Biotechnology and Bioengineering* **103(4)***:*655-663.

Tomasek JJ, Gabbiani G, Hinz B, Chaponnier C, Brown RA (2002). Myofibroblasts and mechano-regulation of connective tissue remodelling. *Nature reviews Molecular Cell Biology* **3(5)***:*349-363.

Toms SR, Dakin GJ, Lemons JE, Eberhardt AW (2002). Quasi-linear viscoelastic behavior of the human periodontal ligament. *Journal of Biomechanics* **35(10)***:*1411-1415.

Tong Z, Sant S, Khademhosseini A, Jia X (2011). Controlling the fibroblastic differentiation of mesenchymal stem cells via the combination of fibrous scaffolds and connective tissue growth factor. *Tissue Engineering Part A* **17(21-22)***:*2773-2785.

Torzilli PA, Grigiene R, Huang C, Friedman SM, Doty SB, Boskey AL *et al.* (1997). Characterization of cartilage metabolic response to static and dynamic stress using a mechanical explant test system. *Journal of Biomechanics* **30(1)***:*1-9.

Toyoda T, Seedhom BB, Yao JQ, Kirkham J, Brookes S, Bonass WA (2003). Hydrostatic pressure modulates proteoglycan metabolism in chondrocytes seeded in agarose. *Arthritis and Rheumatism* **48(10)***:*2865-2872.

Tsubota M, Sasano Y, Takahashi I, Kagayama M, Shimauchi H (2002). Expression of MMP-8 and MMP-13 mRNAs in rat periodontium during tooth eruption. *Journal of Dental Research* **81(10)***:*673-678.

Tsuji K, Uno K, Zhang GX, Tamura M (2004). Periodontal ligament cells under intermittent tensile stress regulate mRNA expression of osteoprotegerin and tissue inhibitor of matrix metalloprotease-1 and -2. *Journal of Bone and Mineral Metabolism* **22(2)***:*94-103.

Twentyman PR, Luscombe M (1987). A study of some variables in a tetrazolium dye (MTT) based assay for cell growth and chemosensitivity. *British Journal of Cancer* **56(3)***:*279-285.

Uematsu S, Mogi M, Deguchi T (1996). Interleukin (IL)-1 beta, IL-6, tumor necrosis factor-alpha, epidermal growth factor, and beta 2-microglobulin levels are elevated in gingival crevicular fluid during human orthodontic tooth movement. *Journal of Dental Research* **75(1)***:*562-567.

van Leeuwen EJ, Maltha JC, Kuijpers-Jagtman AM (1999). Tooth movement with light continuous and discontinuous forces in beagle dogs. *European Journal of Oral Sciences* **107(6)***:*468-474.

Vande Geest JP, Di Martino ES, Vorp DA (2004). An analysis of the complete strain field within Flexercell membranes. *Journal of Biomechanics* **37(12)***:*1923-1928.

Vandenburgh HH, Karlisch P (1989). Longitudinal growth of skeletal myotubes *in vitro* in a new horizontal mechanical cell stimulator. *In vitro Cellular & Developmental Biology* **25(7)***:*607-616.

Vanderhooft JL, Alcoutlabi M, Magda JJ, Prestwich GD (2009). Rheological properties of cross-linked hyaluronan-gelatin hydrogels for tissue engineering. *Macromolecular Bioscience* **9***:*20-28.

Verma RP, Hansch C (2007). Matrix metalloproteinases (MMPs): chemical-biological functions and (Q)SARs. *Bioorganic & Medicinal Chemistry* **15(6)***:*2223-2268.

Verna C, Melsen B (2003). Tissue reaction to orthodontic tooth movement in different bone turnover conditions. *Orthodontics & Craniofacial Research* **6(3)***:*155-163.

Viecilli RF, Kar-Kuri MH, Varriale J, Budiman A, Janal M (2013). Effects of initial stresses and time on orthodontic external root resorption. *Journal of Dental Research* **92(4)***:*346-351.

von Bohl M, Maltha JC, Von Den Hoff JW, Kuijpers-Jagtman AM (2004). Focal hyalinization during experimental tooth movement in beagle dogs. *American Journal of Orthodontics and Dentofacial Orthopedics* **125(5)***:*615-623.

Von Euler US (1934). Naunym-Schmeidegberg's Archib fur. *Experimental Pathologie and Pharmakologie* **175**, 78–84.

Waddington RJ, Embery G (2001). Proteoglycans and orthodontic tooth movement. *Journal of Orthodontics* **28(4)***:*281-290.

Wahl SM (1992). Transforming growth factor beta (TGF-beta) in inflammation: a cause and a cure. *Journal of Clinical Immunology* **12(2)***:*61-74.

Wall ME, Weinhold PS, Siu T, Brown TD, Banes AJ (2007). Comparison of cellular strain with applied substrate strain *in vitro*. *Journal of Biomechanics* **40(1)***:*173-181.

Wang JC, Yang G, Li Z (2005). Controlling Cell Responses to Cyclic Mechanical Stretching. *Annals of Biomedical Engineering* **33(3)***:*337-342.

Wang JH, Yang G, Li Z, Shen W (2004). Fibroblast responses to cyclic mechanical stretching depend on cell orientation to the stretching direction. *Journal of Biomechanics* **37(4)***:*573-576.

Wang WJ, Zhao YM, Lin BC, Yang J, Ge LH (2012). Identification of multipotent stem cells from adult dog periodontal ligament. *European Journal of Oral Sciences* **120(4)***:*303-310.

Wang Y, Li Y, Fan X, Zhang Y, Wu J, Zhao Z (2011). Early proliferation alteration and differential gene expression in human periodontal ligament cells subjected to cyclic tensile stress. *Archives of Oral Biology* **56(2)***:*177-186.

Webb K, Hitchcock RW, Smeal RM, Li W, Gray SD, Tresco PA (2006). Cyclic strain increases fibroblast proliferation, matrix accumulation, and elastic modulus of fibroblast-seeded polyurethane constructs. *Journal of Biomechanics* **39(6)***:*1136-1144.

Wescott DC, Pinkerton MN, Gaffey BJ, Beggs KT, Milne TJ, Meikle MC (2007). Osteogenic gene expression by human periodontal ligament cells under cyclic tension. *Journal of Dental Research* **86(12)***:*1212-1216.

Wilhelm J, Pingoud A, Hahn M (2003). Real-time PCR-based method for the estimation of genome sizes. *Nucleic Acids Research* **31(10)***:*e56.

Williams KR, Edmundson JT (1984). Orthodontic tooth movement analysed by the Finite Element Method. *Biomaterials* **5(6)***:*347-351.

Wills DJ, Picton DC, Davies WI (1972). An investigation of the viscoelastic properties of the periodontium in monkeys. *Journal Of Periodontal Research* **7(1)***:*42-51.

Wilson AN, Middleton J, Jones ML, McGuinness NJ (1994). The finite element analysis of stress in the periodontal ligament when subject to vertical orthodontic forces. *British Journal Of Orthodontics* **21(2)***:*161-167.

Wong LJ, Bai RK (2006). Real-time quantitative polymerase chain reaction analysis of mitochondrial DNA point mutation. *Methods in Molecular Biology (Clifton, NJ)* **335***:*187-200.

WR P (2000). Biological basis of orthodontic therapy St Louis: Mosby.

Wyllie AH, Kerr JF, Currie AR (1980). Cell death: the significance of apoptosis. *International Review of Cytology* **68***:*251-306.

Xie KY, Yang L, Chen K, Li Q (2012). *In vitro* study of the effect of cyclic strains on the dermal fibroblast (GM3384) morphology—Mapping of cell responses to strain field. *Medical Engineering & Physics* **34(7)***:*826-831.

Xu C, Hao Y, Wei B, Ma J, Li J, Huang Q (2011). Apoptotic gene expression by human periodontal ligament cells following cyclic stretch. *Journal of Periodontal Research* **46(6)***:*742-748.

Xu J, Liu M, Liu J, Caniggia I, Post M (1996). Mechanical strain induces constitutive and regulated secretion of glycosaminoglycans and proteoglycans in fetal lung cells. *Journal of Cell Science* **109 (Pt 6)***:*1605-1613.

Yamaguchi M (2009). RANK/RANKL/OPG during orthodontic tooth movement. *Orthodontics & Craniofacial Research* **12(2)***:*113-119.

Yamaguchi M, Aihara N, Kojima T, Kasai K (2006). RANKL increase in compressed periodontal ligament cells from root resorption. *Journal Of Dental Research* **85(8)***:*751-756.

Yamaguchi M, Ozawa Y, Nogimura A, Aihara N, Kojima T, Hirayama Y *et al.* (2004). Cathepsins B and L increased during response of periodontal ligament cells to mechanical stress *in vitro*. *Connective Tissue Research* **45(3)***:*181-189.

Yamaguchi M, Shimizu N, Goseki T, Shibata Y, Takiguchi H, Iwasawa T *et al.* (1994). Effect of different magnitudes of tension force on prostaglandin E2 production by human periodontal ligament cells. *Archives of Oral Biology* **39(10)***:*877-884.

Yamamoto T, Kita M, Kimura I, Oseko F, Terauchi R, Takahashi K *et al.* (2006). Mechanical stress induces expression of cytokines in human periodontal ligament cells. *Oral Diseases* **12(2)***:*171-175.

Yamamura N, Sudo R, Ikeda M, Tanishita K (2007). Effects of the mechanical properties of collagen gel on the *in vitro* formation of microvessel networks by endothelial cells. *Tissue Engineering* **13(7)***:*1443-1453.

Yamasaki K, Miura F, Suda T (1980). Prostaglandin as a mediator of bone resorption induced by experimental tooth movement in rats. *Journal of Dental Research* **59(10)***:*1635-1642.

Yamasaki K, Shibata Y, Fukuhara T (1982). The effect of prostaglandins on experimental tooth movement in monkeys (Macaca fuscata). *Journal of Dental Research* **61(12)***:*1444-1446.

Yamashiro K, Myokai F, Hiratsuka K, Yamamoto T, Senoo K, Arai H (2007). Oligonucleotide array analysis of cyclic tension-responsive genes in human periodontal ligament fibroblasts. *The International Journal of Biochemistry & Cell Biology* **39(5)***:*910-921.

Yang YQ, Li XT, Rabie AB, Fu MK, Zhang D (2006). Human periodontal ligament cells express osteoblastic phenotypes under intermittent force loading *in vitro*. *Frontiers in Bioscience* **11***:*776-781.

Yao S, Liu D, Pan F, Wise GE (2006). Effect of vascular endothelial growth factor on RANK gene expression in osteoclast precursors and on osteoclastogenesis. *Archives of Oral Biology* **51(7)***:*596-602.

Yasuda H, Shima N, Nakagawa N, Yamaguchi K, Kinosaki M, Mochizuki S *et al.* (1998). Osteoclast differentiation factor is a ligand for osteoprotegerin/osteoclastogenesis-inhibitory factor and is identical to TRANCE/RANKL. *Proceedings of the National Academy of Sciences of the United States of America* **95(7)***:*3597-3602.

Yousefian J, Firouzian F, Shanfeld J, Ngan P, Lanese R, Davidovitch Z (1995). A new experimental model for studying the response of periodontal

ligament cells to hydrostatic pressure. *American Journal Of Orthodontics and Dentofacial Orthopedics* **108(4)***:*402-409.

Yun YR, Won JE, Jeon E, Lee S, Kang W, Jo H (2010). Fibroblast growth factors: biology, function, and application for tissue regeneration. *Journal of Tissue Engineering* **2010***:*218142.

Zengo AN, Pawluk RJ, Bassett CA (1973). Stress-induced bioelectric potentials in the dentoalveolar complex. *American Journal of Orthodontics* **64(1)***:*17-27.

Zentner A, Heaney T, Sergl H (2000). Proliferative response of cells of the dentogingival junction to mechanical stimulation. *The European Journal of Orthodontics* **22(6)***:*639-648.

Zhao LJ, Jiang H, Papasian CJ, Maulik D, Drees B, Hamilton J (2008a). Correlation of obesity and osteoporosis: effect of fat mass on the determination of osteoporosis. *Journal of Bone and Mineral Research* **23(1)***:*17-29.

Zhao Z, Fan Y, Bai D, Wang J, Li Y (2008b). The adaptive response of periodontal ligament to orthodontic force loading – A combined biomechanical and biological study. *Clinical Biomechanics* **23, Suppl 1(0)***:*S59-S66.

Zhong W, Xu C, Zhang F, Jiang X, Zhang X, Ye D (2008). Cyclic stretching force-induced early apoptosis in human periodontal ligament cells. *Oral Diseases* **14(3)***:*270-276.

Zhong W, Zhang W, Wang S, Qin J (2013). Regulation of fibrochondrogenesis of mesenchymal stem cells in an integrated microfluidic platform embedded with biomimetic nanofibrous scaffolds. *PloS one* **8(4)***:*e61283.

Zipper H, Brunner H, Bernhagen J, Vitzthum F (2004). Investigations on DNA intercalation and surface binding by SYBR Green I, its structure determination and methodological implications. *Nucleic Acids Research* **32(12)***:*e103.

Zitka O, Kukacka J, Krizkova S, Huska D, Adam V, Masarik M (2010). Matrix metalloproteinases. *Current Medicinal Chemistry* **17(31)***:*3751-3768.

7.1. Pictures and Tables

Berridge MJ (1985). The molecular basis of communication within the cell. *Scientific American* **253(4)***:*142-152.

Meikle MC (2002). Craniofacial development, growth and evolution Bressingham: Bateson.

Rose LF (2004). Periodontics : medicine, surgery, and implants Philadelphia: Mosby.

Figure 1.1 : www.studiodentaire.com/en/glossary/periodontal_ligament.php.

Flexcell pictures and informations : http://www.flexcellint.com/reports.htm

Appendix 1

Published work

Saminathan A, Vinoth KJ, Wescott DC, Pinkerton MN, Milne TJ, Cao T (2012). The effect of cyclic mechanical strain on the expression of adhesion-related genes by periodontal ligament cells in two-dimensional culture. *Journal of Periodontal Research* **47(2)***:*212-221.

Journal of
PERIODONTAL RESEARCH

J Periodont Res 2012; 47: 212–221

JOURNAL OF PERIODONTAL RESEARCH
doi:10.1111/j.1600-0765.2011.01423.x

The effect of cyclic mechanical strain on the expression of adhesion-related genes by periodontal ligament cells in two-dimensional culture

A. Saminathan[1], K. J. Vinoth[1], D. C. Wescott[2], M. N. Pinkerton[2], T. J. Milne[2], T. Cao[1], M. C. Meikle[1]

[1]Faculty of Dentistry, National University of Singapore, Singapore and [2]Department of Oral Sciences, Faculty of Dentistry, University of Otago, Dunedin, New Zealand

Saminathan A, Vinoth KJ, Wescott DC, Pinkerton MN, Milne TJ, Cao T, Meikle MC. The effect of cyclic mechanical strain on the expression of adhesion-related genes by periodontal ligament cells in two-dimensional culture. J Periodont Res 2012; 47: 212–221. © 2011 John Wiley & Sons A/S

Background and Objective: Cell adhesion plays important roles in maintaining the structural integrity of connective tissues and sensing changes in the biomechanical environment of cells. The objective of the present investigation was to extend our understanding of the effect of cyclic mechanical strain on the expression of adhesion-related genes by human periodontal ligament cells.

Material and Methods: Cultured periodontal ligament cells were subjected to a cyclic in-plane tensile deformation of 12% for 5 s (0.2 Hz) every 90 s for 6–24 h in a Flexercell FX-4000 Strain Unit. The following parameters were measured: (i) cell viability by the MTT assay; (ii) caspase-3 and -7 activity; and (iii) the expression of 84 genes encoding adhesion-related molecules using real-time RT-PCR micro-arrays.

Results: Mechanical stress reduced the metabolic activity of deformed cells at 6 h, and caspase-3 and -7 activity at 6 and 12 h. Seventy-three genes were detected at critical threshold values < 35. Fifteen showed a significant change in relative expression: five cell adhesion molecules (*ICAM1*, *ITGA3*, *ITGA6*, *ITGA8* and *NCAM1*), three collagen α-chains (*COL6A1*, *COL8A1* and *COL11A1*), four MMPs (*ADAMTS1*, *MMP8*, *MMP11* and *MMP15*), plus *CTGF*, *SPP1* and *VTN*. Four genes were upregulated (*ADAMTS1*, *CTGF*, *ICAM1* and *SPP1*) and 11 downregulated, with the range extending from a 1.76-fold induction of *SPP1* at 12 h to a 2.49-fold downregulation of *COL11A1* at 24 h.

Conclusion: The study has identified several mechanoresponsive adhesion-related genes, and shown that onset of mechanical stress was followed by a transient reduction in overall cellular activity, including the expression of two apoptosis 'executioner' caspases.

Murray C. Meikle, Faculty of Dentistry, National University of Singapore, 11 Lower Kent Ridge Road, Singapore 119083
Tel: +65 6772 6840
Fax: + 65 6773 2602
e-mail: pndmcm@nus.edu.sg

Key words: adhesion-related gene; apoptosis; cyclic mechanical strain; periodontal ligament cell; real-time RT-PCR microarray

Accepted for publication September 2, 2011

The periodontal ligament is a specialized connective tissue that has evolved to provide attachment of teeth to the bone of the jaws. The periodontal ligament functions in a mechanically active environment and, in addition to its attachment role, serves as a shock absorber to protect the tooth-supporting alveolar bone from excessive

occlusal loading, not only during mastication, deglutition and speech, but also due to occlusal trauma and man-made orthodontic appliances.

Numerous *in vitro* studies have investigated the effects of cyclic and continuous mechanical strain on gene expression by human periodontal ligament cells. Most have focused on alterations in the expression of a small number of cytokine and osteogenic genes (1–4), but microarrays which allow the activity of numerous genes to be monitored simultaneously have also been reported (5–8). Alterations in cell–matrix and cell–cell adhesion play important roles not only in maintaining the structural integrity of connective tissues, but also in sensing changes in the biomechanical environment of cells and mediating the transmission of bidirectional forces across their plasma membranes (9–11). Periodontal ligament cells, derived as they are from a biomechanically active tissue, therefore offer an excellent experimental model for investigating the expression of genes involved in these interactions.

All cells have a finite life span, and apoptosis, a form of programmed cell death in which cells are induced to activate their own death or suicide, plays an important role in many pathophysiologcal processes, including tissue remodelling and homeostasis (12,13). However, cultured bone and periodontal ligament cells deprived of the normal functional loading to which they are exposed *in vivo* are in a physiological default state, raising the question of what effect mechanical stimuli might have on apoptosis-mediated cell death. The *in vitro* evidence to date is equivocal. Although complicated by the use of different model systems and strain regimens, unlike cultured bone cells, where mechanical stimuli have typically been shown to inhibit apoptosis (14,15), in cultured human periodontal ligament cells cyclic mechanical strain has been reported to trigger a transient increase in apoptosis (16,17). This is important because any reductions in metabolic activity may compromise quantification of alterations in gene expression.

In the present investigation, human periodontal ligament cells in two-dimensional culture were screened for adhesion-related genes using targeted real-time RT-PCR microarrays, and we report, for the first time, the effect that a predominantly tensile cyclic mechanical strain has on their expression. We further show that the immediate response of the cells to a change in their biophysical environment was a short-term reduction in overall cellular activity, including the expression of two apoptosis 'executioner' caspases.

Material and methods

Preparation of human periodontal ligament cells

Premolar teeth that had been extracted for orthodontic reasons were used to establish human periodontal ligament cell cultures as described previously (18). Approval to harvest human tissue from extracted teeth with the consent of the donor and/or parent was granted by the Ethics Committees of the University of Otago (reference 05/069) and National University of Singapore (NUS-IRB reference 08-015). Teeth were washed with phosphate-buffered saline and fragments of the periodontal ligament attached to the middle third of the root removed with a scalpel. Tissue explants were plated onto 3 cm Petri dishes in Dulbecco's modifiied Eagle's medium (Gibco, Invitrogen, Auckland, NZ, USA) supplemented with 10% fetal calf serum (Gibco) and antibiotic–antimycotic reagent (10,000 units penicillin, 10,000 μg streptomycin and 25 μg/mL amphoter icin B; Invitrogen), 100 mmol L-glutamine (Invitrogen) and gentamicin (10 mg/mL; Gibco) and cultured at 37°C in a humidified atmosphere of 5% CO_2–95% air. On reaching confluence, the cells were lifted with trypsin–EDTA (Gibco) and serially passaged through 25, 75 and 175 cm^2 tissue culture flasks (Cellstar; Greiner Bio-One AG, Munroe, NC, USA). Passage two cells were frozen in Cell Culture Freezing Medium (Gibco) at −80°C and transferred to liquid nitrogen for long-term storage. Third or fourth passage cells were used for experimental purposes.

Application of cyclic mechanical strain to periodontal ligament cells

Human periodontal ligament cells (3×10^5 per well) were subcultured into six-well, 35 mm flexible-bottomed UniFlex® Series culture plates containing a centrally located rectangular strip (15.25 × 24.18 mm) coated with type I collagen. When the cells had reached confluence (commonly 3–4 d), the silicon rubber membranes were subjected to an in-plane deformation of 12% for 5 s (0.2 Hz) every 90 s using a square waveform, around rectangular ArcTangle™ loading posts (required to correctly apply uniaxial strain to the cells) in a standard Bioflex baseplate linked to a Flexercell FX-4000 strain unit (Flexcell Corp., Hillsborough, NC, USA). The strain value of 12% was based on data derived from a finite element model, which suggested that maximal periodontal ligament strains for horizontal displacements of a human maxillary central incisor under physiological loading lies in the vicinity of 8–25%, depending upon the apico-crestal position. Deformation of 12% correlates well with strain conditions predicted at the mid-root (19). Experimental and control plates were allocated to each of the three time points (6, 12 and 24 h) and separate experiments performed for light microscopy, cell activation, caspase activity and RNA extraction. As discussed in detail later, the deformation of the silicon membrane is not uniform, but generates a tension gradient; any changes in expression will therefore represent the global average of cells exposed to different amounts of strain.

Changes in cell morphology

At the end of the experimental period, plates were examined by light microscopy to determine changes in the orientation of the cells and evidence of cellular detachment or collagen delamination. Some cultures were fixed with acetic methanol (one part glacial acetic acid; three parts methanol) for 5 min at 25°C and, after aspirating the fixative, 1% Giemsa stain (G9641; Sigma-Aldrich, Singapore) in acetic

methanol was added for 2–5 min at 25°C. After washing with 60% methanol in water for 1–2 min, rectangular segments were cut from the silicon membranes and, after mounting on glass slides, viewed by light microscopy.

MTT assay for cell viability

Cell activation was measured by the MTT assay (Sigma-Aldrich), a colorimetric assay for estimating mammalian cell survival, proliferation and activation based on the ability of viable cells to reduce yellow 3-(4, 5-dimethythiazol-2-yl)-2, 5-diphenyl tetrazolium bromide (MTT) by mitochondrial succinate dehydrogenase (20,21). At the end of each time point the cells were harvested by trypsinization and resuspended in fresh media; 50 μL of this cell suspension was added to 96-well plates and spun at 1800 *g* for 5 min. The supernatant was removed and 50 μL of the MTT solution (4 mg/mL in Dulbecco's modifiied Eagle's medium) added to each well. The cells were incubated at 37°C for 2 h in the dark. Following incubation, the plate was centrifuged and the supernatant discarded. The resulting formazan crystals were dissolved by the addition of 200 μL of dimethylsulfoxide (Sigma-Aldrich), and absorbance was measured at 570 nm in a microplate reader (Tecan SpectrophorPlus, Singapore).

Caspase-3 and -7 assay

Caspases, a family of cysteine proteinases that specifically cleave proteins following aspartate residues, play key roles in mammalian apoptosis. Two 'executioner' caspases (3 and 7) were measured by the Caspase-Glo 3/7 Assay (Promega Corp., Madison, WI, USA), which provides a luminescent Caspase-3/7 substrate containing the tetrapeptide sequence (Asp-Glu-Val-Asp) in a reagent optimized for caspase activity, luciferase activity and cell lysis. At the end of each time period, the collagen-coated rectangular area was cut and treated with the Caspase-Glo® 3/7 reagent for 1 h in the dark at room temperature according to the manufacturer's instructions. Each sample was aliquoted into triplicate tubes, and luminescence, expressed as relative light units (RLU), was measured with a Sirius Single Tube Luminometer (Berthold Detection Systems GmbH, Pforzheim, Germany).

Extraction of RNA

Culture media were removed from the wells and total RNA isolated by a modification of the method of Chomczynski and Sacchi (22). Briefly, 0.5 mL of TRIzol® reagent (Invitrogen) was added to each well of the Uniflex plate. After a 5 min incubation period, the cell lysate was added to a tube containing 0.1 mL of chloroform and shaken vigorously by hand for 15 s. A further incubation of 2–3 min at room temperature was required prior to centrifugation of the samples at 12,000*g* for 15 min at 4°C. Following centrifugation, 300 μL of the clear aqueous phase was added to an equal volume of 70% ethanol and vortexed to disperse the precipitate. Sample purity was achieved using the Purelink Micro-to-Midi Total RNA Purification System (Invitrogen) in accordance with the manufacturer's instructions. Total RNA samples were eluted from the columns in 50 μL of RNase-free water and stored at −80°C. The concentration and purity (based on the A260/280 absorbance ratio) of the samples was determined using a Nanodrop ND-1000 Spectrophotometer (Nanodrop Technologies, Rockland, DE, USA). This combined extraction technique yielded 180–250 ng RNA from six wells with an A260/280 value of 1.96 ± 0.07; an A260/280 value > 1.9–2.0 corresponds to a pure sample free of contaminating protein (Applied Biosystems, Life Technologies Corporation, Carlsbad, CA, USA).

Real-time PCR array analysis

Total RNA samples were assessed for degradation status by denaturing agarose gel electrophoresis, prior to analysis. Contaminating genomic DNA was removed from total RNA samples by DNase I digestion prior to first strand synthesis. First strand synthesis was performed using the RT^2 PCR array First Strand Kit (SABiosciences, Fredrick, MD, USA). Samples were then screened for the expression of 84 genes encoding extracellular matrix and adhesion molecules using the RT^2 Profiler PCR Array System (SABiosciences). SABiosciences PCR arrays are sets of optimized PCR primer assays that perform gene expression analysis using the principle of real-time PCR. They achieve a multigene profiling capability similar to that of microarray or SuperArray technology by setting up multiple PCRs in a 96-well plate format. Experimental and control samples at each of the three time points were analysed in triplicate to allow for biological variation between samples and provide a statistically sound data set.

Statistical methods

Data from the viability and caspase assays are expressed as means ± SEM. Differences between groups was determined by Student's *t*-test (two-tailed) using GRAPHPAD PRISM (GraphPad Software Inc., San Diego, CA, USA) and the level of significance set at $p < 0.05$. For the gene expression study, expression profiles of the target genes were measured relative to the mean critical threshold (C_t) values of five different calibrator genes (*GAPDH*, β2-microglobulin, β-actin, *HPRT1* and *RPLI3A*) using the $\Delta\Delta C_t$ method described by Livak and Schmittgen (23). Student's *t*-tests were used for statistical comparison of the control and experimental groups using mean C_t values derived from the triplicate samples (24).

Results

Under light microscopy, a difference in cellular orientation was observed as early as 6 h after the application of cyclic strain, with no evidence of cell detachment or plate delamination. While control cells remained randomly orientated, mechanically deformed cells had become reorientated away from the direction of the applied force, as previously reported (25,26). However, realignment of the cells was not uniform across the whole surface of the centrally located collagen strip, tending

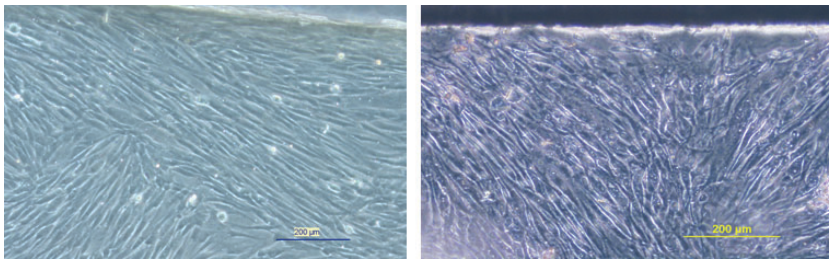

Fig. 1. The application of an in-plane deformation of 12% for 5 s (0.2 Hz) every 90 s, using a square waveform, around rectangular ArcTangle™ loading posts resulted in reorientation of the cells. Both images were taken at the edge of the centrally located type I collagen strip. Left, control culture in which cells tend to be randomly orientated. Right, 12 h stressed culture stained by the Giemsa method. Cells become aligned at varying angles to the long axis of the applied strain.

to be more pronounced towards the edges (Fig. 1).

The MTT assay showed that intermittent substrate deformation resulted in a small, but statistically significant, reduction in overall metabolic activity at 6 h (Table 1). There was also a reduction in caspase-3 and -7 activity by mechanically strained cells at 6 and 12 h, suggesting that the strain regimen had delivered a transient anti-apoptotic signal to the cells (Fig. 2).

A total of 84 cell adhesion and extracellular matrix genes were screened, and the effect of intermittent tensile strain on their differential expression is summarized in Table 2. A gene was regarded as being expressed if it was detected at a C_t value of < 35, and using these criteria 73 genes were detectable, thereby demonstrating significant levels of basal expression. Eleven genes had C_t values ≥ 35, which were outside the detection threshold of the system and were therefore considered not to have been expressed. This group comprised the genes for three matrix metalloproteinases (*MMP7*, *MMP9* and *MMP13*), two integrins (*ITGAL* and *ITGAM*) and three selectins (*SELE*, *SELL* and *SELP*), plus E-cadherin (*CDH1*); Kallmann syndrome 1 sequence (*KAL1*) and ϵ-sarcoglycan (*SGCE*).

Over the 24 h time course, we found statistically significant changes in the relative expression of mRNAs for 16 genes, suggesting a role for cyclic mechanical strain in regulating their function. These included six cell adhesion molecules (*ICAM1*, *ITGA3*, *ITGA6*, *ITGA8, ITGB1* and *NCAM1*) and three genes encoding collagen α-chains (*COL6A1*, *COL8A1* and *COL11A1*; Fig. 3); also four members of the MMP family (*ADAMTS1*, *MMP8*, *MMP11* and *MMP15*), connective tissue growth factor (*CTGF*), secreted phosphoprotein (*SPP1*; also known as bone sialoprotein/osteopontin) and the cell-attachment protein vitronectin (*VTN*; Fig. 4).

Of the mechanoresponsive genes, only four were found to be upregulated (*ADAMTS1*, *CTGF*, *ICAM1* and *SPP1*), the remaining 11 being downregulated, with the range extending from a 2.49-fold downregulation of *COL11A1* at 24 h (Fig. 3) to a 1.76-fold induction of *SPP1* at 12 h (Fig. 4). No genes were found to be consistently up- or downregulated across all three time points, and only two [*ADAMTS1* (upregulated) and *ITGA8* (downregulated)] were expressed across two time points. Four genes (*HAS*, *ITGB4*, *LAMA2* and *TIMP3*) showed treated/control ratios of ± 2, but none reached statistical significance ($p < 0.05$).

Table 1. Effect of cyclic mechanical strain on the viability of periodontal ligament cells

	6 h	12 h	24 h
Control	2.932 ± 0.077	3.176 ± 0.195	2.021 ± 0.199
Stressed	2.535 ± 0.135*	3.266 ± 0.148	1.888 ± 0.182

Following the application of a uniaxial, cyclic tensile strain of 12% for 5 s (0.2 Hz) every 90 s, the colorimetric MTT (tetrazolium) assay was used to detect living cells; absorbance was measured at 570 nm. Data are expressed as means ± SEM for six wells; data are from three separate experiments. There was a small but statistically significant (*$p < 0.05$) reduction in cell viability at 6 h in mechanically stressed cultures.

Discussion

In the Flexercell™ system, a silicone membrane is stretched across a loading post by the application of vacuum pressure and, depending on the shape of the loading post, either a biaxial or a uniaxial strain (as in the present study) may be applied to the cells. Although the most widely used commercially available apparatus for delivering controlled mechanical strain to cells *in vitro*, the Flexercell system does have limitations, particularly when it comes to determining the physical characteristics of the strain. First, the mechanical in-plane deformation applied to Uniflex plates™ does not produce a purely tensional strain because tension in one plane is always accompanied by compressive and shear strains due to the Poisson effect (27,28). Second, cells cultured on a Uniflex plate will experience about half the applied substrate strain programmed into the computer (29). And third, the amount of cellular deformation will vary with the distance from the middle of the membrane; cells near the perimeter of the field will experience greater deformation (27). Nevertheless, despite the shortcomings of all existing model systems in precisely defining the strain profile, *in vitro* methodology still remains the most effective way to screen cells for the expression of mechanoresponsive genes. In any event, three-dimensional finite element analysis of the von Mises and principal stresses generated in different parts of the periodontal ligament when multirooted teeth are mechanically loaded by a masticatory force indicates that the deformation profile of the cells *in vivo* is also complex (30).

The MTT assay data, which suggested a reduction in cellular activity in mechanically deformed cultures at 6 h,

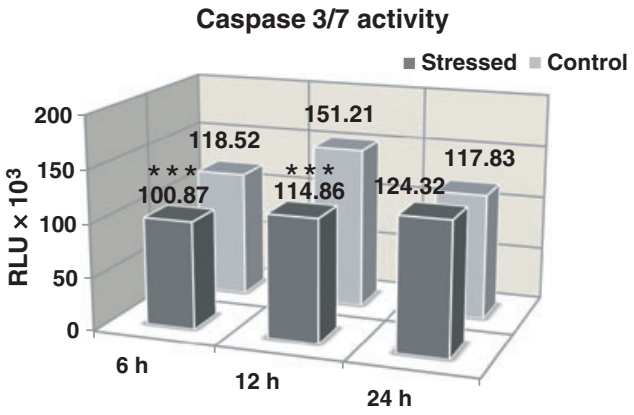

	6 h	12 h	24 h
Control × 10^3	118.52 ± 0.59	151.21 ± 0.48	117.83 ± 0.27
Stressed × 10^3	100.87 ± 0.35	114.86 ± 0.86	124.32 ± 0.43

Fig. 2. The effect of cyclic mechanical strain on the activity of two 'executioner' caspases (caspase-3 and caspase-7) in response to a uniaxial, cyclic tensile strain of 12%. Mechanically induced strain resulted in a significant reduction in caspase activity at 6 and 12 h. Data are expressed in relative light units (RLU) as means ± SEM for six wells; data are from three separate experiments with the same batch of cells. ***$p < 0.001$.

supports the findings of a recent study using an out-of-plane, four-point bending system, which reported that a cyclic tensile strain as low as 0.5%, applied to human periodontal ligament cells for only 2 h, had an inhibitory effect on cell proliferation and viability (31). That is not to say that mechanical stress is cytotoxic, although the MTT assay is commonly used to study cytotoxicity; the signal generated in the assay is dependent upon the number and activity of living cells (20,21), but reductions in the MMT formazan product can occur without a decrease in the number of viable cells. Moreover, Wang *et al.* (31) also performed a microarray analysis using a whole-genome oligonucleotide chip and were able to identify 110 genes that were differentially expressed, 97 of which were upregulated. These data and the findings of the present study indicate that mechanically deformed cells remain metabolically active, and suggest that any changes in gene expression represent a short-term adjustment to alterations in their biophysical environment.

Our caspase-3 and -7 data suggest that the application of an in-plane cyclic strain to periodontal ligament cells has a positive, albeit transient, effect on apoptosis, an observation supported by comparable data for gingival fibroblasts (32). It does, however, contrast with previous reports showing that an out-of-plane cyclic mechanical strain transiently increases apoptosis in periodontal ligament cells (16,17). This seems likely to have been due to the more vigorous strain regimens used (1, 10 and 20% deformation at 0.25 Hz for 10 and 6 cycles/min, respectively), suggesting that the cells might have been overstressed. Experiments conducted on human lung fibroblasts, for example, have shown that 20% cyclic deformation activated apoptotic signalling pathways (33), while 25% strain induced cell death (34). In other words, induction of apoptosis in mechanically deformed cells *in vitro* appears to be related to the magnitude and frequency of the applied strain. This is likely to be reflected in real life, where the periodontal ligament will be more heavily stressed by occlusal loading during mastication than in swallowing. The relationship between the biophysical environment of a cell and the mechanisms of programmed cell death appears to be a complicated one and would benefit from further investigation.

Cells in culture are not uniformly attached to their substrate, but are 'tack-welded' at focal adhesions, where integrin receptors physically link actin-associated cytoskeletal proteins (talin, vinculin, α-actinin and paxillin) to the extracellular matrix (11), as well as to adhesion molecules on the surface of adjacent cells. Integrin-mediated adhesive interactions play key roles in cell migration, proliferation and differentiation, and also regulate intracellular signal transduction pathways that control adhesion-induced (outside-in) changes in cell physiology (9,10). Integrins thus function both as cell adhesion molecules and intracellular signalling receptors, and it is likely that the previously reported changes in cell signalling in response to mechanical deformation are downstream of events mediated by integrins (35). Fourteen integrin subunits were detected at C_t values < 35, confirming previous findings that human periodontal ligament cells express numerous integrin receptors (36). Of these, *ITGA3*, *ITGA6*, *ITGA8* and *ITGB1* were significantly downregulated at various points in the time scale. All are involved in cell attachment to collagen and other substrate adhesion molecules and function to provide cell–matrix linkage. Integrin α3β1 is one of the integrin heterodimers that binds to type I collagen, while the adhesion of fibroblastic cells to laminin is mediated by both α3β1 and α6β1 integrins (37). Integrin α8 also forms heterodimers with integrin β1 and functions as a receptor for tenascin, fibronectin and vitronectin (38). Reduction in the expression of these genes is therefore consistent with detachment and reorientation of the cells observed microscopically, as was downregulation in the expression of the *NCAM1* and *VTN* genes.

The next puzzle is how this might be mediated. Members of the MMP family of proteolytic enzymes are the most likely candidates. Sixteen members of the MMP family were constitutively expressed at C_t values < 35, including seven MMPs, three membrane type matrix metalloproteinases (MT-MMPs), three a disintegrin and metalloproteinases with thrombospondin motifs (ADAMTSs) and three TIMPs. TIMPs are important extracellular regulators of MMPs, and numerous studies suggest that pathophysiological resorption is correlated with an

Table 2. Alterations in the expression of adhesion-related genes by human periodontal ligament cells following cyclic mechanical strain

Name of gene	Description	Fold up- or downregulation (experimental/control)					
		6 h	*p*-Value	12 h	*p*-Value	24 h	*p*-Value
ADAMTS1	Metallopeptidase thrombospondin I motif 1	1.29	0.0066	1.11	0.3452	1.32	0.0226
ADAMTS13	Metallopeptidase thrombospondin I motif 13	−1.53	0.3163	1.28	0.4690	−1.81	0.2037
ADAMTS8	Metallopeptidase thrombospondin I motif 8	1.04	0.9293	−1.07	0.8240	1.48	0.5384
CD44	CD44 molecule	1.03	0.6003	1.06	0.3214	1.05	0.1468
CDH1	Cadherin 1, type 1, E-cadherin (epithelial)	ND	ND	ND	ND	ND	ND
CLEC3B	C-type lectin domain family 3, member B	1.02	0.8951	−1.13	0.7379	1.12	0.6066
CNTN1	Contactin 1	−1.04	0.8663	−1.15	0.5570	−1.41	0.0926
COL1A1	Collagen, type I, α1	−1.08	0.4576	−1.04	0.9074	1.02	0.8773
COL4A2	Collagen, type IV, α2	1.04	0.7795	1.06	0.7367	−1.04	0.6374
COL5A1	Collagen, type V, α1	−1.01	0.9314	−1.19	0.3741	1.15	0.3449
COL6A1	Collagen, type VI, α1	−1.06	0.5398	−1.64	0.0425	1.06	0.6791
COL6A2	Collagen, type VI, α2	−1.11	0.2276	−1.44	0.1504	−1.14	0.5632
COL7A1	Collagen, type VII, α1	−1.03	0.8950	1.13	0.6816	1.10	0.7741
COL8A1	Collagen, type VIII, α1	−1.19	0.3865	−1.35	0.0165	−1.28	0.2641
COL11A1	Collagen, type XI, α1	1.03	0.9373	1.13	0.4348	−2.49	0.0169
COL12A1	Collagen, type XII, α1	−1.18	0.5391	−1.21	0.6089	−1.14	0.2274
COL14A1	Collagen, type XIV, α1	−1.37	0.1790	1.07	0.4394	−1.01	0.9558
COL15A1	Collagen, type XV, α1	−1.06	0.7353	−1.20	0.6717	1.09	0.3297
COL16A1	Collagen, type XVI, α1	−1.09	0.3610	−1.07	0.5466	1.01	0.9213
CTGF	Connective tissue growth factor	−1.29	0.1011	−1.26	0.3554	1.36	0.0156
CTNNA1	Catenin (cadherin-associated protein), α1	1.06	0.7314	−1.61	0.1544	−1.03	0.5492
CTNNB1	Catenin (cadherin-associated protein), β1	−1.13	0.2498	−1.13	0.3472	−1.08	0.1917
CTNND1	Catenin (cadherin-associated protein), δ1	1.02	0.8601	−1.66	0.1624	−1.05	0.4233
CTNND2	Catenin (cadherin-associated protein), δ2	−1.02	0.9193	1.02	0.8303	−1.30	0.3117
ECM1	Extracellular matrix protein 1	−1.03	0.6846	−1.04	0.7175	−1.04	0.4154
FN1	Fibronectin 1	−1.09	0.5283	1.27	0.1587	1.10	0.4764
HAS1	Hyaluronan synthase 1	−1.01	0.9887	ND	ND	−2.34	0.1135
ICAM1	Intercellular adhesion molecule 1 (CD54)	1.62	0.1396	1.74	0.0262	1.00	0.9986
ITGA1	Integrin, α1	−1.17	0.2650	−1.32	0.1899	−1.27	0.1350
ITGA2	Integrin, α2	−1.03	0.8958	−1.69	0.1760	−1.20	0.3546
ITGA3	Integrin, α3	1.03	0.8138	−1.22	0.0469	−1.09	0.6196
ITGA4	Integrin, α4	−1.05	0.7425	−1.13	0.6331	−1.19	0.2664
ITGA5	Integrin, α5	1.01	0.8561	−1.05	0.5481	1.17	0.2033
ITGA6	Integrin, α6	−1.16	0.1839	−1.11	0.6650	−1.23	0.0283
ITGA7	Integrin, α7	−1.13	0.4213	1.01	0.9716	−1.06	0.7357
ITGA8	Integrin, α8	−1.14	0.0157	−1.25	0.0348	1.23	0.3822
ITGAL	Integrin, αL	ND	ND	ND	ND	ND	ND
ITGAM	Integrin, αM	ND	ND	ND	ND	ND	ND
ITGAV	Integrin, αV	−1.14	0.4016	−1.03	0.8566	−1.14	0.1614
ITGB1	Integrin, β1	−1.30	0.6177	−1.18	0.0367	−1.03	0.7270
ITGB2	Integrin, β2	−1.15	0.4842	1.28	0.1568	1.00	0.9833
ITGB3	Integrin, β3	1.06	0.9117	−1.65	0.5671	−1.71	0.1364
ITGB4	Integrin, β4	−1.31	0.3184	−1.15	0.5688	−2.25	0.1559
ITGB5	Integrin, β5	−1.02	0.8581	−1.07	0.1374	1.09	0.1953
KAL1	Kallmann syndrome 1 sequence	ND	ND	ND	ND	ND	ND
LAMA1	Laminin, α1	1.08	0.5504	−1.06	0.7369	1.01	0.8778
LAMA2	Laminin, α2	4.77	0.4376	−1.31	0.2733	−1.16	0.3614
LAMA3	Laminin, α3	−1.13	0.4386	−1.16	0.0702	−1.07	0.7036
LAMB1	Laminin, β1	−1.17	0.3092	−1.06	0.3932	−1.10	0.2048
LAMB3	Laminin, β3	−1.05	0.5515	−1.23	0.1162	−1.16	0.2154
LAMC1	Laminin, γ1 (formerly *LAMB2*)	−1.03	0.8356	−1.40	0.2434	−1.20	0.1382
MMP1	Matrix metallopeptidase 1	1.08	0.5536	ND	ND	1.03	0.5905
MMP2	Matrix metallopeptidase 2	−1.10	0.3379	−1.04	0.6927	−1.08	0.4806
MMP3	Matrix metallopeptidase 3	−1.03	0.7509	1.30	0.0759	−1.29	0.0609
MMP7	Matrix metallopeptidase 7	ND	ND	ND	ND	ND	ND
MMP8	Matrix metallopeptidase 8	−1.33	0.0788	−1.21	0.5606	−2.02	0.0103
MMP9	Matrix metallopeptidase 9	ND	ND	ND	ND	ND	ND
MMP10	Matrix metallopeptidase 10	−1.21	0.2620	1.14	0.2692	1.03	0.8722
MMP11	Matrix metallopeptidase 11	−1.23	0.1800	−1.35	0.0364	−1.09	0.5464
MMP12	Matrix metallopeptidase 12	−1.13	0.4218	1.20	0.1692	−1.16	0.3762

Table 2.(Continued)

Name of gene	Description	Fold up- or downregulation (experimental/control)					
		6 h	*p*-Value	12 h	*p*-Value	24 h	*p*-Value
MMP13	Matrix metallopeptidase 13	ND	ND	ND	ND	ND	ND
MMP14	Matrix metallopeptidase 14	1.01	0.9360	−1.22	0.1830	1.11	0.4988
MMP15	Matrix metallopeptidase 15	−1.92	0.0077	1.54	0.2398	ND	ND
MMP16	Matrix metallopeptidase 16	−1.04	0.8018	−1.07	0.6069	−1.16	0.1985
NCAM1	Neural cell adhesion molecule 1	−1.09	0.0268	−1.31	0.3457	1.22	0.0535
PECAM1	Platelet/endothelial cell adhesion molecule	1.23	0.6156	−1.11	0.8371	ND	ND
SELE	Selectin E (endothelial adhesion molecule 1)	ND	ND	ND	ND	ND	ND
SELL	Selectin L (lymphocyte adhesion molecule 1)	ND	ND	ND	ND	ND	ND
SELP	Selectin P	ND	ND	ND	ND	ND	ND
SGCE	Sarcoglycan, ϵ	ND	ND	ND	ND	ND	ND
SPARC	Secreted protein, acidic, cysteine-rich	−1.06	0.4308	1.08	0.5330	1.16	0.2112
SPG7	Spastic paraplegia 7	1.00	0.9901	1.06	0.6940	−1.24	0.5028
SPP1	Secreted phosphoprotein 1	1.12	0.4623	1.76	0.0037	1.08	0.4308
TGFBI	Transforming growth factor, β1	−1.07	0.6058	−1.42	0.2495	−1.06	0.5762
THBS1	Thrombospondin 1	1.03	0.8460	−1.00	0.9998	−1.06	0.0916
THBS2	Thrombospondin 2	−1.06	0.7065	−1.13	0.1886	−1.38	0.1202
THBS3	Thrombospondin 3	−1.16	0.3227	−1.00	0.9994	−1.07	0.6746
TIMP1	TIMP metallopeptidase inhibitor 1	−1.04	0.8334	1.46	0.3405	1.29	0.1863
TIMP2	TIMP metallopeptidase inhibitor 2	−1.06	0.5450	−1.22	0.1819	−1.07	0.5713
TIMP3	TIMP metallopeptidase inhibitor 3	1.45	0.4867	−2.41	0.2673	ND	ND
TNC	Tenascin C (hexabrachion)	−1.00	0.9796	1.62	0.0853	1.37	0.1043
VCAM1	Vascular cell adhesion molecule 1	−1.48	0.0619	−1.08	0.8198	1.16	0.6055
VCAN	Versican	−1.08	0.8172	−1.23	0.7692	−1.32	0.2985
VTN	Vitronectin	−1.78	0.0051	1.26	0.6872	−1.70	0.0995
Calibrator genes							
B2M	β2-Microglobulin	−1.11	0.1353	−1.02	0.7025	−1.10	0.4223
HPRT1	Hypoxanthine phosphoribosyltransferase 1	−1.05	0.4378	−1.02	0.9281	−1.07	0.3070
RPL13A	Ribosomal protein L13A	1.07	0.3091	1.15	0.2733	−1.02	0.8371
GAPDH	Glyceraldehyde-3-phosphate dehydrogenase	1.04	0.5191	−1.25	0.2964	1.19	0.0824
ACTB	Actin, β	1.05	0.0990	1.13	0.1943	1.01	0.8100

A grey box indicates a statistically significant change (*$p < 0.05$). ND, not detected.

imbalance of inhibitors and proteinases (39). Many biological processes have been linked to these enzymes, but given the similarities in the functional domains of MMPs, MT-MMPs and ADAMTSs and the fact they are all inhibited by TIMPs to varying degrees, considerable potential exists for functional redundancy in their biological activities. Four members of the MMP family showed significant alterations in expression; *MMP8* (neutrophil collagenase), *MMP11* (stromelysin-3) and *MMP15* (MT2-MMP) were all downregulated, while *ADAMTS1* was upregulated. The upregulation of *ADAMTS1* at 6 and 24 h suggests an important role for this enzyme in mechanically induced matrix remodelling, and of interest in this regard is the finding that parathyroid hormone stimulates ADAMTS-1 synthesis and collagen degradation by human osteoblasts in culture (40). Both *TIMP1* and *TIMP2* were expressed at high copy numbers, but were not responsive to mechanical deformation.

Of the twelve genes encoding collagen α-chains that were constitutively expressed, three were significantly downregulated, the short-chain collagens *COL6A1* and *COL8A1* at 12 h and *COL11A1* at 24 h. We have previously reported that cyclic tensile strain downregulates *COL3A1* and *COL11A1* expression (6). Collagen type VI is a ubiquitous extracellular matrix protein, which forms microfibrillar networks with other matrix proteins (41,42), while collagen type - VIII is a nonfibrillar collagen present in a variety of extracellular matrices, including basement membranes (43). Although the function of these collagens is not well understood, their binding activity suggests that they have an anchoring function and play a role in cell migration and differentiation.

Although not a cell-adhesion factor, CTGF, which functions as a growth factor for fibroblasts and other connective tissue cells (44), was included in the gene array. Connective tissue growth factor is mitogenic and chemotactic for fibroblasts and is selectively induced by transforming growth factor-β (TGF-β; 45), and its role as a downstream mediator of TGF-β signalling has led to it being widely studied in wound repair and various types of fibrotic disease (46). Most recently, CTGF has been shown to direct fibroblast differentiation from periodontal ligament progenitor cells (47) and human mesenchymal stem/stromal cells (48), which has implications for

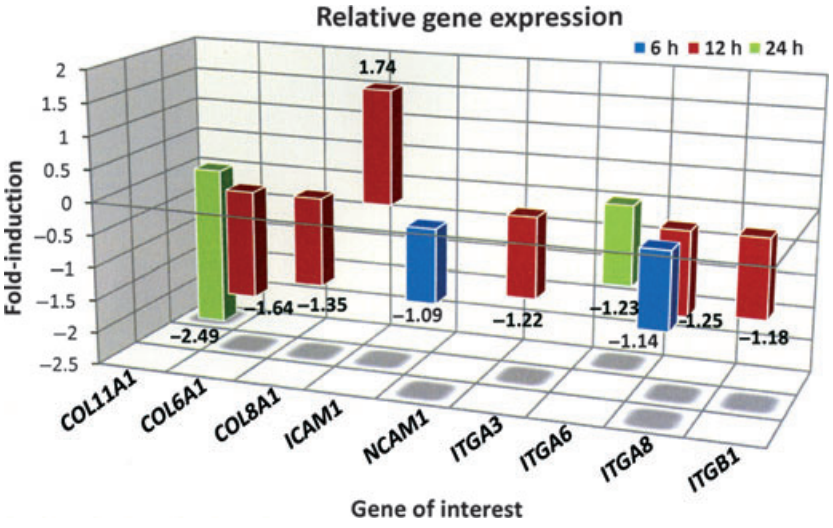

Fig. 3. Fold-induction (C_t ratio) of nine genes showing a statistically significant ($p < 0.05$) change in mRNA expression in response to a uniaxial, cyclic tensile strain of 12%, three coding collagen α-chains, two cell-adhesion molecules and four integrin subunits. All were downregulated, with the exception of the transmembrane protein *ICAM1*, which was upregulated 1.74-fold.

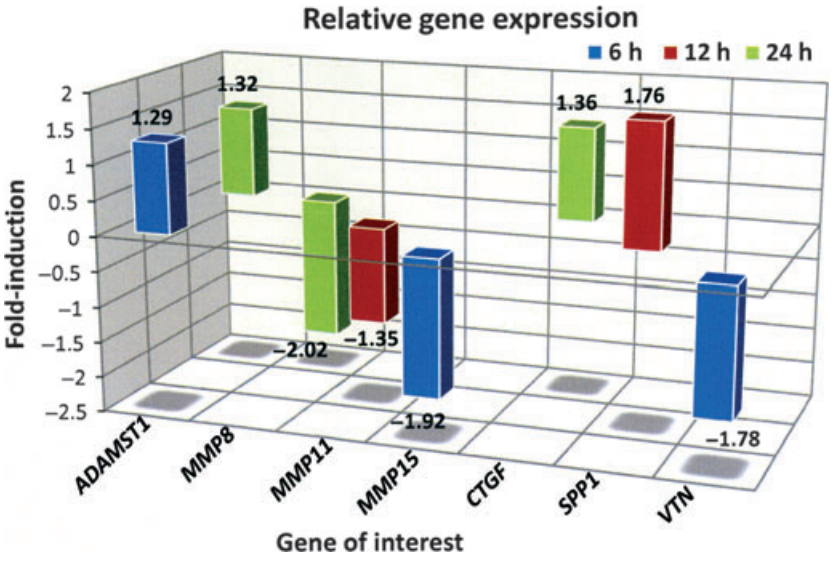

Fig. 4. Three-dimensional profile showing statistically significant alterations ($p < 0.05$) in mRNA expression (C_t ratio) of the following seven genes encoding four members of the MMP family of proteolytic enzymes: the fibroblast differentiation gene, *CTGF*, and the extracellular matrix proteins, *SPP1* (osteopontin) and *VTN*. *ADAMST1* was one of only two genes altered across two time points.

the present study. The increase in *CTGF* expression together with upregulation of the genes for two TGF-β isoforms (*TGFB1* and *TGFB3*) in the same model system (8) is strongly indicative of a causal relationship, and suggests that CTGF functions in the periodontal ligament to maintain the fibroblast phenotype.

Previous studies of the effect of mechanical strain on gene expression by periodontal ligament cells have been referenced against a single calibrator or housekeeping gene, most commonly *GAPDH* or *ACTB*. By measuring expression profiles relative to the mean C_t values of five different calibrator genes (Table 1), the present methodology represents an important advance. Ideally, the experimental conditions should not influence the expression of the calibrator gene, but calibrator gene expression is invariably affected by the experimental conditions (49). If validation data do exist, calibrator genes should be selected on the basis of their predicted stability in specific experimental conditions, because currently there is no calibrator gene that is stable in every system, in every circumstance and for every cell type (50). In other words, because an all-purpose calibrator gene does not exist, accurate normalization of real-time RT-PCR data can only be achieved by averaging multiple calibrator gene expression (51,52). Another advantage of the experimental design is that by measuring the samples in triplicate, it is possible to obtain more statistically robust data than obtainable by using a treated/control ratio of ± 2 as representing significant change. The present study indicates that use of the latter will result in a considerable number of false negatives as well as some false positives; of the fifteen genes recording a statistically significant change in expression, for the majority ($n = 13$) the C_t ratio was < 2.

In conclusion, this investigation has demonstrated a complex set of interactions between human periodontal ligament cells cultured *in vitro* and a mechanically active two-dimensional collagen substrate. The C_t ratios may seem modest, but the alterations in relative expression represent averages over the entire strain field, where the magnitude and type of strain experienced will vary depending on the location of the cells within the field. Nevertheless, alterations in the pattern of expression are suggestive of a homeostatic mechanism whereby cell adhesion molecules are predominately downregulated to facilitate cellular reorientation in response to their altered functional environment. Some of these genes are also involved in cellular mechanosensing, and changes in their pattern of expression carry implications for the activation of a number of downstream mechanotransduction pathways.

Nevertheless, additional studies will be necessary to establish whether the

expressed genes are translated into protein and, if they are, whether they are biologically active. This will require assaying culture supernatants for the expressed proteins of interest and immunolocalization of the proteins *in situ* with specific antibodies in animal models of tooth movement. Another consideration is that the traditional two-dimensional culture systems in widespread use for investigating the response of cells to mechanical strain *in vitro* have a number of limitations, not least the fact that periodontal ligament cells are normally surrounded by a complex network of collagens, proteoglycans and noncollagenous proteins, which are not grown on tissue culture plastic or films of matrix proteins, such collagen or fibronectin. Some attempt has been made to address this shortcoming for compressive force application by seeding periodontal ligament cells into type I collagen gels (4,5), but collagen is only one of the major structural macromolecules found in extracellular matricies. For the field to progress, therefore, it is clear that future *in vitro* analyses of mechanoresponsive gene and protein expression require well-characterized three-dimensional models incorporating periodontal ligament cells into hydrogel matrices designed to produce a tissue construct resembling more closely the periodontal ligament *in vivo*.

Acknowledgements

We are grateful for financial support from the National University of Singapore Academic Research Fund (R222-000-029-112), the New Zealand Lottery Grants Board, NZ Dental Association Research Foundation, NZ Association of Orthodontists, and the University of Otago Research Committee.

References

1. Shimizu N, Yamaguchi M, Goseki T *et al.* Cyclic-tension force stimulates interleukin-1β production by human periodontal ligament cells. *J Periodont Res* 1994;**29:** 328–333.
2. Long P, Hu J, Piesco N, Buckley M, Agarwal S. Low magnitude of tensile strain inhibits IL-1β-dependent induction of pro-inflammatory cytokines and induces synthesis of IL-10 in human periodontal ligament cells *in vitro*. *J Dent Res* 2001;**80:**1416–1420.
3. Kanzaki H, Chiba M, Shimizu Y, Mitani H. Periodontal ligament cells under mechanical stress induces osteoclastogenesis by receptor activator of nuclear factor κB ligand up-regulation via prostaglandin E_2 synthesis. *J Bone Miner Res* 2002;**17:**210–220.
4. Lee Y-H, Nahm D-S, Jung Y-K *et al.* Differential gene expression of periodontal ligament cells after loading of static compressive force. *J Periodontol* 2007;**78:** 446–452.
5. de Araujo RMS, Oba Y, Moriyama K. Identification of genes related to mechanical stress in human periodontal ligament cells using microarray analysis. *J Periodont Res* 2007;**42:**15–22.
6. Wescott DC, Pinkerton MN, Gaffey BJ, Beggs KT, Milne TJ, Meikle MC. Osteogenic gene expression by human periodontal ligament cells under cyclic tension. *J Dent Res* 2007;**86:**1212–1216.
7. Yamashiro K, Myokai F, Hiratsuka K *et al.* Oligonucleotide array analysis of cyclic tension-responsive genes in human periodontal ligament fibroblasts. *Int J Biochem Cell Biol* 2007;**39:** 910–921.
8. Pinkerton MN, Wescott DC, Gaffey BJ, Beggs KT, Milne TJ, Meikle MC. Cultured human periodontal ligament cells constitutively express multiple osteotropic cytokines and growth factors, several of which are responsive to mechanical deformation. *J Periodont Res* 2008;**43:** 343–351.
9. Wang N, Butler JP, Ingber DE. Mechanotransduction across the cell surface and through the cytoskeleton. *Science* 1993;**269:**1124–1127.
10. Clarke EA, Brugge JS. Integrins and signal transduction pathways: the road taken. *Science* 1995;**268:**233–239.
11. Sastry SK, Burridge K. Focal adhesions: a nexus for intracellular signaling and cytoskeletal dynamics. *Exp Cell Res* 2000;**261:**25–36.
12. Wyllie AH, Kerr JFR, Currie AR. Cell death: the significance of apoptosis. *Int Rev Cytol* 1980;**68:**251–307.
13. Elmore S. Apoptosis: a review of programmed cell death. *Toxicol Pathol* 2007;**35:**495–516.
14. Bakker A, Klein-Nulend J, Burger E. Shear stress inhibits while disuse promotes osteocyte apoptosis. *Biochem Biophys Res Commun* 2004;**320:**1163–1168.
15. Aguirre JI, Plotkin LI, Stewart SA *et al.* Osteocyte apoptosis is induced by weightlessness in mice and precedes osteoclast recruitment and bone loss. *J Bone Miner Res* 2006;**21:**605–615.
16. Zhong W, Xu C, Zhang F, Jiang X, Zhang X, Ye D. Cyclic stretching force-induced early apoptosis in human periodontal ligament cells. *Oral Dis* 2008;**14:**270–276.
17. Hao Y, Xu C, Sun S, Zhang F. Cyclic stretching force induces apoptosis in human periodontal ligament cells via Caspase-9. *Arch Oral Biol* 2009;**54:** 864–870.
18. Somerman MJ, Archer SY, Imm GR, Foster RA. A comparative study of human periodontal ligament cells and gingival fibroblasts *in vitro*. *J Dent Res* 1988;**67:**66–70.
19. Natali AN, Pavan PG, Scarpa C. Numerical analysis of tooth mobility: formulation of a non-linear constitutive law for the periodontal ligament. *Dent Mater* 2004;**20:**623–629.
20. Mosmann T. Rapid colorimetric assay for cellular growth and survival: application to proliferation and cytotoxicity assays. *J Immunol Methods* 1983;**65:**55–63.
21. Twentyman PR, Luscombe M. A study of some variables in a tetrazolium dye (MTT) based for cell growth and chemosensitivity. *Br J Cancer* 1987;**56:**279–285.
22. Chomczyski P, Sacchi N. Single-step method of RNA isolation by acid guanidium thiocyanate-phenol-chloroform extraction. *Anal Biochem* 1987;**162:**156–159.
23. Livak KJ, Schmittgen TD. Analysis of relative gene expression data using real-time quantitative PCR and the $2^{-\Delta\Delta C(T)}$ method. *Methods* 2001;**25:**402–408.
24. Yuan JS, Reed A, Chen F, Stewart CN. Statistical analysis of real-time PCR data. *BMC Bioinformatics* 2006;**7:**85–97.
25. Buckley MJ, Banes AJ, Levin LG *et al.* Osteoblasts increase their rate of cell division and align in response to cyclic, mechanical tension in vitro. *Bone Miner* 1988;**4:**225–236.
26. Neidlinger-Wilke C, Grood E, Claes L, Brand R. Fibroblast orientation to stretch begins within three hours. *J Orthop Res* 2002;**20:**953–956.
27. Matheson LA, Fairbank NJ, Maksym GN, Santerre JP, Labow RS. Characterization of the Flexcell^{TM} cyclic strain culture system with U937 macrophage-like cells. *Biomaterials* 2006;**27:**226–233.
28. Vande Geeste JP, Di Martino ES, Vorp DA. An analysis of the complete strain field within Flexercell^{TM} membranes. *J Biomech* 2004;**37:**1923–1928.
29. Wall ME, Weinhold PS, Siu T, Brown TD, Banes AJ. Comparison of cellular strain with applied substrate strain in vitro. *J Biomech* 2007;**40:**173–181.
30. Milne TJ, Ichim I, Patel B, McNaughton A, Meikle MC. Induction of osteopenia during experimental tooth movement in the rat: alveolar bone remodelling and the mechanostat theory. *Eur J Orthodont* 2009;**31:**221–231.

31. Wang Y, Li Y, Fan X, Zhang Y, Wu J, Zhao Z. Early proliferation alteration and differential expression in human periodontal ligament cells subjected to cyclic tensile stress. *Arch Oral Biol* 2011;**56:**177–186.
32. Danciu TE, Gagari E, Adam RM, Damoulis PD, Freeman MR. Mechanical strain delivers anti-apoptotic and proliferative signals to gingival fibroblasts. *J Dent Res* 2004;**83:**596–601.
33. Boccafoschi F, Sabbatini M, Bosetti M, Cannas M. Overstressed mechanical stretching activates survival and apoptotic signals in fibroblasts. *Cells Tissues Organs* 2010;**192:**167–176.
34. Boccafoschi F, Bosetti M, Gatti S, Cannas M. Dynamic fibroblast cultures: response to mechanical stretching. *Cell Adh Migr* 2007;**1:**124–128.
35. Meyer CJ, Alenghat FJ, Rim P, Fong JH, Fabry B, Ingber DE. Mechanical control of cyclic AMP signaling and gene transcription through integrins. *Nat Cell Biol* 2000;**2:**666–668.
36. Lallier TE, Yukna R, Moses RL. Extracellular matrix molecules improve periodontal ligament cell adhesion to anorganic bone matrix. *J Dent Res* 2001; **80:**1748–1752.
37. Kikkawa Y, Sanzen N, Fujiwara H, Sonnenberg A, Sekiguchi K. Integrin binding specificity of laminin-10/11: laminin-10/11 are recognized by α3β1, α6β1 and α6β4 integrins. *J Cell Sci* 2000;**113:**859–876.
38. Schnapp LM, Hatch N, Ramos DM, Klimanskaya IV, Sheppard D, Pytela R. The human integrin α8β1 functions as a receptor for tenascin, fibronectin and vitronectin. *J Biol Chem* 1995;**270:**23196–23202.
39. Murphy G, Reynolds JJ. Extracellular matrix degradation. In: Royce PM, Steinmann B, eds. *Connective Tissue and Its Heritable Disorders*. New York: Wiley-Liss Inc, 1993:287–316.
40. Rehn AP, Birch MA, Karlström E, Wendel M, Lind T. ADAMTS-1 increases the three-dimensional growth of osteoblasts through type I collagen processing. *Bone* 2007;**41:**231–238.
41. Engel J, Furthmayr H, Odermatt E *et al*. Structure and macromolecular organization of type VI collagen. *Ann N Y Acad Sci* 1985;**460:**25–37.
42. Lampe AK, Bushby KMD. Collagen VI related muscle disorders. *J Med Genet* 2005;**42:**673–685.
43. Shuttleworth CA. Type VIII collagen. *Int J Biochem Cell Biol* 1997;**29:**1145–1148.
44. Igarashi A, Okochi H, Bradham DM, Grotendorst GR. Regulation of connective tissue growth factor gene expression in human skin fibroblasts and during wound repair. *Mol Biol Cell* 1993;**4:**637–645.
45. Kothapalli D, Frazier KS, Welphy A, Segarini PR, Grotendorst GR. Transforming growth factor b induces anchorage-independent growth of NRK fibroblasts via a connective tissue growth factor-independent signaling pathway. *Cell Growth Differ* 1997;**8:**61–68.
46. Werner S, Grose R. Regulation of wound healing by growth factors and cytokines. *Physiol Rev* 2003;**83:**835–870.
47. Dangaria SJ, Ito Y, Walker C, Druzinsky R, Luan X, Diekwisch TGH. Extracellular matrix-mediated differentiation of periodontal progenitor cells. *Differentiation* 2009;**78:**79–90.
48. Lee CH, Shah B, Moioli EK, Mao JJ. CTGF directs fibroblast differentiation from human mesenchymal stem/stromal cells and defines connective tissue healing in a rodent injury model. *J Clin Invest* 2010;**120:**3340–3349.
49. Schmittgen TD, Zakrajsek BA. Effect of experimental treatment on housekeeping gene expression: validation by real-time, quantitative RT-PCR. *J Biochem Biophys Methods* 2000;**46:**69–81.
50. Farrel R. *RNA Methodologies. A Laboratory Guide for Isolation and Characterization*. Burlington: Elsevier Academic Press, 2005.
51. Vandesompele J, De Preter K, Pattyn F *et al*. Accurate normalization of real-time quantitative RT-PCR data by geometric averaging of multiple internal control genes. *Genome Biol* 2002;**3:** research 0034.1–0034.11.
52. Dheda K, Huggett JF, Chang JS *et al*. The implications of using an inappropriate reference gene for real-time reverse transcription PCR data normalization. *Anal Biochem* 2005;**344:**141–143.

Appendix 2

Agilent 2100 Bioanalyzer output – RNA integrity check

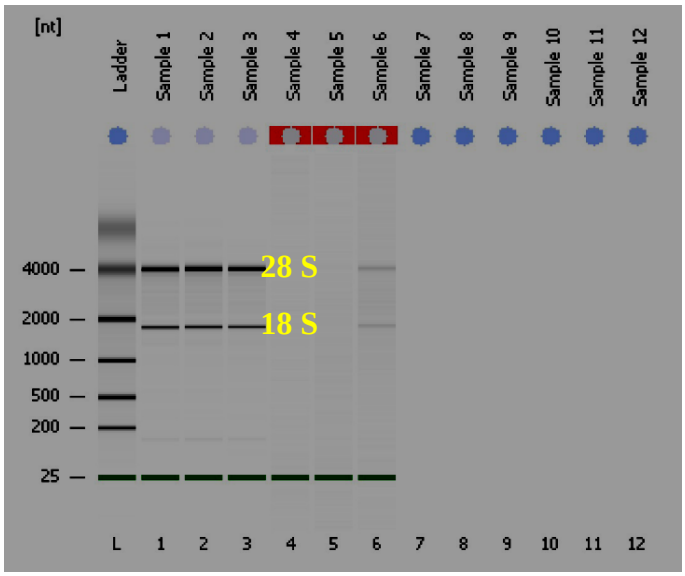

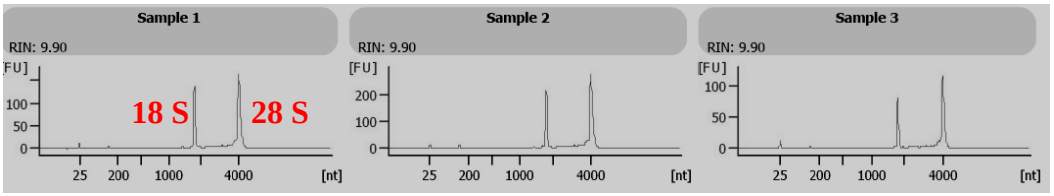

Overall Results for sample 1 : Sample 1

RNA Area:	432.9
RNA Concentration:	215 ng/µl
rRNA Ratio [28s / 18s]:	1.9

Fragment table for sample 1 : Sample 1

Name	Start Size [nt]	End Size [nt]
18S	1,738	1,910
28S	3,635	4,448

Overall Results for sample 2 : Sample 2

RNA Area:	740.5
RNA Concentration:	368 ng/µl
rRNA Ratio [28s / 18s]:	1.9

Fragment table for sample 2 : Sample 2

Name	Start Size [nt]	End Size [nt]
18S	1,744	2,042
28S	3,656	4,463

Overall Results for sample 3 : Sample 3

RNA Area:	273.2
RNA Concentration:	136 ng/µl
rRNA Ratio [28s / 18s]:	2.0

Fragment table for sample 3 : Sample 3

Name	Start Size [nt]	End Size [nt]
18S	1,749	1,927
28S	3,662	4,434

Sample Name	Sample Comment	Statu s	Result Label
Sample 1		✔	RIN: 9.90
Sample 2		✔	RIN: 9.90
Sample 3		✔	RIN: 9.90
Sample 4		✔	RIN N/A
Sample 5		✔	RIN N/A
Sample 6		✔	RIN N/A

Appendix 3

Agarose gel images – Chapter 4:

Agarose gel electrophoresis of amplified real-time PCR products following mechanical stress on gene expression by human periodontal ligament cells ± CTGF (100 ng/mL) and FGF-2 (10 ng/mL), ± cyclic mechanical strain for 6 h/day ,reverse transcription of RNA extracted from PDL/Extracel constructs for 7, 14 and 21 days in Tissue Train® plates. The images are representative examples of the results of four independent experiments.

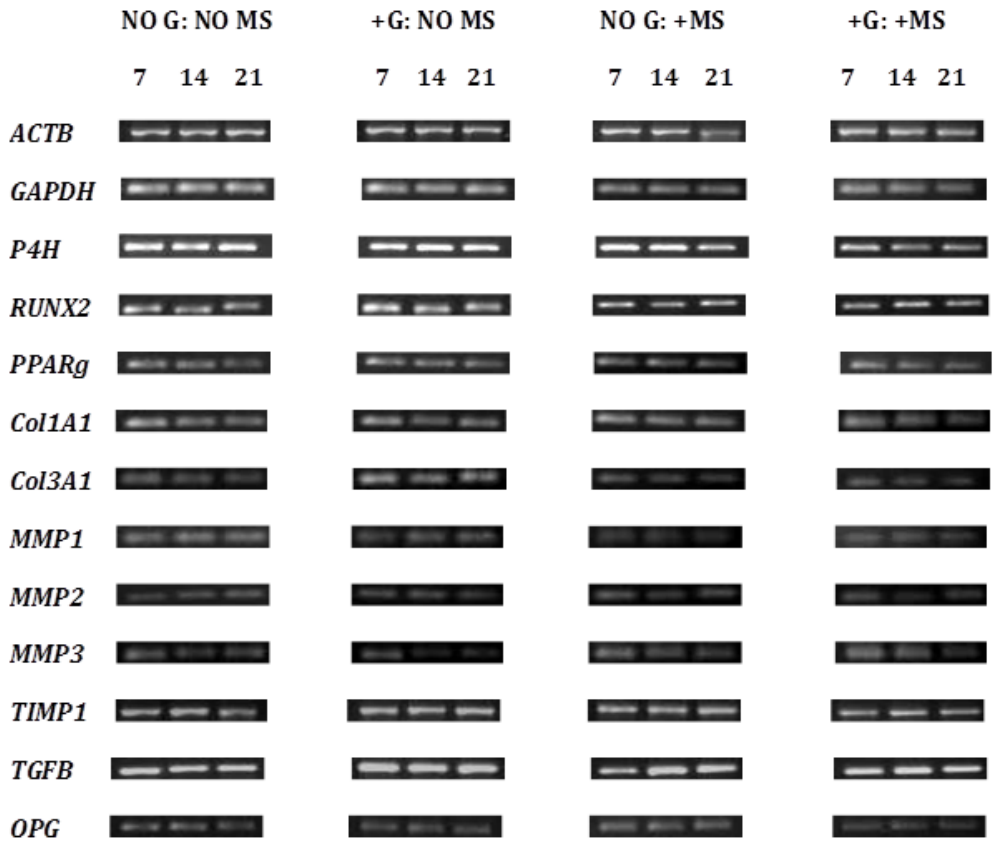

Appendix 4

Published work

Saminathan A, Vinoth KJ, Low HH, Cao T, Meikle MC (2013). Engineering three-dimensional constructs of the periodontal ligament in hyaluronan–gelatin hydrogel films and a mechanically active environment. *Journal of periodontal research* 48(6)*:*790-801.

JOURNAL OF PERIODONTAL RESEARCH
doi:10.1111/jre.12072

Engineering three-dimensional constructs of the periodontal ligament in hyaluronan–gelatin hydrogel films and a mechanically active environment

A. Saminathan, K. J. Vinoth, H. H. Low, T. Cao, M. C. Meikle
Faculty of Dentistry, National University of Singapore, 11 Lower Kent Ridge Road, Singapore, 119083, Singapore

Saminathan A, Vinoth KJ, Low HH, Cao T, Meikle MC. Engineering three-dimensional constructs of the periodontal ligament in hyaluronan–gelatin hydrogel films and a mechanically active environment. J Periodont Res 2013; doi: 10.1111/jre.12072. © 2013 John Wiley & Sons A/S. Published by John Wiley & Sons Ltd

Background and Objective: Periodontal ligament (PDL) cells in stationary two-dimensional culture systems are in a double default state. Our aim therefore was to engineer and characterize three-dimensional constructs, by seeding PDL cells into hyaluronan–gelatin hydrogel films (80–100 μm) in a format capable of being mechanically deformed.

Material and Methods: Human PDL constructs were cultured with and without connective tissue growth factor (CTGF) and fibroblast growth factor (FGF)-2 in (i) stationary cultures, and (ii) mechanically active cultures subjected to cyclic strains of 12% at 0.2 Hz each min, 6 h/d, in a Flexercell FX-4000 Strain Unit. The following parameters were measured: cell number and viability by laser scanning confocal microscopy; cell proliferation with the MTS assay; the expression of a panel of 18 genes using real-time RT-PCR; matrix metalloproteinases (MMPs) 1–3, TIMP-1, CTGF and FGF-2 protein levels in supernatants from mechanically activated cultures with Enzyme-linked immunosorbent assays. Constructs from stationary cultures were also examined by scanning electron microscopy and immunostained for actin and vinculin.

Results: Although initially randomly distributed, the cells became organized into a bilayer by day 7; apoptotic cells remained constant at approximately 5% of the total. CTGF/FGF-2 stimulated cell proliferation in stationary cultures, but relative quantity values suggested modest effects on gene expression. Two transcription factors (*RUNX2* and *PPARG*), two collagens (*COL1A1*, *COL3A1*), four MMPs (*MMP-1–3*, *TIMP-1*), *TGFB1*, *RANKL*, *OPG* and *P4HB* were detected by gel electrophoresis and Ct values < 35. In mechanically active cultures, with the exception of *P4HB*, *TGFB1* and *RANKL*, each was upregulated at some point in the time scale, as was the synthesis of MMPs and TIMP-1. *SOX9*, *MYOD*, *SP7*, *BMP2*, *BGLAP* or *COL2A1* were not detected in either stationary or mechanically active cultures.

Murray C. Meikle, DDSc MSD PhD, Faculty of Dentistry, National University of Singapore, 11 Lower Kent Ridge Road, Singapore 119083, Singapore
Tel: +6772 6840 ext 1481
Fax: +6778 5742
e-mail: denmcm@nus.edu.sg

Key words: periodontal ligament; in vitro model; real-time RT-PCR; growth factors; matrix metalloproteinase

Accepted for publication February 05, 2013

Conclusion: Three-dimensional tissue constructs provide additional complexity to monolayer culture systems, and suggest some of the assumptions regarding cell growth, differentiation and matrix turnover based on two-dimensional cultures may not apply to cells in three-dimensional matrices. Primarily developed as a transitional *in vitro* model for studying cell–cell and cell–matrix interactions in tooth support, the system is also suitable for investigating the pathogenesis of periodontal diseases, and importantly from the clinical point of view, in a mechanically active environment.

Two-dimensional culture systems have been widely used to investigate the pathophysiology and mechanobiology of the periodontal ligament (PDL), a specialized connective tissue that evolved to provide attachment of teeth to the bones of the jaws (1–4). However, two-dimensional systems are limited by the fact that cells are normally embedded in a complex extracellular network of collagens, proteoglycans and non-collagenous proteins, not attached to tissue culture plastic or substrates composed of matrix proteins such as collagen or fibronectin. The PDL also functions in a mechanically active environment, which means that cells in conventional stationary two-dimensional culture systems lack the mechanical stimuli to which they are exposed *in vivo*. In other words, PDL cells in monolayer culture are effectively in a double default state. First, by the absence of the three-dimensional structure of a tissue construct, and second, the lack of biomechanical stimuli provided by mastication and other forms of occlusal loading.

Because they have material properties that resemble naturally occurring extracellular matrices and bridge the gap between two-dimensional cell culture systems and animal models, hydrogels have been widely used to create three-dimensional tissue constructs for use in cell biology, bioengineering and regenerative medicine. Hydrogels are a class of polymer materials that can absorb large amounts of water without dissolving, due to the physical or chemical cross-linkage of the various hydrophilic polymer chains from which they are composed (5,6). Not only do hydrogels mimic more closely the environment experienced by cells *in vivo*, they also confer beneficial effects on gene expression, cell adhesion, morphology and phenotype (7–10).

Collagens are the most abundant proteins in connective tissues, and collagen hydrogels have been widely used as tissue culture scaffolds for numerous cell types since first being described by Elsdale and Bard (11) 40 years ago. Nevertheless, collagen is just one of the major structural macromolecules found in extracellular matrices. The challenge for engineering three-dimensional tissue constructs has been to replicate not only connective tissue complexity with minimal components, but also the mechanical and viscoelastic characteristics of the native tissue – the intention being to enable the incorporated cells reproduce their parent tissue as closely as possible (12,13). To address the limitations posed by two-dimensional cultures, the aim of the present investigation was to engineer and characterize a tissue that more closely resembled the structure of the PDL by seeding cells into Extracel™, a commercially-available hydrogel matrix composed of hyaluronan (HA) and gelatin (14,15), and in a format that could be mechanically deformed. Although primarily developed as a transitional *in vitro* model for studying mechanisms of tooth support, the system is also suitable for investigating the pathogenesis of periodontal diseases.

Material & methods

Preparation of periodontal ligament cell/Extracel™ constructs in stationary culture

Primary human PDL fibroblasts were purchased from a commercial source (ScienCell Research Laboratories, Carlsbad, CA, USA; Lot number: 5145). The cells, isolated from human periodontal tissue from several donors are cryopreserved at passage 1, delivered frozen on dry ice, and immediately transferred to liquid nitrogen on receipt. They were subsequently thawed and expanded in Dulbecco minimal Eagle's medium (DMEM) supplemented with 10% fetal bovine serum (FBS; Gibco, Invitrogen, Singapore) and antibiotic–antimycotic reagents as described below. The expanded cells were harvested, aliquoted and stored in liquid N_2 until required; passage three cells were used in all subsequent experiments. Extracel™ was purchased from Glycosan Biosystems (Salt Lake City, UT, USA). The hydrogel is formed when the cross-linking agent, Extralink™ (polyethylene glycol diacetate) is added to a mixture of Glycosil™ (thiol-modified HA) and Gelin-S™ (thiol-modified gelatin). The three components come as lyophilized solids, and DG Water™ (degassed, deionized water) was used to dissolve the Glycosil, Gelin-S and Extralink in individual vials. Glycosil and Gelin-S were mixed 1 : 1 and 2.5×10^6/mL PDL cells added. Extralink was added to the Glycosil–Gelin-S mix at a ratio of 1 : 4, and after blending in a pipette, 300 μL of the gel mixture was added to 35 mm diameter type I collagen coated six-well plates (Sigma-Aldrich, Singapore) and spread to form a film 80–100 μm in thickness. The constructs were allowed to gel at 37°C, which occurred after about 20 min; PDL/Extracel cultures were then incubated in 3 mL DMEM (Gibco, Invitrogen, Singapore) supplemented with 10% FBS, antibiotic–antimycotic reagent (10,000 units, penicillin, 10,000 μg streptomycin and 25 μg/mL amphotericin B;

Invitrogen), 100 mM L-glutamine (Invitrogen) and Gentamycin (10 mg/mL, Gibco) and cultured at 37°C in a humidified atmosphere of 5% CO_2/95% air. The culture medium was changed every 2 d.

To promote fibroblast proliferation and differentiation, gel constructs were cultured with and without human recombinant connective tissue growth factor (CTGF; 100 ng/mL; BioVendor Laboratories, Guangzhou, China) and human recombinant fibroblast growth factor (FGF)-2 (10 ng/mL; Gibco). Growth factors were incorporated into both the gel matrix and culture media.

Scanning electron microscopy

To examine the tissue constructs by scanning electron microscopy, culture media was aspirated from the 35 mm culture dishes and the constructs fixed in 2.5% glutaraldehyde at 4°C overnight, washed in phosphate-buffered saline (PBS) twice and then post-fixed for 2 h at room temperature in 2% osmium tetroxide. They were then dehydrated in a graded series of ethanols and dried by transferring the specimens in 100% ethanol to a critical point drying apparatus (Leica EM CPD030, Singapore) and ethanol exchanged for liquid CO_2 under pressure. After six cycles of this exchange, the temperature of the chamber was raised to 40°C, a point at which the liquid changes into a gas and drying occurs. The dried specimens were mounted on to aluminium specimen stubs with conductive tape and sputter coated with gold–palladium alloy for 120 s, placed in a vacuum and viewed in a scanning electron microscope (Philips/FEI XL30 FEG scanning electron microscopy, Singapore) at an accelerating voltage of 10 kV.

Laser scanning confocal microscopy

Laser scanning confocal microscopy was used for the following.

Analysis of cell viability— The effect on cell viability of incorporating cells into Extracel was determined by the fluorescein diacetate (FDA)–propidium iodide (PI) method (16). At the end of each time point, culture supernatants were discarded and the cells stained with 0.1 mL (2 μg) FDA and 0.3 mL (6 μg) PI from stock solutions (Sigma-Aldrich) and viewed with a Carl Zeiss, LSM 510 META confocal imaging system – viable cells fluoresce bright green, nonviable cells bright red. Three fields (120 μm × 120 μm), one in the centre and two approximately 1 cm on either side were chosen for analysis, and the number of viable and nonviable cells in three wells at each time point counted using Image-Pro Plus (version 6.1.0.346) software (Media Cybernetics, Bethesda, MD, USA).

Immunostaining— The cells were washed with PBS and fixed in 4% formaldehyde at room temperature for 15 min. The Extracel gel constructs were permeabilized with 0.1% Triton X-100 in PBS, and blocked with 5% normal goat serum or FBS for 1 h at room temperature. The cells were then triple-stained with an Actin Cytoskeleton/Focal Adhesion Staining Kit (Merck Millipore, Singapore) as follows: first, a mouse antivinculin monoclonal antibody (1 mg/mL) diluted with blocking solution in the ratio of 1 : 150 was incubated with prepared cells at 4°C overnight. The constructs were washed with PBST (0.1% Tween-20 in PBS) for 2 h and a secondary antibody, goat antimouse IgG conjugated to fluorescein isothiocyanate (2 mg/mL) added at a dilution of 1 : 300. Second, orientation of the actin filaments was mapped by adding tetramethyl rhodamine isothiocyanate-conjugated phalloidin (60 μg/mL) at a dilution of 1 : 250, and after 60 min incubation the cells washed three times with PBST. Finally, the constructs were incubated with 4′,6-diamidino-2-phenylindol (0.1 mg/mL) to stain nuclei. Cells were viewed with an Olympus Fluoview FV 1000 (Olympus, Japan) confocal imaging system at 60 × magnification and processed using Imaris version 6.1.5 software.

Application of cyclic mechanical strain to constructs of the periodontal ligament

PDL/Extracel constructs 80–100 μm in thickness were formed on type I collagen-coated silicone membranes in six-well, 35 mm flexible-bottomed Tissue Train® culture plates (Flexcell International Corporation, Hillsborough, NC, USA) fitted with a bonded foam perimeter to improve cell attachment. The constructs were subjected to an in-plane biaxial cyclic strain of 12% for 5 s (0.2 Hz) every 60 s for 6 h/d, using a square wave-form around circular loading posts in a standard Bioflex baseplate linked to a Flexercell FX-4000T Tension Plus Strain Unit (Flexcell International). The strain value of 12% was based on data derived from a finite element model, which suggested that maximal PDL strains for horizontal displacements of a human maxillary central incisor under physiological loading lies close to 8–25% depending upon the apico-crestal position (17). We have previously used the figure of 12% corresponding to the mid-root position, to deform PDL cells in two-dimensional cultures (3,4,18).

Cell recovery from Extracel

At the end of the experimental period the culture medium was aspirated from each well and the hydrogel surface washed with PBS; 1.5 mL trypsin-EDTA (Invitrogen) was added and incubated at 37°C for 3 h. After a further wash, 1.5 mL of 10 × collagenase/hyaluronidase in DMEM (StemCell Technologies, Singapore) was added and incubated overnight at 37°C. This was based on a protocol developed and recommended by Glycosan Biosystems, the manufacturers of Extracel. At the end of the second incubation, 3 mL DMEM supplemented with 10% FBS was added to the hydrolysed gel and the cell suspension centrifuged at 290 *g* for 5 min. The resulting pellet was resuspended in 1.5 mL DMEM and centrifuged again at 6708 *g* for 2 min.

RNA extraction

Extraction of RNA was carried out using an RNeasy Plus Mini kit (Qiagen, Singapore) according to the manufacturer's instructions. This yielded RNA with an A260/280 value > 1.95 and an A230/280 value > 1.2 in a NanoDrop 2000 Spectrophotometer (Thermo Scientific, Wilmington, DE, USA), indicative of a pure sample. Integrity of the RNA was assessed by gel electrophoresis on an Agilent 2100 Bioanalyser (Agilent Technologies, Santa Clara, CA, USA); the RIN (RNA Integrity Number) values were in the range 9.0–9.9.

Gene expression using real-time polymerase chain reaction

A known amount (500 ng) of total RNA was reverse transcribed using the iScript cDNA Synthesis Kit (Bio-Rad Laboratories, Hercules, CA, USA) and a MyCycler™ thermal cycler (Bio-Rad). Real-time PCR was performed in triplicate using Fast SYBR® Green Master Mix (Applied Biosystems, Singapore) with a StepOnePlus™ Real-Time PCR System (Applied Biosystems). Samples were screened for the expression of 18 genes; the primer sequences (First Base, Singapore) used and the annealing temperatures are listed in Table 1. The amplification was carried out via the first step at 95°C for 10 min, followed by 40 cycles with 15 s at 95°C, 10 s at the particular annealing temperature, and 20 s at 72°C. The fluorescence signal was acquired at 72°C. The relative expression of these genes was normalized to the expression of two calibrator genes: *ACTB* (β-actin) and *GAPDH* (glyceraldehyde-3-phosphate dehydrogenase) using the standard curve method. Critical threshold (Ct) values were calculated using the StepOnePlus™ Version2.1 software

Table 1. Genes and primer sequences used for real-time RT-PCR

HGNC agreed gene symbol	Description	Primer sequences	Annealing temperature
ACTB	Actin, beta	F: CCAAGGCCAACCGCGAGAAGATGAC R: AGGGTACATGGTGGTGCCGCCAGAC	58
GAPDH	Glyceraldehyde-3-phosphate dehydrogenase	F: ACCACAGTCCATGCCATCAC R: TCCACCACCCTGTTGCTGTA	60
P4HB	Prolyl-4-hydroxylase, beta subunit	F: GTCTTTGTGGAGTTCTATGCCC R: GTCATCGTCTTCCTCCATGTCT	62
RUNX2	Runt-related transcription factor 2	F: TGAGAGCCGCTTCTCCAACC R: GCGGAAGCATTCTGGAAGGA	58
SOX9	SRY (sex determining region Y)-Box 9	F: GAACGCACATCAAGACGGAG R: TCTCGTTGATTTCGCTGCTC	58
PPARG	Peroxisome proliferator-activated receptor-gamma	F: ATTGACCCAGAAAGCGATTC R: CAAAGGAGTGGGAGTGGTCT	62
MYOD	Myogenic differentiation antigen 1	F: CGGCGGAACTGCTACGAAG R: GCGACTCAGAAGGCACGTC	60
COL1A1	Collagen type I, Alpha-1	F: GAACGCGTGTCATCCCTTGT R: GAACGAGGTAGTCTTTCAGCAACA	60
COL2A1	Collagen type II, Alpha-1	F: TTCAGCTATGGAGATGACAATC R: AGAGTCCTAGAGTGACTGAG	58
COL3A1	Collagen Type III, Alpha-1	F: AACACGCAAGGCTGTGAGACT R: GCCAACGTCCACACCAAATT	60
MMP1	Matrix metalloproteinase 1; collagenase 1	F: GGGAGATCATCGGGACAACTC R: GGGCCTGGTTGAAAAGCAT	60
MMP2	Matrix metalloproteinase 2; gelatinase A (72 kDa)	F: TGATCTTGACCAGAATACCATCGA R: GGCTTGCGAGGGAAGAAGTT	60
MMP3	Matrix metalloproteinase3; stromelysin 1	F: TGGCATTCAGTCCCTCTATGG R: AGGACAAAGCAGGATCACAGTT	60
TIMP1	Tissue inhibitor of metalloproteinases 1	F: CTGTTGTTGCTGTGGCTGATA R: CCGTCCACAAGCAATGAGT	60
TGFB1	Transforming growth factor, beta 1	F: GCAACAATTCCTGGCGATACCTC R: AGTTCTTCTCCGTGGAGCTGAAG	60
BGLAP	Gamma carboxyglutamic acid protein; Osteocalcin	F: ATGAGAGCCCTCACACTCCTC R: GCCGTAGAAGCGCCGATAGGC	60
SP7	Transcription factor Sp7; Osterix	F: TGGCGTCCTCTCTGCTTGA R: TCAGTGAGGGAAGGGTGGGT	58
BMP2	Bone morphogenetic protein 2	F: CAGAGACCCACCCCCAGCA R: CTGTTTGTGTTTGGCTTGAC	58
TNFSF11	Tumour necrosis factor ligand superfamily, member 11; RANKL	F: TCCCATCTGGTTCCCATAAA R: GGTGCTTCCTCCTTTCATCA	60
TNFRSF11B	Tumour necrosis factor receptor superfamily member 11B; Osteoprotegerin	F: TTCCGGAAACAGTGAATCAA R: CGCTGTTTTCACAGAGGTCA	60

(Applied Biosystems); a gene was excluded if it could not be detected by agarose gel electrophoresis or had a threshold value exceeding 33–35.

Agarose gel electrophoresis

The PCR products were checked by electrophoresis with 1.5% agarose gel stained with 1 × SYBR® Safe DNA Gel Stain (Invitrogen). Two microlitres of 6 × loading dye (10 mM Tris-HCl, 0.03% bromophenol blue, 0.03% xylene cyanol FF, 60% glycerol and 60 mM EDTA; Fermentas, Singapore) was mixed with 8 μL of the PCR products and loaded against 8 μL of 100 bp DNA ladder (Fermentas). The gels were run for 55 min at 75V in 1 × TBE buffer and observed by ultraviolet transillumination on a BioRad imaging system using Quantity One® v 4.6 software (BioRad, Hercules, CA, USA).

MTS assay for cell proliferation

The laser beam in confocal microscopy does not penetrate the silicone membrane used to support cell cultures in Flexcell Bioflex plates. For the mechanical stress experiments, cell proliferation was therefore measured by the CellTiter 96® AQueous One Solution Cell Proliferation Assay (Promega, Singapore), a colorimetric assay based on the ability of viable cells to reduce the novel tetrazolium compound [3-(4,5-dimethylthiazol-2-yl)-5-(3-carboxymethoxyphenyl)-2-(4-sulfophenyl)-2H-tetrazolium, inner salt; MTS] with an electron coupling reagent (phenazine ethosulphate) by mitochondrial NADPH or NADH dehydrogenase into a coloured formazan product (19). At the end of each time point, the supernatant was removed and 1.2 mL of MTS solution (200 μL of CellTiter 96® AQueous One Solution reagent/mL of DMEM) was added to each well of the tissue train plates. The plates were incubated at 37°C in 5% CO_2/95% air for 30 min. Absorbance was measured at 490 nm by an uQuant microplate spectrophotometer (Biotek, Singapore) the formazan product being directly proportional to the number of viable cells.

Measurement of enzymes and growth factors in culture supernatants by Enzyme-linked immunosorbent assays

Conditioned media from the 24 h period before each end-point were harvested. Enzyme-linked immunosorbent assays (ELISAs) were used to quantitate levels of a selection of proteolytic enzymes used by fibroblasts to remodel their extracellular matrices: the panel included matrix metalloproteinase MMP-1 (collagenase-1); MMP-2 (gelatinase-A; 72 kDa); MMP-3 (stromelysin-1); and TIMP-1 (tissue inhibitor of metalloproteinases-1). All were assayed using Quantikine® colorimetric sandwich ELISAs (R&D Systems China, Shanghai, China) accor ding to the manufacturer's instructions. We also assayed the culture media for CTGF (Aviscera Bioscience, Santa Clara, CA, USA) and FGF-2 (R&D Systems China).

Statistical methods

Differences between the groups were determined by Student's *t*-test (two-tailed) using GraphPad Prism (GraphPad Software Inc., San Diego, CA, USA) with the level of significance set at $p < 0.05$.

Results

Our initial experiments were carried out on stationary cultures in 35 mm six-well culture plates – these were chosen because the wells are the same diameter as the Tissue Train plates, with the added advantage that laser scanning confocal microscopy can be used to visualize the cells. On being encapsulated into the HA–gelatin matrix, PDL cells remained rounded over the first few days, gradually acquiring a fibroblastic phenotype, and although initially distributed evenly throughout the gel, with cell growth the central two-thirds of the wells became densely populated with the peripheral one-third less so. When the constructs were viewed in profile, the cells were found to be initially distributed randomly throughout the gel, but by the second wk had became organized into a double cell layer, one at the gel–substrate interface, and the other near the surface (Fig. 1).

Laser scanning confocal microscopy and FDA/PI staining proved effective at distinguishing viable and nonviable cells (Fig. 2). A progressive increase in the number of cells in stationary cultures occurred both with and without the addition of growth factors, which plateaued about 2 wk, the number of nonviable cells remaining fairly constant at approximately 5%. However, the addition of CTGF and FGF-2 resulted in a significant increase in the number of cells per field compared to controls (Table 2). We also found that maintaining the cultures for up to 6 wk had no significant effect on the number of viable cells, but increased the number undergoing apoptosis to about 14% in cultures with growth factors, and 12% in those without (data not shown).

Lack of stiffness of the gel was a disadvantage when attempting to examine the tissue constructs by scanning electron microscopy, the specimens collapsing during the critical point drying stage of preparation. Nevertheless, adequate images of the cells and the dense network of HA and gelatin fibrils were still obtained, although the density of the fibrillary matrix is likely to be exaggerated by shrinkage during dehydration (Fig. 3). Laser scanning confocal microscopy and triple staining for vinculin, actin and DNA, however, enabled images of the morphology and organization of the cells within the hydrogel matrix to be captured. At the gel–substrate interface the cells assumed an amoeboid-like morphology, and near the surface the characteristic elongated fusiform appearance of fibroblasts in two-dimensional culture (Fig. 4).

We next examined the effects of CTGF and FGF-2 on gene expression by cells in the stationary cultures. Of the panel of 18 genes screened (Table 1), 12 were detected at Ct values < 35 (Table 3), and subsequently confirmed by agarose gel electrophoresis (Fig. 5). We failed to detect *SOX9*, *MYOD*, *SP7* (osterix), *BMP2*, *BGLAP* (osteocalcin) or *COL2A1* in either stationary or mechanically

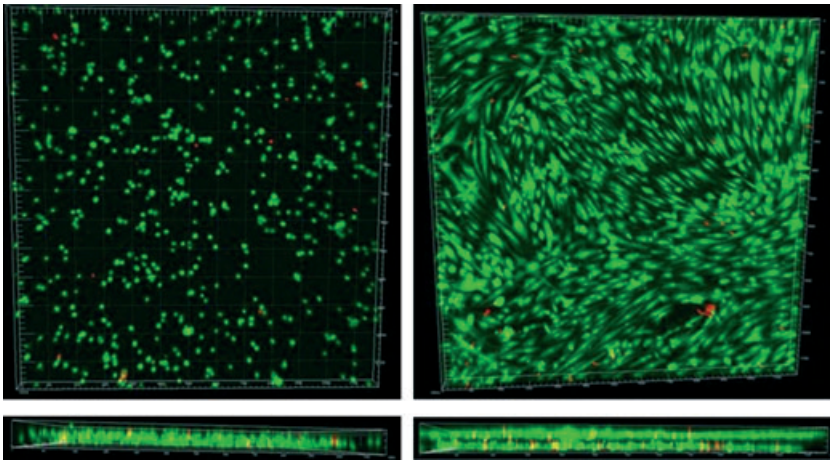

Fig. 1. Human periodontal ligament cells in hyaluronan–gelatin hydrogel films (80–100 μm in thickness) in 35 mm diameter type I collagen coated six-well plates, cultured with connective tissue growth factor (100 ng/mL) and fibroblast growth factor-2 (10 ng/mL). Left: 24 h. Right: 2 wk. The cells were stained with 0.1 mL (2 μg) fluorescein diacetate and 0.3 mL (6 μg) propidium iodide and viewed with a Carl Zeiss, LSM 510 META confocal imaging system; viable cells fluoresce bright green, non-viable cells bright red. Images are viewed from above and in profile. Profile view shows that cells are initially distributed randomly throughout the gel, but as they proliferate they become organized into a double cell layer; the field measures 120 × 120 μm.

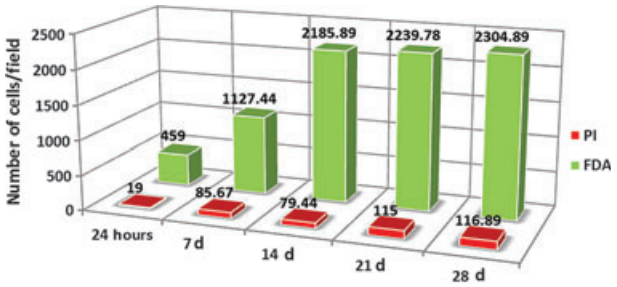

Fig. 2. Viability of human periodontal ligament cells incorporated into Extracel films (80–100 μm thickness) cultured in 35 mm diameter type I collagen coated six-well plates in the presence of connective tissue growth factor (100 ng/mL) and fibroblast growth factor-2 (10 ng/mL). At the end of each time-point the cells were stained with fluorescein diacetate and propidium iodide and viewed with a Carl Zeiss, LSM 510 META confocal imaging system; viable cells (green) and non-viable cells (red). Three fields were selected from three wells and the number of viable and nonviable cells counted using Image-Pro Plus (version 6.1.0.346) software.

activated cultures. The relative quantity (RQ) values suggested addition of growth factors had modest effects on gene expression, apart from *RUNX2*, *COL1A1* and *TGFB1*, which were upregulated at RQ values > 2.00 at some point in the time-scale; *MMP1* was upregulated across all three time-points (Table 3).

The effect of mechanical stress on gene expression with and without growth factors is shown in Table 4. A higher number of genes were expressed at RQ values > 2.00, particularly *COL3A1*, *MMP3*, *TIMP1* and *OPG*. However, we were unable to detect any significant additive or synergistic effects between the effects of mechanical stress alone and CTGF/FGF-2 with the sole exception of *PPARG*. Protein levels of MMP-1–3 and TIMP-1 in supernatants from cultures that had been mechanically stressed in the absence of CTGF/FGF-2 were significantly upregulated at various points in the time-scale, with MMP-3 and TIMP-1 across all three time-points (Fig. 6).

Finally, we performed an experiment to exclude the possibility that increases in gene and protein expression in mechanically stressed cultures were due to an increase in cell population. As Flexercell plates are unsuitable for use with laser scanning confocal microscopy, cell growth was measured by the MTS (tetrazolium) assay; this showed that mechanical stress did not have a significant effect on cell number (Table 5). Assays of the supernatants from these cultures showed that CTGF was constitutively synthesized by the cells in picogram quantities; however, no significant differences in CTGF synthesis could be

Table 2. Effect of growth factors on the proliferation of periodontal ligament cells

	7 d	14 d	21 d	28 d
Control	288.44 ± 47.04	1619.67 ± 234.50	1543.00 ± 76.36	1731.67 ± 117.89
Experimental	1127.44 ± 59.22***	2185.89 ± 156.14***	2239.78 ± 44.52***	2304.89 ± 52.43***

Human periodontal ligament cells were incorporated into Extracel films and cultured with and without connective tissue growth factor (100 ng/mL) and fibroblast growth factor-2 (10 ng/mL). At the end of each time-point the cells were stained with fluorescein diacetate and propidium iodide and viewed with a Carl Zeiss, LSM 510 META confocal imaging system. Three fields were chosen from three wells and the number of viable and non-viable cells counted using Image-Pro Plus (version 6.1.0.346) software. The data are cross-sectional and expressed as means ± SEM.
***$p < 0.001$.

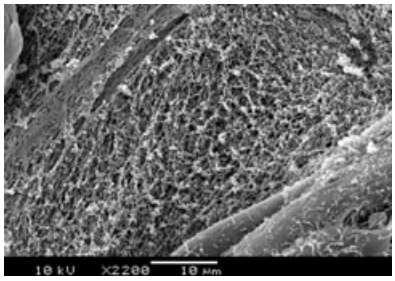

Fig. 3. Scanning electron micrograph showing the ultrastructure of the dense network of cross-linked hyaluronan and gelatin fibrils of the hydrogel matrix. This is likely to be exaggerated to some extent by dehydration during specimen preparation. In the lower right-hand corner are three periodontal ligament cells.

detected between control and mechanically stressed cultures (Fig. 7). FGF-2 was also detected in the media in picogram quantities, but at levels (12–17 pg/mL) close to the detection limit of the assay.

Discussion

A number of attempts to engineer three-dimensional constructs of the PDL *in vitro* by incorporating ligament cells into various natural and synthetic polymers have been reported. Collagen has been most commonly used for obvious reasons given that collagens are the major structural proteins in connective tissues (20–25), but one disadvantage of collagen constructs is a tendency for fibroblast-populated collagen gels to contract over time unless cultured in the presence of MMP inhibitors (26,27).

We therefore carried out preliminary experiments to compare the suitability of 2% agarose gels with the commercially available preparation, Extracel. Agarose, a naturally occurring linear polysaccharide composed of galactose subunits obtained from agar, has been widely used in orthopaedic research due its ability to support the chondrocyte phenotype (28–30). The attraction of Extracel was that it is composed of two major structural molecules, HA and collagen (albeit in denatured form). It soon became apparent, however, that a marked difference existed between the two polymers in terms of cell survival; after 24 h in agarose almost 50% of the ligament cells were non-vital compared to about 5% in Extracel (unpublished findings). There was an improvement in cell growth in agarose cultures over a 4 wk time-course, but the added difficulty of spreading agarose into films that could be mechanically deformed led to our focus on Extracel.

Our reason for adding growth factors to the constructs was based on reports that CTGF is mitogenic for fibroblasts, and able to direct fibroblast differentiation from PDL progenitor cells and mesenchymal stem cells (31,32), while FGF-2 is a mitogen for PDL cells (33). Originally identified as a polypeptide growth factor and downstream mediator of transforming growth factor-β (34,35), CTGF has been reclassified as a matricellular protein, residing in the pericellular matrix and a member of the CCN family, the nomenclature of which is based on Cysteine-rich protein 61 (Cyr61/CCN1), CTGF/CCN2 and Nephroblastoma overexpressed (Nov/CCN3). In addition to being a mitogen, FGF-2 has been shown to regulate the expression of another matricellular protein osteopontin in PDL cells (36); also known as bone sialoprotein 1 and secreted phosphoprotein 1, as the name implies it was originally discovered in bone cells but is synthesized by many cell types. Both CTGF and osteopontin in common with other matricellular proteins do not play a structural role in the extracellular matrix, but serve to regulate cell–matrix interactions and cell function (37). This is achieved via direct binding to specific integrin receptors and heparin sulphate proteoglycans, triggering signal transduction in a wide variety of events such as cell adhesion, migration, proliferation, differentiation and apoptosis (38).

Previous investigations, including our own, have shown that in monolayer culture, *CTGF* is a mechanoresponsive gene (18,39–41). However, we were unable to confirm this finding. The present data further suggest that the addition of exogenous CTGF or FGF-2 to either stationary or mechanically stressed constructs was of limited benefit. In retrospect this is perhaps not surprising, given that real-time RT-PCR microarrays (3,4) have shown that PDL cells *in vitro* constitutively express numerous cytokines and growth factors that exhibit overlapping biological activities (redundancy), as well as multiple biological effects (pleiotropy); it would seem that endogenous production of growth factors by the cells was sufficient to promote growth. Another unexpected finding was that while mechanical stress upregulated the expression of multiple genes, we were

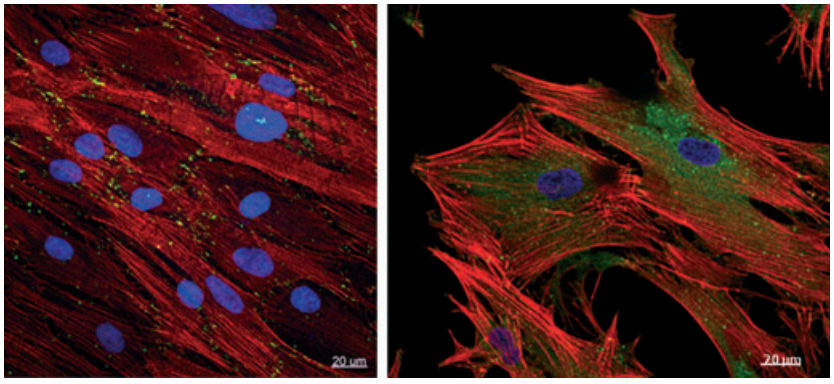

Fig. 4. Confocal immunofluorescent images of human periodontal ligament cells in three-dimensional Extracel films. Left: Cells near the gel surface. Right: cells at the gel substrate interface. Cells were fixed, permeabilized and triple stained with: (i) an antibody against vinculin (green), which links integrin receptors at focal adhesions to the actin cytoskeleton; (ii) rhodamine (TRITC) conjugated-phalloidin, which binds actin filaments (F-actin; red); and (iii) DAPI, a fluorescent stain that binds strongly to DNA (nuclei, blue).

Table 3. Effect of growth factors on gene expression by human periodontal ligament cells

	7 d	14 d	21 d
P4HB	1.41 ± 0.73	0.72 ± 0.25	0.44 ± 0.19
RUNX2	0.94 ± 0.27	2.01 ± 0.77	2.21 ± 0.82
PPARG	1.48 ± 0.84	0.95 ± 0.30	0.53 ± 0.25
COL1A1	0.81 ± 0.35	3.35 ± 0.49	1.27 ± 0.82
COL3A1	0.89 ± 0.37	1.35 ± 0.25	0.61 ± 0.27
MMP1	4.02 ± 1.18	4.62 ± 1.42	3.16 ± 0.86
MMP2	1.21 ± 0.82	0.47 ± 0.26	1.45 ± 1.03
MMP3	0.42 ± 0.18	0.31 ± 0.09	1.15 ± 0.46
TIMP1	0.78 ± 0.26	0.30 ± 0.19	0.66 ± 0.57
TGFB1	0.97 ± 0.35	0.82 ± 0.38	3.07 ± 0.71
RANKL	1.06 ± 0.16	1.14 ± 0.28	0.61 ± 0.22
OPG	0.67 ± 0.37	1.29 ± 1.08	0.83 ± 0.23

Human periodontal ligament cells were cultured in three-dimensional hyaluronan/gelatin films ± connective tissue growth factor (100 ng/mL) and fibroblast growth factor-2 (10 ng/mL) and gene expression quantified by real-time RT-PCR. The data are cross-sectional, expressed as relative quantity ± SEM, and represents the mean of four separate determinations. Relative quantity values > 1.00 signify an increase in gene expression by growth factor-treated cultures over controls.

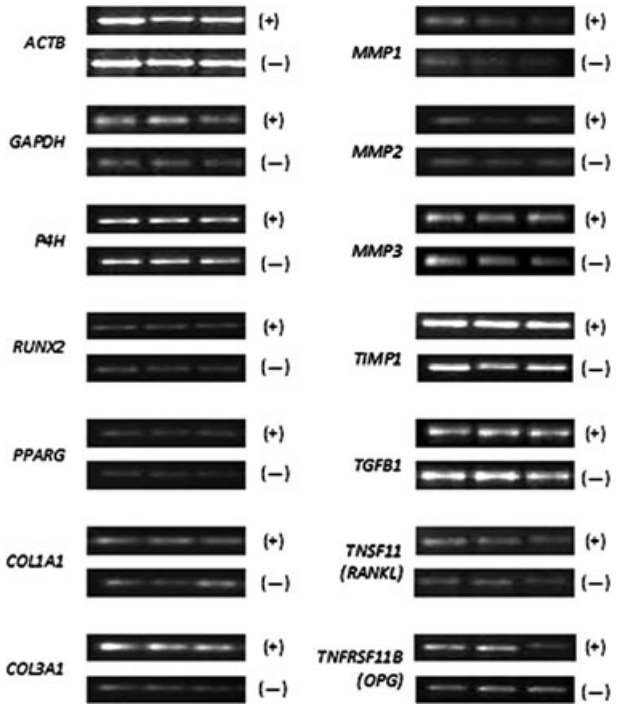

Fig. 5. Agarose gel electrophoresis of amplified real-time polymerase chain reaction products following reverse transcription of RNA extracted from periodontal ligament/Extracel constructs cultured with (+) and without (−) connective tissue growth factor (100 ng/mL) and fibroblast growth factor-2 (10 ng/mL) for 7, 14 and 21 d in 35 mm six-well plates. The images are representative examples of the results of four independent experiments. For description of gene symbols please see Table 1.

unable to detect a significant increase in cell proliferation as previously reported for epithelial cells and osteoblasts strained in monolayer culture (42,43).

While predominantly fibroblastic in phenotype, cells cultured from the PDL and expanded *in vitro* constitute a heterogeneous cell population that includes STRO-1-positive mesenchymal stem cells with the potential to differentiate into osteoblasts, chondroblasts, myoblasts and adipocytes (44–46). The osteoblast-specific transcription factor *RUNX2* was expressed by the cells and upregulated by growth factors and mechanical stress and given its location one might expect to find precursors for osteogenic and cementogenic cells. However, none of the downstream mediators of osteogenesis such as *SP7* (Osterix), *BMP2* or *BGLAP* (Osteocalcin) were detected, which suggests that *RUNX2*-expressing osteoprogenitor cells were part of the mesenchymal stem cell pool, but remained just that. Unlike *SOX9* and *MYOD*, which we failed to detect, expression of the adipocyte-related transcription factor *PPARG* and its responsiveness to mechanical strain was intriguing. PPAR-γ ligands induce bone marrow stem cell adipogenesis but also inhibit osteogenesis (47), and the secretion of adipocyte hormones such as leptin, which affect bone development, goes some way to explaining the poorly understood pathophysiological association between fat and bone (48). The reasons for this in the present context are not immediately obvious, but with the PDL bordered on one side by a surface lined with osteoblasts and on the other by cementoblasts, inhibition of osteogenesis by peroxisome proliferator-activated receptor -γ ligands may form part of a mechanism preventing ossification of the ligament.

The genes for RANKL and OPG, two cytokines customarily synthesized by osteoblasts and stromal cells were expressed, *OPG* being highly responsive to mechanical stress. RANKL, which exists in both membrane-bound and soluble forms stimulates the differentiation and function of osteoclasts, an effect mediated by RANK, a member of the TNF receptor family expressed primarily on cells of the monocyte/macrophage lineage, including osteoclasts and their precursor cells (49). OPG is a secreted protein that inhibits bone resorption by acting as a decoy receptor, binding to and neutralizing both cell-bound and soluble RANKL (50). The RANK/RANKL/OPG triad thus constitutes a

Table 4. Effect of mechanical stress on gene expression by human periodontal ligament cells

	No growth factors ± mechanical stress			Growth factors ± mechanical stress		
	7 d	14 d	21 d	7 d	14 d	21 d
P4HB	0.78 ± 0.21	0.84 ± 0.15	1.08 ± 0.10	0.85 ± 0.10	0.91 ± 0.42	1.02 ± 0.22
RUNX2	0.86 ± 0.29	1.13 ± 0.12	2.62 ± 0.48	1.20 ± 0.41	1.66 ± 0.17	1.38 ± 0.37
PPARG	0.49 ± 0.15	1.00 ± 0.39	3.00 ± 0.41*	1.47 ± 0.36	1.78 ± 0.18	1.00 ± 0.26
COL1A1	0.87 ± 0.21	1.53 ± 0.45	1.40 ± 0.09	0.85 ± 0.08	2.01 ± 0.73	0.84 ± 0.15
COL3A1	2.02 ± 0.92	0.98 ± 0.19	3.14 ± 1.15	1.49 ± 0.24	1.35 ± 0.52	3.46 ± 0.45
MMP1	0.44 ± 0.18	1.48 ± 0.67	4.31 ± 1.46	1.06 ± 0.26	2.05 ± 1.13	5.41 ± 1.70
MMP2	1.00 ± 0.25	1.44 ± 0.58	1.83 ± 0.17	0.88 ± 0.27	2.34 ± 0.65	2.11 ± 0.33
MMP3	2.66 ± 0.47	2.56 ± 0.26	13.47 ± 2.27	0.77 ± 0.10	1.53 ± 0.62	13.00 ± 4.49
TIMP1	0.88 ± 0.23	2.10 ± 0.17	2.71 ± 0.62	1.17 ± 0.22	3.45 ± 0.62	5.54 ± 1.70
TGFB1	0.78 ± 0.27	1.13 ± 0.48	1.03 ± 0.14	0.63 ± 0.11	1.39 ± 0.22	1.05 ± 0.46
RANKL	0.12 ± 0.01	0.56 ± 0.38	1.12 ± 0.40	0.12 ± 0.05	0.05 ± 0.02	0.63 ± 0.59
OPG	1.26 ± 0.11	2.31 ± 0.84	5.02 ± 1.37	0.37 ± 0.13	2.58 ± 1.06	2.28 ± 0.31

Human periodontal ligament cells were cultured in three-dimensional hyaluronan/gelatin films ± connective tissue growth factor (100 ng/mL) and fibroblast growth factor-2 (10 ng/mL), ± cyclic mechanical strain for 6 h/d and gene expression quantified by real-time RT-PCR. The data are cross-sectional, expressed as relative quantity ± SEM, and represents the mean of four separate determinations. Relative quantity values > 1.00 signify an increase in gene expression by mechanically active cultures over the corresponding controls.
*$p < 0.05$.

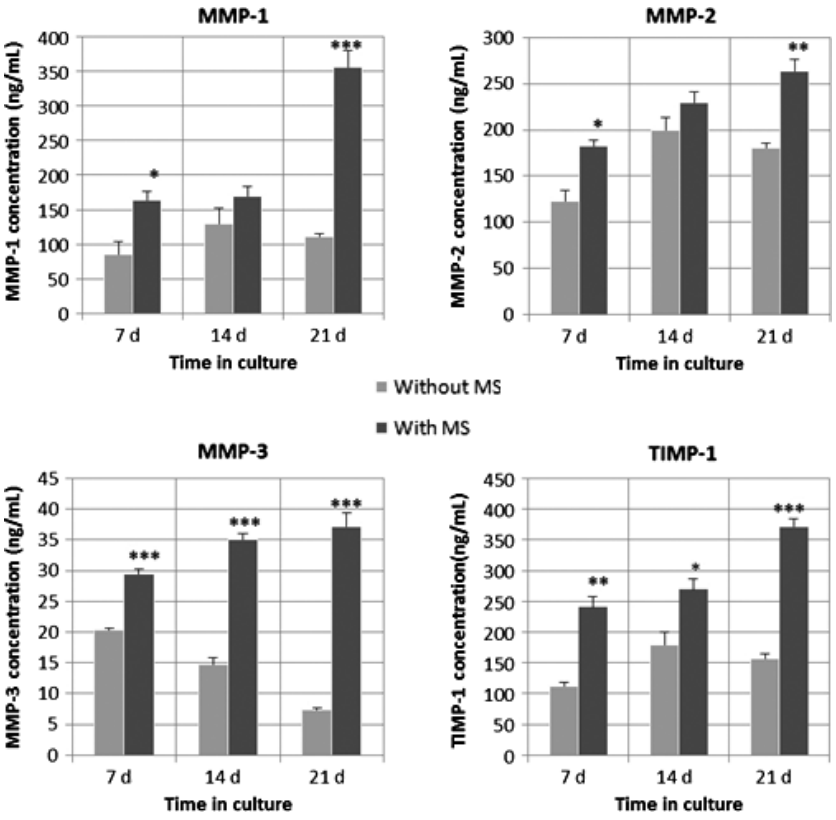

Fig. 6. Matrix metalloproteinases (MMP)-1–3 and TIMP-1 synthesis by human periodontal ligament cells in Extracel films subjected to an in-plane biaxial cyclic strain of 12% for 5 s (0.2 Hz) every 60 s for 6 h/d. At each end-point the culture media from six wells was pooled in pairs and assayed in triplicate. The antibodies to MMP-1 recognize pro-MMP-1 only, not active enzyme or MMP-1 complexed to TIMP. The TIMP-1 immunoassay only recognizes natural TIMP-1. The data are cross-sectional and expressed as means ± SEM. *$p < 0.05$, **$p < 0.01$, ***$p < 0.001$.

ligand–receptor system that directly regulates the final steps of the bone resorptive cascade, irrespective of the initiating signal (51). The finding that PDL cells also express *RANKL* and *OPG* has led to their being widely investigated *in vitro*, both genes being upregulated by compressive and tensile mechanical strain (52–54). Again, the reasons for this are not clear, but again may be related to limiting ossification of the ligament; the clinical observation that most ankylosed teeth are lower deciduous molars out of occlusion (55) is perhaps relevant.

The MMPs (matrixins) are a family of proteolytic enzymes synthesized in either secreted forms or bound to the plasma membrane, that play key roles in cell–cell and cell–matrix interactions during growth, morphogenesis and pathophysiological remodelling (56). MMPs function at neutral pH and are released as latent proforms, activation involving the loss of a propeptide of about 80 residues (57). TIMPs, of which TIMP-1 is the major form (58), closely regulate MMP activity by forming high affinity, essentially irreversible complexes with the activated enzyme to prevent uncontrolled resorption. The three major secreted MMPs, MMP-1 (collagenase-1), MMP-2 (gelatinase-A) and MMP-3 (stromelysin-1), as well as

Table 5. Effect of mechanical stress on periodontal ligament cell proliferation

	7 d	14 d	21 d
Control	0.281 ± 0.017	0.864 ± 0.136	1.104 ± 0.105
Experimental	0.225 ± 0.015	0.838 ± 0.110	0.996 ± 0.100

The effect on cell proliferation of an in-plane, biaxial cyclic mechanical strain of 12% for 5 s (0.2 Hz) every 60 s for 6 h/d measured by the colorimetric MTS (tetrazolium) assay to detect living cells; absorbance was measured at 490 nm. Data are expressed as means ± SEM for six wells from three separate experiments. Mechanical strain did not have a significant effect on cell number.

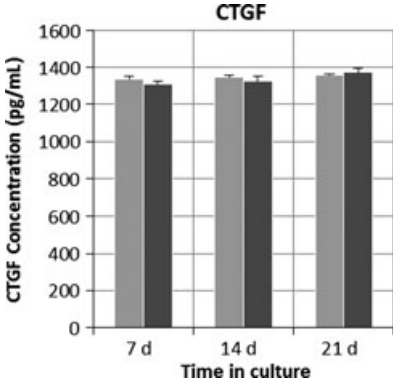

Fig. 7. The effect of an in-plane cyclic mechanical strain of 12% for 5 s (0.2 Hz) every 60 s for 6 h/d on the synthesis of CTGF by human periodontal ligament cells. At each end-point the culture media from six wells was pooled in pairs and assayed in triplicate. The data are cross-sectional and expressed as means ± SEM. There was no statistically significant difference between control and mechanically stressed cultures. CTGF, connective tissue growth factor.

their inhibitor TIMP-1, were all released into the culture media as well as being stimulated by mechanical stress at various points in the time-scale. However, whether they were involved in degrading the pericellular matrix, the supporting scaffold or both is unclear and additional research using activity assays and gelatin and casein zymography will be necessary to establish whether the enzymes are in the active, latent or complexed forms; the MMP-1 ELISA, for example, only recognizes proMMP-1. We have previously reported that human PDL cells in monolayer culture constitutively expressed 16 members of the MMP family at Ct values < 35 (18). The list included seven *MMPs*, three *MT-MMPs* (membrane type-MMPs) and three *ADAMTSs* (a disintegrin and metalloproteinase with thrombospondin motifs), a family of proteinases anchored to the extracellular matrix whose actions include cleavage of the matrix proteoglycans aggrecan and versican (59), plus three *TIMPs*. There are therefore plenty of alternative enzymes available for matrix degradation depending on the substrate, and MMP-1 in addition to cleaving native collagen can also act as a gelatinase (60).

Engineering three-dimensional tissue constructs is rather more complicated than it might first appear, and the challenge is to replicate not only the complexity, but also the mechanical and viscoelastic characteristics (resistance to elastic deformation or stiffness) of the native tissue. One of the disadvantages of hydrogels is their poor mechanical properties, resulting in tissue constructs with significantly poorer mechanical strength than the real tissue (12). In an analysis of the rheological properties of cross-linked HA–gelatin hydrogels for use in soft tissue engineering, the elastic moduli ranged from 11 Pa to 3.5 kPa depending on the concentration of HA (61); Extracel has a shear elastic modulus of about 70 Pa (Glycosan Biosystems; personal communication), which is similar to the 90 Pa reported recently for a three-dimensional collagen gel populated with PDL cells (24). For the purposes of the present investigation this enabled the gel to be mechanically deformed, but for tissue engineering applications a much higher stiffness is required. One problem in trying to reconstruct the biophysical properties of the human PDL, a complex fibre-reinforced tissue that responds to mechanical loading in a viscoelastic and nonlinear manner (62), is that the elastic modulus is, for all practical purposes, unknown. The difficulty of examining thin tissue sandwiched between bone and cementum has resulted in a lack of consistency regarding its elastic properties, highlighted by a recent systematic review where Young's modulus in 23 studies using finite element analysis, was found to range from 10 kPa to 1750 MPa, a difference approaching six orders of magnitude (63).

Culturing cells in three dimensions complicates the perennial question of the strain profile experienced by the cells. As discussed previously (18), this is difficult enough to determine with the methods commonly used to deform cells in two dimensions. When a substrate is deformed, irrespective of whether in-plane or out-of-plane, uniaxial or biaxial, the cells will be exposed to a combination of tensile, compressive and shear strains; the amount of deformation will also vary with the position of the cells within the field, and in the Flexercell system deformation of the substrate will only be about half that programmed into the computer (64,65). In the present study, the strain experienced by the cells at the gel–substrate interface, will clearly be different from that experienced by the cells of the surface layer or within the body of the gel. The stress profile is therefore likely to be similar to the complexity revealed by the finite element analysis of the von Mises and principal stresses generated in the PDL when multirooted teeth are mechanically loaded *in vivo* (66). One thing is certain, understanding the strain distribution within the hydrogel matrix and its effect on the biomechanical behaviour of the cells will require sophisticated three-dimensional finite element modelling.

In summary, we have demonstrated that the addition of a third dimension provides another level of complexity to the existing two-dimensional culture systems designed to investigate the mechanobiology of the PDL. While thin films are suitable for studies of tensile strain, thicker constructs will be needed for investigating the

effects of compression. This will require increasing the complexity of the scaffold by incorporating additional structural molecules such as type I collagen and fibronectin into the matrix to provide extra RGD (Arg-Gly-Asp) binding sites; these will aid cell attachment, proliferation and function, enabling cells to populate the entire gel, while the triple helices of intact collagen will stiffen the matrix. Although primarily developed as a transitional *in vitro* model for studying cell–cell and cell–matrix interactions in tooth support, the system is also suitable for investigating the pathogenesis of periodontal diseases, and importantly from the clinical point of view, in a mechanically active environment.

Acknowledgements

Supported by the Academic Research Fund of the National University of Singapore: (R222-000-029-112) and (R221-000-043-112).

References

1. Somerman MJ, Archer SY, Imm GR, Foster RA. A comparative study of human periodontal ligament cells and gingival fibroblasts in vitro. *J Dent Res* 1988;**67**:66–70.
2. Agarwal S, Chandra CS, Piesco NP, Langkamp HH, Bowen L, Baran C. Regulation of periodontal ligament cell functions by interleukin-1β. *Infect Immun* 1996;**66**:932–937.
3. Wescott DC, Pinkerton MN, Gaffey BJ, Beggs KT, Milne TJ, Meikle MC. Osteogenic gene expression by human periodontal ligament cells under cyclic tension. *J Dent Res* 2007;**86**:1212–1216.
4. Pinkerton MN, Wescott DC, Gaffey BJ, Beggs KT, Milne TJ, Meikle MC. Cultured human periodontal ligament cells constitutively express multiple osteotropic cytokines and growth factors, several of which are responsive to mechanical deformation. *J Periodont Res* 2008;**43**:343–351.
5. Lee KY, Mooney DJ. Hydrogels for tissue engineering. *Chem Rev* 2001;**101**: 1869–1879.
6. Schacht EH. Polymer chemistry and hydrogel systems. *J Phys Conf Series* 2004;**3**:22–28.
7. Hoffman RM. To do tissue culture in two or three dimensions? That is the question. *Stem Cells* 1993;**11**:105–111.
8. Roskelley CD, Desprez PY, Bissell MJ. Extracellular matrix-dependent issue specific gene expression in mammary epithelial cells requires both physical and biochemical signal transduction. *Proc Natl Acad Sci USA* 1994;**91**: 12378–12382.
9. Wang F, Weaver VM, Petersen OW, *et al.* Reciprocal interactions between beta 1-integrin and epidermal growth factor receptor in three-dimensional basement membrane breast cultures: a different perspective in epithelial biology. *Proc Natl Acad Sci USA* 1998;**95**:14821–14826.
10. Cukierman E, Pankov R, Stevens DR, Yamada KM. Taking cell-matrix adhesions to the third dimension. *Science* 2001;**294**:1708–1712.
11. Elsdale T, Bard J. Collagen substrata for studies in cell behaviour. *J Cell Biol* 1972;**54**:626–637.
12. Aherne M, Yang Y, El Haj AJ, Then KY, Liu K-K. Characterizing the viscoelastic properties of thin hydrogel-based constructs for tissue engineering applications. *J R Soc Interface* 2005;**2**:455–463.
13. Serban MA, Prestwich GD. Modular extracellular matricies: solutions for the puzzle. *Methods* 2008;**45**:93–98.
14. Pike DB, Cai S, Pomraning KR, *et al.* Heparin-regulated release of growth factors in vitro and angiogenic response in vivo to implanted hyaluronan hydrogels containing VEGF and bFGF. *Biomaterials* 2006;**27**:5242–5251.
15. Serban MA, Scott A, Prestwich GD. Use of hyaluronan-derived hydrogels for three-dimensional cell culture and tumor xenografts. *Curr Protoc Cell Biol* 2008; **40**:10.14.1–10.14.21.
16. Jones KH, Senft JA. An improved method to determine cell viability by simultaneous staining with fluorescein diacetate-propidium iodide. *J Histochem Cytochem* 1985;**33**:77–79.
17. Natali AN, Pavan PG, Scarpa C. Numerical analysis of tooth mobility: formulation of a non-linear constitutive law for the periodontal ligament. *Dent Mater* 2004;**20**:623–629.
18. Saminathan A, Vinoth KJ, Wescott DC, *et al.* The effect of cyclic mechanical strain on the expression of adhesion-related genes by periodontal ligament cells in two-dimensional culture. *J Periodont Res* 2012;**47**:212–221.
19. Berridge MV, Tan AS. Characterization of the cellular reduction of 3-(4,5-dimethylthiazol-2-yl)-2,5-diphenyltetrazolium bromide (MTT): subcellular localization, substrate dependence, and involvement of mitochondrial electron transport in MTT reduction. *Arch Biochem Biophys* 1993;**303**:474–482.
20. de Araujo RMS, Oba Y, Moriyama K. Identification of genes related to mechanical stress in human periodontal ligament cells using microarray analysis. *J Periodont Res* 2007;**42**:15–22.
21. Lee Y-H, Nahm D-S, Jung Y-K, *et al.* Differential gene expression of periodontal ligament cells after loading of static compressive force. *J Periodontol* 2007;**78**:446–452.
22. Ku S-J, Chang Y-I, Chae C-H, *et al.* Static tensional forces increase osteogenic gene expression in three-dimensional periodontal ligament cell culture. *BMB Rep* 2009;**42**:427–432.
23. Nagai N, Hirakawa A, Otani N, Munekata M. Development of tissue-engineered human periodontal ligament constructs with intrinsic angiogenic potential. *Cells Tissues Organs* 2009;**190**:303–312.
24. Kim SG, Kim S-G, Viechnicki B, Kim S, Nah H-D. Engineering of a periodontal ligament construct: cell and fibre alignment induced by shear stress. *J Clin Periodontol* 2011;**38**:1130–1136.
25. Ootgiesen DAW, Yu N, Bronckers AL, Yang F, Walboomers XF, Jansen JA. A three-dimensional cell culture model to study the mechano-biological behavior in periodontal ligament regeneration. *Tissue Eng Part C Methods* 2012;**18**:81–89.
26. Myers SA, Wolowacz RG. Tetracycline-based MMP inhibitors can prevent fibroblast-mediated collagen gel contraction in vitro. *Adv Dent Res* 1998;**12**:86–93.
27. Bildt MM, Bloemen M, Kuijpers-Jagtman AM. Von den Hoff JW, Matrix metalloproteinase inhibitors reduce collagen gel contraction and α-smooth muscle actin expression by periodontal ligament cells. *J Periodont Res* 2008;**44**:266–274.
28. Benya PD, Shaffer JD. Dedifferentiated chondrocytes reexpress the differentiated collagen phenotype when cultured in agarose gels. *Cell* 1982;**30**:215–224.
29. Buschmann MD, Gluzband YA, Grodzinsky AJ, Kimura JH, Hunziker EB. Chondrocytes in agarose culture synthesize a mechanically functional extracellular matrix. *J Orthop Res* 1992;**10**: 745–758.
30. Kelly T-NA, Ng KW, Wang CC-B, Ateshian GA, Hung CT. Spatial and temporal development of chondrocyte-seeded agarose constructs in free-swelling and dynamically loaded cultures. *J Biomech* 2006;**39**:1489–1497.
31. Dangaria SJ, Ito Y, Walker C, Druzinsky R, Luan X, Diekwisch TGH. Extracellular matrix-mediated differentiation of periodontal progenitor cells. *Differentiation* 2009;**78**:79–90.
32. Lee CH, Shah B, Moioli EK, Mao JJ. CTGF directs fibroblast differentiation from human mesenchymal stem/stromal cells and defines connective tissue healing in a rodent injury model. *J Clin Invest* 2010;**120**:3340–3349.

33. Dereka XE, Markopoulou CE, Vrotsos IA. Role of growth factors on periodontal repair. *Growth Factors* 2006;**24**: 260–267.
34. Bradham DM, Igarashi A, Potter RL, Grotendorst GR. Connective tissue growth factor: a cysteine-rich mitogen secreted by human vascular endothelial cells is related to the SRC induced immediate gene product CEF-10. *J Cell Biol* 1991;**114**:1285–1294.
35. Igarashi A, Okochi H, Bradham DM, Grotendorst GR. Regulation of connective tissue growth factor gene expression in human skin fibroblasts and during wound repair. *Mol Biol Cell* 1993;**4**: 637–645.
36. Terashima Y, Shimabukuro Y, Terashima H, *et al*. Fibroblast growth factor-2 regulates expression of osteopontin in periodontal ligament cells. *J Cell Physiol* 2008;**216**:640–650.
37. Bornstein P, Sage EH. Matricellular proteins: extracellular modulators of cell function. *Curr Opin Cell Biol* 2002;**14**: 608–616.
38. Chen C-C, Lau LF. Functions and mechanisms of action of CCN matricellular proteins. *Int J Biochem Cell Biol* 2009;**41**:771–783.
39. Miyake Y, Furumatsu T, Kubota S, Kawata K, Ozaki T, Takigawa M. Mechanical stretch increases CCN2/CTGF expression in anterior cruciate igament-derived cells. *Biochem Biophys Res Comm* 2011;**409**:247–252.
40. Guo F, Carter DE, Leask A. Mechanical tension increases CCN2/CTGF expression and proliferation in gingival fibroblasts via a TGFβ-dependent mechanism. *PLoS ONE* 2011;**6**:e19756.
41. Kanazawa Y, Nomura J, Yoshimoto S, *et al*. Cyclical cell stretching of skin-derived fibroblasts downregulates connective tissue growth factor (CTGF) production. *Connect Tissue Res* 2009;**50**: 323–329.
42. Brunette DM. Mechanical stretching increases the number of epithelial cells synthesizing DNA in culture. *J Cell Sci* 1984;**69**:35–45.
43. Buckley MJ, Banes AJ, Levin LG, *et al*. Osteoblasts increase their rate of division and align in response to cyclic mechanical tension. *Bone Miner* 1988;**4**:225–236.
44. Lekic P, Rojas J, Birek C, Tenenbaum H, McCulloch CA. Phenotypic comparison of periodontal ligament cells in vivo and in vitro. *J Periodont Res* 2001;**36**: 71–79.
45. Seo B-M, Miura M, Gronthos S, *et al*. Investigation of multipotential postnatal stem cells from human periodontal ligament. *Lancet* 2004;**364**:149–155.
46. Nagatomo K, Komaki M, Sekiya I, *et al*. Stem cell properties of human periodontal ligament cells. *J Periodont Res* 2006; **41**:303–310.
47. Lecka-Czernick B, Moerman EJ, Grant DF, Lehmann JM, Manolagas SC, Jilka RL. Divergent effects of selective peroxisome proliferator-activated receptor-γ2 ligands on adipocyte versus osteoblast differentiation. *Endocrinology* 2002;**143**: 2376–2384.
48. Zhao L-J, Jiang H, Papasian CJ, *et al*. Correlation of obesity and osteoporosis: effect of fat mass on the determination of osteoporosis. *J Bone Miner Res* 2008; **23**:17–29.
49. Nakagawa N, Kinosaki M, Yamaguchi K, *et al*. RANK is the essential signaling receptor for osteoclast differentiation factor in osteoclastogenesis. *Biochem Biophys Res Commun* 1998;**253**:395–400.
50. Simonet WS, Lacey DL, Dunstan CR, *et al*. Osteoprotegerin: a novel secreted protein involved in the regulation of bone density. *Cell* 1997;**89**:309–319.
51. Filvaroff E, Derynck R. Bone remodelling: a signalling system for osteoclast regulation. *Curr Biol* 1998;**8**:R679–R682.
52. Kanzaki H, Chiba M, Shimizu Y, Mitani H. Periodontal ligament cells under mechanical stress induce osteoclastogenesis by receptor activator of nuclear factor B ligand up-regulation via prostaglandin E_2 synthesis. *J Bone Miner Res* 2002; **17**:210–220.
53. Tsuji K, Uno K, Zhang GX, Tamura M. Periodontal ligament cells under intermittent tensile stress regulate mRNA expression of osteoprotegerin and tissue inhibitor of metalloproteinase-1 and -2. *J Bone Miner Res* 2004;**22**: 94–103.
54. Kanzaki H, Chiba M, Sato A, *et al*. Cyclic tensile force on periodontal ligament cells inhibits osteoclastogenesis through OPG induction. *J Dent Res* 2006;**85**: 457–462.
55. Biederman W. Etiology and treatment of tooth ankylosis. *Am J Orthod* 1962;**48**: 670–684.
56. Murphy G, Nagase H. Progress in matrix metalloproteinase research. *Mol Aspects Med* 2008;**29**:290–308.
57. Reynolds JJ, Meikle MC. Mechanisms of connective tissue matrix destruction in periodontitis. *Periodontology 2000* 1997; **14**:144–157.
58. Docherty AJP, Lyons A, Smith BJ, *et al*. Sequence of human tissue inhibitor of metalloproteinases and its identity to erythoid potentiating activity. *Nature* 1985; **318**:66–69.
59. Porter S, Clark IM, Kevorkian L, Edwards DR. The ADAMTS metalloproteinases. *Biochem J* 2005;**386**:15–27.
60. Welgus HG, Jeffrey JJ, Stricklin GP, Eisen AZ. The gelatinolytic activity of human skin fibroblast collagenase. *J Biol Chem* 1982;**257**:11534–11539.
61. Vanderhooft JL, Alcoutlabi M, Magda JJ, Prestwich GD. Rheological properties of cross-linked hyaluronan-gelatin hydrogels for tissue engineering. *Macromol Biosci* 2009;**9**:20–28.
62. Jónsdóttir SH, Giesen EB, Maltha JC. Biomechanical behaviour of the periodontal ligament of the beagle dog during the first 5 hours of orthodontic force application. *Eur J Orthod* 2006;**28**: 547–552.
63. Fill T, Carey JP, Toogood RW, Major PW. Experimentally determined mechanical properties of, and models for, the periodontal ligament: critical review of current literature. *J Dent Biomech* 2011; doi:10.4061/2011/312980.
64. Vande Geeste JP, Di Martino ES, Vorp DA. An analysis of the complete strain field within Flexercell membranes. *J Biomech* 2004; **37**, 1923–1928.
65. Wall ME, Weinhold PS, Siu T, Brown TD, Banes AJ. Comparison of cellular strain with applied substrate strain *in vitro*. *J Biomech* 2007;**40**:173–181.
66. Milne TJ, Ichim I, Patel B, McNaughton A, Meikle MC. Induction of osteopenia during experimental tooth movement in the rat: alveolar bone remodelling and the mechanostat theory. *Eur J Orthodont* 2009;**31**:221–231.